11-19-2015

Mass Spectrometry-Based Investigation of APP-Dependent Mechanisms in Neurodegeneration

Dale Chaput
University of South Florida, chaput@mail.usf.edu

Mass Spectrometry-Based Investigation of APP-Dependent Mechanisms in Neurodegeneration

by

Dale Chaput

A dissertation submitted in partial fulfillment
of the requirements for the degree of
Doctor of Philosophy
Department of Cell Biology, Microbiology, and Molecular Biology
College of Arts and Sciences
University of South Florida

Co-Major Professor: Stanley M. Stevens, Jr, Ph.D.
Co-Major Professor: Jaya Padmanabhan, Ph.D.
Kristina Schmidt, Ph.D.
Patrick Bradshaw, Ph.D.

Date of Approval:
November 2nd, 2015

Keywords: proteomics, phosphoproteomics, stable-isotope labeling, Alzheimer's Disease

Dedication

I dedicate this to my parents, Tim and Lori, my brother, Noel, and my grandma, Sheila. Without your persistent support along the way, this would not have been possible. Thank you for always encouraging me and pushing me to challenge myself.

.

Acknowledgements

This was made possible by the guidance and support of both my mentors Dr. Stanley M Stevens, Jr., and Dr. Jaya Padmanabhan. I also want to thank Dr. Kristina Schmidt and Dr. Patrick Bradshaw for your advice and feedback during the development of this project. I also need to extend a special thank you to Dr. Kent Seeley and Dr. Harris Bell-Temin who helped me immensely through my first few years of graduate school. Finally, I'd like to thank Dr. Anne Messer for taking a chance and hiring an inexperienced undergrad and giving me the confidence to pursue my dreams. Thank you all for your advice and encouragement, teaching me to solve problems and think critically as I have grown into a young scientist.

.

Table of Contents

List of Tables

List of Figures

Abstract

Alzheimer's disease (AD) is the most prevalent form of dementia affecting the elderly, and as the aging population increases the social and economic burden of AD grows substantially. Pathological hallmarks of AD include the accumulation of extracellular amyloid plaques and intracellular neurofibrillary tangles (NFTs), as well as significant neuron loss. Amyloid plaques consist of aggregated amyloid beta (Aβ) peptide, which is generated from the proteolytic processing of amyloid precursor protein (APP) in addition to several other peptides. While the processing of APP has been characterized, its primary physiological function and its involvement in AD pathology are poorly understood. Developing a greater understanding of the function of APP, and the molecular and cellular functions it is involved in or other proteins it is associated with, could provide insight into its role in AD pathology. To investigate the function of APP695, the neuronal isoform of APP, we used mass spectrometry to compare changes in protein expression and phosphorylation between APP-null B103 and APP695-expressing B103-695 rat neuroblastoma cells.

Mass spectrometry-based proteomics has become a powerful technique for the unbiased identification of proteins from complex mixtures. Quantitative proteomics using labeling techniques, such as stable isotope labeling by amino acids in cell culture (SILAC), allow relative quantitation of multiple samples at once. More recently, with advances in mass spectrometer technology, label-free quantitation has become a reliable quantitative proteomics approach. Additionally, mass spectrometry can be used for the analysis of post-translational modifications, such as phosphorylation, a dynamic modification involved in the regulation of many cellular processes. Phosphoproteomics identifies site-specific phosphorylation and surrounding sequence information, which can be used for consensus motif analysis to provide further information about potential changes in kinase activity. Identifying

changes in phosphorylation and kinase activity also provides information about signaling pathways and functions that may be affected by APP695 expression. Comprehensive proteomic and phosphoproteomic datasets can be used to gain insight into the molecular mechanisms that may be regulated by APP695 expression, or involved in AD progression and pathology, leading to the development of novel therapeutic and preventative strategies for AD.

Proteomic and phosphoproteomic analysis of B103 and B103-695 cells identified several significant protein expression and phosphorylation changes that may be mediated by APP695-expression. Global-scale proteomic analysis identified increased expression of Ras and γ-synuclein in B103-695 cells, which was further validated in human AD brain tissue. Phosphoproteomic analysis showed increased phosphorylation of Histone H4 at Ser47, and led to the investigation of PCTAIRE-2 (Cdk17), and PCTAIRE-3 (Cdk18) expression, which were all shown to be increased in AD transgenic mouse tissue, culture primary rat neurons treated with Aβ, as well as mild cognitive impairment (MCI) and AD human brain tissue.

Label-free quantitative proteomics was used for the analysis of human brain tissue from the cortex of individuals affected by AD, MCI, Parkinson's disease (PD), and progressive supranuclear palsy (PSP) compared to cognitively normal, control samples. A number of differentially expressed proteins were identified in AD, MCI, PD, and PSP tissue. Bioinformatic analysis of the comprehensive proteomic datasets from AD, MCI, PD, and PSP human brain tissue identified several proteins consistent with corresponding disease pathology and neurodegeneration, such as inflammatory proteins. While some of the molecular and cellular functions were unique among neurodegenerative diseases, there also appears to be overlap of affected functions, suggesting there may be a more common mechanism of neurodegeneration.

Chapter 1 – Introduction

Alzheimer's Disease

Alzheimer's disease (AD) is the most prevalent neurodegenerative disorder, affecting an estimated 5.3 million Americans of all ages and costing an expected $226 billion in 2015 [1]. With advances in medicine, social and environmental conditions, life expectancy has increased, and the number of people living into their 80s and 90s has also increased. Additionally, a large portion of the American population, often referred to as 'the baby boom generation', is beginning to reach the age of 65 when the risk of developing AD is greater. As the elderly population is expected to grow, the financial and medical burdens of AD also increase substantially, which increases the need for development of better treatments and preventative strategies. Symptoms of AD include memory loss and significant cognitive decline. The two major pathological hallmarks of AD are extracellular amyloid plaques and intracellular neurofibrillary tangles (NFTs) found in the neocortex, entorhinal cortex, and hippocampus; brain regions associated with learning and memory [2-4]. Neurofibrillary tangles (NFTs) are composed of paired helical filaments (PHFs) of hyperphosphorylated tau, a microtubule associated protein that accumulates within neurons [5, 6]. Tau is a cytoplasmic protein that normally functions to promote microtubule assembly and stability by binding to tubulin during its polymerization [7]. Hyperphosphorylation of tau affects its ability to bind and stabilize microtubules and impairs axonal transport [8, 9]. Amyloid plaques consist of aggregated amyloid-beta (Aβ) peptides, and are typically surrounded by dystrophic axons and dendrites, as well as activated microglia and reactive astrocytes [10-12]. Amyloid-beta peptides result from the sequential proteolytic cleavages of APP, which are secreted and accumulate extracellularly. The precise molecular mechanisms that promote the formation of amyloid plaques and NFTs in AD are not fully understood. While the symptoms of AD and

the pathology observed in AD brains have been characterized, the cause and progression of AD pathology is still unclear.

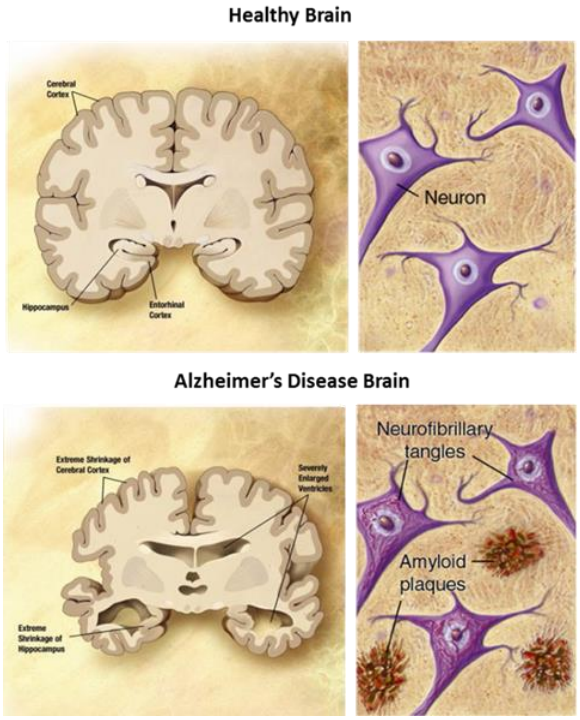

Figure 1. Pathological hallmarks of Alzheimer's disease. Extracellular amyloid plaques and intracellular neurofibrillary tangles (NFTs), as well as significant shrinkage of the cerebral cortex and enlarged ventricles, are observed in the brains of AD patients. *Images adapted from the National Institute of Aging.*

Of the 5.3 million Americans living with AD, approximately 5.1 million are age 65 and older [1]. The majority of AD is considered sporadic, or late-onset AD, and is thought to be caused by a variety of factors including age, environment, and inflammatory proteins [13-15]. The major genetic risk factor for late-onset AD is Apolipoprotein E4 (ApoE4) [16]. Three major isoforms of ApoE exist; ApoE2, ApoE3, and ApoE4. ApoE2 is a relatively rare isoform and has been shown to be potentially protective against AD [17]. ApoE3, the most common isoform, is thought to neither increase nor decrease the risk of AD, while ApoE4 is associated with increased risk of late-onset AD. ApoE4 may be involved in increased Aβ aggregation and reduced Aβ clearance [18, 19]. A small portion of AD cases (<10%) occur before the age of 65 and are considered early-onset, referred to as familial AD (FAD). Familial AD is the result of inherited autosomal dominant gene mutations found in APP or presenilins (PS1 or PS2), proteins

involved in APP processing [20-22]. These mutations will be discussed later in this chapter in the context of APP proteolytic processing. The pathology of early-onset FAD and late onset or sporadic AD is identical. While some treatments are available for the symptoms of mild AD, disease progression remains inevitable as there is no preventative strategy.

The diagnosis of AD remains difficult and relies heavily on neuropsychological findings and the exclusion of other possible causes of dementia. AD can only be confirmed by post-mortem autopsy. Measuring levels of Aβ42, total tau and phosphorylated tau in the cerebrospinal fluid (CSF) is used as an indication of AD. Decreased levels of Aβ42, indicating reduced clearance of the peptide, and increased tau and phosphorylated tau have been observed in the CSF of AD and early AD patients [23]. Brain amyloid imaging can also be used in combination with measuring CSF levels of Aβ42, total tau, and phosphorylated tau. Imaging Aβ in the brain was made possible in 2004 using Pittsburgh Compound B-based positron emission tomography (PET) scanning [24]. A specific and effective diagnostic biomarker for AD is yet to be discovered, and there are no known biomarkers to detect early AD before the accumulation of Aβ42 and the eventual onset of symptoms. There is a crucial need to discover biomarkers for the detection of early AD so that preventative strategies can be implemented to delay or avoid disease progression.

Amyloid Precursor Protein

The amyloid precursor protein (APP) gene is located on chromosome 21 in humans [25]. Three major isoforms exist; APP695, APP751, and APP770, composed of 695, 751, and 770 amino acids, respectively [20]. While APP751 and APP770 are expressed in most tissues, APP695 is predominantly expressed in neurons. APP is a single transmembrane protein [26] synthesized in the endoplasmic reticulum (ER) of neurons and transported through the Golgi apparatus to the trans-Golgi-network (TGN) where it can be shuttled to the cell surface by TGN-derived secretory vesicles where it undergoes proteolytic processing [27-29].

APP belongs to a protein family that includes APP-like protein 1 (APLP1) and APP-like protein 2 (APLP2) [30, 31]. The protein family includes conserved domains in their extracellular sequence and APLP1 and APLP2 are processed similarly to APP; however, the Aβ domain is unique to APP. Studies using knockout mice have provided some insight into the partially redundant functions of APP protein family members. *APP*, *APLP1*, and *APLP2* single knockout mice and *APP/APLP1* double knockout mice are all viable and fertile [32-35]. *APP/APLP2*, *APLP1/APLP2* double knockout mice and *APP/APLP1/APLP2* triple knockout mice, however, show early postnatal lethality, suggesting a crucial role for *APLP2* in the absence of *APP* or *APLP1* [34-36]. A large amount of research has been directed at understanding the expression, processing, and function of APP and its role in AD pathogenesis.

Proteolytic Processing

APP is proteolysed by 2 different pathways; the amyloidogenic and non-amyloidogenic pathways. The non-amyloidogenic pathway avoids the generation of Aβ as APP is first cleaved by α-secretase between Lys612 and Leu613 (numbering based on the 695 isoform) within the Aβ domain, generating a membrane-bound C-terminal fragment (CTFα) C83 and sAPPα from the N-terminal domain. sAPPα has been shown to be involved in early central nervous system (CNS) development [37], neural stem cell proliferation [38], and have neuroprotective effects [39, 40]. The membrane bound CTFα fragment C83 is then cleaved by γ-secretase producing P3 and APP-intracellular domain (AICD) fragments. P3 is rapidly degraded and is unlikely to have an important function. Studies have identified disintegrin and metalloproteinase domain-containing proteins ADAM10 [41] and ADAM17 (also called tumor necrosis factor-α converting enzyme, TACE) [42] as the primary α-secretases that cleave APP within the Aβ domain.

Alternatively in the amyloidogenic pathway, APP is cleaved between Met596 and Asp597 (numbering based on the 695 isoform) by β-site APP cleaving enzyme (BACE or β-secretase) [43, 44], producing C-terminal fragment (CTFβ) C99, and sAPPβ. The sAPPβ fragment is very similar to sAPPα,

however, it has been shown to cause defective axonal transport resulting in axonal dystrophy and neuronal cell death [45, 46]. Cleavage of the membrane bound CTFβ fragment C99 by y-secretase releases the AICD fragment, leaving Aβ bound to the membrane. Finally, different sizes of Aβ fragments are generated, including the 40-42 amino acid long peptide fragments (Aβ40 and Aβ42), as it is thought that y-secretase cleaves Aβ at multiple sites every 3-4 amino acids until it is released from the membrane [47-49]. The APP intracellular domain (AICD) fragment is generated in both the amyloidogenic and non-amyloidogenic pathways following y-secretase cleavage. AICD is known to be translocated into the nucleus and regulate the transcription of several genes including *APP* [50], *GSK3β* [51], and *EGFR* [52]. It has also been suggested that AICD can induce apoptosis [53] and increases the sensitivity of neurons to toxic insult [54].

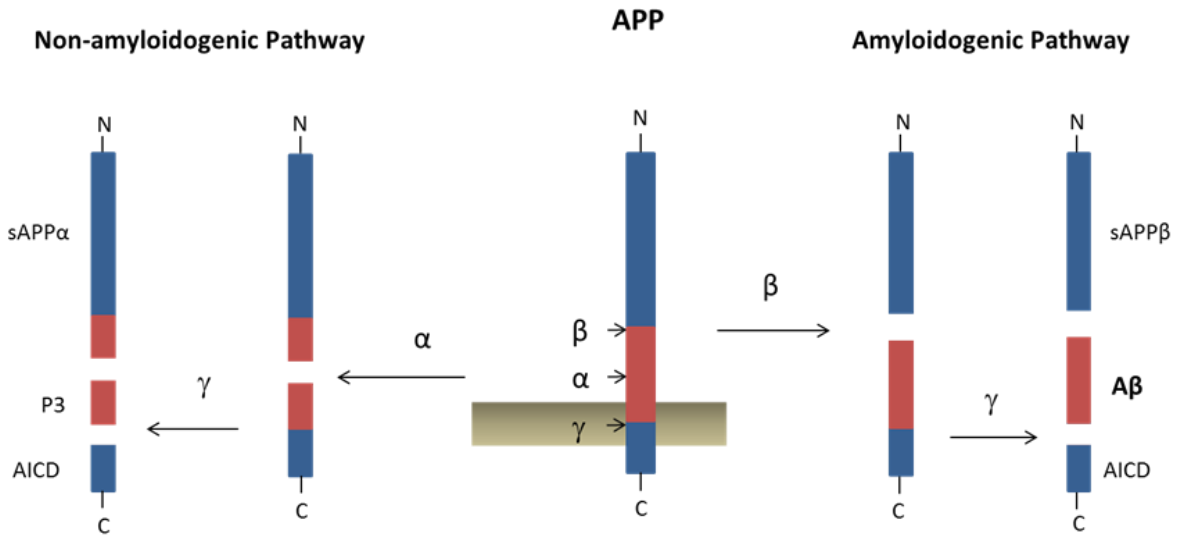

Figure 2. Proteolytic processing of Amyloid Precursor Protein (APP). APP is proteolysed by α-, β-, and y-secretases leading to the generation of several peptides including the Aβ peptide, which aggregates to form amyloid plaques in AD.

The y-secretase protease complex is found within the cell membrane and consists of 4 different proteins: presenilin-1 (PS1) or presenilin-2 (PS2), nicastrin, anterior pharynx-defective 1 (APH1) and presenilin enhancer 2 (PEN2) [55]. Presenilin 1 and 2 are the catalytic subunits of the y-secretase

complex, possessing two highly conserved aspartate residues required for γ-secretase activity [56, 57]. Familial AD mutations in PS1 and PS2 have been shown to promote the production of Aβ peptides, especially Aβ42 [58-60].

Increasing evidence suggests that the intracellular trafficking and subcellular localization of APP influences its processing and the production of Aβ; this is likely attributed to the localization of β- and γ-secretases [61]. BACE is found in endosomes and Golgi compartments, and is most efficient at lower pH [44], while α-secretase activity is observed at the cell surface [62]. The γ-secretase complex components are localized to the endoplasmic reticulum (ER), lysosome, and cell surface [63, 64]. APP localized to the cell surface is proteolysed by α-secretase in the non-amyloidogenic pathway, while APP internalized into endosomes is proteolysed by BACE in the amyloidogenic pathways, increasing Aβ production.

The exact sites of γ-secretase cleavage have a significant influence on the ability of Aβ to aggregate. Aβ42 is more hydrophobic than other Aβ peptides as it includes C-terminal alanine and isoleucine amino acid residues causing it to have a strong tendency to aggregate quickly. A large amount of AD research has focused on determining the role of insoluble Aβ42 oligomers in amyloid plaques and its toxicity; however, it is important to consider that proteolytic cleavage of APP generates a variety of Aβ peptides, and it is possible that the aggregation and toxicity of Aβ42 may be influenced by the presence of other Aβ peptides [65]. Several types of Aβ oligomers have been characterized following isolation from brain tissue, or using synthetic Aβ peptides. Some of the oligomeric Aβ assemblies that have been described and characterized include protofibrils (PFs), annular protofibrils (APFs), soluble Aβ oligomers, and amyloid fibrils [65, 66]. While a significant amount of research has been carried out to determine the involvement of insoluble Aβ42 oligomers in AD pathogenesis, the number of amyloid plaques does not correlate with the degree of cognitive decline in AD, and amyloid plaques are often observed years before the onset of symptoms. Increasing evidence suggests that

soluble Aβ oligomeric species are involved in AD pathology. Soluble Aβ oligomers have been extracted from human brain tissue and have shown stronger correlation with levels of dementia and AD symptoms than amyloid plaques [67, 68]. Though we are developing a greater understanding of Aβ oligomerization and the types of Aβ oligomers that exist, the Aβ assemblies that are primarily responsible for toxicity and triggering downstream pathology are not fully understood.

Whether the accumulation of Aβ in the brain is related to increased APP expression, increased secretase activity, decreased Aβ clearance, or some other mechanism, remains largely unknown. Some studies have shown that Aβ accumulation can be attributed to reduced Aβ clearance, which may be mediated by ApoE4 [69]. It has also been suggested that soluble Aβ is cleared by ApoE4, while deposited Aβ is phagocytosed by microglia [70, 71]. APP mutations associated with early-onset AD occur either within or adjacent to the Aβ region of APP. Mutations within the Aβ region of APP involved in early-onset AD have been shown to promote the aggregation of Aβ or decrease its degradation, not affecting Aβ production [72, 73], while mutations adjacent to Aβ proteolytic sites promote the amyloidogenic processing of APP and increase Aβ42 production [74, 75]. Mutations in PS1 and PS2, also involved in early-onset AD, have been shown to increase Aβ generation [58-60]. The oligomerization and accumulation of Aβ, the formation of amyloid plaques, and the role of Aβ in AD pathology development are highly complex and further research is necessary to understand this process.

Function

While the regulation of APP expression, trafficking, and proteolytic processing are fairly well described, the primary function of APP has yet to be fully understood. APP has been proposed to be involved in several processes including cell growth and maturation, neural stem cell proliferation and differentiation, as well as neurite outgrowth and synaptogenesis [76]. Much of APPs ability to promote growth may be attributed to sAPPα. It has been reported that sAPPα can promote proliferation of neural stem cells [38] and progenitor cells [77]. Alternatively, another study reported that APP

influenced neural stem cell and progenitor cell proliferation by cystatin C secretion and not sAPPα secretion, indicating that APP may increase proliferation through two different mechanisms [78]. It has also been demonstrated that APP and sAPPα can increase glial cell differentiation [79] as well as the differentiation of neural stem cells and progenitor cells into neurons [78, 80]. Multiple studies have shown that APP promotes neurite outgrowth in cell culture [81-83]. The proposed mechanisms for how APP promotes neurite outgrowth are based on its ability to bind proteins involved in cell-substrate adhesion that are known to influence neurite outgrowth, such as laminin [84], collagen [85], and heparin [86]. There is also evidence for the involvement of APP in the regulation of synaptogenesis, as increased APP expression is observed in pre- and postsynaptic sites during the formation of synapses [87, 88]. Based on the structure of APP, it has also been suggested that it could act as a cell-surface receptor; however, it has not been established whether it actually functions as a cell-surface receptor and activating ligands of APP as a receptor have not been identified. It appears that APP likely has a role in cell growth and differentiation; however, the precise mechanisms of its growth-regulatory function are still unclear.

Hypotheses of Alzheimer's Disease Pathogenesis

Many factors are hypothesized to influence the onset and progression of AD. Aβ deposition, tau hyperphosphorylation, oxidative stress, mitochondrial dysfunction, cholinergic deficits, progressive synaptic loss, and neurodegeneration are all characteristics of AD. A considerable amount of research has been directed at discovering the ultimate cause of AD, hoping to develop therapeutics and preventative strategies. Several hypotheses have been proposed including the inflammatory and oxidative stress hypotheses, the tau hypothesis, the cell cycle hypothesis, and the amyloid cascade hypothesis. Studies have shown that tau pathology has a stronger correlation with the severity of dementia and neuronal loss than Aβ deposition and amyloid plaque formation [89-91]. However, it has also been hypothesized that soluble Aβ correlates more strongly with severity of dementia than amyloid

plaques [67]. Despite the findings that tau pathology better correlates with AD associated neuronal loss and dementia than amyloid plaques, it is hypothesized that AD-related tau pathology, occurs downstream of aberrant Aβ production. Other pathologies, such as oxidative stress, aberrant cell cycle re-entry, and mitochondrial dysfunction, have also been proposed to follow Aβ deposition, and so the main focus of this research is to examine the role of APP-dependent mechanisms in AD pathology development.

Amyloid Cascade Hypothesis

The amyloid cascade hypothesis proposes that Aβ initiates AD pathology and that neurofibrillary tangles, cell loss, oxidative stress, and dementia are consequences of Aβ deposition [2, 92, 93]. While Aβ may not be primarily responsible for all of the neurodegeneration that occurs in AD, it is argued that Aβ acts as a trigger initiating a complex pathogenic cascade. Early-onset FAD provides strong evidence that AD can be initiated by abnormal APP processing and Aβ accumulation, as the genes associated with FAD (APP, PS1, and PS2) are involved in APP processing promoting the production or oligomerization of Aβ42. While early-onset AD is a strong indication that APP and Aβ may be the primary source for the initiation of AD pathology, a significant amount of controversy surrounds the amyloid cascade hypothesis.

The primary argument against the amyloid cascade hypothesis is that the localization of tau pathology and NFTs better correlates with neuronal loss, occurring largely in the entorhinal cortex and hippocampus, whereas amyloid plaques are found primarily in the frontal cortex [90, 94, 95]. Tau pathology has been observed in the entorhinal cortex of young, cognitively normal individuals and in the hippocampus of aging, cognitively normal individuals without Aβ or amyloid plaque accumulation [96]. It is also possible that soluble Aβ, which was not tested for in these studies, may be present in these regions. In the presence of Aβ pathology, however, tau pathology appears to spread to the neocortex, and similar cortical tau pathology is not observed in individuals lacking Aβ pathology [96]. These

observations suggest that Aβ accumulation and aggregation are required for the increase and spread of tau pathology. The toxicity of tau pathology appears to require Aβ accumulation and amyloid plaques, supporting the idea of the amyloid cascade hypothesis. Haass and Selkoe suggest small soluble Aβ oligomers are responsible for neurodegeneration and synaptic dysfunction [66]. Soluble Aβ oligomers correlate more closely with the appearance of tau pathology and are found in brain regions such as the hippocampus that undergo significant neuronal loss [67, 97, 98]. It has been demonstrated that oligomeric Aβ can initiate tau phosphorylation *in vitro* and *in vivo* [99-101]. The amyloid cascade hypothesis is complex and controversial, and a greater understanding of the function of APP and the potential functions of Aβ are necessary to further understand their role in AD pathology development.

Aberrant Cell Cycle Re-entry

Neuronal cell cycle dysregulation is an early abnormality observed in mild cognitive impairment (MCI) and AD. Neurons are terminally differentiated and considered quiescent; however, there is evidence that neurons aberrantly re-enter the cell cycle in AD. Instead of successfully dividing into two daughter cells, the cells that exhibit aberrant expression of cell cycle regulatory proteins undergo apoptosis. A relationship exists between cell cycle activation and neuronal cell death, and inhibition of cell cycle activation aids in preventing neuronal apoptosis [102, 103]. Expression of cell cycle proteins, including cyclins A, B, D, E, cdc2/cdk1, cdk4, cdk7, proliferating cell nuclear antigen (PCNA), and p16, has been observed in the brains of AD patients [104-108]. Mitogenic signaling has also been implicated in AD as increased expression and activation of ERK and Ras have been observed in early stages of AD [109, 110]. Mitotic kinases are also involved in the phosphorylation of tau and APP, potentially contributing to the formation of neurofibrillary tangles and amyloid plaques. It has recently been proposed that microglial derived tumor necrosis factor-α (TNFα) may be involved in promoting AD-related neuronal cell cycle events [111]. Additionally, microRNA MiR-26b has been found to be upregulated in AD and is shown to be potentially involved in cell cycle activation, tau phosphorylation and apoptosis [112]. Other

findings have suggested that Aβ may be involved in induction of aberrant cell cycle re-entry [113].

In vitro studies have shown that APP is phosphorylated at Thr668 (numbering based on APP695 isoform) in a cell cycle-dependent manner and *in vivo* studies showed that it correlates with the expression of cell cycle regulatory proteins Cyclin D1, Cyclin E, p-cdc2/Cdk1, and E2F1 in mouse models of AD [113]. Further, studies suggest that GSK3β [114, 115], JNK3 [116], Cdk5 [117], and cdc2/Cdk1 [118] influence APP phosphorylation at Thr668. It has also been reported that Aβ peptides can cause cell cycle activation and apoptosis in primary cortical neurons [119, 120] and that Aβ also induces phosphorylation of APP at Thr668 [113]. The mechanisms of aberrant cell cycle activation in AD remain to be fully understood, but these findings have suggested that APP may be processed in a cell cycle dependent matter and that Aβ can cause cell cycle activation.

Proteomics & Alzheimer's Disease

Mass Spectrometry and Proteomics

Mass spectrometry-based proteomics enables the unbiased, large-scale study of protein expression changes and post-translational modifications (PTMs) of proteins in various model systems and tissues. Mass spectrometry-based proteomics does not rely on antibody availability or specificity for identifying proteins or changes in protein expression. Quantitative proteomic techniques have been developed that allow for the comparison of control and treated samples or healthy and disease tissue. Many quantitative proteomic techniques rely on labeling proteins or peptides with isotopic labels, which was first described by Gygi et al., using isotope-coded affinity tags (ICAT) [121]. Since then, several other isotopic labeling techniques have been developed. Stable isotope labeling with amino acids in cell culture (SILAC) is an approach that allows quantification of protein expression changes in cell models by mass spectrometry. Developed by the Mann lab, cells metabolically incorporate 'heavy' and 'light' amino acids during protein synthesis, enabling the differentiation of protein from two different treatment groups simultaneously [122, 123]. SILAC is consistent, reproducible, and also decreases

variability during sample processing, however it is generally restricted to cultured cells. Other methods for quantitative proteomics have also been developed, such as iTRAQ (isobaric tags for relative or absolute quantitation) [124] or isotopic dimethyl labeling [125, 126], which also use isotope-coded covalent tags for quantitation of peptides within a complex sample, and can be used with tissue samples as peptides are labeled following protein digestion. With advances in mass spectrometers and increased mass measurement accuracy and resolution, label free quantification has become possible which eliminates the need for isotope labels or chemical labeling [127].

Proteomics has become an invaluable tool for the identification and quantification of proteins within a complex mixture, and reducing sample complexity for the identification of low abundance proteins has been essential. Using fractionation techniques increases the identification, quantification, and sequence coverage of low abundance proteins. One of the earliest and most commonly used techniques was two-dimensional gel electrophoresis (2-DE) [128]. Using 2-DE, proteins are first separated based on charge using a pH gradient and isoelectric focusing, and proteins migrate until their net charge is 0. Proteins are then further separated by size using SDS-PAGE in the second dimension of 2-DE. Protein spots can be quantified by comparing staining intensity, and then spots of interest are excised and enzymatically digested for identification by mass spectrometry [129]. Differential gel electrophoresis (DIGE) is a variation of 2-DE that involves fluorescent labeling of proteins so that more than one sample can be run simultaneously on a gel, and can also incorporate an internal standard for more accurate comparison and quantitation of spots between multiple gels [130, 131]. While 2-DE has been widely used, it does have limitations as it is not compatible with many detergent-containing lysis buffers, which are necessary to solubilize membrane proteins. It can also be difficult to detect low abundant proteins using 2-DE, as well as being time consuming and laborious to perform image analysis and in-gel digests of many protein gel spots.

The development of multidimensional protein identification technology (MudPIT) enabled protein identification from complex mixtures coupled with high performance liquid chromatography (HPLC) separation techniques [132, 133]. HPLC offers powerful sample fractionation techniques resulting in multiple fractions from a single sample with reduced complexity allowing for an increased number of identified proteins. Strong cation exchange (SCX) and anion exchange (ACX) are popular HPLC peptide fractionation techniques that separate peptides based on charge. SCX columns have a negatively charged stationary phase that bind positively charged peptides at low pH, which can be subsequently eluted by increasing the pH and salt content of the mobile phase. Alternatively, ACX columns have positively charged stationary phase that bind negatively charged peptides at high pH, which can be eluted by increasing the salt concentration of the mobile phase. These HPLC separation techniques coupled with mass spectrometry have allowed high-throughput analyses of complex proteomes.

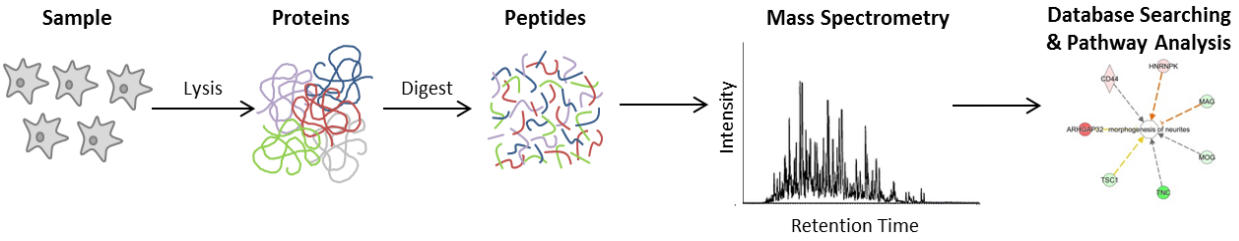

Figure 3. General proteomics workflow. Cells or tissue samples are lysed to extract protein, which are digested to peptides using proteolytic enzymes such as Trypsin. Peptide samples can be further fractionated using strong-cation exchange (SCX) before mass spectrometry analysis. Raw data files can be searched using various software packages against protein sequence databases, and identified proteins can be used for bioinformatics analysis.

Identifying changes in protein expression in AD provides insight into pathways and functions that may be altered, which can help determine mechanisms of pathology development as well as development of interventions or therapeutic strategies. There are several challenges associated with studying neurodegeneration and AD, particularly the complexity of both the brain and the disease. The brain consists of various cell types, such as neurons and glia, which can function differently in different regions of the brain. The mechanistic complexity of AD is also challenging as its pathology can be both stage-specific and region-specific. Proteomic studies have been performed using various cell models,

animal models, as well as human brain tissue in an effort to identify novel proteins and/or pathways that may be involved in the onset and progression of AD, which will be discussed in the next sections. Moreover, proteomic studies using blood and cerebrospinal fluid (CSF) have also been conducted in search of novel diagnostic and therapeutic biomarkers in an effort to potentially detect and treat AD at an early stage [134-136].

Proteomic Studies Using Cell Models

While *in vitro* studies have their limitations, they are useful as they can be easily manipulated to study the effect of various pharmacological agents or differential expression of proteins and to identify the specific changes for further studies in more complex models. Immortalized cell lines are cost effective, convenient, and grow indefinitely. Primary cells, on the other hand, are isolated from tissue; they have a limited lifespan but are often considered a better representation of that cell type than immortalized cell lines as they have not been genetically altered. For example, undifferentiated neuroblastoma cell lines often lack proteins related to neuronal function such as neuronal specific nuclear protein (NeuN), neuron-specific enolase (NSE) and microtubule-associated protein 2 (MAP2), which are present in primary neurons. Neuroblastoma cell lines can be differentiated by manipulating growth conditions to display a more neuronal phenotype [137]. Both primary and immortalized cell models can be treated with Aβ oligomers, which can be prepared *in vitro* from synthetic Aβ peptide. Alternatively, cell lines can be stably transfected to express different proteins, such as APP695, and analyzed for specific changes in expression or function of other cellular proteins, which will provide insights into the function of the newly introduced protein. There have been a number of proteomic studies on cell models of AD, a few of which are described below [138-141].

Foldi and colleagues performed a study using differentiated SH-SY5Y cells, a human neuroblastoma cell line, treated with small Aβ42 oligomers [138]. Aβ oligomers were prepared *in situ* from an Aβ isopeptide precursor that allows for more standardized aggregation [142]. After an 8 hour

Aβ42 treatment, 2-DE was used to separate proteins and quantify expression changes. A total of 1000 spots were detected on the gel, and 649 of these spots matched across treated and untreated gels; 52 of the matched spots were determined to be significantly altered and 47 of them were identified by matrix-assisted laser deposition ionization (MALDI)-time of flight (TOF) mass spectrometry. Elongation factor 2 (EEF2) (-3.6 fold) and Heat-shock protein 70 (Hsp70) (3.5 fold), showed the most significant decrease and increase in expression, respectively, and these changes in expression were further validated by western blot analysis. In addition to identifying changes in protein expression, the study also observed decreased cell viability and altered cell morphology with Aβ42 treatment but did not identify any differences in post-translational modifications.

Another proteomic study examined the cytosolic fractions of SN56 cells, a mouse cholinergic neuroblastoma cell line, also using Aβ treatment and 2-DE. Aβ treatment resulted in significant changes in protein expression and phosphorylation [139]. This study also compared the proteomes of Aβ-treated cells with H_2O_2-treated cells to assess whether changes in protein expression could be attributed to the 'oxidative potential' of Aβ; their findings suggested that Aβ and H_2O_2 treatment had different effects on the proteome profile of SN56 cells. Three unique proteins were identified to show altered expression following Aβ treatment; Calreticulon, MAPK 6c, and γ-actin. The study also identified decreased phosphorylation of 3 proteins; RHO GDI-1 homolog AHO/GDP dissociation inhibitor, ubiquitin carboxyl terminal hydroxylase (UCHL1), and tubulin. The findings that Aβ and H_2O_2 treatment affected protein expression differently is interesting; however, only a few significant changes in protein expression were detected, thus limiting detailed mechanistic information regarding the impact of Aβ on neuron-like cell function.

Studies by Butterfield and colleagues have investigated Aβ-mediated protein oxidation using redox proteomic analysis of Aβ-treated primary neurons [140, 141]. Redox proteomics focuses on the addition of protein carbonyls, lipid peroxidation adducts (HNE-adducts), and tyrosine nitration, which

are protein modifications resulting from oxidative damage [143]. Both studies investigated the impact of 24hr treatment of primary rat neurons with 10μM Aβ using 2-DE for protein separation and 2D-Oxyblots for enrichment and quantification of oxidized proteins, which were subsequently identified by mass spectrometry. One study found that pre-treatment with gamma-glutamylcysteine ethyl ester (GCEE) increased levels of glutathione (GSH), an endogenous antioxidant found to decrease with aging, and protects against protein oxidation [140]. The second study identified specific targets of protein oxidation in response to Aβ treatment and assessed the protective effect of D609, a known inhibitor of phosphatidylcholine specific phospholipase-C (PC-PLC), on these oxidized proteins [141]. Both studies observed increased oxidation of regulatory and structural proteins as well as energy and metabolism-related proteins following Aβ treatment, and demonstrated the potential of 2 different compounds for reducing Aβ-induced oxidative stress.

The studies mentioned above, using cell models, have focused on Aβ treatments to examine changes in protein expression and potentially affected cellular processes and molecular function. The effectiveness of novel compounds in reducing oxidative modification of proteins, and whether Aβ-related protein expression changes are attributed to its oxidative potential, were also investigated. These types of studies are possible in cell models, and are necessary to assess whether potential treatments should be further tested in animal models of AD. The sample preparation approaches used in these studies, primarily relying on 2-DE for protein separation and quantification, may be limiting their proteome coverage and quantitation. The use of SILAC, which is possible in cell models, in combination with other fractionation techniques such as SCX, would likely increase the number of proteins identified and improve relative quantification. It is also interesting that proteomic studies in cell models have relied on Aβ treatments and that cell models expressing full-length APP have not been compared to APP-null cells.

Proteomic Studies Using Animal Models

In vivo studies using animal models that develop Aβ pathology have provided major advances in AD research. While human brain tissue is available post-mortem, animal models allow the study of disease progression from early, asymptomatic stages, which is essential to determine early molecular changes for the development and preliminary testing of preventative strategies and therapeutics to slow disease progression. Proteomic studies have been conducted in a non-mammalian *C.elegans* model of AD, as well as transgenic mouse and rat models of AD.

C.Elegans Models

Caenorhabditis elegans is a non-mammalian model useful for testing the *in* vivo effects of Aβ42 as they have a short life span, they can be easily grown, and their entire genome has also been sequenced. The Butterfield group conducted a redox proteomics study of a transgenic model of *C.elegans* expressing human Aβ42 to identify targets of oxidation. The study identified 16 oxidized proteins associated with similar pathways as in mammalian models [144]. While gene expression studies have been performed in this *C.elegans* model of AD, this appears to be the only proteomics study to date on an *in vivo* model.

Mouse Models

There are a number of transgenic mouse models of AD with mutations in several different genes hypothesized to be involved in disease pathology. Some of the more common mouse models include APP (Tg2576) [145], PS1 (M146L) [146], and PS2 (N141I) [147] single mutant transgenic models, PS/APP double mutant transgenic models [148], as well as tau (P301L) [149] and APP/PS/Tau triple transgenic models [150, 151]. Of the APP transgenic mouse models, the APP Swedish mutant, APP Swedish/London double mutants, and PS/APP double mutants have been used for proteomic studies.

The most common APP transgenic mouse models are Tg2576 and PS/APP mice, with the most common mutations of APP being the Swedish double mutant (K595N/M596L), and London mutant

(V642I) (numbering based on the 695 isoform). The Tg2576 transgenic mouse model overexpresses human APP695 with the Swedish mutation (K595N/M596L). Tg2576 mice develop Aβ deposits at around 1 year, but do not form NFTs [145]. The PS/APP double transgenic mouse model was created by crossing the Tg2576 mouse model with the PSEN1 (M146L) transgenic mouse model. These PS/APP mice therefore overexpress human APP695 with the Swedish mutation and human PSEN1 with the M146L mutation. PS/APP mice, like Tg2576 mice, exhibit accelerated plaque pathology and increased Aβ42 accumulation at an early age, followed by significant fibrillar Aβ accumulation in the cerebral cortex and hippocampus at 6 months. Increased plaque-associated astrocytes and microglia are also observed in PS/APP mice which suggest increased neuroinflammation. Neurofibrillary tangles are not seen in PS/APP mice, however hyperphosphorylated tau is detected [148]. The behavior and cognitive function of both PS/APP and Tg2576 mouse models have been well characterized [148, 152, 153].

Proteomic analysis of the cortex from 24 month old Tg2576 mice determined changes in protein expression, oxidation, and nitration using 2-DE, 2D-Oxyblots, and MALDI-TOF mass spectrometry [154]. The study identified several proteins involved in various physiological functions; increased expression of glial fibrillary acidic protein (GFAP), an inflammatory marker, increased expression of glyeraldehyde-3-phosphate dehydrogenase (GAPDH), pyruvate kinase (PK), and decreased malate dehydrogenase (MDH), proteins involved in metabolism, as well as increased dihydropyrimidase-like 2 (DRP2), involved in synaptic and axonal integrity [154]. Another study performed a proteomic analysis of crude synaptosomal fractions from cortex and hippocampus of Tg2576 mice using 2D-DIGE and hybrid quadrupole-TOF (Q-TOF) mass spectrometry. This study detected 1100 spots in crude synaptosomal fractions where 6 spots were determined to be significantly altered in young Tg2576 mice before Aβ deposition compared with non-transgenic mice. Of the 6 spots, only 2 were confidently identified by mass spectrometry, including Grp75, also referred to as mitochondrial heat shock protein 70 (mtHsp70).

The study revealed changes in mitochondrial protein expression and function prior to Aβ deposition [155].

Proteomic studies of PS/APP transgenic mice have been performed using 2-DE for protein separation and quantification, and protein identification by mass spectrometry using a hybrid linear ion trap-Orbitrap mass spectrometer (LTQ-Orbitrap XL). Previously, the antioxidant N-acetylcysteine (NAC) has been shown to protect against oxidative stress in MCI and AD in PS/APP mice [156]. To investigate the potential mechanisms by which NAC reduced oxidative stress, a proteomic analysis examined PS/APP mice that were administered NAC from 4-9 months of age before Aβ deposition (representing MCI) and from 7-12 months of age after Aβ deposition (representing more advanced AD). Significant changes in protein expression were observed in wild-type (WT), 9-month, and 12-month old mice, and NAC treatment did appear to reduce protein oxidation [157]. Another proteomic study compared PS/APP mice with non-transgenic mice at 1 month, 6 months, 9 months, 12 months, and 15 months of age. The redox proteomic study revealed an age-dependent increase in carbonylated proteins, particularly beta-actin and pyruvate dehydrogenase (PDH), that also correlated with levels of Aβ peptide [158]. These findings support the notion that elevated Aβ levels are associated with increased oxidative damage.

The proteomes of cortex samples from 14 month old Thy1-APP751 transgenic mice have been compared with WT mice. Thy1-APP751 mice express APP751 with both the Swedish and London mutations, have high levels of human Aβ peptide and develop fibrillary amyloid deposits at 6 months of age [159]. Using 2D-DIGE and MALDI-TOF mass spectrometry, this study identified 25 proteins with altered expression in AD mice, 8 of which have also shown increased expression in human AD including GFAP, ApoE precursor, peroxiredoxin 6 (Prdx6), DRP2, PK, synaptotgamin I, serum albumin precursor, and N-ethylmaleidmide sensitive fusion protein, supporting the use of this transgenic mouse as a model of human AD and increasing the potential that these proteins are involved in AD pathology. The

identified proteins differentially expressed in AD mice are involved in molecular and cellular functions consistent with AD, including inflammation and oxidative stress, cholesterol metabolism, and neuronal and synaptic signaling [160].

Rat Models

Proteomic studies have also been conducted using Aβ42-injected rat models [161] and transgenic rats expressing human mutant APP [162] to investigate changes in protein expression and protein carbonylation to identify oxidatively modified proteins. Redox proteomics were used to examine the cortex and hippocampus of rats injected with Aβ42 using 2-DE and 2D-Oxyblots for protein separation and quantitation, and mass spectrometry for protein identification. A number of oxidatively modified proteins were identified in different regions of Aβ-injected rat cortex and hippocampus that have also been shown to be modified in human AD brains, increasing the possibility that these oxidative modifications are involved in AD. This study also demonstrated the profound effect that Aβ-injection into the nucleus basalis can have in other brain regions [161]. Another study by Wilson and colleagues examined the proteome of transgenic rats expressing human APP with the Swedish mutation. This study was primarily focused on developing a proteomic method incorporating laser microdissection to isolate specific cell types from the brain. Using laser microdissection and 2D-DIGE, they were able to observe over 5000 protein spots, and 100 protein spots appeared to be significantly altered; however, with limited amounts of protein only 12 differentially expressed proteins were identified by mass spectrometry [162]. The study by Wilson and colleagues exemplifies the drawbacks of 2D-DIGE and MALDI-TOF for protein identification, and the need to use more advanced and sensitive mass spectrometry approaches for protein identification.

Proteomic Studies Using Human Tissue

While animal models are useful, the differences between the complexity of human biology and animal models can make direct comparisons difficult. Complexity of the central nervous system and the

mechanisms underlying the disease, as well as the availability of human brain tissue, however, makes human studies difficult. One challenge when examining human tissue is the post-mortem interval (PMI) between time of death and specimen collection/processing. It is also important to consider the region of the brain being studied, and how different regions are affected by the disease and composed of different cell types. Different brain regions are also affected at different stages of the disease, while tissue is collected post-mortem when pathology is most severe. Nevertheless, studies using human tissue affected by AD are invaluable for gaining a deeper understanding of the molecular changes that exist with the progression of disease pathology.

Proteomic analyses of the temporal cortex have been performed, which is a brain region affected early in AD. Andreev and colleagues performed a label-free quantitative proteomic analysis of the temporal cortex from 10 AD and 10 non-AD brain samples using the accurate mass and time tag (AMT) approach. The study identified 1400 unique proteins, with 197 proteins determined to be differentially abundant in AD compared with non-AD brains [163]. A more recent proteomic analysis of the temporal cortex analyzed brain tissue specimens from 10 AD patients compared with 5 non-AD controls and used stable isotope dimethyl labeling for protein quantitation. A total of 827 unique proteins were identified, 227 of which were identified in nine out of ten AD/non-AD pairs. Of the 227 proteins, 69 proteins were differentially expressed in AD compared with non-AD, including 27 novel proteins not previously reported in AD including neuronal-specific septin-3, septin-2, septin-5, dihydropteridine reductase and clathrin heavy chain 1 [164].

The hippocampus plays an important role in memory and cognitive function and is one of the primary brain regions affected early in AD. A study by the Butterfield group examined the hippocampal proteome from 6 AD and 6 age-matched controls using 2-DE and MALDI-TOF mass spectrometry. Significant changes were identified in the abundance of 18 proteins [165]. Another proteomic analysis of the hippocampus was performed by Begcevic et al., using 3 AD and 3 non-AD biological replicates,

which were pooled together. Using SCX for peptide fractionation, followed by analysis on an LTQ Orbitrap XL, a total of 2954 proteins were identified with 1203 proteins detected at a minimum of 2 unique peptides. Pooling of biological replicates prevented statistical analysis, instead they reported that 204 proteins were exclusively identified in AD, and 600 proteins were exclusively identified in control samples [166].

A number of studies have used proteomics to investigate certain subcellular fractions, such as membrane or synaptic fractions, while others have been interested in protein post-translational modifications. Since APP and its secretases are transmembrane proteins, Donovan and colleagues performed a label free quantitative proteomic analysis of the membrane-enriched proteome from the frontal cortex of human brain samples. The study identified 1709 proteins from membrane-enriched fractions, 13 showing significant expression changes. Increased levels of ubiquitin carboxy-terminal hydrolase 1 (UCHL1) and syntaxin binding protein 1 (Munc-18) in AD compared with non-AD samples were validated by western blot [167]. Another study examined detergent insoluble proteins from the temporal cortex of AD, early-AD, and control brains, which include the amyloid plaques that develop during AD. The study identified 125 proteins from insoluble fractions including proteins involved in Aβ production, synaptic scaffolding, and proteins associated with increased risk of AD. The study validated the expression changes of 15 proteins, however further research is required to determine whether these proteins are associated with AD pathology or involved in the formation of Aβ plaques [168].

The synaptic proteome has also been investigated as a considerable amount of synaptic dysfunction and degeneration is observed in AD, however the underlying molecular mechanisms are unknown [169-171]. An early analysis of the synaptic proteome from the hippocampus and frontal cortex of AD and control individuals used 2D-DIGE for protein quantitation and separation prior to mass spectrometry-based protein identification. The study identified 26 synaptic proteins differentially expressed in AD compared with control brain involved in energy metabolism, signal transduction, vesicle

transport, and antioxidant activity [169]. The Chang group then performed targeted analysis of the synaptic proteome using multiple reaction monitoring (MRM), which allows multiple proteins of interest to be specifically targeted during mass spectrometry analysis. Ten proteins identified in their previous study were targeted, and significantly increased levels of peroxiredoxin-1 and dihydropyrimidinase-related protein-1 (DRP1) were found in AD [170]. More recently, Chang and colleagues examined the synaptic proteome using a data-independent acquisition (DIA) mass spectrometry approach referred to as SWATH™ (Sequential Window Acquisition of Theoretical fragment ion spectra). The study identified 2077 unique proteins, with 30 proteins having significant expression changes in AD compared with non-AD. Seventeen of the 30 significant proteins had not previously been suggested to be involved in AD, with cellular functions including structural maintenance, oxidative stress, and synaptic-vesicle related functions [171].

Other published studies have examined human brain tissue using redox proteomics to identify nitrated proteins [172] and oxidatively modified proteins [173, 174]. Protein nitration was investigated using 2-DE and western blotting using an anti-nitrotyrosine antibody followed by MALDI-TOF mass spectrometry for protein identification. An overall increase in protein nitration was observed in AD compared with control hippocampus samples; α enolase, GAPDH, carbonic anhydrase II (CAH II), ATP synthase alpha chain, and voltage-dependent anion channel protein 1 (VDAC-1) showed significant increases in levels of nitration [172]. Two separate redox proteomic studies of human cortex used 2-DE and 2D-Oxyblots with MALDI-TOF mass spectrometry to identify specific targets of oxidation. Increased oxidation of creatine kinase BB, glutamate synthase, UCHL1 [173], α enolase, (DRP2, and heat shock cognate 71 (HSC 71) were observed [174]. These redox proteomic studies provide further evidence for the involvement of protein oxidation in AD pathology and identify specific protein targets of oxidative modification in AD.

These proteomic studies using human tissue have provided valuable insight into both protein expression changes as well as cellular and molecular functions affected in AD. Surprisingly, many of these studies rely on similar proteomic approaches, often using 2-DE for protein separation and quantification and MALDI-TOF for protein identification. Implementing more advanced proteomic techniques, such as gel-free fractionation and using mass spectrometry-based proteomics can greatly increase protein identification, as was demonstrated by Begcevic's study; however, pooling of biological replicates in this study limited statistical analysis to identify robust biomarkers or molecular mechanisms associated with AD. Increasing number of proteomic studies of different brain regions will also improve proteome coverage and provide a more complete picture of molecular changes in AD.

Significance of Protein Phosphorylation in Alzheimer's Disease

Phosphorylation is one of the most important regulatory post-translational modifications involved in many biological processes including signal transduction, cell cycle, and gene expression. Serine, threonine, and tyrosine are the most commonly phosphorylated amino acid residues. Protein phosphorylation is a reversible modification; protein kinases are responsible for the addition of phosphate groups, while phosphatases remove phosphate groups. Aberrant phosphorylation is often associated with disease including neurodegenerative diseases such as AD [175]. Mass spectrometry also enables the investigation of post-translational modifications such as phosphorylation.

Hyperphosphorylation of tau is the primary example of aberrant phosphorylation in AD. The effect of tau hyperphosphorylation on axonal transport and the ability of tau to stabilize microtubules exemplifies the impact aberrant phosphorylation can have on protein function and cellular processes [8, 9]. In addition to tau, other proteins demonstrate altered phosphorylation in AD, including neuronal filaments [176, 177] and MAP1B [178, 179]. Increased expression and/or activity of kinases such as GSK3 and CDK5, and decreased expression and/or activity of phosphatases such as PP1, PP2A and PP5 have also been observed in AD brains [175].

The sorting and processing of APP has been shown to be affected by its phosphorylation state, as well as the phosphorylation of proteins associated with APP. The dynamic regulation of APP protein sorting has been reported to be dependent on the phosphorylation state of its interacting proteins [180]. Phosphorylation of components of TGN vesicles by protein kinase C (PKC) appears to promote the sorting of APP toward the cell surface, where it is processed by the non-amyloidogenic pathway avoiding the production of Aβ [181]. The C-terminal domain of APP contains several amino acid residues known to be phosphorylated. Phosphorylation of APP at Thr654/Ser655 by PKC has been suggested to favor non-amyloidogenic processing of APP and to be a protective modification [182]. Decreased PKC expression and activity has been observed in AD brains, which may contribute to the increased amyloidogenic processing of APP. Increased phosphorylation of APP695 at Thr668 has been observed in AD [183]. APP695 phosphorylation at Thr668 is mediated by multiple proline-directed kinases, including GSK3 [114], Cdk5 [117], cdc2 [118], and JNK3 [116, 184], which have also shown to be elevated in AD. NMR studies have shown that phosphorylation of APP at Thr668 causes a conformational change affecting interactions with binding partners [185]. Further, mutation of Thr668 to alanine (T668A) appeared to significantly reduce Aβ production in primary neurons [183]. These findings indicate the potential involvement and significance of phosphorylation in APP processing and AD pathology.

An increasing number of studies suggest aberrant protein phosphorylation is involved in AD pathology, impacting both tau pathology and Aβ production. It has become apparent that we need to gain a deeper understanding of the influence that abnormal phosphorylation has on AD progression and pathology. The knowledge of specific phosphorylated proteins and affected pathways and functions, as well as changes in kinase and phosphatase activity will hopefully lead to development of novel therapeutic and preventative strategies for AD.

Phosphoproteomics

Mass spectrometry can also be used to determine changes in PTMs, such as phosphorylation, which can provide further insight into alterations in activity of kinases or phosphatases and associated signaling pathways. Many of the quantitative techniques used in proteomics can also be applied to phosphoproteomics, such as SILAC. Phosphopeptides are low abundant in a complex mixture of peptides based on the low stoichiometry of this modification, and therefore enrichment prior to mass spectrometry analysis is beneficial in order to increase their identification and site-specific information. Several phosphopeptide/protein enrichment strategies have been developed at the protein and peptide level. Phosphoproteins can be separated and identified using 2-DE in combination with the ProQ Diamond stain, a proprietary fluorescent dye that selectively detects phosphate groups attached to serine, threonine, and tyrosine residues in polyacrylamide gels [186, 187]. ProQ Diamond is useful as it does not require the use of phosphorylation specific antibodies or radioisotopes, such as P^{32}. Alternative approaches have been developed such as immobilized-metal affinity chromatography (IMAC), that exploit the negatively charged phosphate groups affinity for positively charged metal ions, such as Fe^{3+} [188-190], Ga^{3+} [191], or Ti^{4+} [192]. Metal oxide affinity chromatography (MOAC) can also be used for phosphopeptide enrichment, most commonly using TiO_2 particles [193, 194]. Polymer-based metal ion affinity capture (PolyMAC) has more recently been introduced for phosphopeptide enrichment [195]. Strong cation exchange (SCX) has also been used for the enrichment of phosphopeptides [196]. While each phospho-enrichment technique offers unique advantages, the combination of multiple phospho-enrichment strategies has proven to be the most effective for increasing the identification of phosphorylation sites [197-199].

Not only can phosphoproteomics determine changes in protein phosphorylation, but the identification of specific phosphorylation sites and surrounding sequence information can be used for further bioinformatics analysis. Most kinases, or families of kinases, phosphorylate serine, threonine, or

tyrosine residues within a specific amino acid sequence, also referred to as a consensus motif. Gygi and colleagues developed an approach that uses the phosphorylation site and surrounding sequence information obtained from mass spectrometry analysis to determine over-represented consensus sequences, which can reveal potential changes in kinase or phosphatase activity [200].

Phosphoproteomic Studies

There are a limited number of phosphoproteomic studies related to Alzheimer's disease. With the advancement of phospho-enrichment techniques and mass spectrometer performance, there will likely be an increase in the number of phosphoproteomic studies of AD, which is important to further understand changes in phosphorylation of proteins, kinase activity, and pathway signaling that may be involved in AD pathology.

Cell Models

It appears that only one phosphoproteomic study has been performed using a cell model of AD. Wang and colleagues performed a phosphoproteomic analysis of N2aSW cells treated with sodium selenate, a compound shown to reduce tau hyperphosphorylation, improving spatial learning and motor performance in AD mice. N2aSW cells are a mouse neuroblastoma cell line expressing human APP with the Swedish mutation and have increased extracellular Aβ accumulation. This study used2-DE and ProQ Diamond stain, where 65 proteins with changes in phosphorylation were identified corresponding to 39 proteins with increased phosphorylation and 26 proteins with decreased phosphorylation [201].

Mouse Models

Wang et al., conducted a phosphoproteomic analysis of an early onset mouse model to identify changes in phosphorylation that may be involved in the transition from presymptomatic to symptomatic AD in response to Aβ42 accumulation [202]. TgCRND8 mice are an early onset transgenic mouse model of AD overexpressing human APP-695 with the Swedish (K670M/N671L) and Indiana mutation (V717F). TgCRND8 mice exhibit early amyloid plaque formation, activated microglia, and dystrophic neurites

[203]. The study compared the phosphoproteomes of the hippocampus from 2 month old presymptomatic TgCRND8 mice, 6 month old symptomatic TgCRND8 mice, and non-transgenic mice [202]. Triple isotopic dimethylation labeling was used for quantitation and phosphopeptide enrichment was performed using Ti^{4+}-IMAC microspheres (described by [Ref 19]). Additional sample fractionation was implemented using a biphasic C18 trap column followed by in-line SCX fractionation and C18 reverse-phase separation. This study identified 1026 phosphopeptides of which 595 phosphopeptides were confidently quantified, and 139 phosphopeptides were found to be significantly altered.

Human Tissue

There have only been five phosphoproteomic analyses of human brain tissue, 3 of which were performed using frontal cortex, including one earliest (2008) and most recent (2015) phosphoproteomic studies. The first phosphoproteomic study of human AD cortex was published in 2008 using calcium phosphate precipitation for phosphopeptide enrichment and an LTQ Orbitrap mass spectrometer for protein identification [179]. The most recent published phosphoproteomic study also analyzed the frontal cortex of AD brains compared with control samples using IMAC for phosphopeptide enrichment and label free quantitation, also using an LTQ Orbitrap mass spectrometer [204]. The 2008 study identified 466 phosphorylation sites on 185 proteins, while the 2015 study identified 5569 phosphopeptides, 1559 phosphoproteins, and 4185 unique phosphosites, with 253 phosphopeptides significantly altered in AD compared with control (>1.75-fold). The 2015 study by Dammer et al., identified changes in the regulation of the heat shock and protein misfolding response pathways between AD and control samples, which may have further implications in maintaining protein quality and clearance [204]. The third phosphoproteomic analysis examined frontal cortex and substantia nigra from AD and control patients using 2-DE for protein separation and ProQ Diamond stain to identify changes in levels of protein phosphorylation, followed by Q-TOF mass spectrometry for protein identification [205]. Approximately 600 spots were detected, 125 of which appeared to be

phosphorylated in both the cortex and substantia nigra, and were subsequently identified corresponding to 72 different proteins. Significant changes in phosphorylation (>2-fold) among both brain regions were observed in 9 proteins, including GAPDH, DRP2, and aldolase A (ALDOA) [205]. All of the above studies identified significant changes in phosphorylation of cytoskeletal and microtubule-associated proteins, as well as proteins involved in synaptic function, which are consistent with AD pathology. Determining changes in phosphorylation of specific proteins at different sites can further indicate potential changes in kinase activity and altered signaling pathways that may be associated with the progression of AD.

Phosphoproteomic analyses of neurofibrillary tangles (NFTs) and neuronal intermediate filament proteins (NF-M/H) have also been conducted [177, 206]. Rudrabhatla and colleagues characterized the abundance and sites of phosphorylation of NF-M/H from frontal cortex of AD brain compared with control brains using TiO_2 for phosphopeptide enrichment and iTRAQ for quantitative phosphoproteomic analysis [177]. Phosphorylation of several sites were identified that are proline-directed Ser/Thr residues suggesting increased activity of proline-directed kinases such as Cdk5, GSK3β, or MAPKs or the down-regulation of protein phosphatases such as protein phosphatase 2A (PP2A) [177]. In a later study they examined the phosphoproteins associated with NFTs from frontal cortex of AD and control brains, and found that phosphorylated NF-M and NF-H are integral components of NFTs, which was controversial prior to this proteomic study due to the cross reactivity of phospho-NF antibodies. Also identified phosphorylated MAP1B and MAP2 in NFTs isolated from AD patients. These studies further characterize and quantify the site-specific phosphorylation of cytoskeletal and microtubule-associated proteins identified in NFTs [206].

There has only been one published phosphoproteomic analysis of the hippocampus, which is one of the primary brain regions affected by AD. The Butterfield group performed a semi-quantitative phosphoproteomic analysis of hippocampus from AD and normal brains using 2-DE and ProQ Diamond

stain to identify changes in phosphorylation [207]. The authors did not report the total number of phosphorylation site or phosphoproteins that they were able to identify, but they did report significant changes in phosphorylation of 17 proteins; 9 having increased phosphorylation, and 8 with decreased phosphorylation in AD hippocampus.

These phosphoproteomic studies contribute to our knowledge of AD pathology and provide information about potentially altered signaling pathways and cellular processes. While these changes need to be further studied to determine the mechanisms of altered phosphorylation and related biological consequences, they are important to the progress of AD research. It will be necessary to conduct more phosphoproteomic studies to determine the consistency and reproducibility of identified changes in phosphorylation. Also, more studies of different brain regions and at different stages of disease progression are needed to increase phosphoproteome coverage and improve our understanding of the role of phosphorylation in AD. It will also be important to expand the phosphoproteomic approaches used, as the majority of the phosphoproteomic studies of AD have relied on 2-DE in combination with ProQ Diamond phosphoprotein gel stain.

Summary of Approaches and Project Aims

Despite the number of proteomic studies in various models of AD, the precise mechanism of APP and Aβ-induced neurodegeneration remains unclear. In order to gain a deeper understanding of proteomic changes in different brain regions at different stages of AD, more studies are needed to increase proteome coverage, as well as determine reproducible changes. Many of the cell model studies have relied on treatment with Aβ42 and have employed somewhat limited mass spectrometry techniques, primarily relying on 2-DE for protein separation and quantitation, and MALDI-TOF mass spectrometry for protein identification. In this dissertation, we report APP-dependent proteomic and phosphoproteomic changes by comparing an APP-null B103 neuroblastoma cell model with a stably transfected B103-695 cell model expressing APP695. As this cell model expresses moderate levels of

APP695, it is likely more representative of early AD where changes in protein expression or phosphorylation may be related to APP695 expression and not the accumulation Aβ oligomers. We also use more comprehensive mass spectrometry techniques that enable greater proteome coverage, as well as SILAC labeling for quantification of proteomic and phosphoproteomic changes. These studies required optimization of phosphopeptide enrichment techniques to increase phosphoproteome coverage of B103 and B103-605 cells. Identifying APP-mediated changes in global protein expression and phosphorylation provides information about the molecular and cellular functions and signaling pathways that may be affected by APP695. Gaining understanding of changes in protein expression and phosphorylation, as well as affected cellular functions and signaling pathways that may be associated with early AD, provides insight into potential biomarkers of early AD and the development of therapeutic targets to hopefully delay the onset or progression of AD

Finally, we report the proteomic analyses of human tissue from normal, healthy brains compared with brains affected by several neurodegenerative disorders: AD, mild cognitive impairment (MCI), progressive supranuclear palsy (PSP), and Parkinson's disease (PD). Additionally, we developed an improved sample processing method when working with limited starting material, such as human tissue or isolated primary cells. Comprehensive proteomic studies provide information about the cellular and molecular functions that may be involved in disease pathology, and aid in the development of hypotheses for targeted validation and mechanistic studies. Proteomics can also potentially identify proteins with altered expression not yet associated with certain neurodegenerative diseases, as well as identify potential biomarkers, which have been difficult to establish for these neurodegenerative diseases

.

Chapter 2: Global Proteomic Analysis of a Cell Model of Alzheimer's Disease

Summary

Proteomic studies using cell models to study changes that occur during Alzheimer's disease (AD) have primarily relied on Aβ42 treatment. Investigating the effect of Aβ42 treatment on protein expression is important as Aβ42 levels are significantly increased in AD, however few proteomic studies have examined the effect of endogenous APP expression. We were particularly interested in the impact of moderate APP695 expression on the proteome, which may represent molecular changes that take place during early AD before there is significant accumulation of Aβ42. To examine APP695-mediated protein expression changes, we used SILAC-based quantitative proteomics to compare APP-null B103 cells with APP695-expressing B103-695 cells. The results of this study were published in a Neuroproteomics Special Issue of Electrophoresis in December 2012 (see Appendix A). In addition to characterizing the proteomes of B103 and B103-695 cells, we were also interested in determining potential APP-mediated protein expression changes during different stages of the cell cycle, and in response to neurotoxic insult/inflammation. SILAC-labeled B103 and B103-695 cells were treated with cell cycle inhibitors or lipopolysaccharide (LPS) to quantify changes in protein expression using mass spectrometry. These comprehensive datasets identified proteins and related cellular pathways that may be affected by APP695 expression and are potentially involved in AD pathology. The datasets were also utilized for bioinformatic analysis to reveal cellular and molecular functions and potentially altered upstream regulators affected by APP695 expression.

Introduction

B103 and B103-695 cells

Cell models previously used for proteomic studies of AD include SH-SY5Y human neuroblastoma cells, N2a mouse neuroblastoma cells, and cultured primary mouse neurons treated with Aβ42 [138, 140, 201]. Studies by Schubert and colleagues have shown that B103 rat neuroblastoma cells do not express detectable levels of APP, APLP1 or APLP2 [81]. B103-695 cells were developed by stable transfection of APP695 into B103 cells. APP695 expression in B103 cells enhanced cell adhesion, neurite outgrowth, and proliferation; however, the molecular mechanisms by which APP induces these cellular functions are unclear [81]. APP or a metabolite of APP may induce these changes either on its own or by affecting expression of genes associated with these functions. B103 and B103-695 cells are a useful model for studying protein expression changes likely related to APP695 expression, and they can also be SILAC-labeled for quantitative proteomic analysis as well as easily treated with different pharmacological compounds to study their effect. The primary goal of this chapter was to characterize the proteomes of B103 and B103-695 cells using SILAC-based quantitative proteomics to identify protein expression changes that may be mediated by APP695 under normal, cell cycle-dependent and inflammatory conditions.

Cell-Cycle Mediated Protein Expression Changes

Cell cycle dysregulation has been suggested to be involved in AD pathogenesis as a number of cell cycle regulatory proteins have shown increased expression in the brains of AD patients and transgenic mouse models [104-108, 113, 208]. APP has also been shown to undergo cell cycle-dependent phosphorylation that influences its metabolism, increasing Aβ production and promoting cell cycle re-entry [113, 118]. Cells expressing APP demonstrate faster growth rates, and the localization of APP to the centromere during mitosis has also been observed, leading to the hypothesis that it may have a role in cell cycle progression [81, 113]. Cell cycle inhibitors, such as Roscovitine, Taxol, and

Nocodazole, provide a strategy to evaluate changes in protein expression during different stages of the cell cycle in B103 and B103-695 cells. Roscovitine is a compound that prevents cell cycle progression at the G1/S and G2/M transition checkpoints by inhibiting Cdk1, Cdk2, Cdk5, and Cdk7 [209]. Taxol, also known as paclitaxel, is a microtubule stabilizer that specifically targets tubulin, interfering with their normal breakdown during cell division and inhibiting progression through the G2/M transition [210]. Nocodazole prevents progression through the G2/M phase by binding tubulin and preventing microtubule polymerization [211]. The goal of this study was to use quantitative proteomic analysis of SILAC labeled B103 and B103-695 cells treated with cell cycle inhibitors to identify novel proteins not previously associated with cell cycle progression that may be mediated by APP695 expression.

Inflammation-Mediated Protein Expression Changes

Inflammation is observed in the brains of individuals affected by AD, and it is believed that inflammatory pathways are activated in AD [212, 213]. However, as with most hypotheses of AD, it remains to be understood whether inflammation is a primary cause of AD or a secondary affect, and it is likely part of a more complex mechanism [213]. To investigate the impact of inflammation on protein expression, B103 and B103-695 cells were treated with lipopolysaccharide (LPS). LPS is part of the outer membrane of gram-negative bacteria and elicits a strong immune response in mammalian immune cells, such as microglia, promoting the secretion of pro-inflammatory cytokines [214, 215]. While LPS treatment activates inflammatory pathways in immune cells, it has a neurotoxic effect on neurons. One study showed that the presence of neurons reduced the inflammatory response of glia to LPS treatment [216]. Using LPS treatment, we investigated the effect of an inflammatory, neurotoxic environment on protein expression and cellular functions in APP-null B103 and APP695 expressing B103-695 cells.

Materials and Methods

Protein Kinase A (PKA) Knockdown

B103 and B103-695 cells were grown in DMEM:F12 SILAC media supplemented with 10% FBS and Penn-Strep-Glutamine. B103 and B103-695 were transfected with increasing amounts of siRNA against PKA, or control siRNA, to reduce expression levels of PKA. Alternatively, B103 and B103-695 were treated with increasing amounts of KT5720 inhibitor, which reduces PKA activity. Cells were collected and lysed in RIPA buffer for western blot analysis. Equal amounts of protein were separated on 15% Tris-glycine gel and probed with antibodies against PKA, p-ERK, and actin.

SILAC Labeling and Roscovitine, Taxol, and LPS Treatments

B103 and B103-695 cells were grown in DMEM:F12 SILAC media supplemented with 10% dialyzed FBS, Penn-Strep-Glutamine, and either unlabeled L-arginine and L-lysine for B103 cells or heavy labelled $^{13}C_6$-L-lysine 2HCl and $^{13}C_6$-$^{15}N_4$-arginine HCl (Cambridge Isotopes) for B103-695 cells. Cells were grown for 5 doublings to achieve >99% incorporation of labeled amino acids. Cells were treated with 20μM Roscovitine, 100ng/ml Taxol, or 100ng/ml LPS for 24 hours. Cells were collected and lysed in 4% SDS, 100mM Tris-HCl pH 7.6, 100mM dithiothreitol (DTT), and incubated at 95°C for 5 minutes, followed by brief sonication. Protein concentrations were determined using the Pierce 660 assay supplemented with ionic detergent compatibility reagent (IDCR) (Pierce). Equal amounts of protein from B103 and B103-695 lysates were combined and processed by filter-aided sample preparation (FASP) as described by Wisniewski and Mann [217]. Proteins were digested overnight at 37°C with Trypsin (Promega) at 1:50 (w/w, enzyme:protein). Peptides were desalted using C18 SPE columns and dried in a vacuum concentrator. Dried peptide samples were resuspended and fractionated by strong cation exchange (SCX).

LC-MS/MS and Data Analysis

Peptide fractions were analyzed using a hybrid linear ion trap-Orbitrap XL (LTQ-Orbitrap XL, Thermo Scientific) using a 90 minute gradient. Raw data files were searched against the current *Rattus norvegicus* UniprotKB protein sequence database using MaxQuant, a quantitative proteomics software package [218]. Significance A, an outlier test, was carried out using Perseus software to determine the statistical significance of protein expression using a false discovery rate (FDR)-based approach developed by Benjamini and Hochberg [219]. Functional and pathway analysis of statistically significant proteins were performed using Ingenuity Pathway Analysis (IPA).

Cell Synchronization and Treatments

Cells were grown in DMEM/F12 media supplemented with 10% FBS and Penn-Strep-Glutamine. Cells were washed with PBS before being grown in serum-free DMEM/F12 media, or DMEM/F12 with 10% FBS and Aphidicolin (5µg/ml) to synchronize cells at either the G_0/G1 or G1/S transition. After 48 hours in serum-free media, or 12 hours in Aphidicolin-containing media, cells were washed with PBS, and media was replaced with DMEM/F12 media containing 10% FBS and either Roscovitine, Nocodazole, or Taxol using the concentrations described above. Cells were collected at various time points following synchronization and lysed in RIPA buffer for western blot analysis. Western blots were probed with a phospho-tyrosine (100) antibody (mouse monoclonal, Cell Signaling #9411), which binds phosphorylated tyrosine independent of surrounding amino acid sequence, PathScan Multiplex Western Cocktail I (Cell Signaling #5301), which binds phosphorylated p90RSK (Ser380), Akt (Ser473), p44/42 MAPK (ERK1/2) (Thr202/Tyr204), and phospho-S6 ribosomal protein, and an antibody against phosphorylated GSK3α/β (Ser21/Ser9) (Cell Signaling #9331).

Results and Discussion

The results for the global proteomic analysis of B103 and B103-695 cells have been previously published and can be found in Appendix A. The article has been reproduced with the consent of the publisher (Appendix C).

Global Proteomic Analysis of B103 and B103-695: Additional Experiments

Some additional experiments were performed to further validate observations from the proteomic analysis of B103 and B103-695 cells. Increased expression of Ras was shown in B103-695 cells and validated by western blot. Ras is a small GTPase involved in regulating cell growth and differentiation. It is well established that Ras activates the MAPK signaling pathway, and while Ras-MAPK signaling is known to have a role in cancer, increasing evidence suggests that it may also be involved in neurodegenerative disease [110, 220, 221]. We also observed increased levels of the active phosphorylated form of MAPK (ERK1/2), while non-phosphorylated ERK levels were not affected. To determine potential mediators of the observed ERK phosphorylation, and to assess potential crosstalk between protein kinase A (PKA), which can also activate ERK, and MAPK signaling, we investigated the impact of both siRNA-mediated knockdown and chemical inhibition of PKA on levels of ERK phosphorylation. KT5720 is an inhibitor of PKA activity through competitive inhibition of the ATP binding site on PKA catalytic subunit [222]. The siRNA-mediated knockdown of PKA reduced PKA levels (Figure 4a) while treatment with the KT5720 inhibitor did not appear to affect levels of PKA (Figure 4b). Additionally, PKA knockdown using siRNA was more effective in B103 cells than in B103-695 cells; which may be caused by the reduced transfection efficiency of B103-695 cells. Inhibition of PKA appeared to have no effect on levels of ERK phosphorylation, demonstrating that ERK is activated by an alternative pathway. These finding suggest that APP expression specifically affects ERK activation but does not impact its expression (Figure 4).

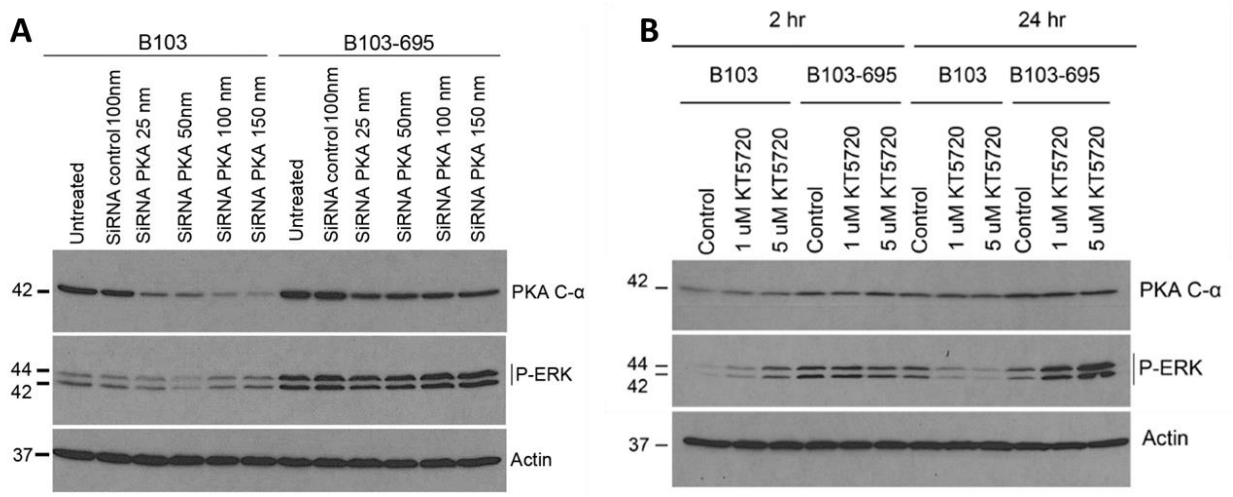

Figure 4. PKA Knockdown in B103 and B103-695 cells. To determine whether ERK phosphorylation was mediated by PKA, a known activator of ERK, PKA was knocked down using siRNA **(A)** or KT5720 chemical inhibition **(B)** in B103 and B103-695 cells. While PKA levels were decreased, there was not a significant reduction in ERK phosphorylation, suggesting ERK is being activated by an alternative pathway.

Based on our results from proteomic analysis of B103 and B103-695 cells, we were also interested in further investigating levels of Ras and γ-synuclein expression in human tissue samples from non-AD, mild cognitive impairment (MCI) and AD brains. MCI involves deficits in memory and is associated with increased risk of developing more advanced forms of dementia and AD. Increased levels of both Ras and γ-synuclein were observed in MCI and AD compared with non-AD individuals (Figure 5), which is in accordance with our B103 proteome datasets. Ras showed a moderate increase in MCI and a statistically significant increase in late-AD (Figure 5a). Levels of γ-synuclein were the highest in MCI, showing a statistically significant increase compared to non-AD samples, but showed less of an increase in late-AD compared with non-AD (Figure 5b). Increased γ-synuclein expression during MCI may indicate an early molecular change during neurodegeneration. Increased expression of Ras in MCI and further increase in late AD provides further evidence that Ras likely has a role in AD progression. Increased Ras activity leads to increased MAPK activity, and it is possible that a Ras-mediated signaling cascade may be involved in aberrant cell cycle re-entry and neurodegeneration associated with AD pathology and progression.

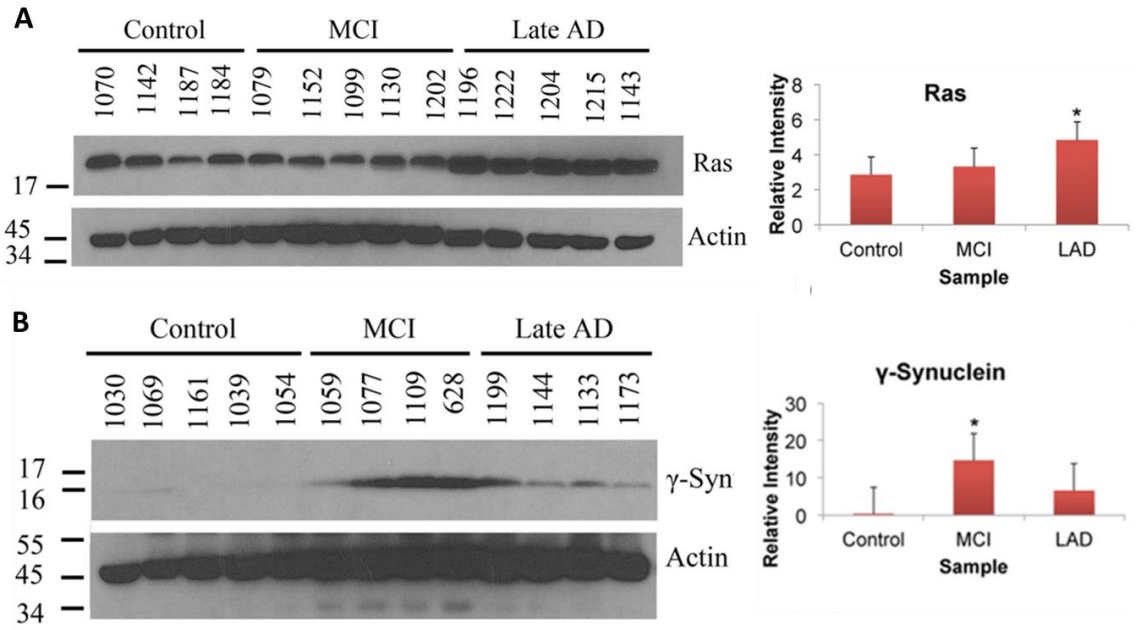

Figure 5. Increased expression of Ras and γ-Synuclein in MCI and AD human brain tissue. (A) Ras was increased in MCI and significantly increased in late-AD (LAD) compared to control tissue. **(B)** γ-synuclein showed a significant increase in MCI and only a moderate increase in LAD compared with control tissue. *p-value ≤ 0.05.

Cell-Cycle Mediated Protein Expression Changes

After completing the SILAC-based global-scale analysis of B103 and B103-695 cells, a similar global-scale analysis was performed to determine cell cycle-mediated changes in protein expression. A preliminary experiment was performed using heavy and light SILAC labeled B103-695 cells. Heavy labeled B103-695 cells were treated with cell cycle inhibitors Roscovitine or Taxol, and changes in protein expression should be attributed to cell cycle inhibition at the G1/S or G2/M transitions, respectively. Proteomic analysis of Roscovitine treated B103-695 cells identified a total of 2265 proteins, of which 1588 proteins had minimum of 2 unique peptides. Taxol treated B103-695 cells identified a total of 2622 proteins, with 1856 proteins having a minimum of 2 unique peptides. Significant protein expression changes were determined using the Benjamini-Hochberg FDR-based Significance A test in Perseus, and only proteins with significant changes in at least 2 out of 3 biological replicates were considered significant. Roscovitine treatment resulted in 43 significantly altered proteins and Taxol treatment resulted in 38 significantly altered proteins.

Roscovitine treatment of B103-695 cells identified several differentially expressed proteins involved in cell growth and proliferation, DNA replication, and cell death and survival. As Roscovitine prevents progression through the G1/S, cells are arrested in the G1 phase of the cell cycle during which biosynthesis takes place in preparation for DNA synthesis during S phase. Therefore, identifying significant changes in proteins involved in gene expression, cell cycle and proliferation is unsurprising as cells are preparing for S phase. Bioinformatic analysis of significantly altered proteins also predicted inhibition of cell cycle progression (z-score: -2.752) based on the decreased expression of several proteins (Figure 6), further confirming the inhibitory effect of Roscovitine on the cell cycle.

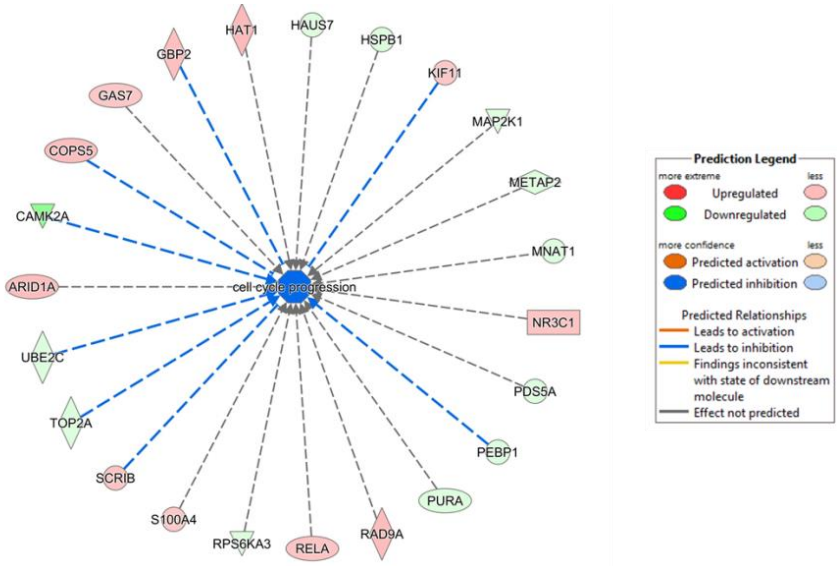

Figure 6. Ingenuity Pathway Analysis predicted inhibition of cell cycle progression in Roscovitine treated B103-695 cells. Based on significant expression changes of proteins involved in the cell cycle, cell cycle progression was predicted to be inhibited, which is expected given that cells were treated with the cell cycle inhibitor Roscovitine.

Bioinformatic analysis of Taxol treated B103-695 cells showed changes in expression of proteins involved in cellular assembly and organization, cellular function and maintenance, and cell morphology. Taxol stabilizes microtubules, preventing progression through the G2/M transition and arresting cells in the G2 phase of the cell cycle, during which microtubule biosynthesis takes place as the cell prepares for mitosis. The enrichment of molecular and cellular functions involved in cellular assembly, organization, and morphology are consistent with expectations based on the microtubule stabilizing function of Taxol.

Cell Synchronization and Preliminary Phosphorylation Analysis

One of the goals of this project was to investigate APP695-mediated changes in phosphorylation by comparing B103 and B103-695 cells. Phosphorylation is a dynamic post-translational modification involved in regulating cell cycle progression, and western blot analysis was performed to evaluate which cell cycle inhibitor, Taxol, Roscovitine, or Nocodazole, had the greatest impact on levels of phosphorylation. B103-695 cells were synchronized by serum-starvation or aphidicolin block, commonly used methods to synchronize cell populations. Aphidicolin is an antibiotic and a selective-inhibitor of DNA polymerase alpha and delta, preventing cells from entering S phase [223]. Serum starvation forces cells to enter G_0 by eliminating growth factors from media. Removal of Aphidicolin and replenishment with regular growth medium or addition of serum to the serum-starved cells enables re-entry into the cell cycle. Following synchronization, B103-695 cells were treated with cell cycle inhibitors Nocodazole, Taxol, or Roscovitine, and collected at several time points following re-entry into the cell cycle and levels of phosphorylation were examined using phospho-specific antibodies.

Serum-starved cells were collected 5 minutes, 15 minutes, 30 minutes, 1 hour, 2 hours, and 4 hours following the addition of serum-containing media. Western blot analysis showed increased phosphorylation in all treatments from 5 minutes to 30 minutes, followed by decreased phosphorylation after 1 hour. Taxol-treated B103-695 cells showed the most significant increase in phosphorylation compared with cells treated with regular media, Nocodazole, or Roscovitine (Figure 7). Following serum-starvation, cells are arrested in G_0, and the addition of serum will activation a number of pathways as cells re-enter G1, resulting in increased phosphorylation. While levels of phosphorylation increase as cells re-enter the cell cycle at G1, we are more interested in phosphorylation events that occur during the G2/M transition and during mitosis.

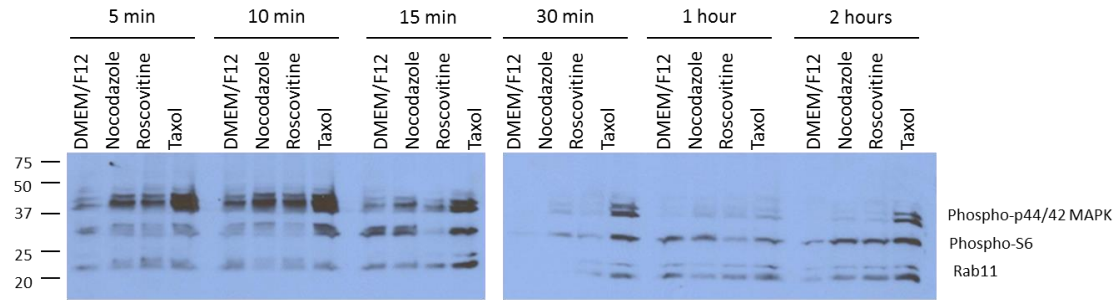

Figure 7. Levels of phosphorylation in B103-695 cells following serum-starvation and inhibitor treatment. B103-695 cells were serum-starved for 48 hours to synchronize cells in G_0, after which cells were treated with either DMEM/F12+10% FBS alone, or DMEM/F12+10% FBS supplemented with 100ng/ml Taxol or 100ng/ml Nocodazole. Western blot analysis using PathScan Multiplex Western Cocktail I (CellSignaling) showed increased phosphorylation in all treatments from 5-30minutes, and decreased after 1 hour. Cells treated with Taxol showed the greatest increase in phosphorylation.

To investigate phosphorylation changes that occur during S and G2 phases of the cell cycles, cells were synchronized using aphidicolin, which arrests cells at the G1/S transition, and cells progress through the S-phase and G2-phase of the cell cycle after Aphidicolin is removed. Following synchronization with Aphidicolin, cells were collected at 0 minutes (before inhibitor treatment), and 30 minutes, 1 hour, 2 hours, and 4 hours after Taxol or Nocodazole treatment. Changes in phosphorylation were assessed by western blot using a phospho-tyrosine (100) antibody and PathScan Multiplex Western Cocktail I. Taxol again showed the most significant increase in phosphorylation from 30 minutes to 1 hour following Aphidicolin release, as cells are replicating DNA during the S phase (Figure 8). Phosphorylation of Akt, a protein kinase essential in controlling survival and apoptosis, is not detected after 12 hour aphidicolin treatment, while phosphorylation of Akt at Ser473 (p-Akt) is detected 30 minutes following aphidicolin release. Phosphorylation of Akt at Ser473 is activating and has been proposed to be regulated in a cell cycle dependent manner [224]. In Taxol and Nocodazole treated B103-695 cells the levels of p-Akt appear to continue to increase until 1 hour, and decrease by 2 hours. In B103-695 cells treated with regular media, p-Akt levels decrease after 30 minutes. Akt is involved in cell cycle regulation by preventing GSK-3β-mediated phosphorylation and degradation of cyclin D1 [225]. Cyclin D1 is synthesized and accumulates during G1 and degraded as the cells enters S phase.

GSK3α is a serine/threonine kinase involved in the phosphorylation of tau protein, regulating the binding of tau to microtubules, as well as its degradation and aggregation [226]. GSK3α has also been shown to regulate the production of amyloid β in AD [227]. Akt-mediated phosphorylation of GSK3α at Ser21 and GSK3β at Ser9 inhibit GSK3 activity [228, 229]. There appears to be in an increase in pGSK3α/β (Ser21/9) that coincides with the observed increase in p-Akt. There was minimal detection of pGSKα/β (Ser21/9) in B103-695 cells following 24 hours of aphidicolin block. Following synchronization with Aphidicolin, activated p-Akt (Ser473) and inhibited pGSK3α/β (Ser21/9) are not detected, however levels of p-Akt (Ser473) and pGSK3α/β (Ser21/9) appear to increase until 1 hour as cells begin progress through the S phase, and are reduced by 2 hours. Taxol treated cells appear to undergo the greatest increase in pAkt (Ser473) and pGSK3α/β (Ser21/9) at 1 hour, followed by Nocodazole treatment, while untreated cells show the greatest pAkt (Ser473 levels) after 30 minutes following Aphidicolin release, suggesting delayed progression through S phase with Taxol and Nocodazole treatment.

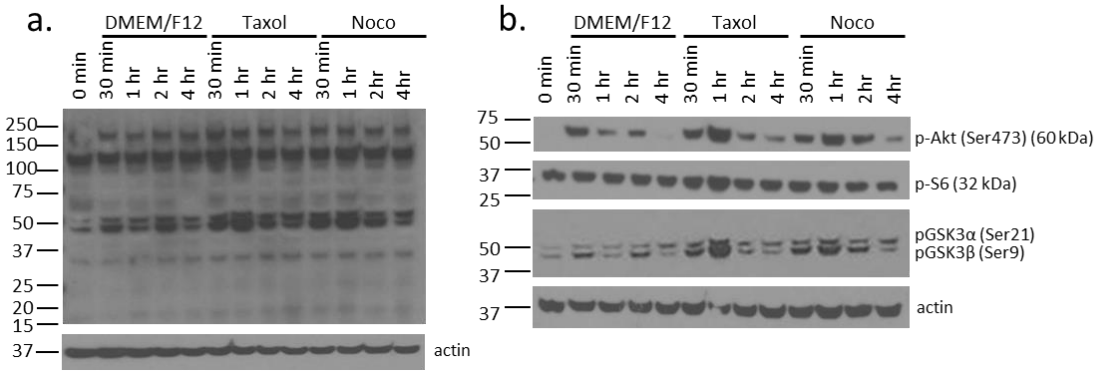

Figure 8. Levels of phosphorylation in B103-695 cells following Aphidicolin block and inhibitor treatment. B103-695 cells were treated with aphidicolin (5μg/ml) for 24 hours to synchronize cells in the S phase, after which cells were treated with either DMEM/F12, 100ng/ml Taxol, or 100ng/ml Nocodazole. **(A)** Global levels of phosphorylated tyrosine were observed used was phospho-Tyrosine(100). **(B)** Primary antibodies PathScan Multiplex Western Cocktail I and phospho-GSK3α/β(Ser21/Ser9) revealed changes in phosphorylation following cell synchronization and release. Actin was used to determine protein loading.

Inflammation Mediated Protein Expression Changes

Lipopolysaccharide is known to promote the inflammatory response in immune cells, and was used to investigate inflammation and neurotoxicity mediated protein expression changes in

APP695 expressing B103-695 cells. A total of 1947 unique proteins were identified, and 1808 proteins were identified with at least 2 unique peptides. Using the Benjamini-Hochberg FDR-based Significance A test, 32 proteins had significant expression changes after LPS treatment and were used for bioinformatics analysis. Based on the observed significant protein expression changes, Ingenuity Pathway Analysis (IPA) predicted activation of interleukin-5 (IL-5) and inhibition of interleukin-10 receptor alpha (IL10RA). Predicted activation of IL-5 (z-score 2.449) was based on increased expression of guanylate binding protein 2 (GBP2), ERO1-like protein (ERO1), cysteine-rich protein 1 (CRIP1), annexin A2 (ANXA2), aldolase C (ALDOC), and prolyl 4-hydroxylase, alpha polypeptide (P4HA1) following LPS treatment (Figure 7a) [230]. IL-5 is a pro-inflammatory cytokine previously shown to be upregulated in immune cells in response to LPS treatment [231]. IL10RA is a receptor for interleukin-10 (IL-10), an anti-inflammatory cytokine, inhibiting the synthesis of pro-inflammatory cytokines. Predicted inhibition of IL10RA (z-score -2.000) was based on the increased expression of GBP2, ERO1, guanine deaminase (GDA), and cysteine and glycine rich protein 2 (CRSP2). Inhibition of IL10RA would prevent the activation of IL-10, no longer inhibiting pro-inflammatory cytokine synthesis, promoting the inflammatory response of immune cells. These findings are consistent with the pro-inflammatory effect of LPS on immune cells as a number of the observed protein expression changes in neuroblastoma cells further indicate the pro-inflammatory response. The significant proteins identified as a result of LPS treatment appear to be consistent with the literature, and pathway analysis did not provide any novel insight into inflammation-mediated protein expression changes APP-695 cells.

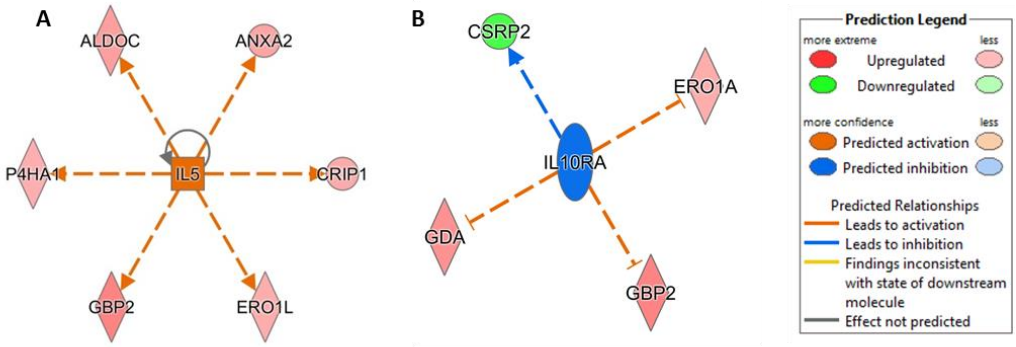

Figure 9. Ingenuity Pathway Analysis of LPS treated B103-695 cells predicts changes in inflammatory proteins. IPA predicted activation of pro-inflammatory cytokine IL-5 **(A)** and inhibition of anti-inflammatory cytokine receptor IL-10RA **(B)** based on changes in protein expression.

Chapter 3: Phosphoproteomic Analysis of a Cell Model of Alzheimer's Disease and Validation Using Cultured Primary Neurons and Human Brain Tissue

Abstract

The Alzheimer's disease (AD) brain is characterized by the presence of two pathogenic lesions: amyloid plaques and neurofibrillary tangles (NFTs). Amyloid plaques are primarily composed of the amyloid-beta (Aβ) peptide, which is generated following cleavage of amyloid precursor protein (APP). Production, oligomerization and deposition of Aβ are thought to be the initiating pathogenic events in AD, however the processes leading up to these events are largely unknown. There has been significant interest in the physiological function of APP and how this function is altered under disease state. Our lab has previously found that under pathogenic conditions, APP undergoes a specific phosphorylation that is thought to induce significant C-terminal conformational change that allows APP to be more readily cleaved by β-secretase. Furthermore, we and others have found that aberrant mitotic events in compromised neurons can initiate this pathogenic modification.

To better understand the molecular events driving mitotic initiation and the subsequent pathogenic alteration of APP, we utilized a B103 rat neuroblastoma cellular model. B103 cells do not express detectable levels of APP or APP-like proteins APLP1 or APLP2, and B103-695 cells express the neuronal APP-695 isoform. Mass spectrometry was used for the identification of phosphopeptides from a complex mixture, including site localization. Identifying changes in phosphorylation can indicate potentially altered pathways as well as overrepresented consensus motifs as an indication of changes in kinase activity. B103 and B103-695 cells were grown in light or heavy SILAC media, respectively, after which the lysates were combined and FASP digested using Trypsin/LysC, fractionated by strong cation exchange and enriched for phosphopeptides using PolyMAC before reverse-phase (RP)-HPLC separation and analysis on a Q-Exactive Plus. A total of 2478 phosphopeptides were identified among 3 biological

replicates. Increased phosphorylation of Histone H4 at Ser47, and increased expression of PCTAIRE-2 (Cdk17) and PCTAIRE-3 (Cdk18) were identified in B103-695 cells compared with B103 cells, and these changes were further validated in PS/APP mice, Aβ-treated primary neurons, and human brain tissue from individuals affected by mild cognitive impairment (MCI) and AD. The comprehensive phosphoproteomic dataset provides insight into pathways that may be affected by APP-695 expression based on changes in phosphorylation as well as consensus motif analysis, providing a foundation for future mechanistic studies.

Introduction

Alzheimer's disease (AD) is the most prevalent form of dementia affecting the elderly, and is associated with decline in higher cognitive function as exhibited through deficits in memory, executive function and complex attention. One of the pathological hallmarks of AD is the presence of extracellular amyloid plaques, composed of aggregated Aβ peptide that accumulates in the brain years before the onset of symptoms associated with the disease [232]. Aβ is derived from the sequential cleavage of APP, a type 1 transmembrane protein [26]. Under pathogenic conditions, APP undergoes proteolytic cleavage by beta-site APP cleaving enzyme (BACE or β-secretase) and γ-secretase, resulting in the production of Aβ and the shedding of the sAPPβ ectodomain [233]. Alternatively, APP can be cleaved by α-secretase, liberating sAPPα and precluding the generation of Aβ by cleaving within the Aβ domain [233]. These cleavages lead to generation of additional fragments such as the intracellular domain of APP (AICD). Since APP expression leads to generation of not only full length APP but also several fragments with various functions, it is difficult to determine the precise cellular function of APP and how its metabolites differentially contribute to AD.

While the genetic factors that contribute to familial AD (FAD) have been well described, relatively little is known about the precise molecular processes that lead to sporadic AD. In both sporadic and familial AD, Aβ accumulation precedes the formation of neurofibrillary tangles (NFTs),

highlighting a key role for Aβ in disease pathogenesis [234]. Furthermore, another prominent feature present in most AD cases is neuroinflammation. In the early stages of AD, Aβ fibrils and oligomers have been shown to induce microgliosis [235, 236]. Interestingly, this immune response has been shown to induce abnormal cell cycle events in compromised neurons of the AD brain [104, 107, 237]. Earlier studies from our lab have demonstrated that mouse models of AD, expressing APP alone or together with presenilin 1 (PS1), show aberrant expression of cell cycle regulatory proteins with a concomitant increase in phosphorylation of APP at Thr668 [113]. Phosphorylation of APP at this residue is associated with enhanced proteolytic processing, and affects APP trafficking [115] and protein-protein interactions [238]. *In vitro* studies have shown that Aβ induces aberrant cell cycle activation and neuronal apoptosis [107]. It is possible that chronic Aβ-induced inflammation in the brain leads to aberrant neuronal cell cycle initiation and cell cycle dependent modifications of APP, altering its proteolysis and leading to increased production of Aβ, thereby promoting the vicious cycle.

Our published studies showing that APP promotes expression of proliferation-associated proteins support the notion that APP has a role in cell cycle regulation [239]. These studies were carried out with B103 rat neuroblastoma cells that are APP-null or express the APP695 isoform (B103-695) using SILAC-based proteomics. These findings indicate that APP expression is able to induce signaling cascades that may play a role in the cell cycle mediated neuronal degeneration observed in AD. To determine the global changes in protein phosphorylation upon APP expression we performed a phosphoproteomic analysis of SILAC-labeled B103 and B103-APP cells. To determine the global changes in protein phosphorylation upon APP expression, we performed phosphoproteome analysis of SILAC-labeled B103 and B103-695 cells.

Mass spectrometry can be used for the identification of phosphopeptides from a complex mixture including site localization and relative quantification. Phosphoproteomics involves the enrichment of phosphopeptides to increase their identification and sequence information, which can be

useful for bioinformatic analysis of affected pathways. Additionally, phosphoproteomics can further identify potential changes in kinase activity by analysis of overrepresented phosphorylated consensus motifs [200]. Several phosphoproteomic enrichment techniques have been developed, including immobilized-metal affinity chromatography (IMAC), which exploits the negatively charged phosphate groups affinity for positively charged metal ions, such as Fe^{3+} [188-190], Ga^{3+} [191], or Ti^{4+} [192]. Metal oxide affinity chromatography (MOAC), most commonly using TiO_2 particles [193, 194], and polymer-based metal ion affinity capture (PolyMAC) enrichment [195] have also be used for phosphopeptide enrichment. To date, there are only a few phosphoproteomic studies related to Alzheimer's disease. In the present study, we used a titanium-based nanopolymer phosphopeptide enrichment in combination with strong cation exchange (SCX) for the enrichment of phosphopeptides, which were analyzed on a Q-Exactive Plus. Phosphoproteomic analysis identified over 2000 phosphopeptides in B103 and B103-695 cells. Compared with B103 cells, B103-695 cells showed increased phosphorylation of Histone H4 at Ser47, and increased expression of PCTAIRE-2 (Cdk17) and PCTAIRE-3 (Cdk18). Increased levels of pS47-Histone H4, PCTAIRE-2, and PCTAIRE-3 were further validated in PS/APP mice, Aβ-treated primary neurons, and human brain tissue from individuals affected by mild cognitive impairment (MCI) and AD.

Materials and Methods

<u>B103 and B103-695 Phosphoproteomic Analysis</u>

Cell Culture and SILAC Labeling

B103 and B103-695 cells were grown in DMEM:F12 SILAC media supplemented 10% dialyzed FBS, Penn-Strep-Glutamine, and either unlabeled L-arginine and L-lysine for B103 or heavy labelled $^{13}C_6$-L-lysine 2HCl and $^{13}C_6$–$^{15}N_4$-arginine HCl (Cambridge Isotopes) for B103-695 cells. Cells were grown for 5 doublings to achieve >99% incorporation of labeled amino acids before being collected.

Sample Preparation and Phosphopeptide Enrichment

Cells were lysed in 100mM Tris-HCl (pH 7.6), 4% SDS, 100mM DTT and Halt protease cocktail inhibitor (Pierce) and incubated at 95˚C for 5 minutes, followed by sonication at 20% amplitude. Protein was quantified using the Pierce 660 assay supplemented with ionic-detergent compatibility reagent (IDCR) (Pierce). Experiments were performed in triplicate. A total of 1.2mg B103 and 1.2mg B103-695 lysate were combined and processed by filter-aided sample preparation (FASP) [217], followed by digestion with Trypsin/Lys-C (Promega) 1:50 (w:w; protease:protein) overnight at 37˚C. Peptides were desalted using C18 SPE columns (Thermo) with a Supelco vacuum manifold and were then dried and resuspended in mobile phase A prior to fractionation. Peptides were fractionated on a Dionex U3000 HPLC system with a 200 x 4.6mm i.d. strong cation-exchange (SCX) column packed with 5 µm 200Å polySULFOETHYL A-SCX material (PolyLC Inc.). One minute fractions were collected using a 45 minute gradient (15-200mM ammonium formate, pH 3-6.5, 25% acetonitrile) at a flow rate of 1ml/minute.

Peptide fractions enriched for phosphopeptides using PolyMAC (Expedeon), a nanopolymer titanium-based enrichment. Following PolyMAC enrichment the samples were dried and resuspended in 0.25% formic acid for LC-MS/MS analysis.

LC-MS/MS

Peptides were analyzed on a Q-Exactive Plus (Thermo Fisher Scientific) following fractionation with a 75µm x 50cm reversed-phase UPLC column (Dionex) packed with 5µm 300Å C18 material using a 90 minute gradient on an EASY-nLC 1000 system (Thermo Fisher Scientific). Full MS survey scans used a resolving power of 60,000, selecting the top ten most abundant ions for MS/MS fragmentation and analysis.

Database Searching and Consensus Motif Analysis

Raw data files were processed in MaxQuant (version 1.5.0.30, http://www.maxquant.org) and searched against the UniprotKB database containing *Rattus norvegicus* protein sequences. The search

parameters included a constant modification of cysteine by carbamidomethylation and variable modifications methionine oxidation and phosphorylation of serine, threonine, and tyrosine. Additional parameters include multiplicity set to 2, with heavy lysine-6 and arginine-10.

Statistical analysis was carried out using Perseus software (version 1.5.0.31, http://141.61.102.17/perseus_doku). Statistically significant changes in phosphopeptide abundance were determined using Significance A, an outlier test with a threshold p-value of 0.05. Only phosphopeptides identified in at least 2 biological replicates with a minimum ratio count of 2 were used for statistical analyses. Phosphopeptide ratios were normalized against total protein ratios from our previous SILAC-based proteomic analysis of B103 and B103-695 cells. Both non-normalized and normalized median phosphopeptide ratios were analyzed to account for potential changes in phosphorylation of proteins that were not identified in our initial proteomic analysis.

Raw data files were searched again with the parameters described above with a multiplicity of 1 for only light lysine and arginine, or heavy lysine-6 and arginine-10, to generate separate light and heavy datasets. Results were analyzed with Scaffold PTM (version 2.1.3) to determine overrepresented kinase motifs surrounding phosphorylation sites, using the method developed by Gygi and Schwartz [200], as well as potential enzyme recognition sites.

Transgenic Mouse Tissue

Heterozygous PDGF-hAPP (V717F) mice (Swiss-Webster x C57BL/6) were crossed with PDGF-hPS1 (M146L) heterozygotes (Swiss-Webster x C57BL/6) to generate $APP^{+/-}/PS1^{+/-}$ genotyped mice. In this study we used these transgenic mice with age-matched non-transgenic (Ntg) mice to serve as control. Mice were anesthetized at 9 months with pentobarbital (10 mg/kg body weight) and perfused with a saline solution. The brains were dissected out and half of each brain was fixed with 4% paraformaldehyde. The brains were processed prior to immunohistochemical analysis as previously

described [240]. Brain sections were prepared using a freezing stage microtome and then stored at 4°C in phosphate buffered saline containing 0.02% sodium azide.

Oligomeric Aβ42 Preparation

1mg of monomeric Aβ42 was dissolved in 1ml trifluoroacetic acid (TFA) and lyophilized in 100µg aliquots. Lyophilized Aβ42 was solubilized in sterile DMSO to a concentration of 5mM and then diluted to 100µM in DMEM media and left at 4°C overnight.

B103 and B103-695 Cell Culture and Aβ Treatment

B103 and B103-695 cells were grown in DMEM:F12 supplemented with 10% FBS and Penn-Strep-Glutamine. B103 and B103-695 cells were plated on 8-chamber slides treated with poly-L-lysine (PLL) (Life Technologies) at a density of approximately $5x10^4$ cells per well. After 24 hours, cells were treated with either 5µM Aβ42 or DMSO, which served as a vehicle control.

Primary Neuron Culture and Aβ Treatment

Primary neurons were cultured in Neurobasal Medium supplemented with 2X B-27, 1% Penicillin/Streptomycin and 2mM glutamine. Neurons were cultured in 8-chamber glass slides and 100mm cell culture dishes that were coated with PLL. Briefly, E18 pregnant rats were euthanized by pentobarbital injection and feti excised and placed in isotonic solution. The meninges were then removed and cortices separated. Cortices were titrated into a single cell suspension in isotonic buffer and spun down at 1500 rpm for 5 mins at 4˚C. The neuronal pellet was resuspended in 2ml Neurobasal media and filtered through a cell strainer. 8 chamber slides were plated with ~$5X10^4$ neurons per well and 100 mm dishes were plated with ~$6X10^6$ neurons. Neurons were fed every third day and grown for 5 days prior to treatment. Neurons grown on 100mm dishes were treated with either DMSO vehicle or 5µM Aβ42 and harvested after 24 hrs. Neurons grown on 8-chamber were treated with either DMSO vehicle or incremental concentrations of Aβ42 ranging from 1µM to 5µM.

Nuclear Fractionation

Cells were collected and pelleted by centrifugation at 500 x g for 15 minutes at 4˚C. Cells were resuspended in 1ml of 10mM Tris-HCl (pH 7.4), 1mM EDTA, 200mM sucrose, and Halt protease inhibitor cocktail (Pierce) and subjected to gentle dounce homogenization. Nuclei and cell debris were pelleted by centrifugation at 900 x g for 10 minutes at 4˚C. The nuclei containing pellet was lysed in 100mM Tris-HCl (pH 7.6), 4% SDS, 100mM DTT and Halt Protease Cocktail Inhibitor (Pierce) as described above. Protein was quantified using the Pierce 660 assay supplemented with ionic-detergent compatibility reagent (Pierce) before preparing 1µg/µl samples in Laemmli Buffer for Western blot analysis.

Human Brain Tissue

Human brain tissue was obtained from Dr. David Cribbs at the University of California Irvine Alzheimer's Disease Research Center. Brain samples were de-identified and categorized based on post-mortem Braak stage and pre-mortem clinical MMSE score. Additional information on this brain material is detailed in Table 1. Samples were categorized based on determined disease stage; Non-AD (NAD), Mild Cognitive Impaired (MCI) or Late-AD (LAD). Tissue was homogenized in 100mM Tris-HCl (pH 7.6) containing 4% SDS, 100mM DTT and Halt protease inhibitor cocktail. Homogenates were briefly sonicated and centrifuged for 15 mins at 14,000 xg. The soluble supernatant fraction was then separated from the insoluble pellet for sample preparation. Brain lysates were analyzed by western blot and disease state confirmed using 6E10 (detecting FL-APP and Aβ) and PHF-1 antibodies (Figure 14).

Immunostaining

For immunostaining analysis of mouse brain sections, sections were mounted onto superfrost slides, air-dried and rehydrated with TBS for 5 minutes. For antigen retrieval, sections were incubated in 10mM citrate buffer, pH 6.0 for 10 mins at 95˚C and cooled to room temperature. After washing with PBS, sections were blocked with 10% normal goat serum (NGS) in TBST with 0.02% sodium azide (NaAz) for 2 hours at room temperature. Sections were then incubated with APP (6E10) primary antibody

(mouse monoclonal 1:500) and either PCTAIRE-2 (1:50) or PCTAIRE-3 (1:50) primary antibody diluted in 1% BSA/TBST at 4˚C in a humidified chamber overnight. Next, sections were washed and incubated for 2 hrs at room temperature with goat anti-mouse IgG Alexa Fluor 488 (1:1000) and goat anti-rabbit IgG Alexa Fluor 594 (1:4000) diluted in blocking buffer. After washing, cells were incubated in 1µg/ml Hoechst 33342 DNA dye in PBS for 3 mins. After thorough washing, the slides were coverslipped with Fluoro-Gel mounting media and analyzed with a Zeiss Fluorescence Axio Imager using AxioVision Rel 4.8 software.

For immunostaining analysis of cultured cells, cells (either B103, B103-695 or primary neurons) were fixed with 4% paraformaldehyde for 10 mins at room temperature and washed with PBS. After, cells were blocked in blocking buffer for 1 hr. B103 and B103-695 cells were then incubated overnight at 4°C with α-tubulin (mouse monoclonal, 1:1000) and either PCTAIRE-2 (1:50) or PCTAIRE-3 (1:50) primary antibodies diluted in 1%BSA/TBST with NaAz. Neurons were incubated with Tau 1 (mouse monoclonal, 1:500) and either PCTAIRE-2 (1:50) or PCTAIRE-3 (1:50) primary antibodies. After incubation, cells were washed and incubated in goat anti-mouse IgG Alexa Fluor 488 (1:1000) and goat anti-rabbit IgG Alexa Fluor 594 (1:4000) diluted in blocking buffer. After brief washing, cells were incubated for 3 mins with 1µg/ml Hoechst 33342 DNA dye. After thorough wash, slides were mounted using Fluoro-gel and visualized as mentioned previously.

Western Blotting

Proteins were selected for validation by western blot analysis based on significance as well as function. Proteins were separated on an AnyKD SDS-PAGE gel (BioRad) and transferred to a PVDF membrane using the Trans Turboblot system (BioRad). Membranes were blocked in 5% non-fat milk in TBS for 1 hour at room temperature. Primary antibodies specific for phospho-Serine47-Histone H4 (Abcam, rabbit polyclonal), Histone H4 (Cell Signaling, mouse monoclonal), PCTAIRE-2 and PCTAIRE-3 (Santa Cruz, rabbit polyclonal), Actin (Sigma Aldrich, mouse monoclonal), APP (6E10 antibody, Covance,

mouse monoclonal), anti-Tau1 (Millipore), anti-PHF1 (phospho Ser396/Ser404-Tau, kindly provided by collaborator Dr. Peter Davies, Albert Einstein College of Medicine) and GAPDH (Cell Signaling, rabbit monoclonal) were diluted in 5% BSA-PBS, with 0.05% NaN_3 and incubated overnight at 4˚C. Membranes were then incubated with appropriate corresponding secondary antibodies, donkey anti-rabbit HRP-conjugated (Cell Signaling) or goat anti-mouse HRP-conjugated (Cell Signaling) for 1.5 hours at room temperature. All blots were developed with Pico Chemiluminescence reagents (Pierce), with the exception of pS47-Histone H4 which was developed using Femto Chemiluminescence reagents (Pierce), using an Amersham Imager 600RGB (GE Healthcare).

Table 1. AD, MCI, and non-AD Human Brain Tissue Information.

Case No.	Age	Sex	Braak Stage	PMI	MMSE	Diagnosis
34	91	F	3	3.33	30	NAD
29	83	F	4	5.25	30	NAD
41	91	F	4	4.82	29	NAD
40	91	F	2	3.8	29	NAD
24	86	F	3	2.92	22	MCI
17	86	F	3	6.17	30	MCI
9	87	M	5	6.17	24	MCI
35	94	M	1	3.87	27	MCI
45	95	F	5	5.30	24	MCI
12	82	F	6	5.92	17	LAD
39	90	M	6	4.17	14	LAD
37	88	F	5	4.50	10	LAD
10	82	F	6	4.58	-5	LAD
40	96	F	6	4.50	20	LAD

Results

<u>B103 and B103-695 Phosphoproteome Comparison</u>

A total of 2478 phosphopeptides were identified across 3 biological replicates in B103 and B103-695 cells; 1082 were quantified in a minimum of 2 biological replicates with a minimum ratio count of 2. Of the 1082 phosphorylation sites confidently identified and quantified, 712 of them corresponded to proteins previously quantified by SILAC in our global scale proteomic analysis of B103 and B103-695 cells [239]. When possible, phosphopeptide ratios were normalized against corresponding protein ratios

previously determined in the B103 and B103-695 proteomic analysis. Perseus was used to identify significant changes in phosphopeptide expression across biological replicates using Significance A, a statistical outlier test, with a p-value threshold of 0.05. Significant changes were identified in 92 phosphosites corresponding to 71 different proteins when using non-normalized ratios, and 50 phosphosites corresponding to 46 proteins when using normalized ratios. Select differentially phosphorylated phosphosites, both normalized and non-normalized, are listed in Table 2. Bioinformatic analysis of statistically significant phosphosites was performed using Ingenuity Pathway Analysis (IPA) which identified several proteins associated with neurological disease and psychological disorders as well as molecular and cellular functions including cell morphology, cellular assembly and organization, function and maintenance, and growth and proliferation.

Table 2. Selected phosphoproteins of interest with significant changes in phosphorylation in APP-695 expressing B103-695 cells compared with APP-null B103 cells. Median phosphopeptide ratios were normalized against corresponding protein ratios when possible.

Protein Name	Gene Name	Protein	Amino Acid	Pos.	Median Phospho Ratio	Variance	Median Protein Ratio	Normalized Median
Heat shock protein beta-1	Hspb1	P42930	S	86	2.90	0.35	0.64	4.50
Heat shock protein beta-1	Hspb1	P42930	S	115	2.04	0.08	0.64	3.16
A-kinase anchor protein 12	Akap12	Q5QD51	S	507	1.79	0.36	0.73	2.46
Cyclin-dependent kinase 17	Cdk17	O35381	S	146	1.86	0.21	N/A	N/A
Cyclin-dependent kinase 17	Cdk17	O35381	S	180	2.27	0.92	N/A	N/A
Cyclin-dependent kinase 18	Cdk18	O35382	S	109	3.85	0.15	N/A	N/A
Cyclin-dependent kinase 18	Cdk18	O35382	S	66	3.5	0.099	N/A	N/A
Histone H4	Hist1h4b	P62804	S	47	2.24	0.018	1.18	1.90
Myristoylated alanine-rich C-kinase substrate	Marcks	P30009	T	143	0.39	0.002	N/A	N/A
Myristoylated alanine-rich C-kinase substrate	Marcks	P30009	S	27	0.25	6.47E-4	N/A	N/A
Myristoylated alanine-rich C-kinase substrate	Marcks	P30009	S	138	0.26	2.17E-5	N/A	N/A
Cell division cycle protein 20	Cdc20	Q62623	T	106	2.15	0.004	0.96	2.25

Consensus Motif Analysis

Mass spectrometry provides site localization of phosphorylated peptides as well as surrounding sequence information, which enables consensus motif analysis. Most kinases phosphorylate residues within a specific consensus motif; determining overrepresented consensus motifs can be an indication of changes in kinase activity. Consensus motif analysis identified several phosphopeptides that were phosphorylated within the growth associated Histone H1 kinase substrate motif in B103-695 cells but not in B103 cells, suggesting increased activity of this kinase in APP695 expressing cells (Figure 10). Growth associated Histone H1 kinase has been shown to be involved in regulating mitotic entry [241], suggesting altered cell cycle regulation in B103-695 cells.

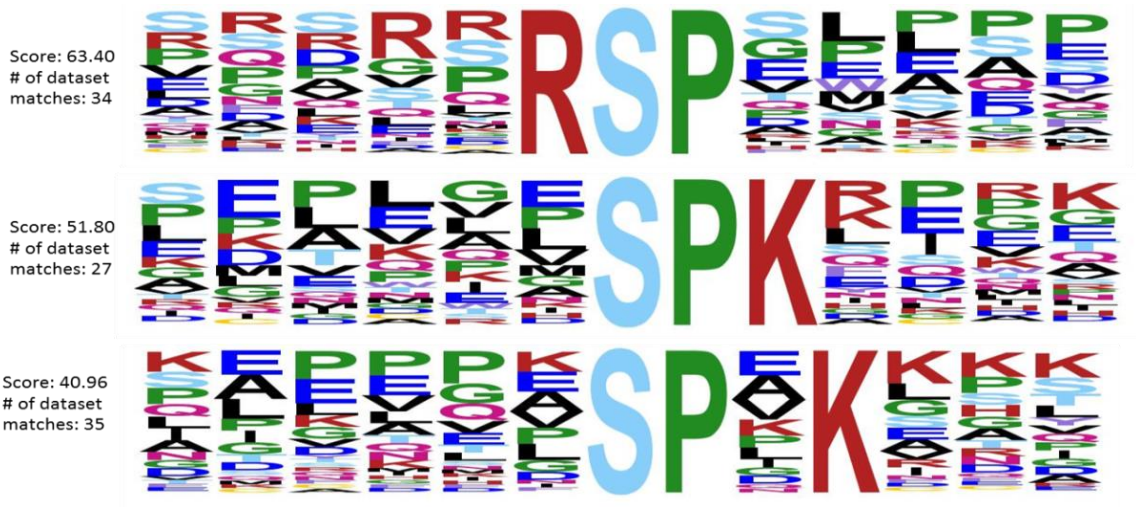

Figure 10. Growth associated Histone H1 kinase motif represented in B103-695 cells but not in B103 cells. Phosphorylation by growth associated histone H1 kinase, a serine/threonine kinase that phosphorylates substrates specifically within the above amino acid sequences; was observed in APP-695 expressing B103-695 cells, while phosphorylation within this motif was not observed in APP-null B103 cells.

Increased Phosphorylation of Histone 4 at Ser47

The normalized ratio of phosphoSer47-Histone H4 (pS47-Histone H4) showed a statistically significant 1.89-fold increase in B103-695 cells compared to B103 cells and was selected for further validation. Histone H4 is involved in chromatin structure and function and modification of Histone H4 influences both dynamic and long term gene expression. Histone H4 is phosphorylated at Ser47 by p21-

protein-activated kinase 2 (Pak2) [242] and Pak2 phosphorylation at Ser141 is required for optimal Pak2 activity [243]. Phosphorylation of Pak2 at Ser141 also showed a very slight increase (1.15-fold after normalization to total Pak2) in B103-695 cells by phosphoproteomics; however this increase could not confirmed by western blot analysis (data not shown). The extracted ion chromatogram (XIC) for the SILAC heavy and light labeled Ser47 phosphorylated Histone H4 peptide identified by LC-MS/MS analysis, as well as their base peak chromatograms, are shown in Figure 11a and 11b. The area under the curve for each XIC is representative of peptide abundance, which is significantly greater in the heavy labeled peptide from B103-695 cells. The annotated MS/MS spectra showing the amino acid sequence determined by LC-MS/MS of the Ser47 phosphorylated Histone H4 peptide is shown in Figure 11c. Increased phosphorylation of Ser47-Histone H4 in B103-695 cells was validated by western blot analysis of nuclear fractions from B103 and B103-695 samples (Figure 12a). To determine whether Aβ42 could increase phosphorylation of Ser47-Histone H4, cultured primary rat neurons were treated with 5μM oligomeric Aβ for 24 hours, which resulted in significantly increased phosphorylation of Histone H4 at Ser47 while total Histone H4 levels were not affected (Figure 15).

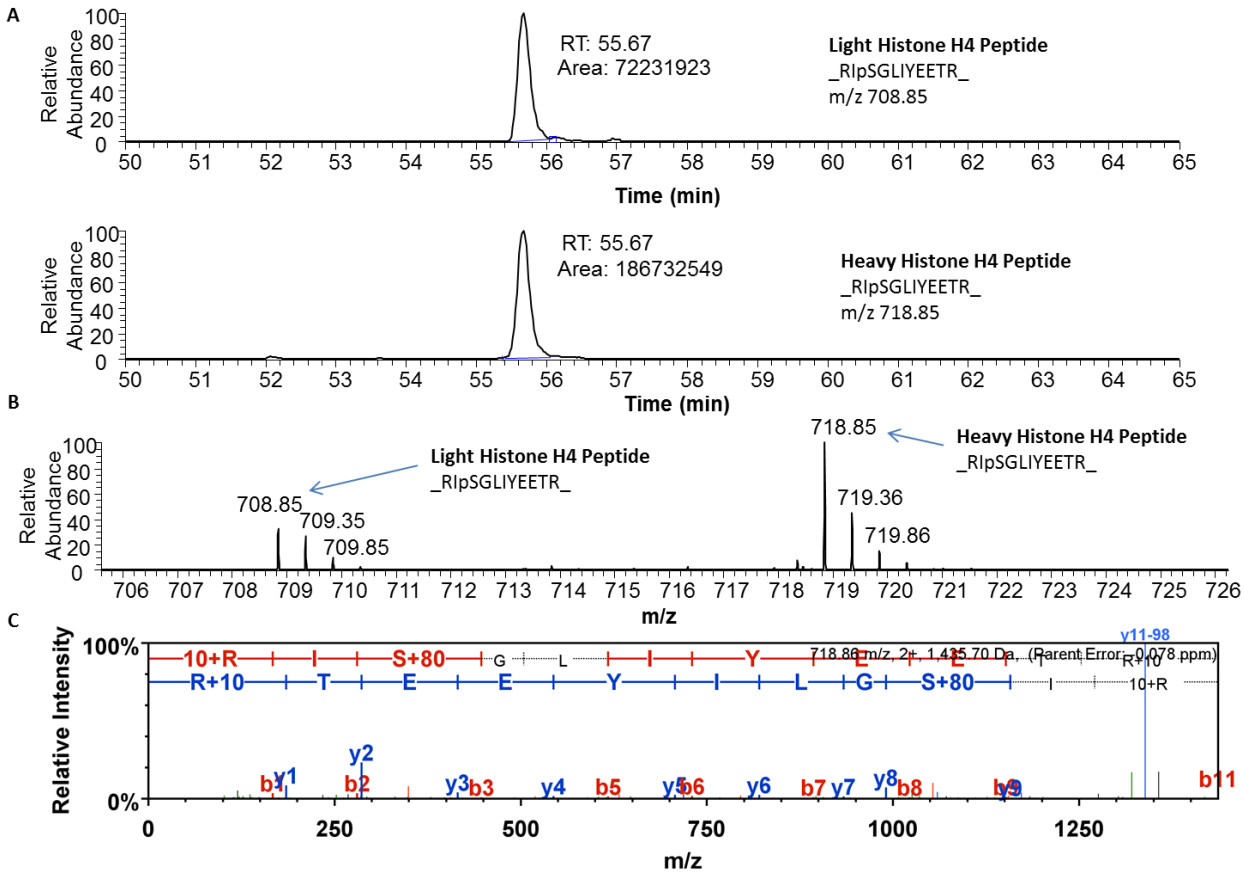

Figure 11. Increased phosphorylation of Histone H4 at Ser47 in B103-695 cells compared with B103 cells. (A) Extracted Ion Chromatogram for "Light" **(top)** and "Heavy" **(bottom)** Histone H4 peptide RpSGLIYEETR. **(B)** Base peak chromatogram showing isotope clusters for both "Light" and "Heavy" peptides with monoisotopic masses labelled. **(C)** Annotated MS/MS spectra of Histone H4 peptide showing phosphorylation detected at Serine 47.

For further validation, human brain samples obtained from the superior frontal gyrus, located in the prefrontal cortex were assessed by western blot analysis. The brain tissue lysate from individuals was categorized as NAD, MCI or LAD. We found that phosphorylation of Histone H4 at Ser47 was significantly higher in LAD individuals compared to their NAD counterparts (Figure 18), suggesting that this phosphorylation is a late-stage modification in AD.

Increased Expression of PCTAIRE-2 and PCTAIRE-3

PCTAIRE-2 (Cdk17) and PCTAIRE-3 (Cdk18), members of the cyclin-dependent kinase (Cdk) family, were found to be differentially phosphorylated in B103-695 cells compared with B103 cells and were selected for further validation. While PCTAIRE-2 and PCTAIRE-3 were not identified in our initial

proteomic analysis of B103 and B103-695 cells, their non-normalized phosphopeptide ratios showed significant increases in phosphorylation. PCTAIRE-2 showed increased phosphorylation at Ser146 (1.86-fold) and Ser180 (2.27-fold). PCTAIRE-3 showed increased phosphorylation at Ser66 (3.5-fold) and Ser109 (3.85-fold). Western blot analysis revealed that expression of both PCTAIRE-2 and PCTAIRE-3 were significantly increased in B103-695 cells compared with B103 cells (Figure 12b).

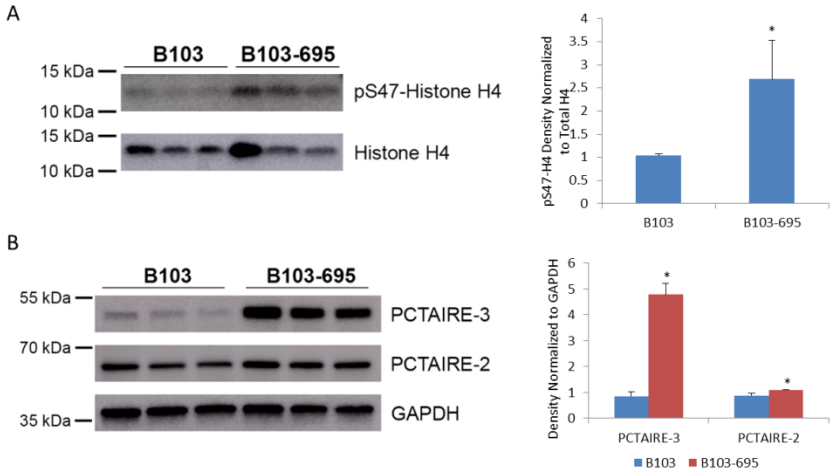

Figure 12. Western blot validation of pS47-Histone H4, PCTAIRE-2, and PCTAIRE-3 in B103 and B103-695 cells. **(A)** Phosphorylation of Histone H4 Ser 47 is significantly increased in B103-695 cells after normalization to Histone H4. **(B)** PCTAIRE-3 and PCTAIRE-2 expression are significantly increased in B103-695 cells after normalization to GAPDH. *p value<0.05, **p value<0.0005.

PCTAIRE-2 and PCTAIRE-3 expression in aged, 9 month old PS/APP double transgenic AD mouse brains were further examined by western blot (Figure 13) and immunostaining (Figure 14). PS/APP transgenic mice demonstrate accelerated plaque pathology and increased accumulation of Aβ42 at a young age, followed by development of fibrillary Aβ deposits in the cerebral cortex and hippocampus at 6 months old [148]. PS/APP transgenic mice showed a significant increase in PCTAIRE-2 expression compared with non-transgenic mice (Figure 13a), while PCTAIRE-3 expression was only slightly increased (Figure 13b). Immunostaining of PCTAIRE-2 and PCTAIRE-3 also revealed increased expression in PS/APP mice compared to their non-transgenic (non-Tg) littermates (Figure 14). Upon analysis of immunofluorescent staining of PS/APP mouse brain sections, we observed strong localization of

PCTAIRE-2 staining to the dense core of the amyloid plaques, detected with 6E10 antibody (Figure 14a). While PCTAIRE-3 staining was not as elevated in PS/APP mice as compared to PCTAIRE-2, it also showed punctate staining within the amyloid plaques in these brain sections (Figure 14b).

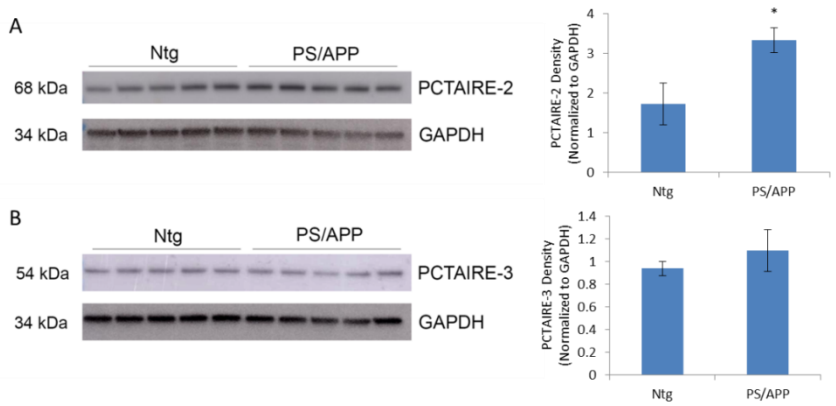

Figure 13. Increased expression of PCTAIRE-2 and PCTAIRE-3 in PS/APP transgenic mice. Western blot analysis showed a significant increase in PCTAIRE-2 **(A)** and only a slight increase in PCTAIRE-3 **(B)** in PS/APP transgenic mice compared with non-transgenic mice after normalization to GAPDH.

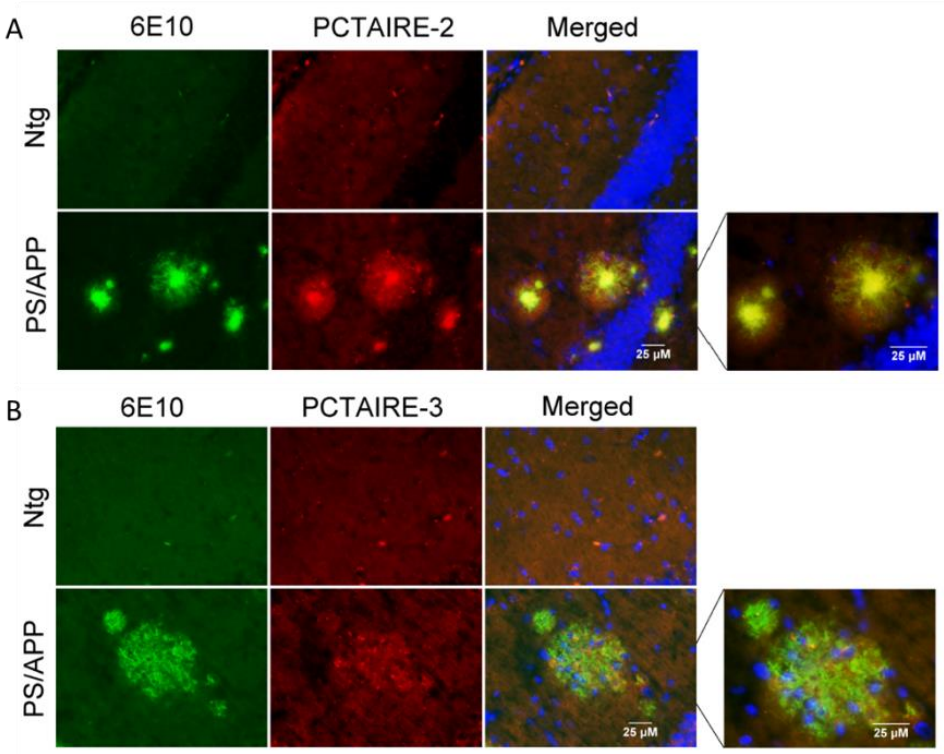

Figure 14. Immunostaining of PCTAIRE-2 and PCTAIRE-3 in PS/APP and non-Tg mice. Co-immunostaining of 6E10 (recognizing Aβ in amyloid plaques) with **(A)** PCTAIRE-2 and **(B)** PCTAIRE-3 reveals localization of PCTAIRE-2 and PCTAIRE-3 to amyloid plaques in PS/APP mice compared with non-transgenic (Ntg) mice.

Because there was strong localization of both PCTAIRE-2 and PCTAIRE-3 to amyloid plaques, we next sought to determine the effect of Aβ treatment on the expression and localization of PCTAIRE-2 and 3 in primary neurons. Primary cortical rat neurons were cultured and treated with 5μM oligomeric Aβ42 for 24 hours and analyzed by western blot (Figure 15) and immunostaining (Figure 16). Western blot analysis revealed a significant increase in levels of both PCTAIRE-2 and PCTAIRE-3 following 24 hour 5μM Aβ treatment (Figure 15). Immunostaining of primary rat neurons treated with 1μM, 2.5μM, and 5μM oligomeric Aβ42 resulted in a dose-dependent alteration of PCTAIRE-2 and PCATIRE-3 expression and localization. Control neurons treated with DMSO exhibited basal, cytoplasmic staining of PCTAIRE-2 (Figure 16a). Upon treatment of the neurons at even the lowest concentration of Aβ, PCTAIRE-2 appears to have enhanced staining that accumulates both in the nuclear and perinuclear areas of the neuron (Figure 16a). PCTAIRE-3 staining in the neurons showed reduced levels of staining compared to that of PCTAIRE-2, which is in agreement with our western blot analysis. In control, DMSO treated neurons, PCTAIRE-3 exhibited basal, punctate nuclear staining (Figure 16b). Upon Aβ treatment, expression of PCTAIRE-3 is increased, as indicated with enhanced staining and the staining appears to localize to not only nuclear regions, but extends into the cell body in a fibrillar pattern (Figure 16b)

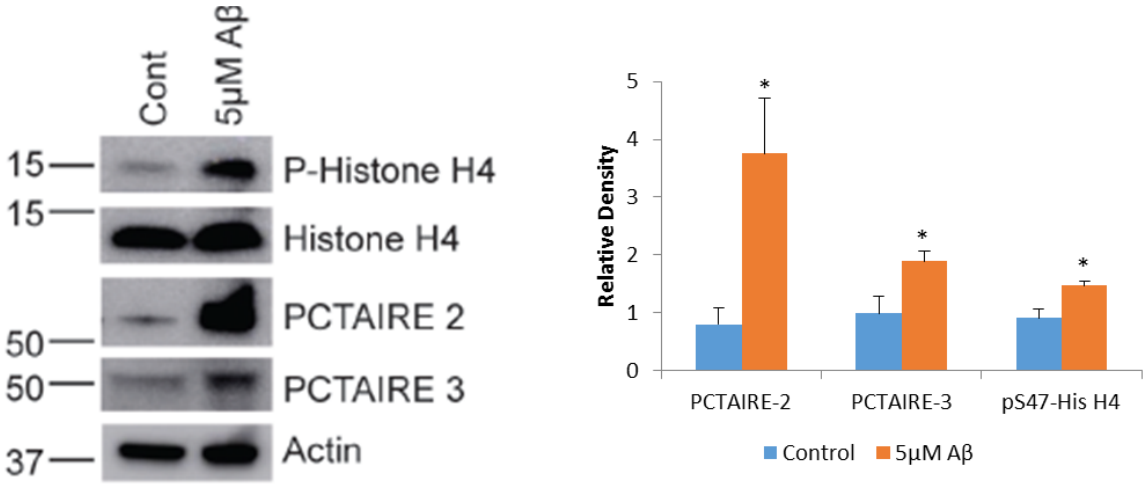

Figure 15. Increased levels of pS47-Histone H4, PCTAIRE-2, and PCTAIRE-3 in Aβ-treated primary neurons. Primary neurons treated with 5μM Aβ for 24 hours resulted in significant increases in pSer47-Histon H4, PCTAIRE-2, and PCTAIRE-3, compared with control cells. *p value<0.05.

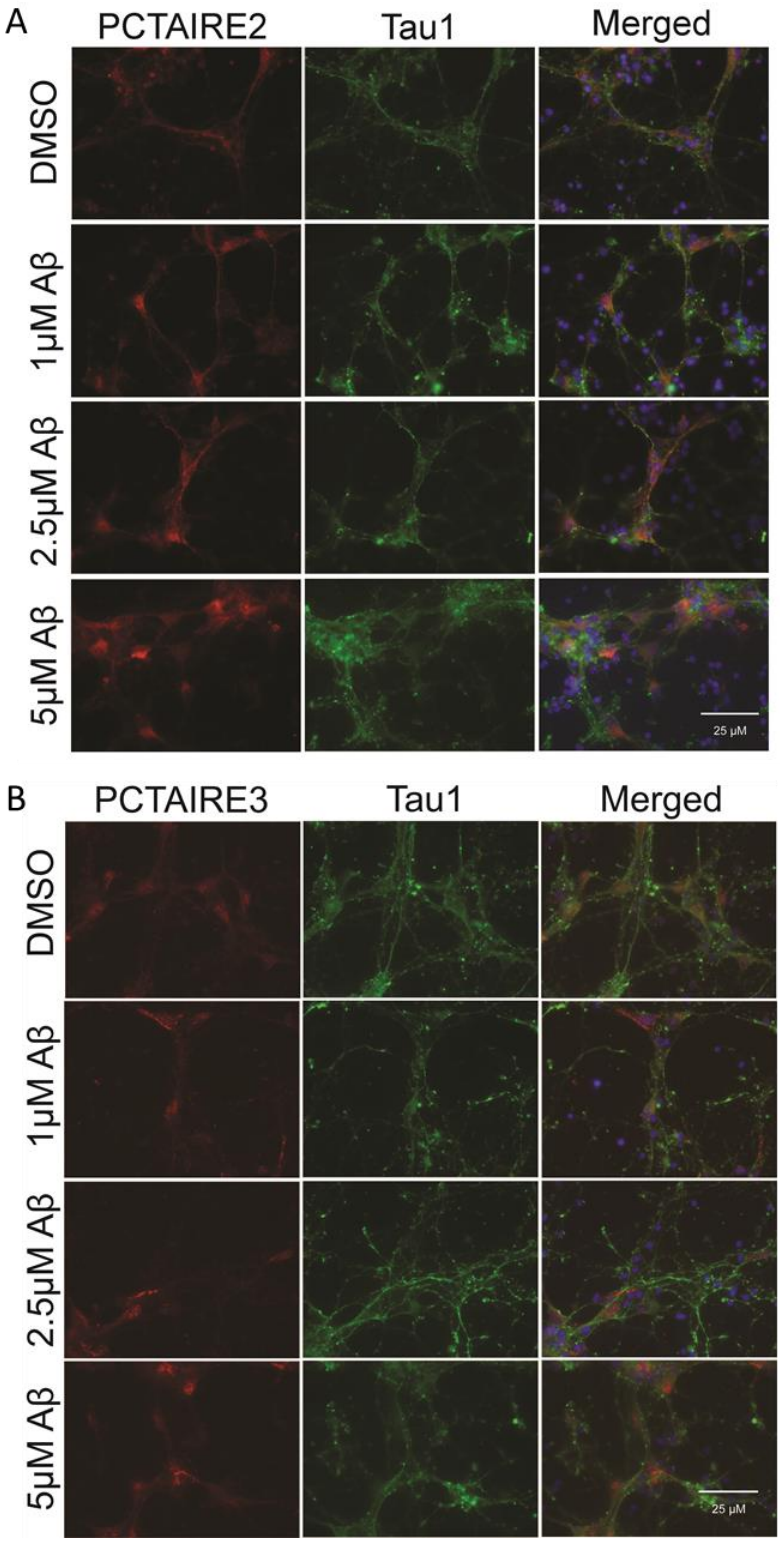

Figure 16. Immunostaining of PCTAIRE-2 and PCTAIRE-3 in Aβ treated primary neurons. Cultured primary neurons were treated with 1μM, 2.5μM, and 5μM Aβ or DMSO (control) for 24 hours and probed for PCTAIRE-2 or PCTAIRE-3 and Tau1. **(A)** PCTAIRE-2 showed enhanced nuclear and perinuclear staining upon Aβ-treatment. **(B)** PCTAIRE-3 also showed enhanced nuclear staining that extends into the cell body upon Aβ-treatment.

Our western blot data in Figure 12b suggests that expression of both PCTAIRE-2 and PCTAIRE-3 are significantly increased in B103-695 cells compared to APP-null B103 cells. This, along with the data from primary neurons treated with oligomeric Aβ, suggests that either APP or Aβ42 are able to induce these Cdks. Aβ toxicity has been shown to be mediated by APP present in the cellular membrane [244]. To examine both the independent and concerted roles of Aβ and APP in inducing expression of PCTAIRE-2 and PCTAIRE-3, B103 and B103-695 cells were treated with oligomeric Aβ42 (Figure 17). Upon treatment of B103 cells with Aβ, we observed subtle changes in localization of PCTAIRE-2 with no increase in staining for the protein (Figure 17a). While DMSO treated B103 cells appeared to have punctate, perinuclear staining in the body of the cell, Aβ treatment seemed to slightly alter the localization to become clustered at the cell's hillock (Figure 17a). B103-695 cells treated with vehicle DMSO showed staining for PCTAIRE-2 primarily in the cell body and, upon Aβ treatment, appeared to translocate to the nucleus of the cell (Figure 17a). Similar to PCTAIRE-2, PCTAIRE-3 showed slight alterations in staining in B103 cells exposed to Aβ. Staining under control DMSO treatment shows a polarized, clustered perinuclear staining and after treatment with Aβ, this staining become slightly more intense and concentrated (Figure 17b). In B103-695 cells, control treatment with DMSO shows perinuclear PCTAIRE-3 staining with slight punctate staining in the nucleus (Figure 17b). This staining was significantly enhanced upon Aβ treatment, translocating into the nucleus and into perinuclear and polarized clusters (Figure 17b).

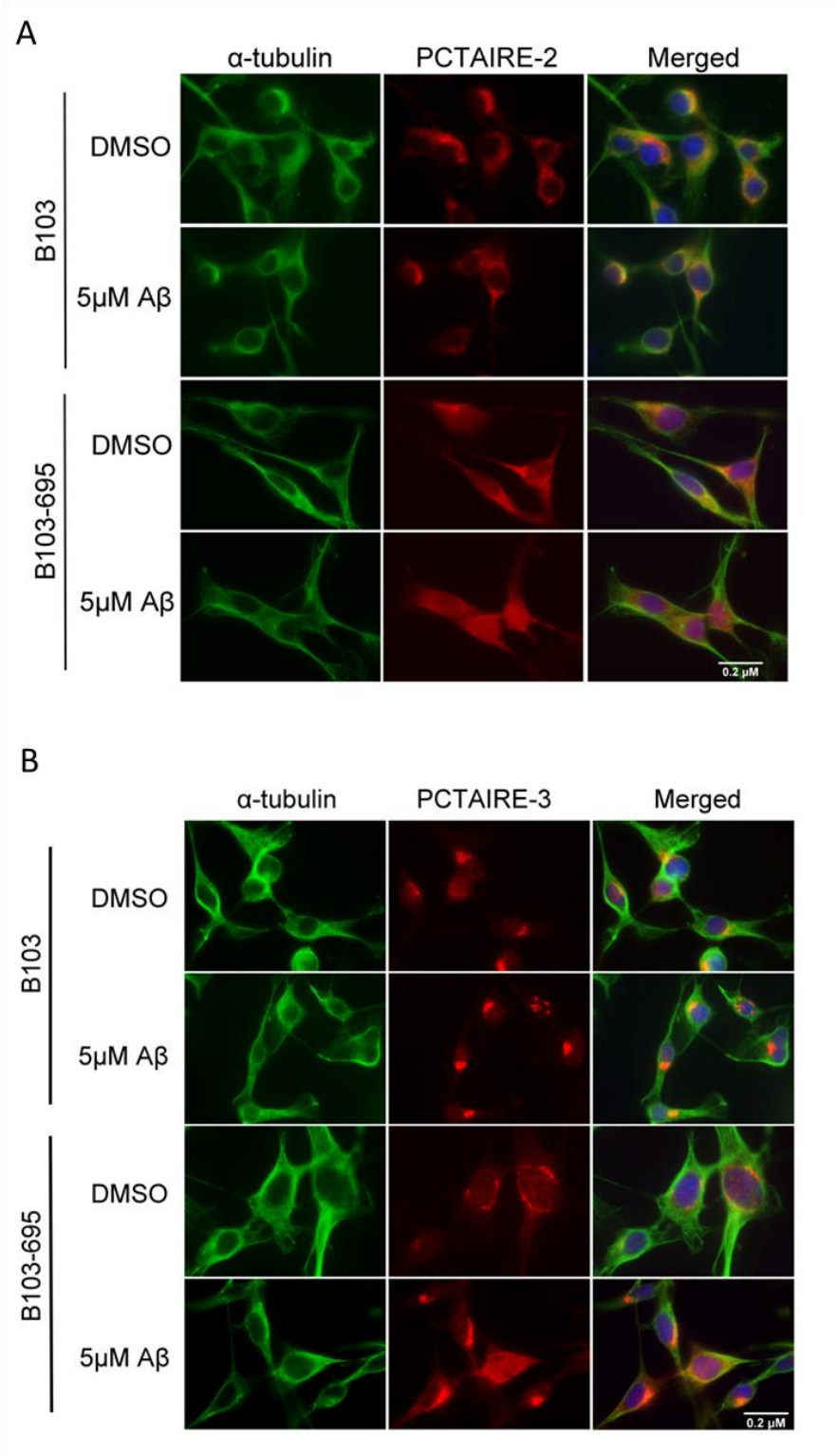

Figure 17. Immunostaining of PCTAIRE-2 and PCTAIRE-3 in Aβ-treated B103 and B103-695 cells. Cells were treated with 5μM Aβ for 24 hours and probed with PCTAIRE-2 or PCTAIRE-3 and α-tubulin. Both PCTAIRE-2 **(A)** and PCTAIRE-3 **(B) s**howed only subtle changes in B103 cells upon Aβ-treatment, However, Aβ-treated B103-695 cells resulted in translocation of PCTAIRE-2 **(A)** and PCTAIRE-3 **(B)** to the nucleus.

Finally, PCTAIRE-2 and PCTAIRE-3 levels were assessed in human brain samples from individuals categorized as NAD, MCI or AD (see Table 1). Both PCTAIRE-2 and PCTAIRE-3 expression levels were found to be significantly increased in AD individuals (Figure 18). PCTAIRE-2 expression was also significantly increased in MCI brain, suggesting that this particular cdk may be relevant in disease progression (Figure 18). Levels of APP, Aβ, and phospho Ser396/Ser404-Tau (PHF1) in human brain tissue were also determined, which confirm disease state pathology based on the increase in Aβ and PHF1 from non-AD to late-AD (Figure 18).

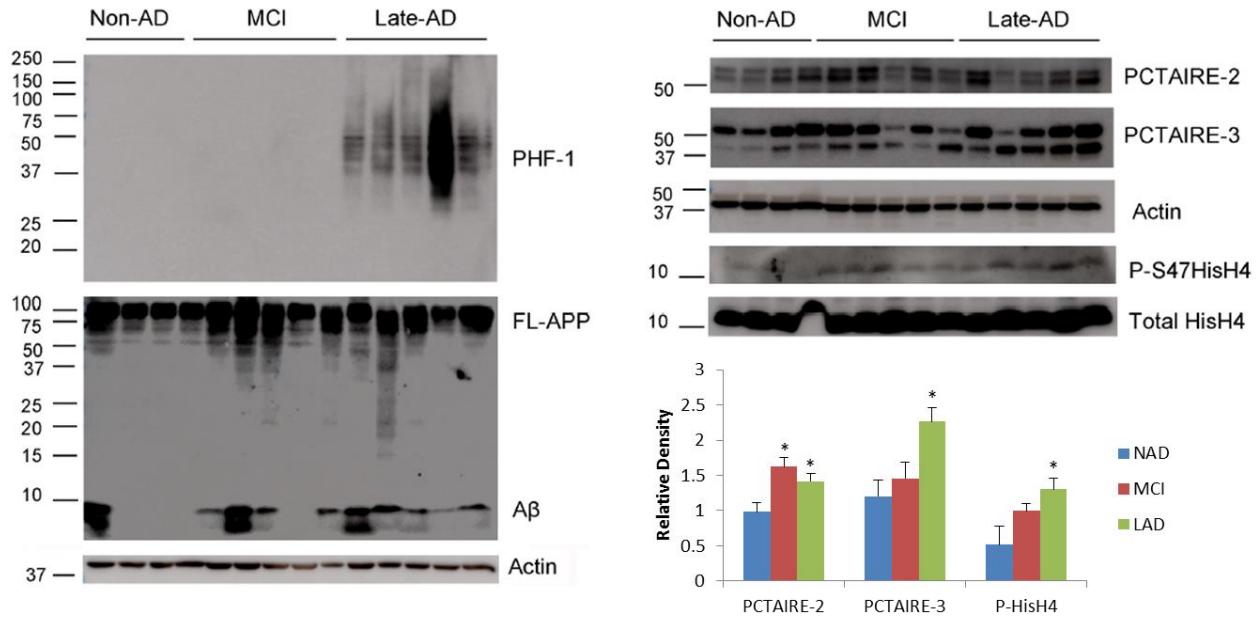

Figure 18. Increased levels of pS47-Histone H4, PCTAIRE-2, and PCTAIRE-3 in MCI and AD human brain tissue. Levels of phospho Ser396/Ser404-Tau (PHF-1), APP and Aβ (6E10) were assessed to confirm disease state based on increases in PHF-1 and Aβ in MCI and late-AD (LAD). Levels of PCTAIRE-2 and PCTAIRE-3, pS47 Histone H4, and total Histone H4 were also found to be increased in MCI and LAD.

Discussion

Comprehensive phosphoproteomic analysis of the B103 and B103-695 cell model of AD resulted in the identification of both changes in phosphorylation and protein expression in APP-695 expressing cells. Selected significant differentially phosphorylated proteins are listed in Table 2. A-kinase anchor protein 12 (AKAP12) showed significantly increased phosphorylation at Ser507 (2.46-fold) in B103-695

cells after normalization against total protein expression. AKAP12 is a scaffolding protein that serves as a negative regulator of G1 to S cell cycle progression [245]. Its regulatory role in cell cycle progression is thought to be due to contact inhibition and AKAP12 has been shown to physically bind cyclin D1, resulting in decreased cellular accessibility of cytoplasmic cyclin D1 pools and decreased translocation of cyclin D1 into the nucleus [246, 247]. AKAP12 is phosphorylated at Ser507/515 by protein kinase C (PKC) and modification of these sites results in disruption of the cyclin binding motifs present on AKAP12 [246]. Increased phosphorylation of AKAP12 was also observed in an early phosphoproteomic study of human AD brain at Ser290 [179], however the functional relevance of this residue is not known.

B103-695 cells also revealed increased phosphorylation of heat shock protein beta 1 (Hspb1) at Ser15 (3.16-fold) and Ser86 (4.49-fold). A recent quantitative phosphoproteomic study of frontal cortex from human AD brains also identified increased phosphorylation of Hspb1 at Ser82, the human analogue to rodent Ser86 [204]. HpsB1 is a molecular chaperone that belongs to a family of survival proteins that modulate cell proliferation and cytoskeletal reorganization [248-250]. The phosphorylation status of HspB1 is thought to dictate both its structure and function [251, 252] and this modification can occur due to a number of kinases that are induced by various stimuli [252]. In an *in vitro* study using a dorsal root ganglion sensory neuron model, phosphorylation of HspB1 was shown to induce cytoskeletal reorganization and promote neurite outgrowth. Further, phosphorylation of Hspb1 at Ser15 and Ser86 has been shown to influence its subcellular localization in hippocampal neurons, increasing its recruitment to dendrites and synaptic sites [253].

Myristoylated alanine-rich C-kinase substrate (MARCKS) showed significant decreases in phosphorylation at several sites in B103-695 cells, however these phosphopeptide ratios were unable to be normalized against total protein ratios as MARCKS was not identified in our global proteomic analysis of B103 and B103-695 cells. A previous studied showed that human AD cortical neurons exhibited an overall decrease in MARCKS phosphorylation, however they also reported increased MARCKS

phosphorylation in microglia from AD brains. MARCKS is phosphorylated by protein kinase C (PKC), and PKC-mediated phosphorylation of MARCKS has been shown to inhibit the actin crosslinking activity of MARCKS [254]. Reduced MARCKS phosphorylation in APP695-expressing cells suggests altered PKC activity, which may further affect actin assembly and organization [255]. We identified a number of differentially phosphorylated proteins that have previously been reported to have altered phosphorylation in AD, which provides confidence in our cell model for the study of AD as well as the quality of our phosphoproteomic dataset.

Phosphorylation of Histone H4 at Ser47, which was significantly increased in B103-695 cells compared with B103 cells, has not previously been implicated in AD. Histone H4 Ser47 phosphorylation has been shown to regulate nucleosome assembly, promoting assembly of H3.3-H4 by the histone chaperone HIRA, while inhibiting CAF-1 mediated assembly of H3.1-H4 [242]. Though Histone variant H3.3 differs from Histone H3.1 by only 5 amino acids, the functions of H3.3 are unique and cannot be substituted by H3.1 [256-258]. H3.3 is localized to gene bodies of actively transcribed genes, and increased levels of H3.3 at gene bodies positively correlates with gene expression [259, 260]. PhosphoSer47-Histone H4 is known to be phosphorylated by Pak2, a member of the p21-activated serine/threonine kinase (Pak) family [242]. Additionally, phosphatases PP1α, PP1β, and Wip1 also regulate phosphoSer47-Histone H4 levels [261]. Depletion of PP1α and PP1β results in increased Pak2 phosphorylation at Ser141 [243], which is required for Pak2 activity, suggesting that PP1α and PP1β may regulate Histone H4 Ser47 phosphorylation through Pak2 activation [261]. Pak2 phosphorylation at Ser141 was identified in our phosphoproteomic dataset but it was not significantly increased in B103-695 cells, which may suggest an alternative kinase is responsible for increased phosphorylation of Histone H4 Ser47. LAD human brain exhibited a significant increase in phosphorylation of Histone H4 at Ser47 compared to MCI and NAD individuals. Furthermore, increased phosphorylation was observed in both APP expressing B103-695 cells and Aβ treated primary neurons, which provides strong evidence

that APP and/or Aβ are involved in promoting Histone H4-Ser47 phosphorylation. While the significance of Histone H4 Ser47 phosphorylation has not been determined, this data suggests that APP-695 expression and Aβ productions may influence its regulation.

PCTAIRE-2 and PCTAIRE-3 were also shown to be differentially phosphorylated in B103-695 cells compared to APP-null B103 cells. Phosphorylation of PCTAIRE-2 at Ser146 and Ser180 has been identified in previous phosphoproteomic studies of human tissue [262-264]. Phosphorylation of PCTAIRE-3 at Ser66 has been shown previously in rat kidney [265], however only PCTAIRE-3a or 3b isoforms have a Ser located at amino acid residue 66 in humans. To our knowledge, this is the first identification of PCTAIRE-3 phosphorylation at Ser109 in rats; none of the human PCTAIRE-3 isoforms have a Ser located at amino acid residue 109. Changes in levels of phosphorylation at these residues could not be confirmed as antibodies are yet to be produced against these phosphorylation sites, but total protein expression was examined.

PCTAIRE-2 and PCTAIRE-3 levels were determined to be significantly increased in B103-695 cells (Figure 12). PCTAIRE-2 expression was also significantly increased in PS/APP transgenic mice, while PCTAIRE-3 levels were only slightly increased (Figure 13). This finding was also reflected in the immunostaining of PCTAIRE-2 and PCTAIRE-3 in corresponding PS/APP Tg mouse brain slices. Staining for both PCTAIRE-2 and PCTAIRE-3 were localized to the dense, amyloid plaques suggesting a possible role for Aβ in inducing their expression (Figure 13). Primary rat neurons treated with oligomeric Aβ42 showed increased expression of these proteins as demonstrated by immunostaining (Figure 16) and western blot (Figure 15). Upon Aβ treatment, PCTAIRE-2 translocated from the cytosol to the perinuclear and nuclear regions of the neuron. Likewise, PCTAIRE-3 demonstrated altered staining with Aβ treatment, translocating into the nucleus and forming fibril structures in the cytoplasmic regions. To further examine the differential roles of APP and Aβ, we further determined that the changes in PCTAIRE localization appear to be APP dependent. APP-null B103 cells treated with Aβ exhibited a slight increase

in staining for both PCTAIRE-2 and PCTAIRE-3, however staining for PCTAIRE-2 and PCTAIRE-3 drastically altered in B103-695 cells upon treatment with Aβ.

PCTAIRE kinases are relatively uncharacterized members of the cyclin-dependent kinase (Cdk) family, and are categorized by a serine to cysteine mutation in the PSTAIRE cyclin binding consensus motif [266]. PCTAIRE-2 and PCTAIRE-3 are Cdc-2-related serine/threonine kinases; however their functions remain to be discovered. Whether PCTAIREs are involved in cell cycle regulation or are regulated by the cell cycle is yet be determined. A study by Meek and colleagues (2004) identified PCTAIRE-2 and PCTAIRE-3 as 14-3-3 binding partners, and furthermore PCTAIRE-2 interacted with 14-3-3 in a cell cycle-regulated manner. Other studies, however, indicate that PCTAIREs may function independently of the cell cycle [267, 268].

PCTAIRE-2 is expressed in terminally differentiated neurons and has been found to phosphorylate Ser and Thr residues of Histone H1 [269]. PCTAIRE-3 is expressed in the brain and testis. A study by Herskovits and Davies (2006) found increased levels of PCTAIRE-3 in the temporal cortex of AD brains compared with control brains and they also found it was localized within paired helical filaments (PHFs). Further, they suggested that PCTAIRE-3 is indirectly involved in promoting phosphorylation of Tau at residues T231 and S235, early modifications in AD pathogenesis [270]. A separate study recently found that PCTAIRE-3 can be activated through association with Cyclin A and/or phosphorylation by Protein Kinase A (PKA) [271]. PKA increased phosphorylation of PCTAIRE-3 at Ser12, Ser66, and Ser109, though only phosphorylation of Ser12 appeared to increase kinase activity; the function of PCTAIRE-3 phosphorylation at S109 and S66 by PKA is still unknown [271]. Interestingly, PKA was also found by Herskovits and Davies (2006) in the same PHF fractions that PCTAIRE-3 was observed in. Bioinformatic analysis of our previous proteomic study of B103 and B103-695 cells suggested increased PKA signaling in B103-695 cells [239] and phosphorylation of PCTAIRE-3 at S109 and S66 was

observed in B103-695 cells in this phosphoproteomic dataset. Additional experiments are necessary to determine the functional significance of PCTAIRE-3 phosphorylation at these sites.

Further investigation is required to determine the function of PCTAIRE-2 and PCTAIRE-3 and their potential role in Alzheimer's disease, as well as the significance of the identified phosphorylation sites. It is possible these phosphorylation sites may be involved in the regulation of PCTAIRE-2 and PCTAIRE-3 activation or deactivation, or have a potential role in cell cycle progression. PCTAIRE-3 may have a role in Alzheimer's disease as an effector of tau phosphorylation, however the mechanism needs to be elucidated. This comprehensive phosphoproteomic dataset provides insights into pathways that may be affected by APP695 expression based on changes in phosphorylation as well as consensus motif analysis, providing a foundation for future mechanistic studies. Additionally, this dataset led to the investigation of PCTAIRE-2 and PCTAIRE-3 whose expression appears to be influenced by APP and Aβ in a number of models of AD including human brain tissue, suggesting their involvement in the complex pathogenesis of AD; whether their increased expression is causative or is a result of AD still needs to be determined.

Chapter 4 – Label-Free Quantitative Proteomic Analysis of Human Neurodegenerative Disorders

Summary

The challenges associated with proteomic analysis of human tissue include the limited accessibility and quantity of samples that can be obtained, as well as the quantitative proteomic approaches available. This chapter had two main goals; to perform label-free quantitative proteomic analysis of human tissue from multiple neurodegenerative diseases, as well as develop a method for increasing proteome coverage when starting material is limited. Proteomic analyses of human tissue from the cortex of individuals affected by Alzheimer's disease (AD), mild cognitive impairment (MCI), Parkinson's disease (PD), and progressive supranuclear palsy (PSP) were compared to cognitively normal, control samples using label-free quantification. Label-free quantitative proteomics has been made possible with advances in mass spectrometers such as increased mass accuracy and resolution. Label-free quantitative proteomic analysis of human tissue identified over 4000 proteins and determined several molecular and cellular functions that may be affected during neurodegeneration.

The filter-aided sample processing (FASP) method typically used for proteomics sample preparation requires at least 100µg of protein, which may not always be available when working with human brain samples or primary cells such as microglia. The second goal of this chapter was to optimize a gel-aided sample processing (GASP) method for proteomic analysis of samples with limited amounts of starting material, as low as 1µg of protein. The GASP method and results were submitted as a chapter for a Methods in Neuroproteomics book and can be found in Appendix D.

Introduction

Mild Cognitive Impairment and Alzheimer's Disease

Alzheimer's disease (AD) was reviewed in Chapter 1 and will not be described here. Mild cognitive impairment (MCI) involves deficits in memory and is associated with increased risk of developing more advanced forms of dementia and AD [272, 273]. MCI affects an estimated 10-20% of Americans age 65 and older [1]. As MCI does not usually result in death, characterizing the neuropathology of MCI has been difficult since tissue is only obtained when a person with MCI dies of other causes. However, studies that have successfully examined MCI pathology observed neurofibrillary tangles (NFTs) in the hippocampus and entorhinal cortex, and Aβ plaques in the neocortex [96, 274, 275]. While MCI is typically associated with AD, an estimated 25% of Parkinson's disease (PD) patients without dementia also suffer from MCI [276]. Additionally, MCI is also known to progress to dementia with Lewy bodies (DLB) [277, 278]. There is unlikely a single cause of MCI as its pathology and progression is variable from case to case, and resulting pathology is observed in a number of different neurodegenerative diseases, such as AD, PD, and LBD. Investigating the molecular changes that occur during MCI is particularly valuable as MCI represents an early stage of dementia often progressing to more severe neurodegenerative diseases. Developing a further understanding of MCI and identifying reliable diagnostic biomarkers would be valuable for earlier diagnosis and the development of therapeutics to delay progression to more severe dementia and neurodegeneration.

Parkinson's Disease

Parkinson's disease (PD) is the second most common neurodegenerative disorder after AD. PD is a progressive movement disorder and symptoms include tremor, rigidity, bradykinesia, weakness, and sometimes dementia [279]. The major pathological hallmarks of PD are loss of dopaminergic neurons in the substantia nigra, a brain region involved in movement, and the presence of Lewy bodies. PD is considered a synucleinopathy as α-synuclein is the primary component of Lewy bodies [280], which are

intracellular aggregates of insoluble proteins, including ubiquitin [281, 282], and neurofilament proteins [283, 284] in addition to α-synuclein. Lewy bodies are observed in both PD and LBD. Lewy bodies are not only found in the substantia nigra where dopaminergic neuron loss occurs, but are also found in the cerebral cortex, amygdala, and hippocampus [285]. It has been suggested that the presence of Lewy bodies in the cortex strongly correlates with cognitive impairment in PD [285, 286]. In addition to Lewy bodies, amyloid plaques and tau-NFTs have also been observed in the brains of PD patients with dementia [287, 288]. Compared with α-synuclein pathology alone, the combination of α-synuclein and amyloid plaque pathology are most common in PD with dementia, and often result in shorter survival and earlier onset of dementia [287]. Tau-NFTs, on the other hand, are not always observed in PD and are not considered to be a major contributor to dementia associated with PD [287].

The majority of PD cases are sporadic, also referred to as idiopathic PD, affecting individuals around the age of 65. A smaller portion of PD is considered early onset, referred to as familial PD, and has been linked to mutations in a number of genes; *α-synuclein (SNCA)* [289], *parkin (PARK2)* [290], *DJ-1 (PARK7)* [291], *leucine rich repeat kinase (LRRK2)* [292, 293], *ubiquitin carboxy-terminal hydrolase L1 (UCHL1)* [294], and *PTEN-induced kinase 1 (PINK-1)* [295] (reviewed in [296]). The primary cause of PD remains to be understood, but it is believed to be a complex process involving both genetic and environmental factors [297]. Mitochondrial dysfunction and oxidative stress, protein folding and processing are processes that have been proposed to be involved in PD pathology [297, 298]. The loss of dopaminergic neurons from the substantia nigra results in decreased dopamine production, the neurotransmitter primarily involved in motor functions, which subsequently results in loss of normal movement control. One of the most common treatments of PD is L-3,4-dihydroxyphenylalanine (L-DOPA), a precursor for the neurotransmitters dopamine, norepinephrine, and epinephrine, which increases dopamine concentrations and improves movement control in PD patients [299]. While medications exist that improve symptoms of PD, there is no cure or preventative treatment, and the

cause of sporadic PD remains largely unknown. There is also a lack of diagnostic and therapeutic markers of PD. Mass spectrometry-based proteomic studies of PD have been performed using animal models, human cerebrospinal fluid (CSF), human brain tissue from the substantia nigra [300-302], and frontal cortex [303, 304], as well as Lewy bodies isolated from human frontal cortex [305, 306]. As cognitive impairment in PD correlates with cortical Lewy body pathology [285], further investigation of the molecular changes occurring in the cortex may provide insights into the molecular changes involved in dementia associated with PD, as well as potentially identify novel proteins or biomarkers not previously associated with PD.

Progressive Supranuclear Palsy

Progressive supranuclear palsy (PSP), also known as Steel-Richardson-Olszewski syndrome, is a rare neurodegenerative disorder. Symptoms of PSP are associated with loss of balance and gait, problems with eye movement, speech and swallowing, as well as progression to dementia [307]. PSP has been described as a tauopathy as tau-NFTs are usually observed in neurons and glia [308, 309]. Deterioration is observed in areas of the brain involved in control of movement and thinking including the brain stem, substantia nigra and cerebral cortex [307-309]. PSP can be difficult to diagnose as its symptoms are very similar to other, more common movement disorders, and it is often misdiagnosed as PD. The cause of PSP remains unknown; however, it is typically associated with age, affecting people around 60 years old. While PSP is not directly life-threatening, it increases the risk of other complications, primarily pneumonia, as well as difficulty swallowing, and injuries caused by falls. While proteomic profiling of CSF from PSP patients has been previously performed [310], as well as proteomic analysis of caudate nucleus, part of the brainstem involved in voluntary movement [311], there has not been a comprehensive proteomic analysis of cortex from PSP affected brain compared with normal brain. As the cause of PSP remains largely unknown, and it is very difficult to diagnose, proteomic studies can identify changes in protein levels to provide some understanding of the cellular and

molecular mechanisms altered in PSP, possibly identifying novel biomarkers of the disease, and aiding in the development of potential therapeutics.

Label Free Quantitative Proteomics

The complexity of the central nervous system and the mechanisms underlying the onset of cognitive decline and dementia makes studying neurodegeneration particularly difficult. When studying human brain tissue it is important to consider the region being studied as different regions are affected at different stages of the disease. One of the limitations of studying human tissue is that tissue is collected post-mortem when pathology is most severe, limiting the discovery of preclinical biomarkers associated with early molecular changes. Researching the molecular changes that occur in MCI is particularly important for the discovery of preclinical biomarkers and molecular changes. Despite the associated challenges, studies using human tissue affected by AD and other neurodegenerative diseases are invaluable for gaining a deeper understanding of the molecular changes that occur with the progression of disease pathology. The causes of disease onset, progression, and pathology are poorly understood for most neurodegenerative conditions, and there is a need to identify novel diagnostic and prognostic biomarkers as well as therapeutic targets. There is also a lack of diagnostic biomarkers to distinguish neurodegenerative diseases from each other, such as PSP from PD. To develop more effective therapeutic strategies, we need to gain a more comprehensive understanding of the molecular mechanisms involved in disease progression and pathology, and identifying molecular changes in MCI is particularly important for the advancement of early diagnosis and development of preventative therapeutics. Mass spectrometry-based proteomics provides an unbiased approach for large scale analysis of protein expression changes that can provide information about affected pathways and functions.

Label free quantitative proteomics does not require metabolic labeling or chemical derivatization and can be applied to all organisms or tissues. With advances in mass spectrometry,

including increased resolution and mass accuracy, label-free quantitative proteomics is becoming more commonly used. Label-free quantitation relies on peptide ion abundance, which has been shown to correlate with protein abundance [312-314]. Spectral counting has also been shown to correlate with protein abundance [315], however current label-free approaches typically use peptide ion abundance based on total or average ion current values [218]. Each peptide ion has a specific mass/charge (m/z) and their signal intensities are recorded over time. Extracted ion chromatograms (XICs) are created by plotting the intensity of the peptide ion, based on its m/z, over time. The area under the XIC curve for a peptide ion is proportional to ion abundance. In this study we used label-free quantitative proteomics for the analysis of human brain tissue from the cortex of MCI, AD, PDP, and PSP patients compared with cognitively normal, control samples.

Materials and Methods

Label-free Quantitative Proteomic Analyses of Human Brain Tissue

Sample Processing and LC-MS/MS

Human AD, MCI, and control tissues were obtained from the University of California Alzheimer's Disease Research Center (UCI-ADRC) and the Institute for Memory Impairments and Neurological Disorders. Brain samples were de-identified and categorized based on post-mortem Braak stage and pre-mortem clinical MMSE score. Additional information on this brain material is detailed in Table 1. Human PD, PSP, and control tissues were obtained from our collaborator Dr. Werner Geldenhuys at the Northeast Ohio Medical University (NEOMED).

All human brain tissue samples were lysed in 4% SDS, 100mM DTT, 100mM Tris-HCl, pH 7.4 at 95˚C for 5 minutes, followed by sonication and centrifugation. Protein was quantified using the Pierce 660 assay supplemented with ionic detergent compatibility reagent (IDCR) (Pierce). Equal amounts of protein from each sample were processed by filter-aided sample processing (FASP), and digested with Trypsin/Lys-C at 1:50 (w:w, enzyme:protein) overnight at 37˚C. Peptides were desalted using Thermo

C18 SPE columns on a Supelco vacuum manifold. Peptides were dried and resuspended in 0.1% formic acid in H_2O for analysis by mass spectrometry.

Peptides were analyzed on a Q-Exactive Plus (Thermo Fisher Scientific) following separation on a 75µm x 50cm reversed-phase (RP) UPLC column (Dionex) packed with 5µm 300Å C18 material using a 120 minute gradient on an EASY-nLC 1000 system (Thermo Fisher Scientific). Full MS survey scans used a resolving power of 60,000, selecting the top ten most abundant ions for MS/MS fragmentation and analysis.

Database Searching, Statistical Analysis, and Pathway Analysis

Raw data files were processed and searched using MaxQuant (version 1.0.30) against the current *Homo sapiens* UniprotKB protein sequence database. Normalization of protein abundances is especially important for label-free proteomic quantification and the MaxQuant label-free quantification feature was used when searching raw data files. Ratios were generated by dividing the intensity of each biological replicate for AD, MCI, PD and PSP by the average of all control intensities. Ratios were generated using both raw intensities as well as the LFQ intensities generated by MaxQuant [316]. Statistical analysis was carried out using the Significance A outlier test in Perseus. Two different approaches were used, Benjamini-Hochberg, which uses a q-value of 0.05 for false discovery rate [219], and a t-test with a p-value cut off of 0.05. Proteins that had a q-value or p-value ≤ 0.05 in five out of seven biological replicates for PD and PSP, or two out of three biological replicates for MCI and AD, were considered significant and submitted to Ingenuity Pathways Analysis (IPA) for bioinformatic analysis.

Western Blotting

AD, MCI and control brain lysates were analyzed by western blot and disease state was confirmed using 6E10 (detecting FL-APP and Aβ) and PHF-1 antibodies (Figure 24). Proteins were selected for validation by western blot analysis based on significance as well as function. Proteins were separated on an AnyKD SDS-PAGE gel (BioRad) and transferred to a PVDF membrane using the Trans

Turboblot system (BioRad). Membranes were blocked in 5% non-fat milk-PBS for 1 hour at room temperature. Primary antibodies specific for CPS1 (Abcam, rabbit monoclonal), SNX17 (Santa Cruz, mouse monoclonal), APP (6E10 antibody, Covance, mouse monoclonal) and GAPDH (Cell Signaling, rabbit monoclonal) were diluted in 5% BSA-PBS, with 0.05% NaN_3 and incubated overnight at 4˚C. Membranes were then incubated with corresponding anti-rabbit (Cell Signaling) and anti-mouse (Cell Signaling) secondary antibodies for 2 hours at room temperature. All blots were developed with Pico Chemiluminescence reagents (Pierce), with the exception of CPS1 which was developed using Femto Chemiluminescence reagents (Pierce), using an Amersham Imager 600RGB (GE Healthcare).

Gel-aided Sample Preparation (GASP)

A detailed description of the GASP protocol can be found in Appendix D.

Results and Discussion

Proteomic Analysis of Human PD, PSP, and Control Brain

A total of 4828 proteins were identified from seven biological replicates of control, PD, and PSP human brain samples, with 3830 proteins having at least 2 unique peptides identified. Of the total identified proteins, 3329 proteins were identified in PD samples, 3237 proteins in PSP samples, and 3324 proteins in control tissue, all having a minimum of 2 unique peptides. Ratio values were log2 transformed, and statistical analysis was performed using the Significance A outlier test, with the Benjamini-Hochberg false-discovery rate (FDR)-based q-value cutoff of 0.05. Ratios needed to have a q-value ≤ 0.05 in at least five of seven replicates to be considered significant. In PD compared with control, 12 proteins were found statistically significant when using raw intensity ratios and 32 proteins were found statistically significant when using LFQ intensity ratios (Table 3 and Table 4). In PSP compared with control, 9 proteins were statistically significant when using raw intensity ratios and 17 proteins were statistically significant when using LFQ ratios (Table 5 and Table 6). Alternatively, statistical analysis using Significance A with a t-test p-value cut off of 0.05 was used to determine

significant expression changes for bioinformatics analysis in Ingenuity Pathway Analysis (IPA). Again, ratios needed to have a p-value ≤ 0.05 in at least five of seven replicates to be considered significant.

Table 3. Benjamini Hochberg FDR Significant Proteins Using LFQ Intensities: PD vs Control. Ratios were generated using LFQ intensity values. LFQ ratios were log2 transformed and analyzed using Significance A with a false discovery rate (FDR)-based q-value threshold of 0.05. Ratios with q-values ≤ 0.05 in five out of seven biological replicates were considered to be statistically significant.

Protein name	Gene name	Median Log2(LFQ Ratio)	Standard Deviation
Vacuolar protein sorting-associated protein 37C	VPS37C	2.13	0.75
Rho GTPase-activating protein 32	ARHGAP32	3.38	0.45
Sorting nexin-17	SNX17	2.85	0.31
DDRGK domain-containing protein 1	DDRGK1	2.70	0.55
Unconventional myosin-Id	MYO1D	-2.78	2.05
Tenascin	TNC	-2.43	1.91
Hormone-sensitive lipase	LIPE	-1.74	2.09
Ectonucleotide pyrophosphatase/phosphodiesterase family member 6	ENPP6	-2.01	2.18
Actin-binding protein anillin	ANLN	-1.61	2.07
Aspartoacylase	ASPA	-2.17	2.14
Perilipin-3	PLIN3	-1.42	1.31
Carnosine synthase 1	CARNS1	-2.26	1.97
Glutathione S-transferase Mu 5	GSTM5	-1.79	0.54
Myelin P2 protein	PMP2	-1.51	2.07
Ermin	ERMN	-1.35	1.67
60S ribosomal protein L36	RPL36	3.00	0.47
Inverted formin-2	INF2	-1.67	1.64
Thyroid hormone receptor-associated protein 3	THRAP3	3.75	0.40
MAGUK p55 subfamily member 5	MPP5	3.38	0.52
Uncharacterized protein C1orf198	C1orf198	-1.48	1.32
Target of rapamycin complex subunit LST8	MLST8	3.71	0.43
Caldesmon	CALD1	2.79	0.29
60S ribosomal protein L35a	RPL35A	3.40	0.04
Glutamate receptor 4	GRIA4	2.80	0.34
Thioredoxin, mitochondrial	TXN2	2.54	0.20
Cytochrome c oxidase subunit 1	MT-CO1	2.50	0.53
Bis(5-nucleosyl)-tetraphosphatase	NUDT2	2.40	0.40
BRISC complex subunit Abro1	FAM175B	2.91	0.31
Golgin subfamily A member 7B	GOLGA7B	2.55	0.19
WD repeat-containing protein 82	WDR82	2.08	0.26
MAP6 domain-containing protein 1	MAP6D1	-2.10	1.37
NAD-dependent protein deacylase sirtuin-5, mitochondrial	SIRT5	1.98	0.38

Table 4. Benjamini Hochberg FDR Significant Proteins Using Raw Intensities: PD vs Control. Ratios were generated using raw intensity values. Raw intensity ratios were log2 transformed and analyzed using Significance A with a false discovery rate (FDR)-based q-value threshold of 0.05. Ratios with q-values ≤ 0.05 in five out of seven biological replicates were considered to be statistically significant.

Protein name	Gene name	Median Log2(Ratio)	Standard Deviation
Signal recognition particle subunit SRP72	SRP72	-2.91	0.59
Phosphatidylinositol 4-phosphate 5-kinase type-1 alpha	PIP5K1A	-2.37	1.83
39S ribosomal protein L3, mitochondrial	MRPL3	2.84	1.00
TBC1 domain family member 10A	TBC1D10A	3.76	0.57
Long-chain-fatty-acid--CoA ligase 4	ACSL4	3.25	0.32
Cholecystokinin	CCK	4.61	0.38
Coagulation factor VII	F7	5.83	0.57
Vacuolar protein sorting-associated protein 41 homolog	VPS41	2.74	1.59
Protein CASP	CUX1	4.30	0.80
Liprin-beta-1	PPFIBP1	2.73	1.26
Protein RMD5 homolog A	RMND5A	4.10	0.93
Nuclear receptor-binding protein 2	NRBP2	3.91	0.37

Table 5. Benjamini Hochberg-FDR Significant Proteins Using LFQ Intensities: PSP vs Control. Ratios were generated using LFQ intensity values. LFQ ratios were log2 transformed and analyzed using Significance A with a false discovery rate (FDR)-based q-value threshold of 0.05. Ratios with q-values ≤ 0.05 in five out of seven biological replicates were considered to be statistically significant.

Protein name	Gene name	Median Log2(LFQ Ratio)	Standard Deviation
Vitamin D-binding protein	GC	-2.69	0.60
Sorting nexin-17	SNX17	3.29	0.35
Malate dehydrogenase, cytoplasmic	MDH1	-3.02	1.87
Coronin-7	CORO7	2.48	0.41
Unconventional myosin-Id	MYO1D	-4.01	2.61
Tenascin	TNC	-3.59	1.97
Perilipin-3	PLIN3	-2.33	1.34
Myelin P2 protein	PMP2	-2.81	1.62
MAP6 domain-containing protein 1	MAP6D1	-2.23	1.16
NAD-dependent protein deacylase sirtuin-5, mitochondrial	SIRT5	2.02	0.29
AP-3 complex subunit sigma-1	AP3S1	3.55	0.40
GH3 domain-containing protein	GHDC	2.35	0.25
Thiosulfate sulfurtransferase/rhodanese-like domain-containing protein 1	TSTD1	3.56	0.48
Leucyl-cystinyl aminopeptidase;Leucyl-cystinyl aminopeptidase	LNPEP	1.75	0.19
Collagen alpha-1(VI) chain	COL6A1	-1.84	0.66
Protein DEK	DEK	1.93	0.81
Hamartin	TSC1	-1.79	0.46

Table 6. Benjamini Hochberg FDR Significant Proteins Using Raw Intensities: PSP vs Control. Ratios were generated using raw intensity values. Raw intensity ratios were log2 transformed and analyzed using Significance A with a false discovery rate (FDR)-based q-value threshold of 0.05. Ratios with q-values ≤ 0.05 in five out of seven biological replicates were considered to be statistically significant.

Protein name	Gene name	Median Log2(Ratio)	Standard Deviation
Protein RMD5 homolog A	RMND5A	5.03	0.91
Tubulin beta-6 chain	TUBB6	-4.38	2.00
MKL/myocardin-like protein 2	MKL2	3.54	0.47
Signal recognition particle subunit SRP72	SRP72	-2.70	1.61
Liprin-beta-1	PPFIBP1	2.32	0.50
Lck-interacting transmembrane adapter 1	LIME1	2.51	0.63
Muscarinic acetylcholine receptor M3	CHRM3	2.87	0.45
Clathrin heavy chain 2	CLTCL1	3.50	0.76
Zinc finger RNA-binding protein	ZFR	3.42	2.05

Functional Enrichment of Differentially Expressed Proteins in PD

Significance A analysis of raw intensity and LFQ intensity ratios comparing PD with control identified statistically significant changes in 65 and 86 proteins, respectively. Pathway analysis of proteins with significant LFQ intensity ratios from PD tissue identified a number of proteins that have previously been shown to be associated with PD and movement disorders (Figure 19). A number of LFQ significant proteins were also associated with mitochondrial dysfunction, which is hypothesized to be involved in PD. Pathway analysis of proteins with significant raw intensity ratios revealed molecular and cellular functions altered in PD, including protein synthesis, cell-to-cell signaling and interaction, and lipid metabolism. Cholecystokinin (CCK), a peptide hormone that showed a significant increase in PD, was shown to be involved in a number of altered cellular functions such as protein oligomerization, dopamine regulation, and cytoskeletal organization. CCK has been shown to exist within dopaminergic neurons in the brain [317], and its carboxy terminal octapeptide (CCK-8) is suggested to modulate dopamine release [318, 319]. One early study examined the distribution of CCK-8 in human PD and control brains, and found that CCK-8 levels were only slightly decreased in the substantia nigra [320]. Our proteomic analysis found CCK significantly increased in the cortex. Two separate studies showed no correlation between mutations found in CCK and CCK-receptor genes and risk of sporadic PD, however

both studies showed one polymorphism was associated with increased vulnerability to hallucinations [321, 322]. While CCK does not appear to be a genetic risk factor for sporadic PD, its function as a regulator of dopamine release may have implications in PD as dopamine has been shown to modulate cortical function [323].

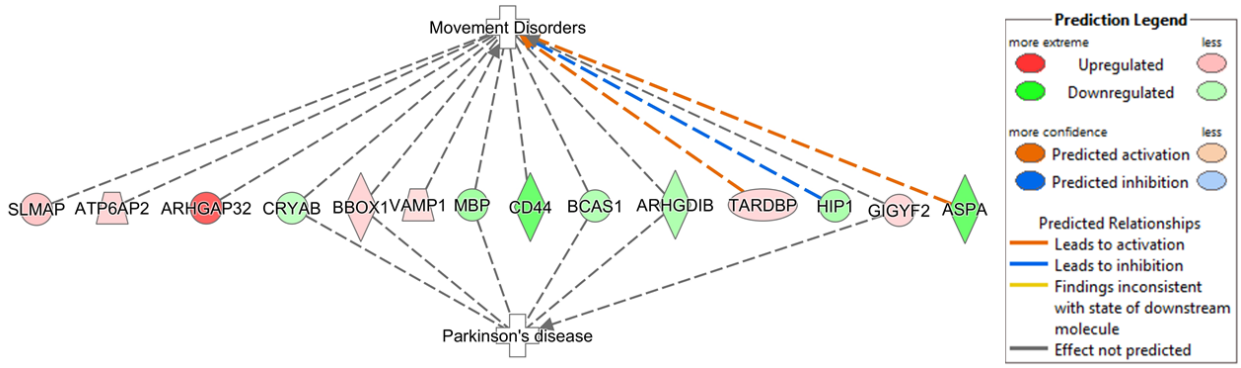

Figure 19. Ingenuity Pathway Analysis of differentially expressed proteins in PD identified a number of proteins previously associated with PD and movement disorders. IPA analysis of proteins with significant LFQ ratios in Parkinson's disease tissue identified a number of proteins previously associated with movement disorders and Parkinson's disease.

Another protein with significant expression changes in PD compared with control tissue is NAD-dependent protein deacylase sirtuin-5 (SIRT5). SIRT5 is a member of the Sirtuin family of protein deacylases, and is localized to the mitochondria [324, 325]. Increasing evidence suggests the involvement of oxidative stress and mitochondrial dysfunction in PD pathology and progression [326, 327]. Mutations in *PINK1* and *PARK2*, which are associated with familial PD, both have roles in mitochondrial function, further implicating mitochondrial dysfunction in PD pathology. The *PARK2* encoded protein Parkin can reduce ROS production and is associated with mitochondrial DNA [326]. PINK-1 is localized to the mitochondrial membrane, and has been shown to be involved in mitochondrial metabolism and dynamics, protein degradation and oxidative stress [328, 329]. SIRT5 has desuccinylase activity [330], and has been suggested to be the primary regulator of succinylated proteins in the mitochondria [331]. A previous proteomic study of liver mitochondria from *Sirt5*$^{-/-}$ knockout mice and wild type (WT) mice found hypersuccinylation of mitochondrial proteins in the absence of SIRT5, causing

disruptions in metabolic pathways including in fatty acid-oxidation, oxidative phosphorylation, and ketone body production [331]. Increased expression of the mitochondrial enzyme SIRT5 in PD brain tissue compared with control tissue further implicates mitochondrial dysfunction in PD. While SIRT5 has been shown to desuccinylate proteins in liver mitochondria [331], a mitochondrial succinyl-transferase has not been identified. Identifying the enzyme(s) responsible for mitochondrial protein succinylation could provide insight in the mechanisms regulating some of the metabolic pathways altered in the absence of SIRT5. Additionally, whether SIRT5 found in the brain has the same mitochondrial function as SIRT5 found in liver mitochondria needs to be further determined.

Gamma-aminobutyric acid receptor subunit alpha-4 (GABRA4) is a $GABA_A$ receptor, and GABA is an inhibitory neurotransmitter, reducing neuronal excitability. GABRA4 showed a 4.99-fold increase in the cortex from PD patients compared with cognitively normal controls. A previous microarray analysis identified decreased gene transcription of GABRA4 in the substantia nigra of human PD compared with control samples [332]. Consistent with these observations, another study found decreased GABRA4 mRNA in the substantia nigra by quantitative PCR (qPCR), and they also observed increased GABRA4 mRNA in the caudate nucleus of PD patients suggesting the involvement of GABAergic neurotransmission in neurodegeneration [333]. $GABA_A$ receptors and the GABAergic system have also been implicated in AD pathology, and evidence supports the involvement of GABAergic neurotransmission in the progression of neurodegeneration. Therapeutics that target GABA and the GABAergic system are promising targets for the treatment of neurodegenerative diseases such as PD [334, 335].

Huntington interacting protein 1(HIP1) is a membrane-associated protein that binds to actin and is involved in actin organization. HIP1 also functions in clathrin-mediated endocytosis and protein trafficking [336, 337]. HIP1 normally binds to the huntingtin protein [338], however this association is disrupted in Huntington's disease (HD), resulting in elevated levels of free HIP1 which is suggested to

promote neuronal apoptosis in HD. HIP1 contains a region homologous to the death effect domain found in proteins that promotes apoptosis [339]. As HIP1 is known to be involved in HD, a neurodegenerative disease that also involves protein aggregation, the increased expression of HIP1 in cortical tissue from PD brains suggests that it may contribute to PD pathology, causing impaired clathrin-mediated endocytosis and/or disrupting membrane-cytoskeletal interactions.

Functional Enrichment of Differentially Expressed Proteins in PSP

Significance A analysis of raw intensity and LFQ intensity ratios comparing PSP with control identified statistically significant changes in 55 and 61 proteins, respectively. Molecular and cellular functions that appear to be altered in PSP affected brain tissue include cellular development, growth and proliferation, cell cycle, and carbohydrate metabolism. Bioinformatic analysis also identified a number of proteins that have previously been associated with neurological disease. For example, cholinergic receptor, muscarinic 3(CHRM3), myosin, heavy chain 11 (MYH11), voltage gated sodium channel, type 4 beta subunit (SCN4B), and gamma-aminobutyric acid (GABA) A receptor, beta 1 (GABRB1) all showed significant increases in PSP compared with control samples and have previously been associated with tauopathies, particularly AD [340-343]. Olanzapine, an antagonist of CHRM3 and GABRB1, has been shown to reduce aggression and prevent psychosis in AD patients [341]. Riluzole treatment, an antagonist of SCN4B, has been shown to slow disease progression and prolong survival in amyotrophic lateral sclerosis (ALS) patients [343]. Additionally, Riluzole was evaluated in a clinical trial for the treatment of PSP, however did not have a significant effect on survival rate or the rate of functional deterioration [342]. The differential expression of GABRB1, a multi-subunit chloride channel, and SCN4B, a voltage gated sodium channel, suggest alterations in postsynaptic transmission in PSP.

The ubiquitin-proteasome system (UPS), responsible for the degradation of misfolded proteins, has been proposed to be involved in a number of neurodegenerative diseases including AD and PD. Ubiquitin-conjugating enzyme E2 G1 (UBE2G1) showed a significant 3.81 fold increase in PSP compared

with control tissue, and is involved in the protein ubiquitination pathway. UBE2G1 catalyzes the covalent attachment of ubiquitin to proteins, and is involved in polyubiquitination. UBE2G1 mediates polyubiquitination of cytochrome P450 3A4 (CYP3A4) in the liver, which oxidizes foreign molecules, such as toxins or drugs, so that they are degraded [344]. Other components of the UPS, including ubiquitin, ubiquitin activating enzyme (E1), ubiquitin conjugating enzyme UbcH7 (E2) and ubiquitin C-terminal hydrolase (UCH-L1) have been identified in Lewy bodies, primarily using immunohistochemistry staining [345, 346]. Additionally, mutations in *UCHL1* have been associated with increased susceptibility for PD [294]. UPS is a major pathway mediating the degradation of abnormal proteins, and many neurodegenerative diseases appear to involve aberrant protein aggregation, which may be a result of reduced protein clearance.

Western Blot Validation of Differentially Expressed Proteins in PD and PSP

Other proteins of interest were selected for western blot validation based on functional significance. Carbamoyl-phosphatase synthase 1 (CPS1) was selected for further validations as CPS1 is typically observed in the liver and has not been known to be significantly expressed in the brain. CPS1 is a mitochondrial enzyme that catalyzes the synthesis of carbamoyl phosphate from ammonia and bicarbonate in the first step of the urea cycle. Our proteomic analysis showed a 2.43 fold increase in PD compared with control brains, which was significant without Benjamini Hochberg FDR correction. Western blot analysis revealed only a slight increased CPS1 expression in PD and PSP (Figure 20). While CPS1 does not show a significant increase in PD or PSP and therefore may not be involved in PD pathology, its identification in the cortex suggests CPS1 functions in the brain. While ammonia is converted to urea in the liver and kidneys with the help of CPS1, in the brain excess ammonia has been found to react with glutamate and glutamine synthetase to form glutamine which is released into the blood stream to be absorbed by the liver or kidneys. Further research is needed to determine the function of CPS1 in the brain and possible involvement in neurodegenerative disease

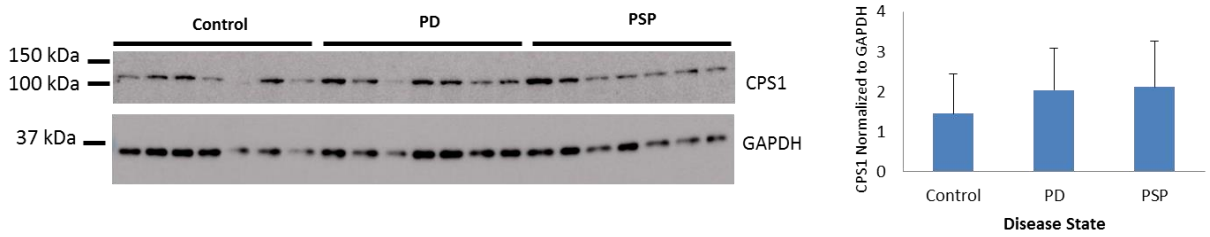

Figure 20. Protein expression levels of CPS1 levels in PD, PSP, and control human brain tissue. After normalization to GAPDH, CPS1 was not significantly increased in PD- or PSP-affected human brain tissue compared with compared with cognitively normal, control tissue.

Based on the involvement of APP in AD, and the observation of amyloid plaque pathology in PD with dementia, we further validated APP levels by western blot. Proteomic analysis showed a 1.87-fold increase in levels of APP in PD, and western blot analysis showed a significant increase in APP in both PD and PSP (Figure 21). While varying degrees of amyloid plaque pathology have been observed in the brains of PD patients [288], increased levels of APP have not been confirmed. One study comparing transgenic mouse models found that Aβ peptides enhanced α-synuclein accumulation and increased cognitive deficits [347]. Other studies have reported reduced levels of Aβ42 in the CSF of PD patients with cognitive impairment [348-350], which is consistent with observations in CSF of AD and MCI patients who have increased levels of Aβ42 in the brain [23]. The mechanisms responsible for Aβ42 accumulation in PD, and the involvement of Aβ42 in PD pathology and progression remain unclear. Increased expression of APP in PD is consistent with observations of amyloid plaque pathology in PD patients and suggests the potential involvement of APP in PD pathology.

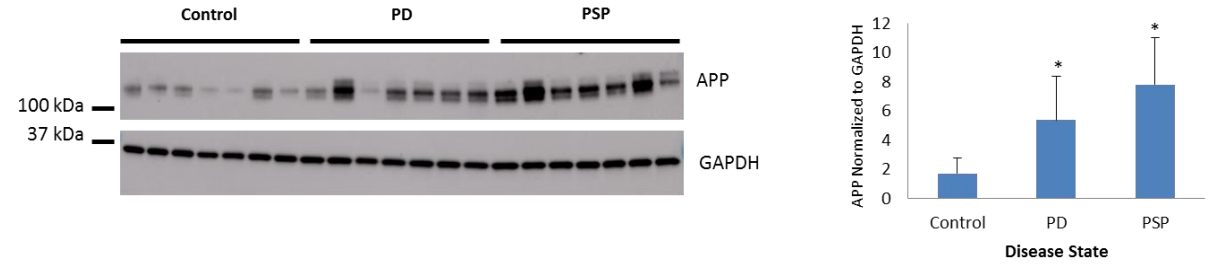

Figure 21. Increased levels of APP in PD and PSP human brain tissue. Western blot analysis shows significant increase in full length APP (6E10 antibody) in PSP- and PD-affected human brain tissue compared with control tissue. *p-value≤0.05.

Comparison of LFQ and Raw Intensity Ratios

Normalization is important for accurate label-free quantification. MaxQuant provides a label-free quantification normalization feature, which produces an 'LFQ' ratio in addition to the non-normalized, raw intensity ratios [316]. Comparing the distribution of ratios generated using raw intensity values with that generated using LFQ intensity values shows that the LFQ distribution is slightly tighter than the raw intensity ratio distribution (Figure 22).

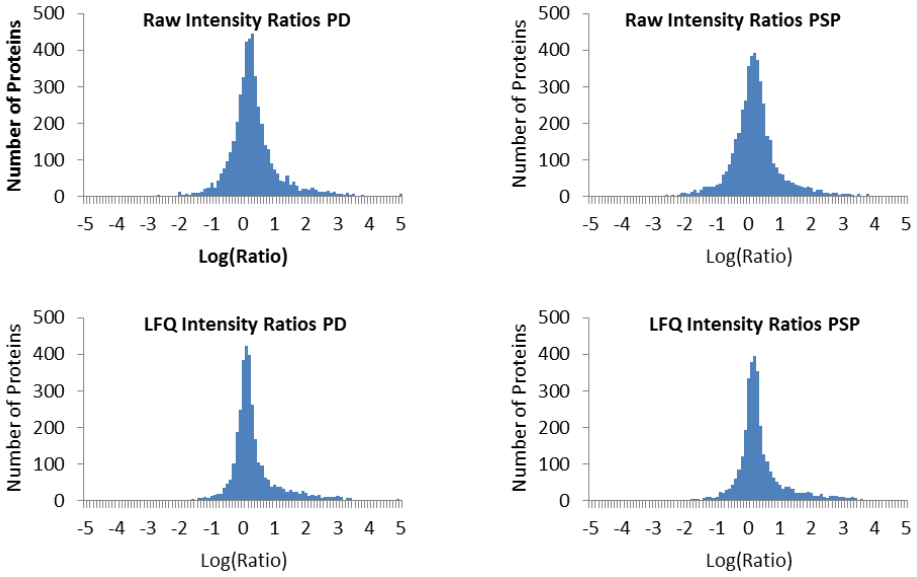

Figure 22. Distribution of LFQ and raw intensity ratios for PD and PSP compared with control human brain tissue. The distribution of log transformed ratios generated using either raw intensities (top) or LFQ intensities (bottom) for proteins identified in either PD or PSP compared with cognitively normal, control tissue. LFQ normalization increases the number of proteins with fold changes around 0, narrowing the distribution curve.

Statistical analysis of LFQ and raw intensity ratios also identifies different numbers of significant proteins, and very few of the proteins with statistically significant ratios overlap when comparing raw intensities and LFQ intensities. In some cases the ratios generated using raw intensities are very different from those generated using LFQ intensities. For example, sorting nexin-17 (SNX17) showed a 2.36-fold increase in PD and a 2.69-fold increase in PSP when using raw intensity values, which were not found statistically significant, but when using LFQ intensity values, SNX17 showed a 7.22-fold increase in PD and a 9.81-fold increase in PSP, in which case both were determined to be statistically significant.

SNX17 levels in PD, PSP, and control tissue were further examined by western blot to evaluate the differences between LFQ and raw intensity ratios. SNX17 was also selected based on its function as a member of the sorting nexin family of proteins, which are involved in membrane and protein trafficking [351]. SNX17 is localized to early endosomes and has been suggested to have a role in recycling endocytosed APP to the cell surface, preventing its degradation [352]. SNX17 knockdown in a human glioblastoma cell line resulted in decreased levels of APP and increased Aβ production [352]. Western blots analysis of SNX17 showed no change (1.05-fold) in PSP and was not significantly increased (1.27-fold) in PD (Figure 23), which are closer to the raw intensity ratios than the LFQ intensity ratios.

APP showed a 1.87-fold increase in PD and a 1.16-fold change in PSP based on raw intensity ratios, and a 1.1-fold increase in PD and a 1.09-fold change in PSP based on LFQ intensity ratios. Western blot analysis of APP levels showed a 3.15-fold increase in PD and a 4.59-fold increase in PSP, both found to be statistically significant. CPS1 showed 2.43-fold and 1.16-fold changes in PD and PSP, respectively, when using raw intensity values, and a statistically significant 4.40-fold increase in PD and 2.07-fold increase in PSP when using LFQ intensity values. Western blot analysis of CPS1 showed a 1.39-fold change in PD which is closer to the raw intensity fold change, and a 1.48-fold increase in PSP which is in-between the raw and LFQ intensity fold changes. In order to control for unequal sample loss that can occur during sample processing, we have implemented a peptide assay before loading samples onto the mass spectrometer. Additionally, we have found that loading too much material onto the RP-UPLC C18 column affects spray stability, which subsequently reduces protein identification and accurate protein quantification. Following the peptide assay, samples are resuspended to achieve a final concentration of 0.5-1µg/µl, depending on the available material, so that no more than 5µg are loaded onto the column with a 5µl injection volume.

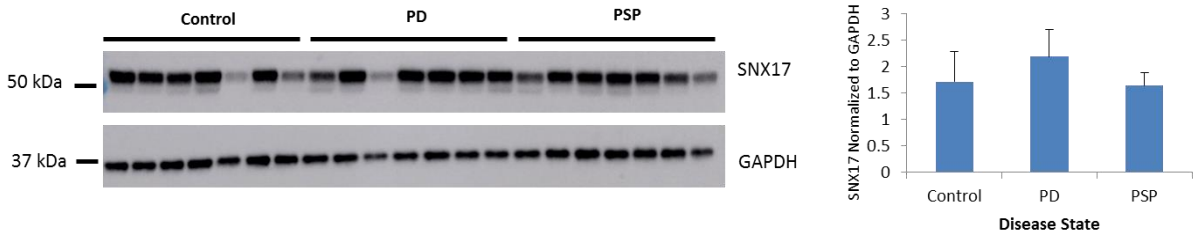

Figure 23. Protein expression levels of SNX17 levels in PD, PSP, and control human brain tissue. After normalization to GAPDH, expression ofSNX17 was slightly increased in PD- and showed no change in PSP-affected human brain tissue compared with compared with cognitively normal, control tissue.

Conclusions of PD and PSP Analyses

While multiple studies have examined protein expression changes in the substantia nigra of human PD brain tissue, we examined proteome changes in the cortex of human PD- and PSP-affected brain tissue. This appears to be the first proteomic analysis of PSP brain tissue. Identifying proteome changes in the cortex is important as cortical pathology is associated with increased cognitive decline in PD [285, 286]. Over 2000 proteins were confidently identified in PD, PSP, and control tissue, and both PD and PSP brain tissue showed significant expression changes in several proteins. Bioinformatic analysis of differentially expressed proteins identified a number of cellular and molecular functions that appear to be altered in PD and PSP. The identification of specific proteins and determination of corresponding expression changes in proteins associated with these functions provides a foundation for future mechanistic studies. Increased expression of APP was shown in PD and PSP, which further implicates the potential involvement of APP in PD. Further validation studies are required to confirm protein expression levels; however these data provide a foundation for additional mechanistic studies to determine the functional significance of protein expression changes.

Proteomic Analysis of Human AD, MCI, and Control Brains

A total of 4389 proteins were identified from three biological replicates of control, MCI, and AD human brain samples, and 3400 proteins were identified with a minimum of 2 unique peptides. Of the total proteins, 2599 proteins were identified in MCI, 2583 proteins in AD, 2689 proteins in control tissue,

all having a minimum of 2 unique peptides. Statistical analysis was performed using the Significance A outlier test, with the Benjamini-Hochberg false-discovery (FDR)-based q-value cutoff of 0.05. Ratios needed to have a q-value ≤ 0.05 for all three replicates to be considered significant. Of the identified proteins, 21 proteins were significantly altered in MCI, and 22 proteins significantly altered in AD. MCI and AD Benjamini-Hochberg significant proteins are listed in Tables 7 and 8, respectively. Alternatively, statistical analysis using Significance A with a t-test p-value cut off of 0.05 was used to determine significant expression changes for further bioinformatics analysis in Ingenuity Pathway Analysis (IPA). Again, ratios needed to have a p-value ≤ 0.05 for all three replicates to be considered significant; 220 significant differentially expressed proteins in MCI and 195 significant differentially expressed proteins in AD were submitted to IPA.

Table 7. Benjamini Hochberg FDR Significant Proteins Using LFQ Intensities: MCI vs Control. Ratios were generated using LFQ intensity values. LFQ intensity ratios were log2 transformed and analyzed using Significance A with a false discovery rate (FDR)-based q-value threshold of 0.05. Ratios with q-values ≤ 0.05 in five out of seven biological replicates were considered to be statistically significant.

Protein name	Gene name	Median Log2(LFQ Ratio)	Standard Deviation
Myosin-11	MYH11	-2.50	3.16
Hemoglobin subunit gamma-1	HBG1	3.42	0.89
Tubulin beta-6 chain	TUBB6	-1.83	0.35
Sodium/calcium exchanger 2	SLC8A2	-1.90	1.50
Microtubule-associated protein tau	MAPT	-3.59	2.02
Prolargin	PRELP	-2.16	1.34
Collagen alpha-1(XIV) chain	COL14A1	-2.26	2.90
Rab3 GTPase-activating protein catalytic subunit	RAB3GAP1	2.42	0.13
Calponin-1	CNN1	0.49	3.31
CB1 cannabinoid receptor-interacting protein 1	CNRIP1	-1.21	0.62
Guanine nucleotide-binding protein subunit gamma	GNG2	-2.00	1.82
Ubiquitin-conjugating enzyme E2 variant 1	UBE2V1	-1.35	1.06
Adenosylhomocysteinase	AHCYL2	-1.33	0.89
T-complex protein 11-like protein 1	TCP11L1	2.44	0.52
Coiled-coil domain-containing protein 92	CCDC92	2.73	0.15
Transportin-3	TNPO3	2.62	0.46
Syntaxin-6	STX6	2.22	0.31
Protein transport protein Sec24A	SEC24A	2.43	0.11

Table 8. Benjamini Hochberg FDR Significant Proteins Using Raw Intensities: MCI vs Control. Ratios were generated using raw intensity values. Raw intensity ratios were log2 transformed and analyzed using Significance A with a false discovery rate (FDR)-based q-value threshold of 0.05. Ratios with q-values ≤ 0.05 in five out of seven biological replicates were considered to be statistically significant.

Protein name	Gene name	Median Log2(Ratio)	Standard Deviation
Exportin-2	CSE1L	-3.96	0.41
116 kDa U5 small nuclear ribonucleoprotein component	SNRP116	-4.55	0.54
Sulfotransferase 1A1	SULT1A1	-3.97	0.23
Dynactin subunit 3	DCTN3	-3.84	1.29
Poly(ADP-ribose) glycohydrolase ARH3	ADPRHL2	3.76	0.36
Tectonin beta-propeller repeat-containing protein 1	TECPR1	3.55	0.32
Putative phospholipase B-like 2	PLBD2	3.52	0.47
Tubulin beta-6 chain	TUBB6	-3.54	0.50
Sodium/calcium exchanger 2	SLC8A2	-2.95	2.13
Diablo homolog, mitochondrial	DIABLO	-2.71	0.24
Zinc transporter 3	SLC30A3	-3.82	1.43
Trans-2-enoyl-CoA reductase, mitochondrial	MECR	-2.86	2.40
Microtubule-associated protein tau	MAPT	-3.74	2.06
Collagen alpha-1(XII) chain	COL12A1	-4.42	3.25
Fibronectin	FN1	0.10	4.30
Vacuolar protein sorting-associated protein 13A	VPS13A	-2.72	1.72
Coagulation factor XIII A chain	F13A1	-3.97	2.56
Carbonyl reductase [NADPH] 3	CBR3	-3.18	2.59
40S ribosomal protein S11	RPS11	-2.69	0.94
Golgin subfamily A member 3	GOLGA3	5.20	0.80
Protein TFG	TFG	-2.69	2.08
Methylthioribose-1-phosphate isomerase	MRI1	-2.77	0.55
Ig alpha-1 chain C region	IGHA1	-3.97	0.33
1-acyl-sn-glycerol-3-phosphate acyltransferase epsilon	AGPAT5	-4.39	0.18
Beta-2-syntrophin	SNTB2	-3.20	1.23
Adenylate cyclase type 5	ADCY5	-2.84	0.74
Histone H2A.V	H2AFV	2.74	0.20
VPS10 domain-containing receptor SorCS2	SORCS2	3.36	0.37
Protein-arginine deiminase type-3	PADI3	3.18	0.40
39S ribosomal protein L22, mitochondrial	MRPL22	-3.51	0.26
Protein DEK	DEK	2.83	1.25
Peptidyl-glycine alpha-amidating monooxygenase	PAM	3.50	1.13
Apoptosis regulator BAX	BAX	3.23	0.39
Semaphorin-4D	SEMA4D	-3.15	0.26
Isovaleryl-CoA dehydrogenase, mitochondrial	IVD	-2.97	1.79
Espin	ESPN	-3.07	0.94
Sodium-coupled neutral amino acid transporter 3	SLC38A3	3.13	0.78

Table 9. Benjamini Hochberg FDR Significant Proteins Using LFQ Intensities: AD vs Control. Ratios were generated using LFQ intensity values. LFQ intensity ratios were log2 transformed and analyzed using Significance A with a false discovery rate (FDR)-based q-value threshold of 0.05. Ratios with q-values ≤ 0.05 in five out of seven biological replicates were considered to be statistically significant.

Protein name	Gene name	Median Log2(LFQ Ratio)	Standard Deviation
Synaptophysin	SYP	-2.09	1.52
ATP synthase subunit delta, mitochondrial	ATP5D	-3.54	0.41
Guanine nucleotide-binding protein G(I)/G(S)/G(O) subunit gamma-2	GNG2	-2.44	0.77
Transgelin	TAGLN	-1.83	0.93
Prolargin	PRELP	-2.61	1.39
Synapsin-3	SYN3	-1.96	1.20
Myelin P2 protein	PMP2	-1.48	1.19
Coiled-coil-helix-coiled-coil-helix domain-containing protein 3	CHCHD3	-1.70	1.03
Perilipin-3	PLIN3	5.79	0.74
Iron-sulfur cluster assembly enzyme ISCU, mitochondrial	ISCU	-2.44	1.27

Table 10. Benjamini Hochberg FDR Significant Proteins Using Raw Intensities: AD vs Control. Ratios were generated using raw intensity values. Raw intensity ratios were log2 transformed and analyzed using Significance A with a false discovery rate (FDR)-based q-value threshold of 0.05. Ratios with q-values ≤ 0.05 in five out of seven biological replicates were considered to be statistically significant.

Protein names	Gene names	AD Median Log2(Ratio)	AD Standard Deviation
Tubulin beta-6 chain	TUBB6	-6.10	1.66
Histone H2A.V;Histone H2A.Z;Histone H2A	H2AFV	4.30	0.55
Peroxisomal acyl-coenzyme A oxidase 3	ACOX3	4.47	0.52
Nuclear pore membrane glycoprotein 210	NUP210	4.77	0.83
Prolargin	PRELP	-4.26	1.68
Calponin-1	CNN1	-4.69	0.28
Zinc transporter 3	SLC30A3	-3.56	0.86
Trans-2-enoyl-CoA reductase, mitochondrial	MECR	-3.41	2.24
Brain acid soluble protein 1	BASP1	-3.75	0.02
Iron-sulfur cluster assembly enzyme ISCU, mitochondrial	ISCU	-4.06	3.15
Poly(ADP-ribose) glycohydrolase ARH3	ADPRHL2	3.77	0.69
Methionine--tRNA ligase, cytoplasmic	MARS	4.30	2.66
Fatty-acid amide hydrolase 1	FAAH	3.94	0.38
Translational activator GCN1	GCN1L1	4.32	0.29
Cartilage acidic protein 1	CRTAC1	-3.16	1.41
Trifunctional purine biosynthetic protein adenosine-3	GART	4.05	0.38
WD repeat-containing protein 61	WDR61	5.14	1.04
Calcium-binding and coiled-coil domain-containing protein 1	CALCOCO1	5.83	1.08
Gamma-aminobutyric acid receptor-associated protein-like 2	GABARAPL2	-4.33	2.40
Microfibrillar-associated protein 2	MFAP2	-9.43	0.21
Lanosterol 14-alpha demethylase	CYP51A1	3.54	0.72
26S proteasome non-ATPase regulatory subunit 8	PSMD8	-4.57	1.21
Alpha-1-antichymotrypsin;Alpha-1-antichymotrypsin His-Pro-less	SERPINA3	-3.03	2.02
60S ribosomal protein L3	RPL3	-3.58	0.13
Endothelin B receptor-like protein 2	GPR37L1	-3.14	2.67
SLIT-ROBO Rho GTPase-activating protein 2C	SRGAP2C	-2.42	1.92
DNA polymerase subunit gamma-1	POLG	-4.85	1.28
Heat shock protein beta-6	HSPB6	5.19	1.10
Guanine nucleotide-binding protein subunit gamma	GNG10	4.83	0.14
Proteasome subunit beta type;Proteasome subunit beta type-6	PSMB6	-4.20	0.31
Coronin-7	CORO7	3.23	0.22
Rabenosyn-5	ZFYVE20	3.12	0.72
Proteasome subunit beta type	PSMB8	4.72	0.51
Potassium-transporting ATPase alpha chain 2	ATP12A	-2.97	0.37

Mass spectrometry analysis demonstrated an increase in APP expression, while western blot analysis showed relatively unchanged levels of full length APP (FL-APP) and a significant increase in Aβ peptide (Figure 24). To further investigate this discrepancy, sequence coverage of FL-APP from mass spectrometry was examined. While no coverage of the Aβ region was observed in non-AD samples, peptides from the Aβ region were identified in MCI and AD samples (Figure 24). As the Aβ region of APP is hydrophobic and near the transmembrane domain, it can be difficult to obtain sequence information from this region by mass spectrometry, and the presence of Aβ peptides in MCI and AD samples are likely contributing to the levels of FL-APP quantified by mass spectrometry, suggesting increased expression in these samples.

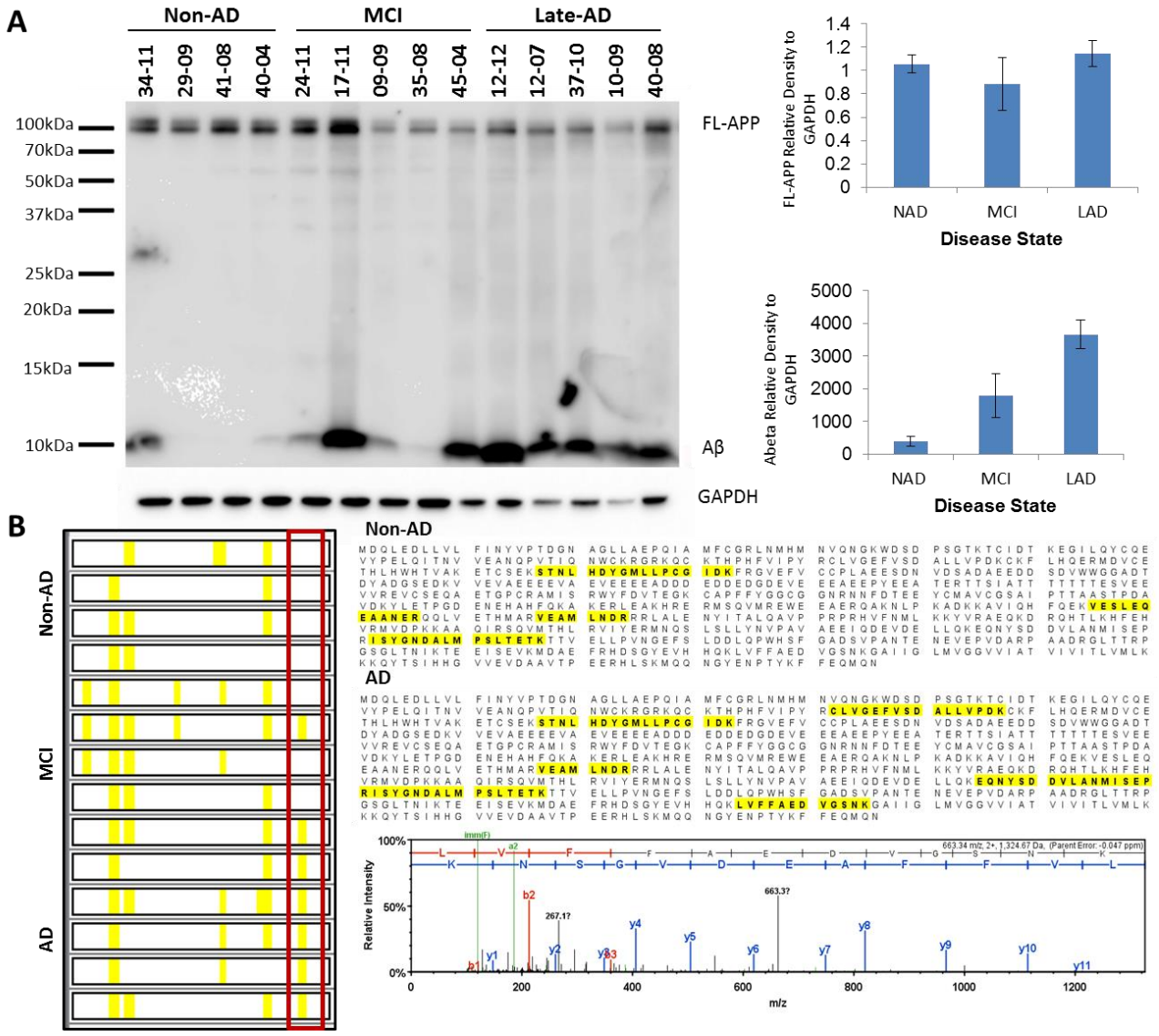

Figure 24. Analysis of APP and Aβ levels in MCI, AD, and non-AD control brains. (A) Western blot analysis of human brain samples show that while full-length APP (FL-APP) levels are not significantly altered in AD or MCI compared with non-AD samples, there is increased Aβ peptide. **(B)** LC-MS/MS analysis of the same human brain samples showed no coverage of the Aβ peptide region of APP (outlined in red) in non-AD samples (top), however peptides were identified in the Aβ region of APP in MCI and AD samples (middle). Annotated MS/MS spectrum of LVFFAEDVGSNK peptide found in Aβ region of APP (bottom).

Functional Enrichment Shows AD and MCI Significant Proteins

Bioinformatic analysis revealed several proteins associated with molecular and cellular functions in AD including post-translational modification, cell cycle, and lipid metabolism. Some of the molecular and cellular functions enriched in MCI included cell death and survival, protein degradation, and protein

synthesis. Both AD and MCI had significant proteins involved in mitochondrial dysfunction and related oxidative phosphorylation as well as EIF2 signaling. Pathway analysis also predicted changes in activity of upstream regulators based on observed protein expression changes. Activation of APP was predicted in MCI (z-score 0.574) and AD (z-score 2.434) based on significant protein expression changes, which is consistent with the disease state (Figure 25). Pathway analysis also predicted the activation of interferon gamma (IFN-gamma) in MCI (z-score 1.221) and AD (z-score 3.087) based on increased expression of several proteins consistent with IFN-gamma activation including intracellular adhesion molecule 1 (ICAM1) [353], ubiquitin-like modifier activating enzyme 2 (UBA2) [354], and ubiquitin-conjugating enzyme E2L 6 (UBE2L6) [355]. The predicted activation of IFN-gamma is consistent with inflammation observed in AD. Interestingly, predicted activation z-scores for both APP and IFN-gamma are not significant in MCI but are significant in AD, suggesting these processes are affected early and are affected during disease progression.

Proteomic analysis identified significant expression changes in fatty acid amide hydrolase (FAAH) in MCI (3.78-fold) and AD (15.36-fold) compared with non-AD, control tissue. FAAH, responsible for the degradation of endocannabinoids in the endocannabinoid system (reviewed in [356]), was significantly increased in AD compared with control tissue. Increased expression and hydrolase activity of FAAH has been observed in glia surrounding amyloid plaques in AD [357], and in blood from AD patients [358]. Supporting a role for FAAH in AD neurodegeneration and pathology development, studies in rats had shown that inhibition of FAAH enhances memory formation [359]. The endocannabinoid system has previously been implicated in AD. Cannabinoid receptors have been shown to be protective against excitotoxicity in mutant mice [360], and cannabinoids have been shown to reduce oxidative stress, and be neuroprotective against Aβ-induced toxicity [361]. Elevated levels of FAAH in the cortex of MCI and AD tissue further supports its involvement in AD pathology, and increasing evidence suggests that dysregulation of the endocannabinoid system may have a role in memory impairment.

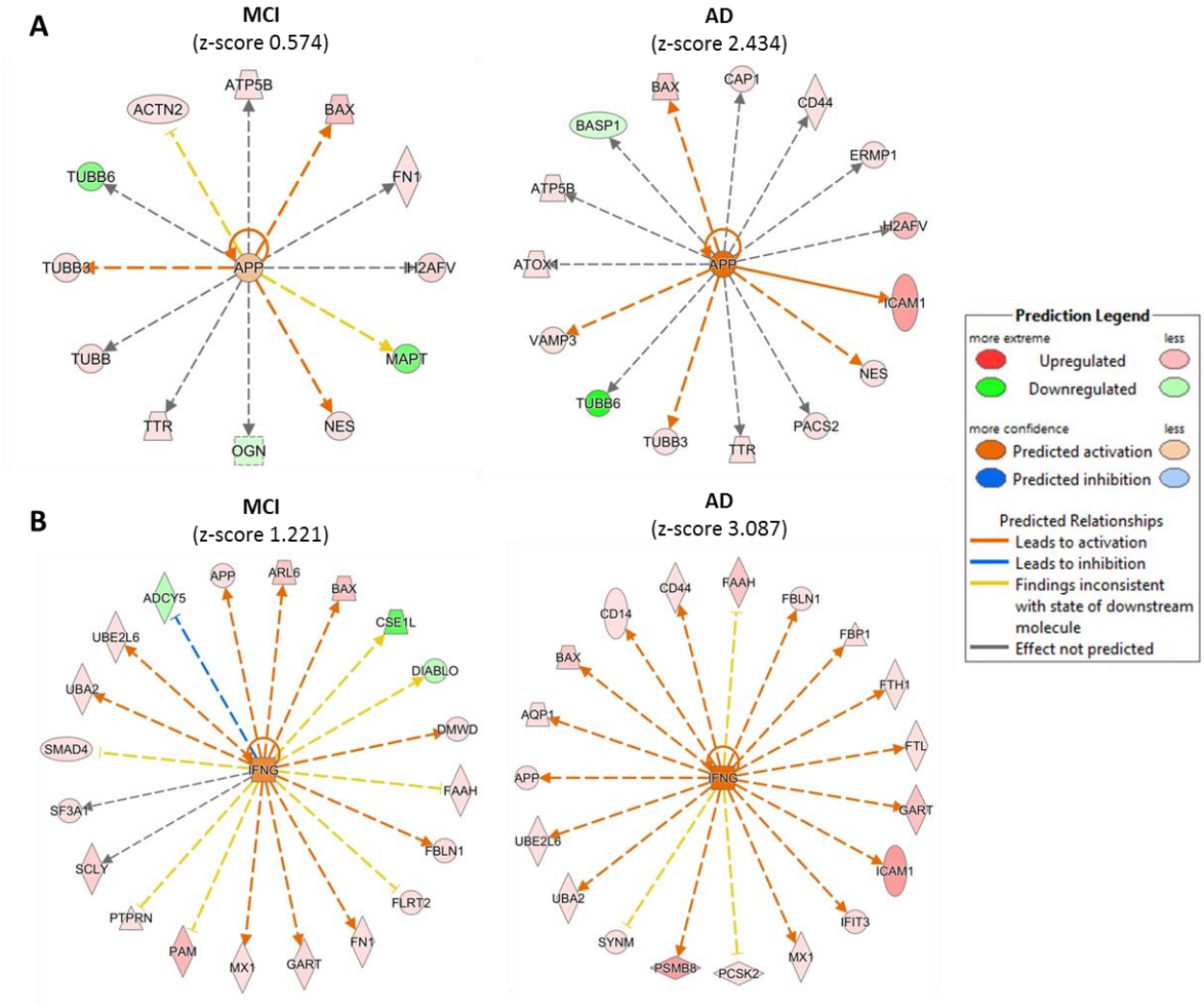

Figure 25. Ingenuity Pathway Analysis predicted activation of APP and IFN-gamma in MCI and AD based on observed protein expression changes. Activation of APP and IFNG were predicted in both MCI (z-score 0.574, and 1.221, respectively, and in AD (z-score 2.434, and 3.087, respectively). APP and Aβ are known to play key roles in AD. The predicted activation of IFNG, a cytokine secreted from immune cells in response to pathogen such as inflammatory proteins, is consistent with inflammation often observed in AD.

Pathway analysis also predicted inhibition of the upstream regulator rapamycin-insensitive companion of mTOR (RICTOR) in AD (z-score 1.633) based on proteins with significant expression changes (Figure 26). RICTOR is a subunit of the mTORC2 complex, a serine/threonine kinase involved in cytoskeletal organization and cell survival. It was previously shown that the RICTOR-mTORC2 complex is involved in cytoskeletal dynamics. Knockdown of RICTOR in HeLa cells resulted in the formation of thick actin bundles, and it was speculated that RICTOR-mTOR regulation of cytoskeletal organization is

mediated by PKCα activity [362]. The RICTOR-mTOR complex has also been shown to phosphorylate Akt at Ser473 and facilitate phosphorylation at Thr308, both phosphorylation events are required for activation [363]. Akt is known to have a role in cell cycle by preventing GSK-3β-mediated phosphorylation and degradation of cyclin D1 [225]. Phosphorylation of Akt at Ser477 and Thr479 by mTORC2 or Cdk2/cyclin A has been shown to trigger Akt activation by promoting mTORC2 phosphorylation of Ser473 [224]. Additionally, it was shown that Akt activation regulates cell cycle progression [224], suggesting the involvement of mTORC2 signaling in the cell cycle. The mTOR complex has also been suggested to be involved in Aβ oligomer induced neuronal cell cycle re-entry events through the PI3K-Akt-mTOR pathway [364]. Finally, Aβ treatment of mouse neuroblastoma cells downregulated mTOR activation, and decreased mTOR activity was also observed in cortex of PS/APP transgenic mice and lymphocytes of human AD patients [365]. These findings are consistent with our data suggesting inhibition of RICTOR, a member of the mTORC2 complex, in AD-affected human brain tissue, suggesting this effect may be mediated by APP or Aβ. The predicted inhibition of RICTOR-mTORC2 may also be involved in aberrant cell cycle re-entry and progression that occurs during AD.

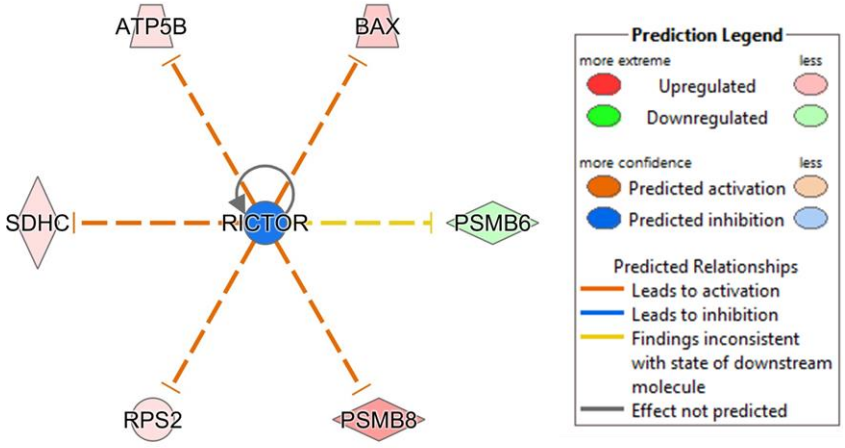

Figure 26. Ingenuity Pathway Analysis showing predicted inhibition of upstream regulator RICTOR in AD based on significantly differentially expressed proteins. (Rapamycin-insensitive companion of mTOR) RICTOR (z-score -1.633 in AD and MCI) is a subunit of the mTORC2 complex, which promotes cell survival through Akt activation and is involved in cytoskeletal dynamics through activation of PKCα.

Though these human brain samples were not enriched for phosphopeptides, phosphorylation of serine, threonine, and tyrosine was included in the database search parameters as a variable modification to determine if any changes in phosphorylation could be identified. While only a small number of phosphorylated proteins were identified, decreased phosphorylation of NAD-dependent protein deacetylase sirtuin-2 (Sirt2) at Ser368 was observed in AD compared with control samples. Annotated MS/MS spectra of the phosphorylated and non-phosphorylated Sirt2 peptide in control and AD brain, respectively, are shown in Figure 27. Reduced phosphorylation of Sirt2 has previously been observed in the hippocampus of AD patients [207], and this phosphoproteomic study provides site-specific information for the observed decrease in phosphorylation. Sirt2 is phosphorylated at Ser368 by CDK1/cyclin B at the G2/M transition, and this phosphorylation event is required for regulating the delay in cell cycle progression [366]. When Sirt2 is constitutively phosphorylated at Ser368 decreased hyperploidy is observed compared with wild type Sirt2, demonstrating the importance of this modification in regulating the mitotic checkpoint [366]. Chromosome missegregation and polyploidy [208], as well as binucleation of hippocampal neurons [367] observed in AD brains further suggest impaired mitotic checkpoint regulation in AD. The observed reduction in Sirt2 Ser368 phosphorylation in AD compared with control brains suggests dysregulation of the mitotic checkpoint, and may contribute to the increased polyploidy observed in the brains of AD patients.

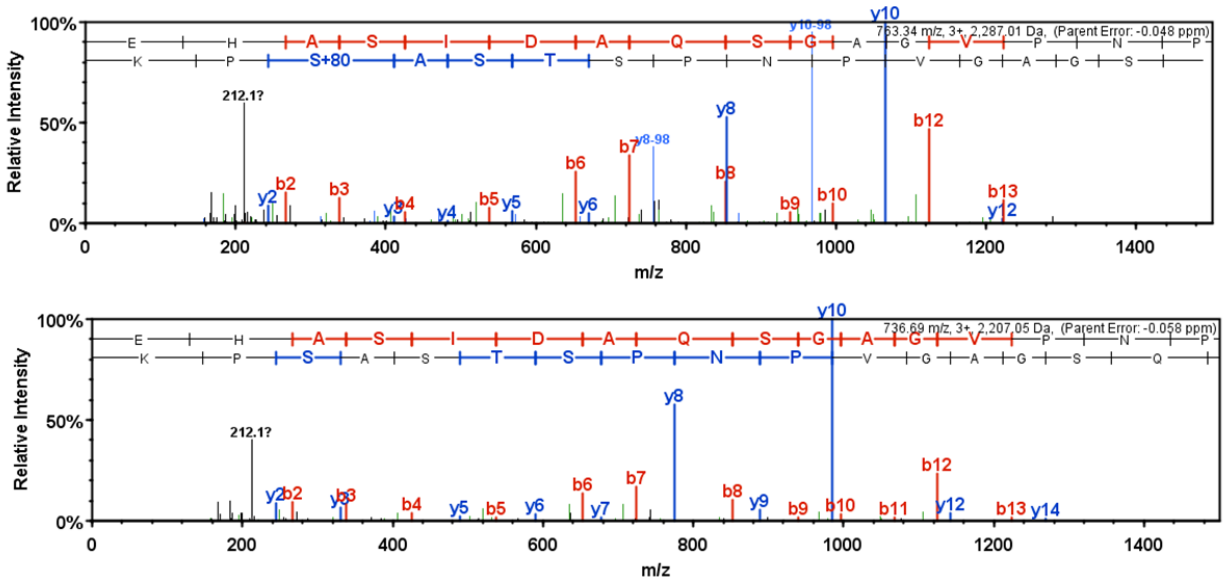

Figure 27. Mass spectrometry identified decreased phosphorylation of Sirt2 at Ser368. Annotated MS/MS spectra of NAD-dependent protein deacetylase sirtuin-2 (Sirt2) in non-AD (top) with phosphorylation at Ser368 and AD (bottom) lacking phosphorylation at Ser368.

Comparison of B103 Cell Model and Alzheimer's Disease Human Tissue Analyses

To further validate findings from our initial proteomic analysis of APP-null B103 and APP695-expressing B103-695 cells, and to identify changes in human AD brain that may be attributed to APP expression, we compared the each dataset. While a number of proteins were identified in each dataset, five proteins showed significant expression changes (p-value≤0.05) in both B103-695 cells and AD human brain tissue. Of the five proteins with significant expression changes in B103-695 cells and AD human brain tissue, four of them demonstrated the same trend in expression change; tubulin polymerization promoting protein family member 3 (TPPP3), Acyl-CoA-binding protein (ACBP), brain acidic soluble protein 1 (BASP1), and glycolipid transfer protein (GLTP). TPPP3, also known as p20, is a tubulin polymerization protein that has been shown to bind and stabilize microtubules [368]. TPPP3 showed a 3.34-fold increase in human AD cortex, and a 1.94-fold increase in B103-695 cells. Previously, a DNA microarray analysis determined increased expression of TPPP3 in the hippocampus of human AD brain compared with control brains [369]. TPPP3 has also been reported to be necessary for proliferation and cell cycle progression in HeLa cells [370]. Microtubule polymerization has a crucial role

in mitosis, and TPPP3 may be involved in regulating spindle formation [370]. ACBP is also known as diazepam-binding inhibitor (DBI) based on its ability to modulate diazepam binding to the benzodiazepine recognition site on the GABA type A receptor [371]. ACBP showed a 2.69-fold increase in AD and a 2.04-fold increase in B103-695 cells. While our study found increased ACBP levels in the cortex, another proteomic analysis of hippocampal tissue observed decreased ACBP levels in human AD compared with control tissue [372]. Elevated levels of ACBP have been observed in the CSF from patients with AD and PD with dementia [373]. These evidence suggest that ACBP may be regulated in a region-specific manner during AD, and may have a role in other neurodegenerative diseases as well. BASP1 showed decreased expression and GLTP showed increased expression in both B103-695 cells compared with B103 cells and human AD cortex compared with control non-AD cortex. The increased expression of TPPP3, ACBP, and GLTP, and the decreased expression of BASP1, in both APP695-expressing cells compared with APP-null cells and human AD tissue, suggests that these proteins and their associated functions are likely regulated by APP or a metabolite of APP. Additionally, as the expression changes observed in human AD tissue are consistent with those observed in APP695-expressing cells, it also suggests that these changes are mediated in an APP695-dependent manner.

Conclusion of AD and MCI Analyses

The predicted activation of APP and IFN-gamma in MCI and further activation in AD, confirm the disease state of the MCI and AD brain tissue samples, and also further support the involvement of APP and IFNG in AD progression. Both APP and IFN-gamma were predicted to be activated in MCI, suggesting that they are affected early during neurodegeneration, and are not just associated with late-stage AD. Differential phosphorylation of Sirt2 and predicted inhibition of RICTOR may have implications in cell cycle deregulation, providing further evidence that aberrant cell cycle re-entry may be involved in AD pathogenesis. Elevated levels of FAAH may represent a disease-specific protein biomarker, as increased FAAH was observed in AD and MCI but not PD or PSP brain tissue. Furthermore,

the findings that FAAH is also increased in the blood samples of AD patients imply that this may serve as a biomarker for early detection of AD. In addition to being a potential biomarker of AD, the endocannabinoid system may have a more complex role in cognitive impairment and AD pathology. Further investigation to further determine the functional significance of the endocannabinoid system in AD would provide insight into the potential neuroprotective effects of cannabinoids in preventing neurodegeneration and dementia [374]. These comprehensive datasets provide information about changes in signaling pathways in MCI and AD brains as well as insight into the mechanisms involved in MCI and AD progression and pathology.

Chapter 5 – Conclusions and Future Directions

Conclusions

Overview

The mechanisms involved in the pathology and progression of dementia in a number of neurodegenerative diseases, including AD, PD, and MCI, are poorly understood. While the neuropathology, such as the presence of amyloid plaques, neurofibrillary tangles, and Lewy Bodies, have been described, the precise molecular mechanisms leading to their deposition and their contribution to the progression of cognitive decline are unclear. As life expectancy has increased, a greater number of people are living into their 80s and 90, and as 'the baby boomer generation' is reaching the age of 65, the medical and financial burdens are growing substantially. The estimated cost of health care and hospice for people with AD in the United States in 2015 is $226 billion, which is expected to rise with the increasing elderly population [1]. There is an increasing need for the identification of reliable biomarkers and development of better treatments and preventative strategies for AD and other neurodegenerative diseases such as PD.

A significant amount of research has focused on the function of amyloid precursor protein (APP) and its role in AD pathology; however, its primary physiological function as well as its involvement in neurodegeneration and AD still need to be further understood. To investigate the impact of APP expression on the proteome, we used mass spectrometry-based proteomics to perform a number of global scale analyses beginning with a cell model of AD, examining both the proteome and phosphoproteome. We then further compared the proteomes of human brain tissues affected by diverse neurodegenerative disorders, including mild cognitive impairment (MCI), Alzheimer's disease (AD), Parkinson's disease (PD), and progressive supranuclear palsy (PSP), with cognitively normal,

control tissue. APP-null B103 and APP695 expressing B103-695 cells were used as a cell model to study APP function, and SILAC-labeling was used for relative quantitation of protein expression changes in both the global proteomic and phosphoproteomic profiles. When working with human tissue, a label-free quantitative approach was used, relying on peptide ion intensity values to determine protein abundance.

Proteomic analysis of SILAC-labeled B103 and B103-695 cells identified nearly 3000 proteins, and proteins with significant expression changes were shown to be involved in cellular assembly and organization, cell cycle, protein folding, and post-translation modification. Increased Ras and y-synuclein expression were further validated by western blot analysis in human AD, MCI, and non-AD brain tissue (Figure 5). Increased y-synuclein expression during MCI may indicate an early molecular change during neurodegeneration, while increased expression of Ras in MCI and further increase in late AD provides further evidence that Ras likely has a role in AD progression. Phosphoproteomic analysis of SILAC labeled B103 and B103-695 cells confidently identified over 2000 phosphorylation sites. Several of the phosphoproteins identified have implications in neurological disease, as well as cellular assembly and organization, and cell growth and proliferation. Increased phosphorylation of Histone H4 at Ser47 was further validated in human MCI and AD tissue (Figure 18), and Aβ treated rat primary cortical neurons (Figure 15). Increased phosphorylation of PCTAIRE-2 (Cdk17) and PCTAIRE-3 (Cdk18) were also found, which led us to further examine their expression in B103 and B103-695 cells (Figure 12), primary neurons (Figure 15), and human tissue (Figure 18).

Label-free quantitative proteomics was then used to investigate human brain tissue from multiple neurodegenerative diseases. Proteomic analysis of human brain tissue from MCI, AD, and cognitively normal, control samples identified a total of 3400 proteins; 2583 in AD, 2599 in MCI, and 2689 in control tissue. A number of proteins with significant expression changes in both MCI and AD are associated with cellular assembly and organization, and development. Bioinformatic analysis also

determined a number of proteins with significant expression changes involved in cell growth and proliferation in AD and cellular morphology in MCI. Identifying significant expression changes in proteins involved in cellular assembly, organization, and morphology, growth and proliferation in APP695-expressing cell model compared with APP-null cells, as well as human MCI and AD tissue suggests that these molecular changes occur early in disease progression and may be mediated by APP. Additionally, it implicates the involvement or dysregulation of structural proteins in disease pathology. A separate proteomic analysis of human tissue from PD, PSP, and control brains identified just over 3800 proteins, 3329 in PD, 3237 in PSP, and 3324 in control tissue. Bioinformatic analysis of proteins with significant expression changes identified a number of proteins involved in protein synthesis and lipid metabolism in PD and cell cycle, growth and proliferation in PSP.

Each comprehensive proteomic dataset identified a number of proteins with significant expression changes and bioinformatics analysis determined potentially affected cellular and molecular functions. Five proteins showed consistent, statistically significant expression changes in the B103 and B103-695 cell model of AD, as well as human AD tissue, increasing the likelihood that these proteins are involved in AD and potentially mediated by APP695. While some of the molecular and cellular functions were unique among neurodegenerative diseases, there also appears to be some overlap of affected functions, suggesting that there may be more common mechanisms among different forms of neurodegeneration.

Inflammation, Protein Aggregation, and Cell Cycle in Neurodegeneration

Analyses of human brain tissue from a number of different neurodegenerative diseases, including MCI, which often progresses to more serious neurodegeneration and dementia, identified a number of significantly altered proteins involved in inflammation. Inflammation, oxidative stress and mitochondrial dysfunction are hypothesized to be involved in AD [212, 213] and PD [375]. Activated microglia are also observed in both AD [10-12, 376] and PD [376, 377] further supporting activation of

the inflammatory response. Pathway analysis of significant proteins in MCI and AD predicted activation of interferon-γ based on increased expression of several proteins including APP, BCL2-associated X protein (BAX), ubiquitin-like modifier activating enzyme 2 (UBA2), and ubiquitin-conjugating enzyme E2L 6 (UNE2L6) in both MCI and AD (Figure 24). Pathway analysis also predicted the activation of the inflammatory cytokines tumor necrosis factor (TNFα) (z-score 2.670) and interleukin 1α (IL1A) (z-score 2.371) in AD, suggesting that inflammation increases during the progression from MCI to AD. These results are consistent with previous reports supporting the involvement of inflammation in AD, and provide specific proteins with altered expression that may contribute to this process. While it is not fully understood whether inflammation is a cause or result of other pathologies, the predicted activation of inflammatory proteins in MCI and increasing in AD, suggests that the inflammatory response is affected early and likely contributes to progression of neuropathology and cognitive decline.

Some of the clinical and pathological characteristics of multiple neurodegenerative diseases overlap. For example, abnormal protein aggregation occurs in AD with the aggregation of Aβ42 into amyloid plaques, as well as PD and LBD, with aggregation of α-synuclein into Lewy Bodies. Additionally tau-neurofibrillary tangles are observed in AD, PSP, and other tauopathies such as frontotemporal lobe dementia. The occurrence of aberrant protein aggregation in a number of common neurodegenerative conditions leads to the idea that protein synthesis, folding, or clearance is likely impaired, and supports the involvement of some more common pathologies leading to cognitive decline. When considering the abnormal accumulation and aggregation of peptides and proteins, it is important to consider the ubiquitin proteasome system (UPS), which is responsible for degrading modified, misfolded, or denatured proteins. Dysregulation of the UPS has previously been implicated in a number of neurodegenerative diseases [378], including AD [379] and PD [380], and our data also support this idea. Several proteins that function in the UPS were identified in the analysis of human tissue, and at least one ubiquitin-related protein showed a statistically significant change after FDR correction in PSP, AD,

and MCI human tissue: Ubiquitin-conjugating enzyme E2 G1 (UBE2G1) showed a 3.81-fold increase in PSP, E3 ubiquitin-protein ligase Itchy homolog (ITCH) showed a 7.82-fold increase in AD, and E3 ubiquitin-protein ligase UBR3 (UBR3) showed a 7.37-fold increase in MCI. Decreased phosphorylation of deubiquitinating protein VCIP135 at Ser473 was observed in APP695 expressing cells compared with APP-null cells, however the significance of phosphorylation at this site is unknown. Whether abnormal protein aggregation occurs as a result of UPS dysfunction, or whether UPS-related proteins are found within Lewy Bodies as a result of failed clearance is still unclear. Increased activity of the UPS has been associated with activation of the inflammatory response [381, 382]. Understanding the precise molecular mechanisms mediating protein aggregation and UPS activity and the role of inflammation could provide novel therapeutic targets as these processes are likely involved in multiple neurodegenerative diseases.

Previous studies have reported the aberrant expression of cell cycle proteins in MCI and AD suggesting the involvement of neuronal cell cycle re-entry in neurodegeneration [104-108]. Additionally, APP and Aβ have been suggested to promote neuronal cell cycle re-entry [113]. Proteomic analysis of the B103 and B103-695 neuroblastoma cell model of AD identified several proteins involved in cell cycle with altered expression in APP695 expressing cells compared with APP-null cells. The cell cycle was also implicated as an altered cellular function in PSP compared with control tissue. Analysis of proteins with significant expression changes in human AD brain tissue predicted inhibition of RICTOR, a component of the mTORC2 complex that activates Akt in a cell cycle dependent manner [224]. Reduced phosphorylation of NAD-dependent protein deacetylase sirtuin-2 (Sirt2) at Ser368 was also found in human AD brain, which is required for regulation the G2/M checkpoint [366]. Both RICTOR and p-Sirt2 (Ser368) have implications in aberrant cell cycle re-entry and progression. Increased expression of TPPP3, a tubulin polymerization promoting protein previously shown to be involved in cell cycle progression, was observed in both APP695-expressing cells and human AD tissue. These findings

suggest that TPPP3 may be involved in neuronal cell cycle progression, and may be mediated by APP695. These findings provide further evidence that aberrant cell cycle re-entry and progression are involved in AD, PD, and PSP, further implicating cell cycle dysregulation in neurodegeneration.

Increased amyloidogenic processing of APP results in increased levels of Aβ42, which forms amyloid plaques in AD, and to a lesser extent in MCI. Amyloid pathology has also been observed in the brains of PD patients with dementia, and the co-existence of α-synuclein pathology and amyloid plaques are associated with earlier onset of dementia and shorter survival [287, 288]. Additionally, our data suggest increased expression of APP in the cortex of individuals with PD and PSP (Figure 23). These findings suggest that APP processing and amyloid pathology can promote cognitive decline in MCI, AD, as well as PD. APP and Aβ have been shown to promote the inflammatory response and promote neuronal cell cycle re-entry [113], which may be involved in MCI, PSP, and PD in addition to AD pathology. The precise mechanism by which APP and/or Aβ induces activation of inflammatory pathways and promotes aberrant neuronal cell cycle re-entry need to be further understood; however, these datasets present significant protein expression changes that may contribute to the specific molecular changes. Whether APP or a metabolite of APP cause changes in protein folding or the UPS needs to be further determined; however, understanding changes in these functions could provide insight into the pathology of a number of neurodegenerative diseases. While Aβ42 and amyloid plaques have been considered major contributors to AD pathology, increasing evidence suggests that soluble Aβ oligomers may be responsible for promoting disease pathology [66]. Moving forward, it is important to consider the potential involvement of other Aβ peptides, oligomers and metabolites of APP in AD pathology. The impact of other APP metabolites and Aβ species on the inflammatory response, cell cycle re-entry and progression, as well as protein misfolding, may provide additional insights into the involvement of APP in neurodegeneration, thereby enabling identification of new targets for therapeutic strategies.

Future Directions

Cell Cycle and Inflammation Studies in a Cell Model of Alzheimer's Disease

Global scale proteomic analysis of a cell model of AD was published in Electrophoresis (2012). Further experiments were performed to investigate protein expression changes associated with cell cycle and inflammation. Only B103-695 cells were assessed with and without cell cycle inhibitors and the observed changes in protein expression under this condition should be attributed to cell cycle inhibition. While expression changes in proteins associated with cell cycle inhibition were observed, a larger study comparing APP-null B103 cells with and without cell cycle inhibitor treatment would be beneficial to determine APP-mediated changes during the cell cycle. Additionally, cell synchronization using aphidicolin treatment and serum starvation synchronizes cells in S phase or G_0, respectively, and flow cytometry experiments using fluorescence activated cell sorting (FACS) analysis can be used to confirm synchronization and monitor progression through the cell cycle. FACS analysis measures DNA content after staining cells with the intercalating agent propidium iodide, and fluorescence can be measured using a flow cytometer. As cells progress from G1 to S phase and G2/M, their DNA content increases until the cell divides, and so the measured fluorescence intensity can be used to assess whether cells are in G1, S, or G2/M phase of the cell cycle. Optimization of cell synchronization in B103 and B103-695 cells to ensure cell populations are synchronized would provide more information about APP-mediated protein expression changes at specific stages of the cell cycle.

B103 and B103-695 cells were also treated with lipopolysaccharide (LPS) to study the impact of inflammation on protein expression; however, LPS has a neurotoxic effect on neurons. A more informative experiment would be to treat B103 and B103-695 cells with conditioned media from LPS treated microglia or astrocytes. Additionally, B103 cells treated with LPS conditioned media should be compared to B103-695 cells treated with LPS conditioned media to determine APP-mediated protein expression changes and not just LPS-mediated changes.

PCTAIREs in Neurodegeneration

PCTAIRE-2 (Cdk17) and PCTAIRE-3 (Cdk18) are members of the cyclin dependent kinase (Cdk) family. PCTAIRE-2 and PCTAIRE-3 showed increased expression in B103-695 cells compared with APP-null B103 cells (Figure 12), as well as in PS/APP transgenic mice compared with non-transgenic control mice (Figure 13) and human MCI- and AD-affected brain tissue compared with control tissue (Figure 18). Additionally, Aβ treatment increased expression of PCTAIRE-2 and PCTAIRE-3 in cultured primary rat neurons (Figure 15). Immunostaining analysis also revealed altered localization of PCTAIRE-2 and PCTAIRE-3 in Aβ-treated primary neurons (Figure 16) and B103 and B103-695 cells (Figure 17). PCTAIREs are relatively uncharacterized Cdc-2-related serine/threonine kinases. The functions of PCTAIRE-2 and PCTAIRE-3 have not been discovered; however, increasing evidence suggests that they may be involved in neurodegeneration. PCTAIRE-3 has been shown to directly promote tau phosphorylation at Thr231 and Ser235, which are early modifications in AD pathogenesis [270]. PCTAIRE-3 has been shown to be activated through association with Cyclin A or phosphorylation by PKA at Ser12 [271], and PKA and PCTAIRE-3 have both been observed in paired helical filament (PHF) fractions [270]. Additionally, our initial proteomic analysis suggested increased PKA signaling in APP-695 expressing B103-695 cells [239]. PCTAIRE-2 and PCTAIRE-3 were initially selected for further validation based on observed changes in phosphorylation; increased phosphorylation of PCTAIRE-2 Ser146 and Ser180, and increased phosphorylation of PCTAIRE-3 at Ser66 and Ser109. After determining increased expression of PCTAIRE-2 and PCTAIRE--3, the levels of phosphorylation may not be significantly increased following normalization to total protein expression. The functional significance of phosphorylation at these sites is unknown.

The functions of PCTAIRE-2 and PCTAIRE-3 can be further investigated by knockdown and overexpression experiments in B103 and B103-695 cells. Knockdown can be achieved using siRNA against PCTAIRE-2 and PCTAIRE-3. Stable or transient transfection of PCTAIRE-2 and PCTAIRE-3 can be

used to increase expression. Levels of PCTAIRE-2 and PCTAIRE-3 can be determined by western blot analysis to confirm knockdown and overexpression. Mass spectrometry can be used to compare the proteomes and phosphoproteomes of PCTAIRE-2 and PCTAIRE-3 knockdown or overexpression cells to determine affected proteins, pathways and functions. In addition to characterizing the function of PCTAIRE-2 and PCTAIRE-3, the functional significance of the phosphorylation sites can also be further investigated. The functional significance of the identified phosphorylation sites can be determined by creating mutations in PCTAIRE-2 and PCTAIRE-3 at known and/or predicted phosphorylation sites. Mutation of phosphorylated serine resides to aspartic acid, which is chemically similar, is commonly used to mimic a phosphorylated protein. Conversely, phosphorylation can be inhibited by mutation of a phosphorylated serine to alanine, a chemically similar amino acid that is not phosphorylated. Reducing endogenous levels of PCTAIRE-2 and PCTAIRE-3 using siRNA, and expression of constitutively phosphorylated or non-phosphorylated PCTAIRE-2 or PCTAIRE-3 may provide insight into the kinase activity, functional significance, and activating or deactivating phosphorylation sites. Validation of phosphorylated PCTAIRE-2 and PCTAIRE-3 is challenging as antibodies have not been generated, and the production of an antibody against phosphorylated residues on PCTAIRE-2 and PCTAIRE-3 could benefit future studies. Knockdown studies can also be performed in existing mouse models of AD, or transgenic models can be developed using siRNA to inhibit PCTAIRE-2 and/or PCTAIRE-3 expression.

phospho-Serine47-Histone H4

Phosphoproteomic analysis showed increased phosphorylation of Histone H4 at Ser47 in APP695 expressing B103-695 cells compared with APP-null B103 cells. Increase pSer47-Histone H4 was further validated by western blot analysis in B103 and B103-695 cells (Figure 12) and in human MCI- and AD-affected tissue compared with control tissue (Figure 18). Treatment of primary neurons with Aβ also increased phosphorylation of Histone H4 at Ser47 (Figure 15). Phosphorylation at Ser47 has been reported to promote the assembly of H3.3-H4 by the histone chaperone HIRA, while inhibiting CAF-1

mediated assembly of H3.1-H4 [242]. While the functional significance of this process is not fully understood, the functions of H3.3 are unique and cannot be substituted by H3.1 [256-258]. H3.3 is localized to gene bodies of actively transcribed genes, and levels of H3.3 at gene bodies positively correlates with gene expression [259, 260]. Chromatin immunoprecipitation (ChIP) sequencing can be used to identify what sequences and genes Histone H4 is associated with when phosphorylated at Ser47. During ChIP sequencing, proteins are cross-linked to DNA and immunoprecipitated using an antibody against the proteins of interest, in this case pSer47-Histone H4, conjugated to beads for purification. Following purification of the protein of interest and associated DNA, protein is dissociated and DNA can be sequenced. As increased pSer47-Histone H4 was observed in APP695-expressing cells compared with APP-null cells, and in human AD brain tissue compared with control tissue, determining sequences or regions that pSer47-Histone H4 binds to would indicate genes that may be differentially transcribed in AD compared with control tissue. Histone H4 Ser47-phosphorylation may be implicated in expression of proteins that have or have not been considered in AD pathology. If ChIP sequencing is successful in B103 and B103-695 cells, it can also be performed using human control, AD, and MCI brain tissue. ChIP sequencing of pS47-Histone H4 would also provide insight into the function and significance of this modification. Mutation of Ser47 to aspartic acid or alanine could also be used to examine proteome changes and functional consequences of constitutively modified or unmodified Histone H4 Ser47. Phosphorylation of Histone H4 at Ser47 may be involved in regulating gene transcription or mitosis, with implications in AD pathology.

Human Tissue Analysis

Future directions include further validation of proteins with statistically significant expression changes in MCI, AD, PD, or PSP, after FDR correction. To date, there are a very limited number of phosphoproteomic analyses of human brain tissue affected by neurodegenerative diseases. Phosphoproteomic analysis of MCI and AD human brain samples can provide insight into

phosphorylation changes that may be involved in the onset and progression of AD. Phosphoproteomic datasets can be used for bioinformatic and consensus motif analysis, which provides further information about changes in kinase activity and affected signaling pathways. One of the limitations of the phosphoenrichment strategy described in Chapter 3 is that it requires of large amounts of starting material, and the filters used with FASP procedure have a loading capacity of 400µg. Gel-aided sample processing (GASP), which was shown to be effective when working with small amounts of protein, does not have a loading capacity and may be more appropriate for phosphoproteomic workflows. Theoretically, GASP could also be applied to very large amounts of protein; however, the efficiency of GASP for processing large amounts of starting material needs to be further tested. As there have been several proteomic analyses of various regions from human MCI and AD brain, increasing the number of phosphoproteomic analysis of human brain tissue would provide insights into affected kinases, phosphatases, and signaling pathways that may be important for progression and development of disease pathology.

References

1. *2015 Alzheimer's disease facts and figures.* Alzheimer's & dementia : the journal of the Alzheimer's Association, 2015. 11(3): p. 332-84.
2. Selkoe, D.J., *The molecular pathology of Alzheimer's disease.* Neuron, 1991. 6(4): p. 487-98.
3. Kosik, K.S., C.L. Joachim, and D.J. Selkoe, *Microtubule-associated protein tau (tau) is a major antigenic component of paired helical filaments in Alzheimer disease.* Proceedings of the National Academy of Sciences of the United States of America, 1986. 83(11): p. 4044-8.
4. Alzheimer, A., et al., *An English translation of Alzheimer's 1907 paper, "Uber eine eigenartige Erkankung der Hirnrinde".* Clinical anatomy, 1995. 8(6): p. 429-31.
5. Goedert, M., et al., *Cloning and sequencing of the cDNA encoding a core protein of the paired helical filament of Alzheimer disease: identification as the microtubule-associated protein tau.* Proceedings of the National Academy of Sciences of the United States of America, 1988. 85(11): p. 4051-5.
6. Grundke-Iqbal, I., et al., *Abnormal phosphorylation of the microtubule-associated protein tau (tau) in Alzheimer cytoskeletal pathology.* Proceedings of the National Academy of Sciences of the United States of America, 1986. 83(13): p. 4913-7.
7. Weingarten, M.D., et al., *A protein factor essential for microtubule assembly.* Proceedings of the National Academy of Sciences of the United States of America, 1975. 72(5): p. 1858-62.
8. Busciglio, J., et al., *beta-amyloid fibrils induce tau phosphorylation and loss of microtubule binding.* Neuron, 1995. 14(4): p. 879-88.
9. Buée, L., et al., *Tau protein isoforms, phosphorylation and role in neurodegenerative disorders.* Brain Research Reviews, 2000. 33(1): p. 95-130.
10. Meyer-Luehmann, M., et al., *Rapid appearance and local toxicity of amyloid-beta plaques in a mouse model of Alzheimer's disease.* Nature, 2008. 451(7179): p. 720-4.
11. Frautschy, S.A., et al., *Microglial response to amyloid plaques in APPsw transgenic mice.* The American journal of pathology, 1998. 152(1): p. 307-17.
12. Pike, C.J., et al., *Beta-amyloid-induced changes in cultured astrocytes parallel reactive astrocytosis associated with senile plaques in Alzheimer's disease.* Neuroscience, 1994. 63(2): p. 517-31.
13. Selkoe, D.J., *Preventing Alzheimer's disease.* Science, 2012. 337(6101): p. 1488-1492.
14. Swerdlow, R.H., *Alzheimer's disease pathologic cascades: who comes first, what drives what.* Neurotoxicity research, 2012. 22(3): p. 182-194.
15. Gandy, S. and S.T. DeKosky, *Toward the treatment and prevention of Alzheimer's disease: rational strategies and recent progress.* Annual review of medicine, 2013. 64: p. 367-83.
16. Corder, E.H., et al., *Gene dose of apolipoprotein E type 4 allele and the risk of Alzheimer's disease in late onset families.* Science, 1993. 261(5123): p. 921-3.
17. Corder, E.H., et al., *Protective effect of apolipoprotein E type 2 allele for late onset Alzheimer disease.* Nature genetics, 1994. 7(2): p. 180-4.
18. Holtzman, D.M., et al., *Apolipoprotein E isoform-dependent amyloid deposition and neuritic degeneration in a mouse model of Alzheimer's disease.* Proceedings of the National Academy of Sciences of the United States of America, 2000. 97(6): p. 2892-7.
19. Kim, J., J.M. Basak, and D.M. Holtzman, *The role of apolipoprotein E in Alzheimer's disease.* Neuron, 2009. 63(3): p. 287-303.

20. Goate, A., et al., *Segregation of a missense mutation in the amyloid precursor protein gene with familial Alzheimer's disease.* Nature, 1991. 349(6311): p. 704-6.
21. Levy-Lahad, E., et al., *Candidate gene for the chromosome 1 familial Alzheimer's disease locus.* Science, 1995. 269(5226): p. 973-7.
22. Sherrington, R., et al., *Cloning of a gene bearing missense mutations in early-onset familial Alzheimer's disease.* Nature, 1995. 375(6534): p. 754-60.
23. Blennow, K. and H. Hampel, *CSF markers for incipient Alzheimer's disease.* The Lancet. Neurology, 2003. 2(10): p. 605-13.
24. Klunk, W.E., et al., *Imaging brain amyloid in Alzheimer's disease with Pittsburgh Compound-B.* Annals of neurology, 2004. 55(3): p. 306-19.
25. Goldgaber, D., et al., *Characterization and chromosomal localization of a cDNA encoding brain amyloid of Alzheimer's disease.* Science, 1987. 235(4791): p. 877-80.
26. Kang, J., et al., *The precursor of Alzheimer's disease amyloid A4 protein resembles a cell-surface receptor.* Nature, 1987. 325(6106): p. 733-6.
27. Xu, H., et al., *Generation of Alzheimer beta-amyloid protein in the trans-Golgi network in the apparent absence of vesicle formation.* Proceedings of the National Academy of Sciences of the United States of America, 1997. 94(8): p. 3748-52.
28. Hartmann, T., et al., *Distinct sites of intracellular production for Alzheimer's disease A beta40/42 amyloid peptides.* Nature medicine, 1997. 3(9): p. 1016-20.
29. Greenfield, J.P., et al., *Endoplasmic reticulum and trans-Golgi network generate distinct populations of Alzheimer beta-amyloid peptides.* Proceedings of the National Academy of Sciences of the United States of America, 1999. 96(2): p. 742-7.
30. Wasco, W., et al., *Identification of a mouse brain cDNA that encodes a protein related to the Alzheimer disease-associated amyloid beta protein precursor.* Proceedings of the National Academy of Sciences of the United States of America, 1992. 89(22): p. 10758-62.
31. Wasco, W., et al., *Isolation and characterization of APLP2 encoding a homologue of the Alzheimer's associated amyloid beta protein precursor.* Nature genetics, 1993. 5(1): p. 95-100.
32. Zheng, H., et al., *beta-Amyloid precursor protein-deficient mice show reactive gliosis and decreased locomotor activity.* Cell, 1995. 81(4): p. 525-31.
33. Dawson, G.R., et al., *Age-related cognitive deficits, impaired long-term potentiation and reduction in synaptic marker density in mice lacking the beta-amyloid precursor protein.* Neuroscience, 1999. 90(1): p. 1-13.
34. von Koch, C.S., et al., *Generation of APLP2 KO mice and early postnatal lethality in APLP2/APP double KO mice.* Neurobiology of aging, 1997. 18(6): p. 661-9.
35. Heber, S., et al., *Mice with combined gene knock-outs reveal essential and partially redundant functions of amyloid precursor protein family members.* The Journal of neuroscience : the official journal of the Society for Neuroscience, 2000. 20(21): p. 7951-63.
36. Herms, J., et al., *Cortical dysplasia resembling human type 2 lissencephaly in mice lacking all three APP family members.* The EMBO journal, 2004. 23(20): p. 4106-15.
37. Caille, I., et al., *Soluble form of amyloid precursor protein regulates proliferation of progenitors in the adult subventricular zone.* Development, 2004. 131(9): p. 2173-81.
38. Ohsawa, I., et al., *Amino-terminal region of secreted form of amyloid precursor protein stimulates proliferation of neural stem cells.* The European journal of neuroscience, 1999. 11(6): p. 1907-13.
39. Furukawa, K., et al., *Increased activity-regulating and neuroprotective efficacy of alpha-secretase-derived secreted amyloid precursor protein conferred by a C-terminal heparin-binding domain.* Journal of neurochemistry, 1996. 67(5): p. 1882-96.

40. Han, P., et al., *Suppression of cyclin-dependent kinase 5 activation by amyloid precursor protein: a novel excitoprotective mechanism involving modulation of tau phosphorylation.* The Journal of neuroscience : the official journal of the Society for Neuroscience, 2005. 25(50): p. 11542-52.
41. Lammich, S., et al., *Constitutive and regulated alpha-secretase cleavage of Alzheimer's amyloid precursor protein by a disintegrin metalloprotease.* Proceedings of the National Academy of Sciences of the United States of America, 1999. 96(7): p. 3922-7.
42. Buxbaum, J.D., et al., *Evidence that tumor necrosis factor alpha converting enzyme is involved in regulated alpha-secretase cleavage of the Alzheimer amyloid protein precursor.* The Journal of biological chemistry, 1998. 273(43): p. 27765-7.
43. Lin, X., et al., *Human aspartic protease memapsin 2 cleaves the beta-secretase site of beta-amyloid precursor protein.* Proceedings of the National Academy of Sciences of the United States of America, 2000. 97(4): p. 1456-60.
44. Vassar, R., et al., *Beta-secretase cleavage of Alzheimer's amyloid precursor protein by the transmembrane aspartic protease BACE.* Science, 1999. 286(5440): p. 735-41.
45. Rodrigues, E.M., A.M. Weissmiller, and L.S. Goldstein, *Enhanced beta-secretase processing alters APP axonal transport and leads to axonal defects.* Human molecular genetics, 2012. 21(21): p. 4587-601.
46. Nikolaev, A., et al., *APP binds DR6 to trigger axon pruning and neuron death via distinct caspases.* Nature, 2009. 457(7232): p. 981-9.
47. Zhao, G., et al., *Identification of a new presenilin-dependent ζ-cleavage site within the transmembrane domain of amyloid precursor protein.* Journal of Biological Chemistry, 2004. 279(49): p. 50647-50650.
48. Zhao, G., et al., *The same γ-secretase accounts for the multiple intramembrane cleavages of APP.* Journal of neurochemistry, 2007. 100(5): p. 1234-1246.
49. Steiner, H., R. Fluhrer, and C. Haass, *Intramembrane Proteolysis by γ-Secretase.* Journal of Biological Chemistry, 2008. 283(44): p. 29627-29631.
50. von Rotz, R.C., et al., *The APP intracellular domain forms nuclear multiprotein complexes and regulates the transcription of its own precursor.* Journal of cell science, 2004. 117(Pt 19): p. 4435-48.
51. Kim, H.S., et al., *C-terminal fragments of amyloid precursor protein exert neurotoxicity by inducing glycogen synthase kinase-3beta expression.* FASEB journal : official publication of the Federation of American Societies for Experimental Biology, 2003. 17(13): p. 1951-3.
52. Zhang, Y.W., et al., *Presenilin/gamma-secretase-dependent processing of beta-amyloid precursor protein regulates EGF receptor expression.* Proceedings of the National Academy of Sciences of the United States of America, 2007. 104(25): p. 10613-8.
53. Kinoshita, A., et al., *The gamma secretase-generated carboxyl-terminal domain of the amyloid precursor protein induces apoptosis via Tip60 in H4 cells.* The Journal of biological chemistry, 2002. 277(32): p. 28530-6.
54. Giliberto, L., et al., *Evidence that the Amyloid beta Precursor Protein-intracellular domain lowers the stress threshold of neurons and has a "regulated" transcriptional role.* Molecular neurodegeneration, 2008. 3: p. 12.
55. Kimberly, W.T., et al., *Gamma-secretase is a membrane protein complex comprised of presenilin, nicastrin, Aph-1, and Pen-2.* Proceedings of the National Academy of Sciences of the United States of America, 2003. 100(11): p. 6382-7.
56. De Strooper, B., et al., *Deficiency of presenilin-1 inhibits the normal cleavage of amyloid precursor protein.* Nature, 1998. 391(6665): p. 387-90.
57. Wolfe, M.S., et al., *Two transmembrane aspartates in presenilin-1 required for presenilin endoproteolysis and gamma-secretase activity.* Nature, 1999. 398(6727): p. 513-7.

58. Borchelt, D.R., et al., *Familial Alzheimer's disease-linked presenilin 1 variants elevate Abeta1-42/1-40 ratio in vitro and in vivo.* Neuron, 1996. 17(5): p. 1005-13.
59. Citron, M., et al., *Mutant presenilins of Alzheimer's disease increase production of 42-residue amyloid beta-protein in both transfected cells and transgenic mice.* Nature medicine, 1997. 3(1): p. 67-72.
60. Scheuner, D., et al., *Secreted amyloid beta-protein similar to that in the senile plaques of Alzheimer's disease is increased in vivo by the presenilin 1 and 2 and APP mutations linked to familial Alzheimer's disease.* Nature medicine, 1996. 2(8): p. 864-70.
61. Selkoe, D.J., *Deciphering the genesis and fate of amyloid beta-protein yields novel therapies for Alzheimer disease.* The Journal of clinical investigation, 2002. 110(10): p. 1375-81.
62. Parvathy, S., et al., *Cleavage of Alzheimer's amyloid precursor protein by alpha-secretase occurs at the surface of neuronal cells.* Biochemistry, 1999. 38(30): p. 9728-34.
63. Ray, W.J., et al., *Cell surface presenilin-1 participates in the gamma-secretase-like proteolysis of Notch.* The Journal of biological chemistry, 1999. 274(51): p. 36801-7.
64. Pasternak, S.H., et al., *Presenilin-1, nicastrin, amyloid precursor protein, and gamma-secretase activity are co-localized in the lysosomal membrane.* The Journal of biological chemistry, 2003. 278(29): p. 26687-94.
65. Benilova, I., E. Karran, and B. De Strooper, *The toxic Abeta oligomer and Alzheimer's disease: an emperor in need of clothes.* Nature neuroscience, 2012. 15(3): p. 349-57.
66. Haass, C. and D.J. Selkoe, *Soluble protein oligomers in neurodegeneration: lessons from the Alzheimer's amyloid beta-peptide.* Nature reviews. Molecular cell biology, 2007. 8(2): p. 101-12.
67. McLean, C.A., et al., *Soluble pool of Aβ amyloid as a determinant of severity of neurodegeneration in Alzheimer's disease.* Annals of neurology, 1999. 46(6): p. 860-866.
68. Walsh, D.M., et al., *Naturally secreted oligomers of amyloid beta protein potently inhibit hippocampal long-term potentiation in vivo.* Nature, 2002. 416(6880): p. 535-9.
69. Mawuenyega, K.G., et al., *Decreased Clearance of CNS β-Amyloid in Alzheimer's Disease.* Science, 2010. 330(6012): p. 1774.
70. Mandrekar-Colucci, S., J.C. Karlo, and G.E. Landreth, *Mechanisms underlying the rapid peroxisome proliferator-activated receptor-gamma-mediated amyloid clearance and reversal of cognitive deficits in a murine model of Alzheimer's disease.* The Journal of neuroscience : the official journal of the Society for Neuroscience, 2012. 32(30): p. 10117-28.
71. Ma, Y., et al., *Activated cyclin-dependent kinase 5 promotes microglial phagocytosis of fibrillar beta-amyloid by up-regulating lipoprotein lipase expression.* Molecular & cellular proteomics : MCP, 2013. 12(10): p. 2833-44.
72. Tsubuki, S., Y. Takaki, and T.C. Saido, *Dutch, Flemish, Italian, and Arctic mutations of APP and resistance of Abeta to physiologically relevant proteolytic degradation.* Lancet, 2003. 361(9373): p. 1957-8.
73. Tomiyama, T., et al., *A new amyloid β variant favoring oligomerization in Alzheimer's-type dementia.* Annals of neurology, 2008. 63(3): p. 377-387.
74. Citron, M., et al., *Mutation of the beta-amyloid precursor protein in familial Alzheimer's disease increases beta-protein production.* Nature, 1992. 360(6405): p. 672-4.
75. Eckman, C.B., et al., *A new pathogenic mutation in the APP gene (I716V) increases the relative proportion of A beta 42(43).* Human molecular genetics, 1997. 6(12): p. 2087-9.
76. Dawkins, E. and D.H. Small, *Insights into the physiological function of the beta-amyloid precursor protein: beyond Alzheimer's disease.* Journal of neurochemistry, 2014. 129(5): p. 756-69.
77. Demars, M.P., et al., *Soluble amyloid precursor protein: a novel proliferation factor of adult progenitor cells of ectodermal and mesodermal origin.* Stem cell research & therapy, 2011. 2(4): p. 36.

78. Hu, Y., et al., *Role of cystatin C in amyloid precursor protein-induced proliferation of neural stem/progenitor cells.* The Journal of biological chemistry, 2013. 288(26): p. 18853-62.
79. Baratchi, S., et al., *Secreted amyloid precursor proteins promote proliferation and glial differentiation of adult hippocampal neural progenitor cells.* Hippocampus, 2012. 22(7): p. 1517-27.
80. Freude, K.K., et al., *Soluble amyloid precursor protein induces rapid neural differentiation of human embryonic stem cells.* The Journal of biological chemistry, 2011. 286(27): p. 24264-74.
81. Schubert, D. and C. Behl, *The expression of amyloid beta protein precursor protects nerve cells from beta-amyloid and glutamate toxicity and alters their interaction with the extracellular matrix.* Brain research, 1993. 629(2): p. 275-82.
82. Small, D.H., et al., *A heparin-binding domain in the amyloid protein precursor of Alzheimer's disease is involved in the regulation of neurite outgrowth.* The Journal of neuroscience : the official journal of the Society for Neuroscience, 1994. 14(4): p. 2117-27.
83. Allinquant, B., et al., *Downregulation of amyloid precursor protein inhibits neurite outgrowth in vitro.* The Journal of cell biology, 1995. 128(5): p. 919-27.
84. Kibbey, M.C., et al., *beta-Amyloid precursor protein binds to the neurite-promoting IKVAV site of laminin.* Proceedings of the National Academy of Sciences of the United States of America, 1993. 90(21): p. 10150-3.
85. Beher, D., et al., *Regulation of amyloid protein precursor (APP) binding to collagen and mapping of the binding sites on APP and collagen type I.* The Journal of biological chemistry, 1996. 271(3): p. 1613-20.
86. Clarris, H.J., et al., *Identification of heparin-binding domains in the amyloid precursor protein of Alzheimer's disease by deletion mutagenesis and peptide mapping.* Journal of neurochemistry, 1997. 68(3): p. 1164-72.
87. Löffler, J. and G. Huber, *β-Amyloid Precursor Protein Isoforms in Various Rat Brain Regions and During Brain Development.* Journal of neurochemistry, 1992. 59(4): p. 1316-1324.
88. Wang, Z., et al., *Presynaptic and postsynaptic interaction of the amyloid precursor protein promotes peripheral and central synaptogenesis.* The Journal of neuroscience : the official journal of the Society for Neuroscience, 2009. 29(35): p. 10788-801.
89. Nagy, Z., et al., *Relative roles of plaques and tangles in the dementia of Alzheimer's disease: correlations using three sets of neuropathological criteria.* Dementia, 1995. 6(1): p. 21-31.
90. Gomez-Isla, T., et al., *Neuronal loss correlates with but exceeds neurofibrillary tangles in Alzheimer's disease.* Annals of neurology, 1997. 41(1): p. 17-24.
91. Arriagada, P.V., et al., *Neurofibrillary tangles but not senile plaques parallel duration and severity of Alzheimer's disease.* Neurology, 1992. 42(3 Pt 1): p. 631-9.
92. Hardy, J.A. and G.A. Higgins, *Alzheimer's disease: the amyloid cascade hypothesis.* Science, 1992. 256(5054): p. 184-5.
93. Hardy, J. and D. Allsop, *Amyloid deposition as the central event in the aetiology of Alzheimer's disease.* Trends in pharmacological sciences, 1991. 12(10): p. 383-8.
94. Gomez-Isla, T., et al., *Profound loss of layer II entorhinal cortex neurons occurs in very mild Alzheimer's disease.* The Journal of neuroscience : the official journal of the Society for Neuroscience, 1996. 16(14): p. 4491-500.
95. Musiek, E.S. and D.M. Holtzman, *Three dimensions of the amyloid hypothesis: time, space and 'wingmen'.* Nature neuroscience, 2015. 18(6): p. 800-6.
96. Price, J.L. and J.C. Morris, *Tangles and plaques in nondemented aging and "preclinical" Alzheimer's disease.* Annals of neurology, 1999. 45(3): p. 358-68.
97. Tomic, J.L., et al., *Soluble fibrillar oligomer levels are elevated in Alzheimer's disease brain and correlate with cognitive dysfunction.* Neurobiology of disease, 2009. 35(3): p. 352-8.

98. Handoko, M., et al., *Correlation of specific amyloid-beta oligomers with tau in cerebrospinal fluid from cognitively normal older adults.* JAMA neurology, 2013. 70(5): p. 594-9.
99. Ma, Q.L., et al., *Beta-amyloid oligomers induce phosphorylation of tau and inactivation of insulin receptor substrate via c-Jun N-terminal kinase signaling: suppression by omega-3 fatty acids and curcumin.* The Journal of neuroscience : the official journal of the Society for Neuroscience, 2009. 29(28): p. 9078-89.
100. Jin, M., et al., *Soluble amyloid beta-protein dimers isolated from Alzheimer cortex directly induce Tau hyperphosphorylation and neuritic degeneration.* Proceedings of the National Academy of Sciences of the United States of America, 2011. 108(14): p. 5819-24.
101. Zhang, Y., et al., *A lifespan observation of a novel mouse model: in vivo evidence supports abeta oligomer hypothesis.* PloS one, 2014. 9(1): p. e85885.
102. Kruman, II, et al., *Cell cycle activation linked to neuronal cell death initiated by DNA damage.* Neuron, 2004. 41(4): p. 549-61.
103. Verdaguer, E., et al., *Inhibition of CDKs: a strategy for preventing kainic acid-induced apoptosis in neurons.* Annals of the New York Academy of Sciences, 2003. 1010: p. 671-4.
104. Arendt, T., et al., *Expression of the cyclin-dependent kinase inhibitor p16 in Alzheimer's disease.* NeuroReport, 1996. 7(18): p. 3047-9.
105. Busser, J., D.S. Geldmacher, and K. Herrup, *Ectopic cell cycle proteins predict the sites of neuronal cell death in Alzheimer's disease brain.* The Journal of neuroscience : the official journal of the Society for Neuroscience, 1998. 18(8): p. 2801-7.
106. Nagy, Z., et al., *Cell cycle markers in the hippocampus in Alzheimer's disease.* Acta neuropathologica, 1997. 94(1): p. 6-15.
107. Vincent, I., et al., *Aberrant expression of mitotic cdc2/cyclin B1 kinase in degenerating neurons of Alzheimer's disease brain.* The Journal of neuroscience : the official journal of the Society for Neuroscience, 1997. 17(10): p. 3588-98.
108. Yang, Y., E.J. Mufson, and K. Herrup, *Neuronal cell death is preceded by cell cycle events at all stages of Alzheimer's disease.* The Journal of neuroscience : the official journal of the Society for Neuroscience, 2003. 23(7): p. 2557-63.
109. Arendt, T., et al., *Increased expression and subcellular translocation of the mitogen activated protein kinase kinase and mitogen-activated protein kinase in Alzheimer's disease.* Neuroscience, 1995. 68(1): p. 5-18.
110. Gartner, U., M. Holzer, and T. Arendt, *Elevated expression of p21ras is an early event in Alzheimer's disease and precedes neurofibrillary degeneration.* Neuroscience, 1999. 91(1): p. 1-5.
111. Bhaskar, K., et al., *Microglial derived tumor necrosis factor-alpha drives Alzheimer's disease-related neuronal cell cycle events.* Neurobiology of disease, 2014. 62: p. 273-85.
112. Absalon, S., et al., *MiR-26b, upregulated in Alzheimer's disease, activates cell cycle entry, tau-phosphorylation, and apoptosis in postmitotic neurons.* The Journal of neuroscience : the official journal of the Society for Neuroscience, 2013. 33(37): p. 14645-59.
113. Judge, M., et al., *Mitosis-specific phosphorylation of amyloid precursor protein at threonine 668 leads to its altered processing and association with centrosomes.* Molecular neurodegeneration, 2011. 6: p. 80.
114. Aplin, A.E., et al., *In Vitro Phosphorylation of the Cytoplasmic Domain of the Amyloid Precursor Protein by Glycogen Synthase Kinase-3β.* Journal of neurochemistry, 1996. 67(2): p. 699-707.
115. Chang, K.A., et al., *Phosphorylation of amyloid precursor protein (APP) at Thr668 regulates the nuclear translocation of the APP intracellular domain and induces neurodegeneration.* Molecular and cellular biology, 2006. 26(11): p. 4327-38.

116. Kimberly, W.T., et al., *Physiological regulation of the beta-amyloid precursor protein signaling domain by c-Jun N-terminal kinase JNK3 during neuronal differentiation.* The Journal of neuroscience : the official journal of the Society for Neuroscience, 2005. 25(23): p. 5533-43.
117. Iijima, K., et al., *Neuron-specific phosphorylation of Alzheimer's beta-amyloid precursor protein by cyclin-dependent kinase 5.* Journal of neurochemistry, 2000. 75(3): p. 1085-91.
118. Suzuki, T., et al., *Cell cycle-dependent regulation of the phosphorylation and metabolism of the Alzheimer amyloid precursor protein.* The EMBO journal, 1994. 13(5): p. 1114-22.
119. Giovanni, A., et al., *Involvement of cell cycle elements, cyclin-dependent kinases, pRb, and E2F x DP, in B-amyloid-induced neuronal death.* The Journal of biological chemistry, 1999. 274(27): p. 19011-6.
120. Varvel, N.H., et al., *Abeta oligomers induce neuronal cell cycle events in Alzheimer's disease.* The Journal of neuroscience : the official journal of the Society for Neuroscience, 2008. 28(43): p. 10786-93.
121. Gygi, S.P., et al., *Quantitative analysis of complex protein mixtures using isotope-coded affinity tags.* Nature biotechnology, 1999. 17(10): p. 994-9.
122. Ong, S.E., et al., *Stable isotope labeling by amino acids in cell culture, SILAC, as a simple and accurate approach to expression proteomics.* Molecular & cellular proteomics : MCP, 2002. 1(5): p. 376-86.
123. Ong, S.E. and M. Mann, *A practical recipe for stable isotope labeling by amino acids in cell culture (SILAC).* Nature protocols, 2006. 1(6): p. 2650-60.
124. Ross, P.L., et al., *Multiplexed Protein Quantitation in Saccharomyces cerevisiae Using Amine-reactive Isobaric Tagging Reagents.* Molecular & Cellular Proteomics, 2004. 3(12): p. 1154-1169.
125. Hsu, J.L., et al., *Stable-isotope dimethyl labeling for quantitative proteomics.* Analytical chemistry, 2003. 75(24): p. 6843-52.
126. Boersema, P.J., et al., *Multiplex peptide stable isotope dimethyl labeling for quantitative proteomics.* Nature protocols, 2009. 4(4): p. 484-94.
127. Old, W.M., et al., *Comparison of Label-free Methods for Quantifying Human Proteins by Shotgun Proteomics.* Molecular & Cellular Proteomics, 2005. 4(10): p. 1487-1502.
128. O'Farrell, P.H., *High resolution two-dimensional electrophoresis of proteins.* The Journal of biological chemistry, 1975. 250(10): p. 4007-21.
129. Rosenfeld, J., et al., *In-gel digestion of proteins for internal sequence analysis after one- or two-dimensional gel electrophoresis.* Analytical biochemistry, 1992. 203(1): p. 173-9.
130. Unlu, M., M.E. Morgan, and J.S. Minden, *Difference gel electrophoresis: a single gel method for detecting changes in protein extracts.* Electrophoresis, 1997. 18(11): p. 2071-7.
131. Marouga, R., S. David, and E. Hawkins, *The development of the DIGE system: 2D fluorescence difference gel analysis technology.* Analytical and Bioanalytical Chemistry, 2005. 382(3): p. 669-678.
132. Link, A.J., et al., *Direct analysis of protein complexes using mass spectrometry.* Nature biotechnology, 1999. 17(7): p. 676-82.
133. Washburn, M.P., D. Wolters, and J.R. Yates, 3rd, *Large-scale analysis of the yeast proteome by multidimensional protein identification technology.* Nature biotechnology, 2001. 19(3): p. 242-7.
134. Kiddle, S.J., et al., *Candidate blood proteome markers of Alzheimer's disease onset and progression: a systematic review and replication study.* Journal of Alzheimer's disease : JAD, 2014. 38(3): p. 515-31.
135. Hendrickson, R.C., et al., *High Resolution Discovery Proteomics Reveals Candidate Disease Progression Markers of Alzheimer's Disease in Human Cerebrospinal Fluid.* PloS one, 2015. 10(8): p. e0135365.

136. Hölttä, M., et al., *An Integrated Workflow for Multiplex CSF Proteomics and Peptidomics · Identification of Candidate Cerebrospinal Fluid Biomarkers of Alzheimer's Disease.* Journal of proteome research, 2014. 14(2): p. 654-663.
137. Gordon, J., S. Amini, and M.K. White, *General overview of neuronal cell culture.* Methods in molecular biology, 2013. 1078: p. 1-8.
138. Foldi, I., et al., *Proteomic study of the toxic effect of oligomeric Abeta1-42 in situ prepared from 'iso-Abeta1-42'.* Journal of neurochemistry, 2011. 117(4): p. 691-702.
139. Joerchel, S., et al., *Oligomeric beta-amyloid(1-42) induces the expression of Alzheimer disease-relevant proteins in cholinergic SN56.B5.G4 cells as revealed by proteomic analysis.* International journal of developmental neuroscience : the official journal of the International Society for Developmental Neuroscience, 2008. 26(3-4): p. 301-8.
140. Boyd-Kimball, D., et al., *Gamma-glutamylcysteine ethyl ester protection of proteins from Abeta(1-42)-mediated oxidative stress in neuronal cell culture: a proteomics approach.* Journal of neuroscience research, 2005. 79(5): p. 707-13.
141. Sultana, R., et al., *Protective effect of D609 against amyloid-beta1-42-induced oxidative modification of neuronal proteins: redox proteomics study.* Journal of neuroscience research, 2006. 84(2): p. 409-17.
142. Bozso, Z., et al., *Controlled in situ preparation of Aβ (1–42) oligomers from the isopeptide "iso-Aβ (1–42)", physicochemical and biological characterization.* Peptides, 2010. 31(2): p. 248-256.
143. Butterfield, D.A., et al., *Mass spectrometry and redox proteomics: applications in disease.* Mass spectrometry reviews, 2014. 33(4): p. 277-301.
144. Boyd-Kimball, D., et al., *Proteomic identification of proteins specifically oxidized in Caenorhabditis elegans expressing human Abeta(1-42): implications for Alzheimer's disease.* Neurobiology of aging, 2006. 27(9): p. 1239-49.
145. Hsiao, K., et al., *Correlative memory deficits, Abeta elevation, and amyloid plaques in transgenic mice.* Science, 1996. 274(5284): p. 99-102.
146. Duff, K., et al., *Increased amyloid-beta42(43) in brains of mice expressing mutant presenilin 1.* Nature, 1996. 383(6602): p. 710-3.
147. Hwang, D.Y., et al., *Alterations in behavior, amyloid beta-42, caspase-3, and Cox-2 in mutant PS2 transgenic mouse model of Alzheimer's disease.* FASEB journal : official publication of the Federation of American Societies for Experimental Biology, 2002. 16(8): p. 805-13.
148. Holcomb, L., et al., *Accelerated Alzheimer-type phenotype in transgenic mice carrying both mutant amyloid precursor protein and presenilin 1 transgenes.* Nature medicine, 1998. 4(1): p. 97-100.
149. Lewis, J., et al., *Neurofibrillary tangles, amyotrophy and progressive motor disturbance in mice expressing mutant (P301L) tau protein.* Nature genetics, 2000. 25(4): p. 402-5.
150. Oddo, S., et al., *Triple-transgenic model of Alzheimer's disease with plaques and tangles: intracellular Abeta and synaptic dysfunction.* Neuron, 2003. 39(3): p. 409-21.
151. Platt, B., et al., *Abnormal cognition, sleep, EEG and brain metabolism in a novel knock-in Alzheimer mouse, PLB1.* PloS one, 2011. 6(11): p. e27068.
152. Arendash, G.W., et al., *Progressive, age-related behavioral impairments in transgenic mice carrying both mutant amyloid precursor protein and presenilin-1 transgenes.* Brain research, 2001. 891(1-2): p. 42-53.
153. Gordon, M.N., et al., *Correlation between cognitive deficits and Abeta deposits in transgenic APP+PS1 mice.* Neurobiology of aging, 2001. 22(3): p. 377-85.
154. Shin, S.J., et al., *Profiling proteins related to amyloid deposited brain of Tg2576 mice.* Proteomics, 2004. 4(11): p. 3359-68.

155. Gillardon, F., et al., *Proteomic and functional alterations in brain mitochondria from Tg2576 mice occur before amyloid plaque deposition.* Proteomics, 2007. 7(4): p. 605-616.
156. Huang, Q., et al., *Potential in vivo amelioration by N-acetyl-L-cysteine of oxidative stress in brain in human double mutant APP/PS-1 knock-in mice: toward therapeutic modulation of mild cognitive impairment.* Journal of neuroscience research, 2010. 88(12): p. 2618-29.
157. Robinson, R.A., et al., *Proteomic analysis of brain proteins in APP/PS-1 human double mutant knock-in mice with increasing amyloid beta-peptide deposition: insights into the effects of in vivo treatment with N-acetylcysteine as a potential therapeutic intervention in mild cognitive impairment and Alzheimer's disease.* Proteomics, 2011. 11(21): p. 4243-56.
158. Sultana, R., et al., *Proteomic identification of specifically carbonylated brain proteins in APP(NLh)/APP(NLh) x PS-1(P264L)/PS-1(P264L) human double mutant knock-in mice model of Alzheimer disease as a function of age.* Journal of proteomics, 2011. 74(11): p. 2430-40.
159. Blanchard, V., et al., *Time sequence of maturation of dystrophic neurites associated with Abeta deposits in APP/PS1 transgenic mice.* Experimental neurology, 2003. 184(1): p. 247-63.
160. Sizova, D., et al., *Proteomic analysis of brain tissue from an Alzheimer's disease mouse model by two-dimensional difference gel electrophoresis.* Neurobiology of aging, 2007. 28(3): p. 357-70.
161. Boyd-Kimball, D., et al., *Proteomic identification of proteins specifically oxidized by intracerebral injection of amyloid beta-peptide (1-42) into rat brain: implications for Alzheimer's disease.* Neuroscience, 2005. 132(2): p. 313-24.
162. Wilson, K.E., et al., *Comparative proteomic analysis using samples obtained with laser microdissection and saturation dye labelling.* Proteomics, 2005. 5(15): p. 3851-3858.
163. Andreev, V.P., et al., *Label-free quantitative LC-MS proteomics of Alzheimer's disease and normally aged human brains.* Journal of proteome research, 2012. 11(6): p. 3053-67.
164. Musunuri, S., et al., *Quantification of the Brain Proteome in Alzheimer's Disease Using Multiplexed Mass Spectrometry.* Journal of proteome research, 2014. 13(4): p. 2056-2068.
165. Sultana, R., et al., *Proteomics analysis of the Alzheimer's disease hippocampal proteome.* Journal of Alzheimer's disease : JAD, 2007. 11(2): p. 153-64.
166. Begcevic, I., et al., *Semiquantitative proteomic analysis of human hippocampal tissues from Alzheimer's disease and age-matched control brains.* Clinical proteomics, 2013. 10(1): p. 5.
167. Donovan, L.E., et al., *Analysis of a membrane-enriched proteome from postmortem human brain tissue in Alzheimer's disease.* PROTEOMICS – Clinical Applications, 2012. 6(3-4): p. 201-211.
168. Woltjer, R.L., et al., *Proteomic determination of widespread detergent-insolubility including Abeta but not tau early in the pathogenesis of Alzheimer's disease.* FASEB journal : official publication of the Federation of American Societies for Experimental Biology, 2005. 19(13): p. 1923-5.
169. Chang, R.Y., et al., *The synaptic proteome in Alzheimer's disease.* Alzheimer's & dementia : the journal of the Alzheimer's Association, 2013. 9(5): p. 499-511.
170. Chang, R.Y., et al., *Targeted quantitative analysis of synaptic proteins in Alzheimer's disease brain.* Neurochemistry international, 2014. 75: p. 66-75.
171. Chang, R.Y., et al., *SWATH analysis of the synaptic proteome in Alzheimer's disease.* Neurochemistry international, 2015.
172. Sultana, R., et al., *Identification of nitrated proteins in Alzheimer's disease brain using a redox proteomics approach.* Neurobiology of disease, 2006. 22(1): p. 76-87.
173. Castegna, A., et al., *Proteomic identification of oxidatively modified proteins in Alzheimer's disease brain. Part I: creatine kinase BB, glutamine synthase, and ubiquitin carboxy-terminal hydrolase L-1.* Free radical biology & medicine, 2002. 33(4): p. 562-71.

174. Castegna, A., et al., *Proteomic identification of oxidatively modified proteins in Alzheimer's disease brain. Part II: dihydropyrimidinase-related protein 2, alpha-enolase and heat shock cognate 71.* Journal of neurochemistry, 2002. 82(6): p. 1524-32.
175. Chung, S.H., *Aberrant phosphorylation in the pathogenesis of Alzheimer's disease.* BMB reports, 2009. 42(8): p. 467-74.
176. Sternberger, N.H., L.A. Sternberger, and J. Ulrich, *Aberrant neurofilament phosphorylation in Alzheimer disease.* Proceedings of the National Academy of Sciences of the United States of America, 1985. 82(12): p. 4274-6.
177. Rudrabhatla, P., et al., *Quantitative phosphoproteomic analysis of neuronal intermediate filament proteins (NF-M/H) in Alzheimer's disease by iTRAQ.* FASEB journal : official publication of the Federation of American Societies for Experimental Biology, 2010. 24(11): p. 4396-407.
178. Ulloa, L., et al., *Microtubule-associated protein MAP1B showing a fetal phosphorylation pattern is present in sites of neurofibrillary degeneration in brains of Alzheimer's disease patients.* Brain research. Molecular brain research, 1994. 26(1-2): p. 113-22.
179. Xia, Q., et al., *Phosphoproteomic analysis of human brain by calcium phosphate precipitation and mass spectrometry.* Journal of proteome research, 2008. 7(7): p. 2845-51.
180. Small, S.A. and S. Gandy, *Sorting through the cell biology of Alzheimer's disease: intracellular pathways to pathogenesis.* Neuron, 2006. 52(1): p. 15-31.
181. Xu, H., P. Greengard, and S. Gandy, *Regulated Formation of Golgi Secretory Vesicles Containing Alzheimer β-Amyloid Precursor Protein.* Journal of Biological Chemistry, 1995. 270(40): p. 23243-23245.
182. Gandy, S.E., et al., *Protein Phosphorylation Regulates Relative Utilization of Processing Pathways for Alzheimer β/A4 Amyloid Precursor Proteina.* Annals of the New York Academy of Sciences, 1993. 695(1): p. 117-121.
183. Lee, M.-S., et al., *APP processing is regulated by cytoplasmic phosphorylation.* The Journal of cell biology, 2003. 163(1): p. 83-95.
184. Standen, C.L., et al., *Phosphorylation of thr668 in the cytoplasmic domain of the Alzheimer's disease amyloid precursor protein by stress-activated protein kinase 1b (Jun N-terminal kinase-3).* Journal of neurochemistry, 2001. 76(1): p. 316-320.
185. Ramelot, T.A. and L.K. Nicholson, *Phosphorylation-induced structural changes in the amyloid precursor protein cytoplasmic tail detected by NMR.* Journal of molecular biology, 2001. 307(3): p. 871-84.
186. Schulenberg, B., et al., *Characterization of dynamic and steady-state protein phosphorylation using a fluorescent phosphoprotein gel stain and mass spectrometry.* Electrophoresis, 2004. 25(15): p. 2526-2532.
187. Schulenberg, B., et al., *Analysis of Steady-state Protein Phosphorylation in Mitochondria Using a Novel Fluorescent Phosphosensor Dye.* Journal of Biological Chemistry, 2003. 278(29): p. 27251-27255.
188. Andersson, L. and J. Porath, *Isolation of phosphoproteins by immobilized metal (Fe3+) affinity chromatography.* Analytical biochemistry, 1986. 154(1): p. 250-4.
189. Stensballe, A., S. Andersen, and O.N. Jensen, *Characterization of phosphoproteins from electrophoretic gels by nanoscale Fe (III) affinity chromatography with off-line mass spectrometry analysis.* Proteomics, 2001. 1(2): p. 207-222.
190. Li, S. and C. Dass, *Iron(III)-immobilized metal ion affinity chromatography and mass spectrometry for the purification and characterization of synthetic phosphopeptides.* Analytical biochemistry, 1999. 270(1): p. 9-14.
191. Posewitz, M.C. and P. Tempst, *Immobilized gallium (III) affinity chromatography of phosphopeptides.* Analytical chemistry, 1999. 71(14): p. 2883-2892.

192. Zhou, H., et al., *Specific phosphopeptide enrichment with immobilized titanium ion affinity chromatography adsorbent for phosphoproteome analysis.* Journal of proteome research, 2008. 7(9): p. 3957-3967.
193. Larsen, M.R., et al., *Highly selective enrichment of phosphorylated peptides from peptide mixtures using titanium dioxide microcolumns.* Molecular & Cellular Proteomics, 2005. 4(7): p. 873-886.
194. Pinkse, M.W., et al., *Selective isolation at the femtomole level of phosphopeptides from proteolytic digests using 2D-NanoLC-ESI-MS/MS and titanium oxide precolumns.* Analytical chemistry, 2004. 76(14): p. 3935-3943.
195. Iliuk, A.B., et al., *In-depth Analyses of Kinase-dependent Tyrosine Phosphoproteomes Based on Metal Ion-functionalized Soluble Nanopolymers.* Molecular & Cellular Proteomics, 2010. 9(10): p. 2162-2172.
196. Ballif, B.A., et al., *Phosphoproteomic Analysis of the Developing Mouse Brain.* Molecular & Cellular Proteomics, 2004. 3(11): p. 1093-1101.
197. Dai, J., et al., *Protein phosphorylation and expression profiling by Yin-yang multidimensional liquid chromatography (Yin-yang MDLC) mass spectrometry.* Journal of proteome research, 2007. 6(1): p. 250-62.
198. Nie, S., et al., *Comprehensive profiling of phosphopeptides based on anion exchange followed by flow-through enrichment with titanium dioxide (AFET).* Journal of proteome research, 2010. 9(9): p. 4585-94.
199. Chen, X., et al., *Increasing phosphoproteome coverage and identification of phosphorylation motifs through combination of different HPLC fractionation methods.* Journal of chromatography. B, Analytical technologies in the biomedical and life sciences, 2011. 879(1): p. 25-34.
200. Schwartz, D. and S.P. Gygi, *An iterative statistical approach to the identification of protein phosphorylation motifs from large-scale data sets.* Nature biotechnology, 2005. 23(11): p. 1391-8.
201. Chen, P., et al., *Phosphoproteomic profiling of selenate-treated Alzheimer's disease model cells.* PloS one, 2014. 9(12): p. e113307.
202. Wang, F., et al., *Phosphoproteome analysis of an early onset mouse model (TgCRND8) of Alzheimer's disease reveals temporal changes in neuronal and glia signaling pathways.* Proteomics, 2013. 13(8): p. 1292-1305.
203. Chishti, M.A., et al., *Early-onset Amyloid Deposition and Cognitive Deficits in Transgenic Mice Expressing a Double Mutant Form of Amyloid Precursor Protein 695.* Journal of Biological Chemistry, 2001. 276(24): p. 21562-21570.
204. Dammer, E.B., et al., *Quantitative phosphoproteomics of Alzheimer's disease reveals cross-talk between kinases and small heat shock proteins.* Proteomics, 2015. 15(2-3): p. 508-519.
205. Zahid, S., et al., *Phosphoproteome profiling of substantia nigra and cortex regions of Alzheimer's disease patients.* Journal of neurochemistry, 2012. 121(6): p. 954-963.
206. Rudrabhatla, P., H. Jaffe, and H.C. Pant, *Direct evidence of phosphorylated neuronal intermediate filament proteins in neurofibrillary tangles (NFTs): phosphoproteomics of Alzheimer's NFTs.* FASEB journal : official publication of the Federation of American Societies for Experimental Biology, 2011. 25(11): p. 3896-905.
207. Di Domenico, F., et al., *Quantitative proteomics analysis of phosphorylated proteins in the hippocampus of Alzheimer's disease subjects.* Journal of proteomics, 2011. 74(7): p. 1091-103.
208. Yang, Y., D.S. Geldmacher, and K. Herrup, *DNA replication precedes neuronal cell death in Alzheimer's disease.* The Journal of neuroscience, 2001. 21(8): p. 2661-2668.

209. Meijer, L., et al., *Biochemical and cellular effects of roscovitine, a potent and selective inhibitor of the cyclin-dependent kinases cdc2, cdk2 and cdk5.* European journal of biochemistry / FEBS, 1997. 243(1-2): p. 527-36.
210. Schiff, P.B., J. Fant, and S.B. Horwitz, *Promotion of microtubule assembly in vitro by taxol.* Nature, 1979. 277(5698): p. 665-7.
211. Samson, F., et al., *Nocodazole action on tubulin assembly, axonal ultrastructure and fast axoplasmic transport.* Journal of Pharmacology and Experimental Therapeutics, 1979. 208(3): p. 411-417.
212. Akiyama, H., et al., *Inflammation and Alzheimer's disease.* Neurobiology of aging, 2000. 21(3): p. 383-421.
213. Wyss-Coray, T. and J. Rogers, *Inflammation in Alzheimer disease-a brief review of the basic science and clinical literature.* Cold Spring Harbor perspectives in medicine, 2012. 2(1): p. a006346.
214. Huang, Y., et al., *Exaggerated sickness behavior and brain proinflammatory cytokine expression in aged mice in response to intracerebroventricular lipopolysaccharide.* Neurobiology of aging, 2008. 29(11): p. 1744-53.
215. Godbout, J.P., et al., *Exaggerated neuroinflammation and sickness behavior in aged mice following activation of the peripheral innate immune system.* FASEB journal : official publication of the Federation of American Societies for Experimental Biology, 2005. 19(10): p. 1329-31.
216. Chang, R.C., et al., *Neurons reduce glial responses to lipopolysaccharide (LPS) and prevent injury of microglial cells from over-activation by LPS.* Journal of neurochemistry, 2001. 76(4): p. 1042-1049.
217. Wisniewski, J.R., et al., *Universal sample preparation method for proteome analysis.* Nature methods, 2009. 6(5): p. 359-62.
218. Cox, J. and M. Mann, *MaxQuant enables high peptide identification rates, individualized ppb-range mass accuracies and proteome-wide protein quantification.* Nature biotechnology, 2008. 26(12): p. 1367-1372.
219. Benjamini, Y. and Y. Hochberg, *Controlling the false discovery rate: a practical and powerful approach to multiple testing.* Journal of the Royal Statistical Society. Series B (Methodological), 1995: p. 289-300.
220. Amigoni, L., et al., *Activation of amyloid precursor protein processing by growth factors is dependent on Ras GTPase activity.* Neurochemical research, 2011. 36(3): p. 392-8.
221. Stornetta, R.L. and J.J. Zhu, *Ras and Rap Signaling in Synaptic Plasticity and Mental Disorders.* The Neuroscientist, 2010.
222. Kase, H., et al., *K-252 compounds, novel and potent inhibitors of protein kinase C and cyclic nucleotide-dependent protein kinases.* Biochemical and biophysical research communications, 1987. 142(2): p. 436-440.
223. Krokan, H., E. Wist, and R.H. Krokan, *Aphidicolin inhibits DNA synthesis by DNA polymerase alpha and isolated nuclei by a similar mechanism.* Nucleic acids research, 1981. 9(18): p. 4709-19.
224. Liu, P., et al., *Cell-cycle-regulated activation of Akt kinase by phosphorylation at its carboxyl terminus.* Nature, 2014. 508(7497): p. 541-545.
225. Diehl, J.A., et al., *Glycogen synthase kinase-3beta regulates cyclin D1 proteolysis and subcellular localization.* Genes & development, 1998. 12(22): p. 3499-511.
226. Lovestone, S., et al., *Alzheimer's disease-like phosphorylation of the microtubule-associated protein tau by glycogen synthase kinase-3 in transfected mammalian cells.* Current biology : CB, 1994. 4(12): p. 1077-86.

227. Phiel, C.J., et al., *GSK-3alpha regulates production of Alzheimer's disease amyloid-beta peptides.* Nature, 2003. 423(6938): p. 435-9.
228. Srivastava, A.K. and S.K. Pandey, *Potential mechanism(s) involved in the regulation of glycogen synthesis by insulin.* Molecular and cellular biochemistry, 1998. 182(1-2): p. 135-41.
229. Cross, D.A., et al., *Inhibition of glycogen synthase kinase-3 by insulin mediated by protein kinase B.* Nature, 1995. 378(6559): p. 785-9.
230. Horikawa, K. and K. Takatsu, *Interleukin-5 regulates genes involved in B-cell terminal maturation.* Immunology, 2006. 118(4): p. 497-508.
231. Masuda, A., et al., *Th2 Cytokine Production from Mast Cells Is Directly Induced by Lipopolysaccharide and Distinctly Regulated by c-Jun N-Terminal Kinase and p38 Pathways.* The Journal of Immunology, 2002. 169(7): p. 3801-3810.
232. Braak, H. and E. Braak, *Neuropathological stageing of Alzheimer-related changes.* Acta neuropathologica, 1991. 82(4): p. 239-59.
233. Zhang, Y.W., et al., *APP processing in Alzheimer's disease.* Molecular brain, 2011. 4: p. 3.
234. Tiraboschi, P., et al., *The importance of neuritic plaques and tangles to the development and evolution of AD.* Neurology, 2004. 62(11): p. 1984-9.
235. Sondag, C.M., G. Dhawan, and C.K. Combs, *Beta amyloid oligomers and fibrils stimulate differential activation of primary microglia.* J Neuroinflammation, 2009. 6(1): p. b7.
236. Maezawa, I., et al., *Amyloid-β protein oligomer at low nanomolar concentrations activates microglia and induces microglial neurotoxicity.* Journal of Biological Chemistry, 2011. 286(5): p. 3693-3706.
237. Varvel, N.H., et al., *NSAIDs prevent, but do not reverse, neuronal cell cycle reentry in a mouse model of Alzheimer disease.* The Journal of clinical investigation, 2009. 119(12): p. 3692-702.
238. Suzuki, T. and T. Nakaya, *Regulation of amyloid beta-protein precursor by phosphorylation and protein interactions.* The Journal of biological chemistry, 2008. 283(44): p. 29633-7.
239. Chaput, D., et al., *SILAC-based proteomic analysis to investigate the impact of amyloid precursor protein expression in neuronal-like B103 cells.* Electrophoresis, 2012. 33(24): p. 3728-37.
240. Padmanabhan, J., et al., *Alpha1-antichymotrypsin, an inflammatory protein overexpressed in Alzheimer's disease brain, induces tau phosphorylation in neurons.* Brain : a journal of neurology, 2006. 129(11): p. 3020-3034.
241. Langan, T.A., et al., *Mammalian growth-associated H1 histone kinase: a homolog of cdc2+/CDC28 protein kinases controlling mitotic entry in yeast and frog cells.* Molecular and cellular biology, 1989. 9(9): p. 3860-8.
242. Kang, B., et al., *Phosphorylation of H4 Ser 47 promotes HIRA-mediated nucleosome assembly.* Genes & development, 2011. 25(13): p. 1359-64.
243. Jung, J.H. and J.A. Traugh, *Regulation of the interaction of Pak2 with Cdc42 via autophosphorylation of serine 141.* The Journal of biological chemistry, 2005. 280(48): p. 40025-31.
244. Lu, D.C., et al., *Caspase cleavage of the amyloid precursor protein modulates amyloid β-protein toxicity.* Journal of neurochemistry, 2003. 87(3): p. 733-741.
245. Frankfort, B.J. and I.H. Gelman, *Identification of Novel Cellular Genes Transcriptionally Suppressed by v-scr.* Biochemical and biophysical research communications, 1995. 206(3): p. 916-926.
246. Lin, X., P. Nelson, and I.H. Gelman, *SSeCKS, a major protein kinase C substrate with tumor suppressor activity, regulates G1→ S progression by controlling the expression and cellular compartmentalization of cyclin D.* Molecular and cellular biology, 2000. 20(19): p. 7259-7272.

247. Lin, X. and I.H. Gelman, *Calmodulin and cyclin D anchoring sites on the Src-suppressed C kinase substrate, SSeCKS.* Biochemical and biophysical research communications, 2002. 290(5): p. 1368-1375.
248. Huot, J., et al., *Oxidative stress-induced actin reorganization mediated by the p38 mitogen-activated protein kinase/heat shock protein 27 pathway in vascular endothelial cells.* Circulation research, 1997. 80(3): p. 383-392.
249. Rane, M.J., et al., *Heat shock protein 27 controls apoptosis by regulating Akt activation.* Journal of Biological Chemistry, 2003. 278(30): p. 27828-27835.
250. Gibert, B., et al., *Inhibition of heat shock protein 27 (HspB1) tumorigenic functions by peptide aptamers.* Oncogene, 2011. 30(34): p. 3672-3681.
251. Gusev, N., N. Bogatcheva, and S. Marston, *Structure and properties of small heat shock proteins (sHsp) and their interaction with cytoskeleton proteins.* Biochemistry (Moscow), 2002. 67(5): p. 511-519.
252. Kostenko, S. and U. Moens, *Heat shock protein 27 phosphorylation: kinases, phosphatases, functions and pathology.* Cellular and molecular life sciences, 2009. 66(20): p. 3289-3307.
253. Schmidt, T., B. Bartelt-Kirbach, and N. Golenhofen, *Phosphorylation-dependent subcellular localization of the small heat shock proteins HspB1/Hsp25 and HspB5/alphaB-crystallin in cultured hippocampal neurons.* Histochemistry and cell biology, 2012. 138(3): p. 407-18.
254. Hartwig, J., et al., *MARCKS is an actin filament crosslinking protein regulated by protein kinase C and calcium–calmodulin.* 1992.
255. Kimura, T., et al., *Phosphorylation of MARCKS in Alzheimer disease brains.* NeuroReport, 2000. 11(4): p. 869-873.
256. Szenker, E., D. Ray-Gallet, and G. Almouzni, *The double face of the histone variant H3.3.* Cell research, 2011. 21(3): p. 421-34.
257. Sakai, A., et al., *Transcriptional and developmental functions of the H3.3 histone variant in Drosophila.* Current biology : CB, 2009. 19(21): p. 1816-20.
258. Couldrey, C., et al., *A retroviral gene trap insertion into the histone 3.3A gene causes partial neonatal lethality, stunted growth, neuromuscular deficits and male sub-fertility in transgenic mice.* Human molecular genetics, 1999. 8(13): p. 2489-95.
259. Ahmad, K. and S. Henikoff, *The histone variant H3.3 marks active chromatin by replication-independent nucleosome assembly.* Molecular cell, 2002. 9(6): p. 1191-200.
260. Mito, Y., J.G. Henikoff, and S. Henikoff, *Genome-scale profiling of histone H3.3 replacement patterns.* Nature genetics, 2005. 37(10): p. 1090-7.
261. Zhang, H., Z. Wang, and Z. Zhang, *PP1alpha, PP1beta and Wip-1 regulate H4S47 phosphorylation and deposition of histone H3 variant H3.3.* Nucleic acids research, 2013. 41(17): p. 8085-93.
262. Daub, H., et al., *Kinase-selective enrichment enables quantitative phosphoproteomics of the kinome across the cell cycle.* Molecular cell, 2008. 31(3): p. 438-48.
263. Dephoure, N., et al., *A quantitative atlas of mitotic phosphorylation.* Proceedings of the National Academy of Sciences of the United States of America, 2008. 105(31): p. 10762-7.
264. Wissing, J., et al., *Proteomics analysis of protein kinases by target class-selective prefractionation and tandem mass spectrometry.* Molecular & cellular proteomics : MCP, 2007. 6(3): p. 537-47.
265. Bansal, A.D., et al., *Phosphoproteomic Profiling Reveals Vasopressin-Regulated Phosphorylation Sites in Collecting Duct.* Journal of the American Society of Nephrology, 2010. 21(2): p. 303-315.
266. Okuda, T., J.L. Cleveland, and J.R. Downing, *PCTAIRE-1 and PCTAIRE-3, two members of a novel cdc2/CDC28-related protein kinase gene family.* Oncogene, 1992. 7(11): p. 2249-58.
267. Meyerson, M., et al., *A family of human cdc2-related protein kinases.* The EMBO journal, 1992. 11(8): p. 2909-17.

268. Whitfield, M.L., et al., *Identification of genes periodically expressed in the human cell cycle and their expression in tumors.* Molecular biology of the cell, 2002. 13(6): p. 1977-2000.
269. Hirose, T., et al., *PCTAIRE 2, a Cdc2-related serine/threonine kinase, is predominantly expressed in terminally differentiated neurons.* European journal of biochemistry / FEBS, 1997. 249(2): p. 481-8.
270. Herskovits, A.Z. and P. Davies, *The regulation of tau phosphorylation by PCTAIRE 3: implications for the pathogenesis of Alzheimer's disease.* Neurobiology of disease, 2006. 23(2): p. 398-408.
271. Matsuda, S., et al., *PCTAIRE kinase 3/cyclin-dependent kinase 18 is activated through association with cyclin A and/or phosphorylation by protein kinase A.* The Journal of biological chemistry, 2014. 289(26): p. 18387-400.
272. Flicker, C., S.H. Ferris, and B. Reisberg, *Mild cognitive impairment in the elderly predictors of dementia.* Neurology, 1991. 41(7): p. 1006-1006.
273. Petersen, R.C., et al., *Mild cognitive impairment: Clinical characterization and outcome.* Archives of Neurology, 1999. 56(3): p. 303-308.
274. Troncoso, J.C., et al., *Neuropathology in controls and demented subjects from the Baltimore Longitudinal Study of Aging.* Neurobiology of aging, 1996. 17(3): p. 365-371.
275. Markesbery, W.R., et al., *Neuropathologic substrate of mild cognitive impairment.* Archives of Neurology, 2006. 63(1): p. 38-46.
276. Aarsland, D., et al., *Mild cognitive impairment in Parkinson disease A multicenter pooled analysis.* Neurology, 2010. 75(12): p. 1062-1069.
277. Ferman, T.J., et al., *Nonamnestic mild cognitive impairment progresses to dementia with Lewy bodies.* Neurology, 2013. 81(23): p. 2032-8.
278. Belden, C.M., et al., *Clinical characterization of mild cognitive impairment as a prodrome to dementia with Lewy bodies.* American journal of Alzheimer's disease and other dementias, 2015. 30(2): p. 173-7.
279. Parkinson, J., *The shaking palsy.* Sherwood, Neely and Jones, London, 1817.
280. Spillantini, M.G., et al., *α-Synuclein in Lewy bodies.* Nature, 1997. 388(6645): p. 839-840.
281. Kuzuhara, S., et al., *Lewy bodies are ubiquitinated.* Acta neuropathologica, 1988. 75(4): p. 345-353.
282. Lennox, G., et al., *Anti-ubiquitin immunocytochemistry is more sensitive than conventional techniques in the detection of diffuse Lewy body disease.* Journal of neurology, neurosurgery, and psychiatry, 1989. 52(1): p. 67-71.
283. Goldman, J.E., et al., *Lewy bodies of Parkinson's disease contain neurofilament antigens.* Science, 1983. 221(4615): p. 1082-4.
284. Schmidt, M., et al., *Epitope map of neurofilament protein domains in cortical and peripheral nervous system Lewy bodies.* The American journal of pathology, 1991. 139(1): p. 53.
285. Mattila, P., et al., *Alpha-synuclein-immunoreactive cortical Lewy bodies are associated with cognitive impairment in Parkinson's disease.* Acta neuropathologica, 2000. 100(3): p. 285-290.
286. Mattila, P.M., et al., *Cortical Lewy bodies and Alzheimer-type changes in patients with Parkinson's disease.* Acta neuropathologica, 1998. 95(6): p. 576-82.
287. Kotzbauer, P.T., et al., *Pathologic accumulation of alpha-synuclein and Abeta in Parkinson disease patients with dementia.* Archives of Neurology, 2012. 69(10): p. 1326-31.
288. Edison, P., et al., *Amyloid load in Parkinson's disease dementia and Lewy body dementia measured with [11C]PIB positron emission tomography.* Journal of Neurology, Neurosurgery & Psychiatry, 2008. 79(12): p. 1331-1338.
289. Polymeropoulos, M.H., et al., *Mutation in the alpha-synuclein gene identified in families with Parkinson's disease.* Science, 1997. 276(5321): p. 2045-7.

290. Kitada, T., et al., *Mutations in the parkin gene cause autosomal recessive juvenile parkinsonism.* Nature, 1998. 392(6676): p. 605-8.
291. Bonifati, V., et al., *Mutations in the DJ-1 Gene Associated with Autosomal Recessive Early-Onset Parkinsonism.* Science, 2003. 299(5604): p. 256-259.
292. Paisán-Ruíz, C., et al., *Cloning of the gene containing mutations that cause PARK8-linked Parkinson's disease.* Neuron, 2004. 44(4): p. 595-600.
293. Zimprich, A., et al., *Mutations in LRRK2 cause autosomal-dominant parkinsonism with pleomorphic pathology.* Neuron, 2004. 44(4): p. 601-607.
294. Leroy, E., et al., *The ubiquitin pathway in Parkinson's disease.* Nature, 1998. 395(6701): p. 451-2.
295. Valente, E.M., et al., *Hereditary early-onset Parkinson's disease caused by mutations in PINK1.* Science, 2004. 304(5674): p. 1158-60.
296. Houlden, H. and A.B. Singleton, *The genetics and neuropathology of Parkinson's disease.* Acta neuropathologica, 2012. 124(3): p. 325-38.
297. Dauer, W. and S. Przedborski, *Parkinson's disease: mechanisms and models.* Neuron, 2003. 39(6): p. 889-909.
298. Licker, V., et al., *Proteomics in human Parkinson's disease research.* Journal of proteomics, 2009. 73(1): p. 10-29.
299. Cotzias, G.C., P.S. Papavasiliou, and R. Gellene, *Modification of Parkinsonism—chronic treatment with L-dopa.* New England Journal of Medicine, 1969. 280(7): p. 337-345.
300. Basso, M., et al., *Proteome analysis of human substantia nigra in Parkinson's disease.* Proteomics, 2004. 4(12): p. 3943-3952.
301. Werner, C.J., et al., *Proteome analysis of human substantia nigra in Parkinson's disease.* Proteome Sci, 2008. 6(8): p. 10.1186.
302. Kitsou, E., et al., *Identification of proteins in human substantia nigra.* Proteomics-Clinical Applications, 2008. 2(5): p. 776-782.
303. Pan, S., et al., *Proteomics identification of proteins in human cortex using multidimensional separations and MALDI tandem mass spectrometer.* Molecular & Cellular Proteomics, 2007. 6(10): p. 1818-1823.
304. Shi, M., et al., *Mortalin: a protein associated with progression of Parkinson disease?* Journal of Neuropathology & Experimental Neurology, 2008. 67(2): p. 117-124.
305. Leverenz, J.B., et al., *Proteomic identification of novel proteins in cortical lewy bodies.* Brain pathology, 2007. 17(2): p. 139-145.
306. Xia, Q., et al., *Proteomic identification of novel proteins associated with Lewy bodies.* Frontiers in bioscience: a journal and virtual library, 2008. 13: p. 3850.
307. Steele, J.C., J. Richardson, and J. Olszewski, *Progressive supranuclear palsy: A heterogeneous degeneration involving the brain stem, basal ganglia and cerebellum with vertical gaze and pseudobulbar palsy, nuchal dystonia and dementia.* Archives of Neurology, 1964. 10(4): p. 333-359.
308. Dickson, D.W., et al., *Neuropathology of variants of progressive supranuclear palsy.* Current opinion in neurology, 2010. 23(4): p. 394-400.
309. Hauw, J.-J., et al., *Constant neurofibrillary changes in the neocortex in progressive supranuclear palsy. Basic differences with Alzheimer's disease and aging.* Neuroscience letters, 1990. 119(2): p. 182-186.
310. Constantinescu, R., et al., *Proteomic profiling of cerebrospinal fluid in parkinsonian disorders.* Parkinsonism & related disorders, 2010. 16(8): p. 545-549.
311. Ebrahim, A., et al., *A proteomic study identifies different levels of light chain ferritin in corticobasal degeneration and progressive supranuclear palsy.* Acta neuropathologica, 2011. 122(6): p. 727-736.

312. Bondarenko, P.V., D. Chelius, and T.A. Shaler, *Identification and relative quantitation of protein mixtures by enzymatic digestion followed by capillary reversed-phase liquid chromatography-tandem mass spectrometry.* Analytical chemistry, 2002. 74(18): p. 4741-4749.
313. Wang, W., et al., *Quantification of proteins and metabolites by mass spectrometry without isotopic labeling or spiked standards.* Analytical chemistry, 2003. 75(18): p. 4818-4826.
314. Wiener, M.C., et al., *Differential mass spectrometry: a label-free LC-MS method for finding significant differences in complex peptide and protein mixtures.* Analytical chemistry, 2004. 76(20): p. 6085-6096.
315. Liu, H., R.G. Sadygov, and J.R. Yates, *A model for random sampling and estimation of relative protein abundance in shotgun proteomics.* Analytical chemistry, 2004. 76(14): p. 4193-4201.
316. Cox, J., et al., *Accurate Proteome-wide Label-free Quantification by Delayed Normalization and Maximal Peptide Ratio Extraction, Termed MaxLFQ.* Molecular & Cellular Proteomics, 2014. 13(9): p. 2513-2526.
317. Ho, T., et al., *A subpopulation of mesencephalic dopamine neurons projecting to limbic areas contains a cholecystokinin-like peptide: evidence from immunohistochemistry combined with retrograde tracing.* Neuroscience, 1980. 5(12): p. 2093-2124.
318. Hommer, D., et al., *Cholecystokinin-dopamine coexistence: electrophysiological actions corresponding to cholecystokinin receptor subtype.* The Journal of neuroscience, 1986. 6(10): p. 3039-3043.
319. Marshall, F.H., et al., *Cholecystokinin Modulates the Release of Dopamine from the Anterior and Posterior Nucleus Accumbens by Two Different Mechanisms.* Journal of neurochemistry, 1991. 56(3): p. 917-922.
320. Studler, J., et al., *CCK-8-immunoreactivity distribution in human brain: selective decrease in the substantia nigra from parkinsonian patients.* Brain research, 1982. 243(1): p. 176-179.
321. Fujii, C., et al., *Association between polymorphism of the cholecystokinin gene and idiopathic Parkinson's disease.* Clinical Genetics, 1999. 56(5): p. 395-400.
322. Wang, J., et al., *Cholecystokinin, cholecystokinin-A receptor and cholecystokinin-B receptor gene polymorphisms in Parkinson's disease.* Pharmacogenetics and Genomics, 2003. 13(6): p. 365-369.
323. Mattay, V.S., et al., *Dopaminergic modulation of cortical function in patients with Parkinson's disease.* Annals of neurology, 2002. 51(2): p. 156-64.
324. Frye, R.A., *Characterization of five human cDNAs with homology to the yeast SIR2 gene: Sir2-like proteins (sirtuins) metabolize NAD and may have protein ADP-ribosyltransferase activity.* Biochemical and biophysical research communications, 1999. 260(1): p. 273-279.
325. Michishita, E., et al., *Evolutionarily conserved and nonconserved cellular localizations and functions of human SIRT proteins.* Molecular biology of the cell, 2005. 16(10): p. 4623-4635.
326. Ciccone, S., et al., *Parkinson's disease: a complex interplay of mitochondrial DNA alterations and oxidative stress.* International journal of molecular sciences, 2013. 14(2): p. 2388-409.
327. Yan, M.H., X. Wang, and X. Zhu, *Mitochondrial defects and oxidative stress in Alzheimer disease and Parkinson disease.* Free Radical Biology and Medicine, 2013. 62: p. 90-101.
328. Heeman, B., et al., *Depletion of PINK1 affects mitochondrial metabolism, calcium homeostasis and energy maintenance.* Journal of cell science, 2011. 124(7): p. 1115-1125.
329. Pridgeon, J.W., et al., *PINK1 protects against oxidative stress by phosphorylating mitochondrial chaperone TRAP1.* PLoS Biol, 2007. 5(7): p. e172.
330. Du, J., et al., *Sirt5 is a NAD-dependent protein lysine demalonylase and desuccinylase.* Science, 2011. 334(6057): p. 806-809.
331. Rardin, M.J., et al., *SIRT5 regulates the mitochondrial lysine succinylome and metabolic networks.* Cell metabolism, 2013. 18(6): p. 920-933.

332. Bossers, K., et al., *Analysis of Gene Expression in Parkinson's Disease: Possible Involvement of Neurotrophic Support and Axon Guidance in Dopaminergic Cell Death.* Brain pathology, 2009. 19(1): p. 91-107.
333. Luchetti, S., et al., *Neurosteroid Biosynthetic Pathway Changes in Substantia Nigra and Caudate Nucleus in Parkinson's Disease.* Brain pathology, 2010. 20(5): p. 945-951.
334. Brickley, S.G. and I. Mody, *Extrasynaptic GABA A receptors: their function in the CNS and implications for disease.* Neuron, 2012. 73(1): p. 23-34.
335. Madsen, K.K., H.S. White, and A. Schousboe, *Neuronal and non-neuronal GABA transporters as targets for antiepileptic drugs.* Pharmacology & therapeutics, 2010. 125(3): p. 394-401.
336. Engqvist-Goldstein, Å.E., et al., *An actin-binding protein of the Sla2/Huntingtin interacting protein 1 family is a novel component of clathrin-coated pits and vesicles.* The Journal of cell biology, 1999. 147(7): p. 1503-1518.
337. Legendre-Guillemin, V., et al., *Huntingtin interacting protein 1 (HIP1) regulates clathrin assembly through direct binding to the regulatory region of the clathrin light chain.* Journal of Biological Chemistry, 2005. 280(7): p. 6101-6108.
338. Kalchman, M.A., et al., *HIP1, a human homologue of S. cerevisiae Sla2p, interacts with membrane-associated huntingtin in the brain.* Nature genetics, 1997. 16(1): p. 44-53.
339. Hackam, A.S., et al., *Huntingtin interacting protein 1 induces apoptosis via a novel caspase-dependent death effector domain.* Journal of Biological Chemistry, 2000. 275(52): p. 41299-41308.
340. Chow, N., et al., *Serum response factor and myocardin mediate arterial hypercontractility and cerebral blood flow dysregulation in Alzheimer's phenotype.* Proceedings of the National Academy of Sciences of the United States of America, 2007. 104(3): p. 823-8.
341. Street, J.S., et al., *Olanzapine treatment of psychotic and behavioral symptoms in patients with alzheimer disease in nursing care facilities: A double-blind, randomized, placebo-controlled trial.* Archives of General Psychiatry, 2000. 57(10): p. 968-976.
342. Bensimon, G., et al., *Riluzole treatment, survival and diagnostic criteria in Parkinson plus disorders: the NNIPPS study.* Brain : a journal of neurology, 2009. 132(Pt 1): p. 156-71.
343. Group II, R.S., et al., *Dose-ranging study of riluzole in amyotrophic lateral sclerosis.* The Lancet, 1996. 347(9013): p. 1425-1431.
344. Pabarcus, M.K., et al., *CYP3A4 ubiquitination by gp78 (the tumor autocrine motility factor receptor, AMFR) and CHIP E3 ligases.* Archives of biochemistry and biophysics, 2009. 483(1): p. 66-74.
345. Shults, C.W., *Lewy bodies.* Proceedings of the National Academy of Sciences of the United States of America, 2006. 103(6): p. 1661-1668.
346. Wakabayashi, K., et al., *The Lewy body in Parkinson's disease: Molecules implicated in the formation and degradation of α-synuclein aggregates.* Neuropathology, 2007. 27(5): p. 494-506.
347. Masliah, E., et al., *β-Amyloid peptides enhance α-synuclein accumulation and neuronal deficits in a transgenic mouse model linking Alzheimer's disease and Parkinson's disease.* Proceedings of the National Academy of Sciences, 2001. 98(21): p. 12245-12250.
348. Siderowf, A., et al., *CSF amyloid {beta} 1-42 predicts cognitive decline in Parkinson disease.* Neurology, 2010. 75(12): p. 1055-61.
349. Andersson, M., et al., *The cognitive profile and CSF biomarkers in dementia with Lewy bodies and Parkinson's disease dementia.* International journal of geriatric psychiatry, 2011. 26(1): p. 100-5.
350. Alves, G., et al., *CSF amyloid-beta and tau proteins, and cognitive performance, in early and untreated Parkinson's disease: the Norwegian ParkWest study.* Journal of neurology, neurosurgery, and psychiatry, 2010. 81(10): p. 1080-6.

351. Worby, C.A. and J.E. Dixon, *Sorting out the cellular functions of sorting nexins.* Nature reviews Molecular cell biology, 2002. 3(12): p. 919-931.
352. Lee, J., et al., *Adaptor Protein Sorting Nexin 17 Regulates Amyloid Precursor Protein Trafficking and Processing in the Early Endosomes.* Journal of Biological Chemistry, 2008. 283(17): p. 11501-11508.
353. Caldenhoven, E., et al., *Stimulation of the human intercellular adhesion molecule-1 promoter by interleukin-6 and interferon-gamma involves binding of distinct factors to a palindromic response element.* Journal of Biological Chemistry, 1994. 269(33): p. 21146-21154.
354. Gade, P., et al., *Critical Role for Transcription Factor C/EBP-β in Regulating the Expression of Death-Associated Protein Kinase 1.* Molecular and cellular biology, 2008. 28(8): p. 2528-2548.
355. Nyman, T.A., et al., *Proteome analysis reveals ubiquitin-conjugating enzymes to be a new family of interferon-α-regulated genes.* European Journal of Biochemistry, 2000. 267(13): p. 4011-4019.
356. Giuffrida, A., M. Beltramo, and D. Piomelli, *Mechanisms of Endocannabinoid Inactivation: Biochemistry and Pharmacology.* Journal of Pharmacology and Experimental Therapeutics, 2001. 298(1): p. 7-14.
357. Benito, C., et al., *Cannabinoid CB2 receptors and fatty acid amide hydrolase are selectively overexpressed in neuritic plaque-associated glia in Alzheimer's disease brains.* The Journal of neuroscience, 2003. 23(35): p. 11136-11141.
358. D'Addario, C., et al., *Epigenetic regulation of fatty acid amide hydrolase in Alzheimer disease.* PloS one, 2012. 7(6): p. e39186.
359. Mazzola, C., et al., *Fatty acid amide hydrolase (FAAH) inhibition enhances memory acquisition through activation of PPAR-α nuclear receptors.* Learning & Memory, 2009. 16(5): p. 332-337.
360. Marsicano, G., et al., *CB1 Cannabinoid Receptors and On-Demand Defense Against Excitotoxicity.* Science, 2003. 302(5642): p. 84-88.
361. Iuvone, T., et al., *Neuroprotective effect of cannabidiol, a non-psychoactive component from Cannabis sativa, on β-amyloid-induced toxicity in PC12 cells.* Journal of neurochemistry, 2004. 89(1): p. 134-141.
362. Sarbassov, D.D., et al., *Rictor, a novel binding partner of mTOR, defines a rapamycin-insensitive and raptor-independent pathway that regulates the cytoskeleton.* Current biology, 2004. 14(14): p. 1296-1302.
363. Sarbassov, D.D., et al., *Phosphorylation and Regulation of Akt/PKB by the Rictor-mTOR Complex.* Science, 2005. 307(5712): p. 1098-1101.
364. Bhaskar, K., et al., *The PI3K-Akt-mTOR pathway regulates Abeta oligomer induced neuronal cell cycle events.* Molecular neurodegeneration, 2009. 4: p. 14.
365. Lafay-Chebassier, C., et al., *mTOR/p70S6k signalling alteration by Aβ exposure as well as in APP-PS1 transgenic models and in patients with Alzheimer's disease.* Journal of neurochemistry, 2005. 94(1): p. 215-225.
366. North, B.J. and E. Verdin, *Mitotic Regulation of SIRT2 by Cyclin-dependent Kinase 1-dependent Phosphorylation.* Journal of Biological Chemistry, 2007. 282(27): p. 19546-19555.
367. Zhu, X., et al., *Neuronal binucleation in Alzheimer disease hippocampus.* Neuropathology and Applied Neurobiology, 2008. 34(4): p. 457-465.
368. Vincze, O., et al., *Tubulin polymerization promoting proteins (TPPPs): members of a new family with distinct structures and functions.* Biochemistry, 2006. 45(46): p. 13818-26.
369. Kong, W., et al., *Independent component analysis of Alzheimer's DNA microarray gene expression data.* Molecular neurodegeneration, 2009. 4(1): p. 1-14.
370. Zhou, W., et al., *Depletion of tubulin polymerization promoting protein family member 3 suppresses HeLa cell proliferation.* Molecular and cellular biochemistry, 2010. 333(1-2): p. 91-98.

371. Gray, P.W., et al., *Cloning and expression of cDNA for human diazepam binding inhibitor, a natural ligand of an allosteric regulatory site of the gamma-aminobutyric acid type A receptor.* Proceedings of the National Academy of Sciences, 1986. 83(19): p. 7547-7551.
372. Edgar, P., et al., *A comparative proteome analysis of hippocampal tissue from schizophrenic and Alzheimer's disease individuals.* Molecular psychiatry, 1999. 4(2): p. 173-178.
373. Ferrarese, C., et al., *Cerebrospinal fluid levels of diazepam-binding inhibitor in neurodegenerative disorders with dementia.* Neurology, 1990. 40(4): p. 632-632.
374. Paradisi, A. and S. Oddi, *The endocannabinoid system in ageing: a new target for drug development.* Current drug targets, 2006. 7(11): p. 1539-1552.
375. Jenner, P. and C.W. Olanow, *Oxidative stress and the pathogenesis of Parkinson's disease.* Neurology, 1996. 47(6 Suppl 3): p. 161S-170S.
376. McGeer, P., et al., *Reactive microglia are positive for HLA-DR in the substantia nigra of Parkinson's and Alzheimer's disease brains.* Neurology, 1988. 38(8): p. 1285-1285.
377. Zhang, W., et al., *Aggregated α-synuclein activates microglia: a process leading to disease progression in Parkinson's disease.* The FASEB Journal, 2005. 19(6): p. 533-542.
378. Ciechanover, A. and P. Brundin, *The ubiquitin proteasome system in neurodegenerative diseases: sometimes the chicken, sometimes the egg.* Neuron, 2003. 40(2): p. 427-446.
379. Lam, Y.A., et al., *Inhibition of the ubiquitin-proteasome system in Alzheimer's disease.* Proceedings of the National Academy of Sciences, 2000. 97(18): p. 9902-9906.
380. Shimura, H., et al., *Familial Parkinson disease gene product, parkin, is a ubiquitin-protein ligase.* Nature genetics, 2000. 25(3): p. 302-305.
381. Marfella, R., et al., *The Ubiquitin-Proteasome System and Inflammatory Activity in Diabetic Atherosclerotic Plaques: Effects of Rosiglitazone Treatment.* Diabetes, 2006. 55(3): p. 622-632.
382. Wang, J. and M.A. Maldonado, *The ubiquitin-proteasome system and its role in inflammatory and autoimmune diseases.* Cell Mol Immunol, 2006. 3(4): p. 255-261.
383. Link, A.J., et al., *Direct analysis of protein complexes using mass spectrometry.* Nature biotechnology, 1999. 17(7): p. 676-682.
384. le Maire, M., P. Champeil, and J.V. Moller, *Interaction of membrane proteins and lipids with solubilizing detergents.* Biochimica et biophysica acta, 2000. 1508(1-2): p. 86-111.
385. Ogorzalek Loo, R., N. Dales, and P. Andrews, *The Effect of Detergents on Proteins Analyzed by Electrospray Ionization*, in *Protein and Peptide Analysis by Mass Spectrometry*, J. Chapman, Editor 1996, Humana Press. p. 141-160.
386. Barnidge, D.R., et al., *Extraction method for analysis of detergent-solubilized bacteriorhodopsin and hydrophobic peptides by electrospray ionization mass spectrometry.* Analytical biochemistry, 1999. 269(1): p. 1-9.
387. Fischer, R. and B.M. Kessler, *Gel-aided sample preparation (GASP)--a simplified method for gel-assisted proteomic sample generation from protein extracts and intact cells.* Proteomics, 2015. 15(7): p. 1224-9.

Appendix A - Electrophoresis: Neuroproteomics Special Issue

Dale Chaput[1]
Lisa Hornbeck Kirouac[2]
Harris Bell-Temin[1]
Stanley M. Stevens Jr.[1*,**]
Jaya Padmanabhan[2*]

[1]Department of Cell Biology, Microbiology, and Molecular Biology, University of South Florida, Tampa, FL, USA
[2]Department of Molecular Medicine, USF Health Byrd Alzheimer's Institute, University of South Florida, Tampa, FL, USA

Received April 27, 2012
Revised August 27, 2012
Accepted August 27, 2012

Research Article

SILAC-based proteomic analysis to investigate the impact of amyloid precursor protein expression in neuronal-like B103 cells

Alzheimer's disease (AD) is the most prevalent form of dementia in the elderly. Amyloid plaque formation through aggregation of the amyloid beta peptide derived from amyloid precursor protein (APP) is considered one of the hallmark processes leading to AD pathology; however, the precise role of APP in plaque formation and AD pathogenesis is yet to be determined. Using stable isotope labeling by amino acids in cell culture (SILAC) and MS, protein expression profiles of APP null, rat neuronal-like B103 cells were compared to B103–695 cells that express the APP isoform, APP-695. A total of 2979 unique protein groups were identified among three biological replicates and significant protein expression changes were identified in a total of 102 nonredundant proteins. Some of the top biological functions associated with the differentially expressed proteins identified include cellular assembly, organization and morphology, cell cycle, lipid metabolism, protein folding, and PTMs. We report several novel biological pathways influenced by APP-695 expression in neuronal-like cells and provide additional framework for investigating altered molecular mechanisms associated with APP expression and processing and contribution to AD pathology.

Keywords:
Alzheimer's disease / Amyloid beta / Amyloid precursor protein / Proteomics / SILAC
DOI 10.1002/elps.201200251

Additional supporting information may be found in the online version of this article at the publisher's web-site

1 Introduction

Alzheimer's disease (AD) is the most common form of dementia that affects elderly and is associated with cognitive decline and loss of executive function. The two major pathological characteristics of the disease are the presence of neuritic plaques and neurofibrillary tangles in the areas of the brain associated with learning and memory [1–3]. Neuritic plaques are formed by extracellular accumulation of amyloid beta (Aβ), a peptide derived from amyloid precursor protein (APP). APP is a single transmembrane domain protein that is expressed at high levels in brain. Studies in AD brains have shown that APP is cleaved by beta-site APP cleaving enzyme (BACE or beta secretase) and gamma secretases to generate Aβ, a peptide fragment that is 40–42 amino acids long (Aβ40 and Aβ42) [4–8]. In addition to beta and gamma secretases, APP is also cleaved by alpha secretase; this secretase cleaves APP within the Aβ domain and thus excludes the formation of Aβ from APP. The secretase cleavages of APP generate ectodomains and intracellular domains of APP in addition to Aβ (Fig. 1A). APP has been reported to enhance neurite outgrowth, inhibit neurodegeneration, and exert anti-apoptotic activity. Out of the different APP fragments, Aβ and AICD (APP intracellular domain) have been shown to enhance neurodegeneration while the secreted alpha-cleaved ectodomain of APP (sAPPα) has been shown to have growth promoting activity.

A number of factors such as age, environment, and inflammatory proteins appear to affect the onset of AD. Several

Correspondence: Dr. Jaya Padmanabhan, Department of Molecular Medicine, USF Health Byrd Alzheimer's Institute, University of South Florida, 4001 E Fletcher Ave, Tampa, FL 33613, USA
E-mail: jpadmana@health.usf.edu

Abbreviations: Aβ, amyloid β; **AD**, Alzheimer's disease; **ApoE4**, apolipoproteins E4 allele; **APP**, amyloid precursor protein; **eIF4A2**, eukaryotic translation initiation factor 4A2; **IPA**, Ingenuity Pathway Analysis; **MAPK**, Mitogen-activated protein kinase; **PDLIM1**, PD2 and LIM domain 1; **RTN4**, Reticulon 4; **SCX**, strong cation-exchange; **SILAC**, stable isotope labeling by amino acids in cell culture

*Dr. Stanley M. Stevens Jr. and Dr. Jaya Padmanabhan are equal last authors.
**Additional corresponding author: Dr. Stanley M. Stevens Jr., E-mail: smstevens@usf.edu

Colour Online: See the article online to view Figs. 1 and 3 in colour.

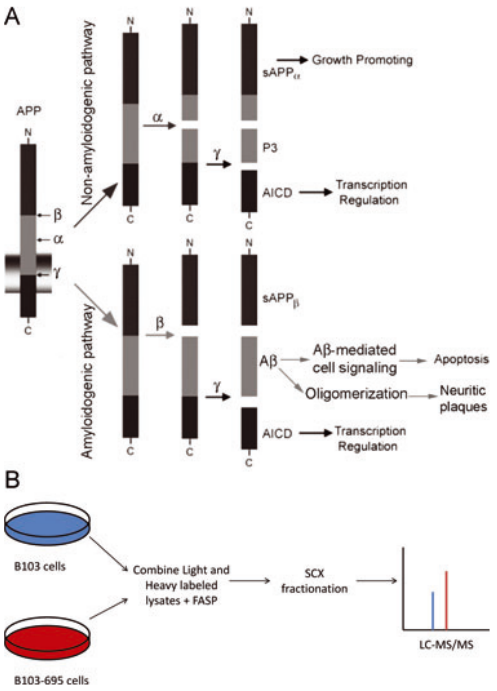

Figure 1. (A) Schematic of proteolytic processing of APP by α, β, and γ secretases. (B) SILAC experimental workflow used for differential protein expression profiling in B103 cells expressing APP-695.

independent studies have shown that cell cycle deregulation correlates with pathology development in AD. Analysis of brains from AD patients and mice expressing AD transgenes has shown increased expression of cell cycle regulatory proteins in neurons, which correlated with APP and tau phosphorylation and pathology development [9–21]. We recently showed that phosphorylation and cellular distribution of APP are affected in a cell cycle-dependent manner and this is associated with altered processing of APP [10]. The discoveries demonstrating that cells expressing APP show enhanced growth rate and the observation that APP localizes to centrosomes under mitotic conditions led to the hypothesis that it may play a role in cell cycle progression. The exact role of APP in cell cycle activation and cell proliferation is not yet identified. Here we sought to determine the mechanism(s) by which APP affects cellular functions using APP null B103 nerve cells.

Elegant studies by Schubert et al. have shown that B103 nerve cells do not express either APP or the APP-like proteins APLP1 or APLP2 [22]. Therefore, these cells are appropriate for studying the cellular functions of APP. These investigators showed that expression of APP in B103 cells enhances cell adhesion, neurite outgrowth, and cell proliferation but the molecular mechanisms by which APP induces these cellular functions are not quite clear. It is possible that APP or a metabolite of APP can induce these either by itself or by affecting expression of genes associated with these functions. In order to determine whether APP affects expression of proteins associated with cell adhesion or cell cycle progression or cell signaling processes in general, we performed an unbiased, global-scale analysis to assess APP-mediated protein expression changes in B103 cells. We used the stable isotope labeling by amino acids in cell culture (SILAC) approach for comparing the protein complement of B103 cells expressing the 695 isoform of APP (referred to as B103–695) to B103 APP null cells (referred to as B103) as shown in Fig. 1B. The advantage of this approach is that B103 cells can be grown in media containing normal or "light" versions of amino acids and B103–695 in media with "heavy" amino acids. The labeled (heavy) amino acids are added to media that are deficient in specific amino acids (in this case *L*-arginine and *L*-lysine) and the cells metabolically incorporate these amino acids during protein synthesis. This technique allows one to differentiate proteins from one cell system to the other and analyze both simultaneously using MS/MS. This approach decreases experimental variability that occurs during sample processing and provides more consistent and reliable data for relative protein quantitation. Here we provide evidence for protein expression changes in B103 cells expressing APP-695 versus APP null cells and validate changes in selected proteins involved in cell signaling as well as cell morphology, assembly, and organization.

2 Materials and methods

2.1 Cell culture and SILAC labeling

B103 and B103–695 rat neuroblastoma cells were initially cultured in DMEM/F12 (1:1) media supplemented with 10% fetal bovine serum, 50 U/mL penicillin, and 50 μg/mL streptomycin, at 37°C and 5% CO_2 [23]. Cells were grown in T75 cm^2 flasks to near confluence, and then split into 3 × T75 cm^2 flasks for stable isotope labeling with heavy or light amino acids in cell culture (SILAC).

B103 and B103–695 cells were labeled for quantitation using SILAC media supplemented with 10% dialyzed fetal bovine serum, pen/strep, and either *L*-lysine and *L*-arginine for B103 or $^{13}C_6$-L-Lysine 2HCl and $^{13}C_6$-$^{15}N_4$-Arginine HCl (Thermo Scientific) for B103–695 cells. Cells were grown in SILAC media for 7 days, during which they were passaged once and media was changed every 48 h, for a minimum of five doublings, corresponding to greater than 98% labeling efficiency.

Cells were collected using Trypsin-EDTA and washed three times with PBS to remove serum proteins. Cells were lysed in 250 μL of 100 mM Tris-HCl (pH 7.6) containing 4% SDS, 100 mM DTT, and Halt protease inhibitor cocktail (Pierce) at 95°C for 5 min. Lysed samples were briefly sonicated. Protein concentrations were determined using the Pierce 660 nm protein assay with the ionic detergent

compatibility reagent (Pierce). These experiments were done in triplicate.

2.2 Sample preparation

Whole cell lysates were digested using the filter-aided sample preparation kit (Protein Discovery), as developed by Wisniewski and Mann [24]. Four digestions of approximately 100 μg of protein were performed for each biological replicate, which were then pooled for a total of 400 μg per biological replicate. Thirty microliters of protein sample and 8 M urea were mixed and added to the 30 kDa filter-aided sample preparation spin filter for buffer exchange. Samples were alkylated according to manufacturer's instructions with iodoacetamide for 30 min in the dark. Following alkylation, samples underwent further buffer exchange with 3 × 100 μL additions of 50 mM ammonium bicarbonate, followed by centrifugation at 14 000 × *g* for 10 min. Samples were incubated with trypsin at 1:100 (w:w, trypsin:protein) for proteolytic digestion of proteins and incubated overnight at 37°C. Peptides were collected by centrifugation with the addition of 2 × 40 μL 50 mM ammonium bicarbonate and 40 μL NaCl. Peptides were desalted using Supelco Discovery DSC-18 SPE columns in combination with a Supelco vacuum manifold. Samples were dried using a vacuum concentrator (Thermo) and resuspended in 20 μL of 0.1% formic acid in H_2O.

Peptides were fractionated on a Dionex U3000 HPLC system with a 15 cm × 1.0 mm id strong cation-exchange (SCX) column (PolyLC Inc.) packed with 5 μm 300 Å polySULFOETHYL A-SCX material. Two-min fractions were collected using a 30-min gradient, where ammonium formate increased from 15–200 mM in 25% ACN at a flow rate of 250 μL/min. Ten peptide-containing fractions were selected for LC-MS/MS analysis from each biological replicate (n = 3 total). Peptides were again dried in a vacuum concentrator and resuspended in 10 μL of 0.1% formic acid in H_2O.

2.3 LC-MS/MS

SCX peptide fractions were separated on a 10 cm × 75 μm id RP column (New Objective) packed with 5 μm 300 Å C18 material (ProteoPep II). MS/MS analysis was carried out using a hybrid linear ion trap-Orbitrap instrument (LTQ Orbitrap XL, Thermo). A 90 min gradient was used, where 0.1% formic acid in ACN increased from 2 to 40%, increasing to 80% at 95 min through 100 min. Orbitrap full MS scans were collected at a mass resolving power of 60 000, with positive polarity in profile mode, and a scan range of m/z 350–1500. The top five most abundant ions were selected for further fragmentation in the ion trap. Global settings include dynamic exclusion of 90 s, with an exclusion list size of 500, and a repeat count of 2.

2.4 Database searching and pathway analysis

Raw files were processed in MaxQuant version 1.2.0.13, a quantitative proteomics software package for the analysis of large, high-resolution MS data sets [25]. The raw files were processed and searched against the current UniprotKB database containing *Rattus norvegicus* protein sequences as well as a second MaxQuant database of known contaminants. The search parameters included a constant modification of cysteine by carbamidomethylation and variable modification of methionine oxidation. Additional parameters include multiplicity set to 2, with a heavy set of lysine-6 and arginine-10. The search tolerance was set to 8 ppm and the fragment ion mass tolerance was set to 0.5 Da with a false discovery rate of less than 1%.

Statistical analysis was carried out using Perseus software, which assesses the statistical significance of protein expression based on the approach developed by Benjamini and Hochberg [26]. A threshold q-value of 0.05 for the Benjamini-Hochberg false discovery rate was used. Functional and pathway analysis of identified proteins was carried out using Ingenuity Pathway Analysis (IPA, Ingenuity Systems).

2.5 Western blotting

Proteins were selected for Western blot validation of protein expression changes based on significance as well as function. Twenty micrograms of B103 and B103–695 cell lysate were separated on a 15% Tris/Glycine SDS-PAGE gel, run at 90 V for 90 min. Proteins were semi-wet transferred to a nitrocellulose membrane (Whatman) at 30 V for 90 min. The membrane was subsequently blocked in 5% nonfat milk-TBS for 1 h at room temperature, and washed using PBS containing Tween-20 (PBST). Primary antibodies specific for Ras (Abcam, mouse monoclonal, 1:1000), P-ERK, and ERK44/42 (Cell Signaling, rabbit polyclonal, 1:1000), and actin (Sigma, mouse monoclonal, 1:7000) were diluted in 3% BSA/TBS/0.02% sodium azide and incubated overnight at 4°C. Membranes were then incubated with corresponding anti-rabbit (Pierce) and anti-mouse (Pierce) secondary antibodies for 90 min at room temperature and washed thoroughly. The blots were developed using the Super Signal chemiluminescence reagents (Pierce).

2.6 Immunostaining analysis

B103 and B103–695 cells were plated onto poly-lysine-coated eight chamber slides and cultured overnight in DMEM/F12 (1:1) medium with serum and Pen-Strep. After 24 h of culturing, cells were washed with PBS and fixed with 4% paraformaldehyde for 10 min at room temperature. At the end of the fixation, cells were washed and incubated in 1% BSA in TBS containing 0.1% Triton X-100 (BSA/TBST) to block any nonspecific binding. After 1 h incubation at room temperature, γ-synuclein (Millipore, rabbit monoclonal, 1:500) and actin (Sigma, mouse monoclonal, 1:500) antibodies diluted in BSA/TBST were added to the cells and incubated overnight at 4°C by gentle rocking. The slides were washed with PBS thoroughly and incubated with Alexa Fluor 488 anti-mouse

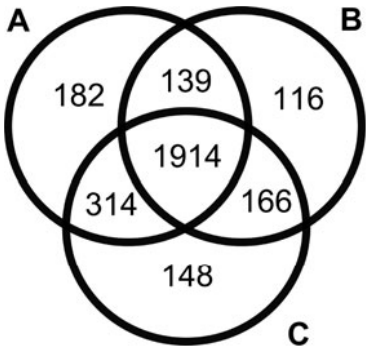

Figure 2. Venn diagram representing the number of unique protein groups identified in biological replicate A, B, and C, and the overlap of proteins identified between the biological replicates.

and Alexa Fluor 594 anti-rabbit secondary antibodies (Invitrogen/Gibco) for 1–2 h at room temperature in the dark. At the end of the incubation, cells were washed again and incubated with 1 μg/mL Hoechst 33258, diluted in PBS, for 10 min at room temperature protected from light. After further washes, the slides were mounted using Fluoro-gel mounting media (Electron Microscopy Sciences) and analyzed under a Zeiss Fluorescent microscope using AxioVision Rel 4.8 software program.

3 Results and discussion

3.1 B103 and B103–695 proteome comparison

A total of 2979 protein groups were identified among three biological replicates, excluding contaminants and false positive identifications. The entire MaxQuant output is provided in Supporting Information Table S1 and the protein list is sorted by H/L ratio counts in order to approximately organize the data in terms of quantitation confidence at the protein level. Biological replicates A, B, and C identified 2549, 2335, and 2542 protein groups, respectively. Over 1900 protein groups were shared by all three biological replicates. Replicates A and B shared 2053, replicates A and C shared 2228, and replicates B and C shared 2080 protein groups. The overlap of protein identifications between biological replicates is demonstrated by the Venn diagram shown in Fig. 2.

Perseus was used to identify proteins with statistically significant changes in expression across multiple biological replicates. Two significance tests were employed, Significance A and Significance B, where the A significance gives no weight to signal intensity and B significance is weighted by signal intensity. Significance A test identified 79 significant proteins, while 83 significant proteins were identified using Significance B, for a combined total of 102 nonredundant proteins that were differentially expressed in B103–695 cells (listed in Supporting Information Table S2). Out of the 102 differentially expressed proteins, seven proteins were downregulated and 95 proteins were upregulated.

3.2 Functional enrichment

Several proteins that are important in cellular and molecular functions including cellular assembly and organization, cell cycle, cell morphology, lipid metabolism, protein folding, and PTMs were identified as having differential expression upon proteome comparison in B103 and B103–695 cells using IPA (Fig. 3). Many of the proteins identified are also involved in regulating physiological system development and function processes such as connective tissue, cardiovascular system, and nervous system development and function, as well as embryonic tissue development (Fig. 3).

IPA also identified significant canonical pathways associated with a number of identified proteins that were differentially expressed including CDK5 signaling, cell cycle G2/M DNA damage checkpoint regulation, actin cytoskeleton signaling, protein kinase A signaling, and ERK5 signaling as shown in the selected canonical pathways in Fig. 3. CDK5 signaling is involved in cell differentiation and morphology regulation and has been implicated in neuron degeneration [27]. CDK5 signaling is important for proper brain development and dysregulation in CDK5 leads to defects in cell migration, plasticity, and other neurological defects [5, 28–30]. Additionally, actin cytoskeleton and protein kinase A signaling were also over-represented from the SILAC dataset. Actin cytoskeleton signaling is associated with cell motility, axon guidance, cellular assembly, organization, function, and maintenance whereas protein kinase A is a serine/threonine kinase that functions as a second messenger regulating a variety of diverse functions including growth, development, and memory. Interestingly, the G2/M DNA damage checkpoint was identified as a potential altered pathway from the SILAC dataset as well and provides additional evidence of the involvement of cell cycle-dependent mechanisms upon APP expression in this cell model system. The G2/M DNA damage checkpoint is the second checkpoint within the cell cycle and is important for maintaining genomic stability as it prevents damaged DNA from entering M-phase.

3.3 Pathway analysis reveals APP-mediated alterations in cell morphology and Ras signaling

The top protein interaction network identified using IPA is primarily involved in cell morphology, assembly, and organization, as well as nervous system development and function which is shown in Fig. 4. Proteins of particular interest include γ-synuclein and Ras, which are both found to be upregulated in B103–695 cells. Western blots were performed to validate the increased expression of γ-synuclein and Ras in B103–695 cells. While Ras showed a significant increase by Western blot analysis (Fig. 5B), we were unable to detect the γ-synuclein with this technique. We believe that this is

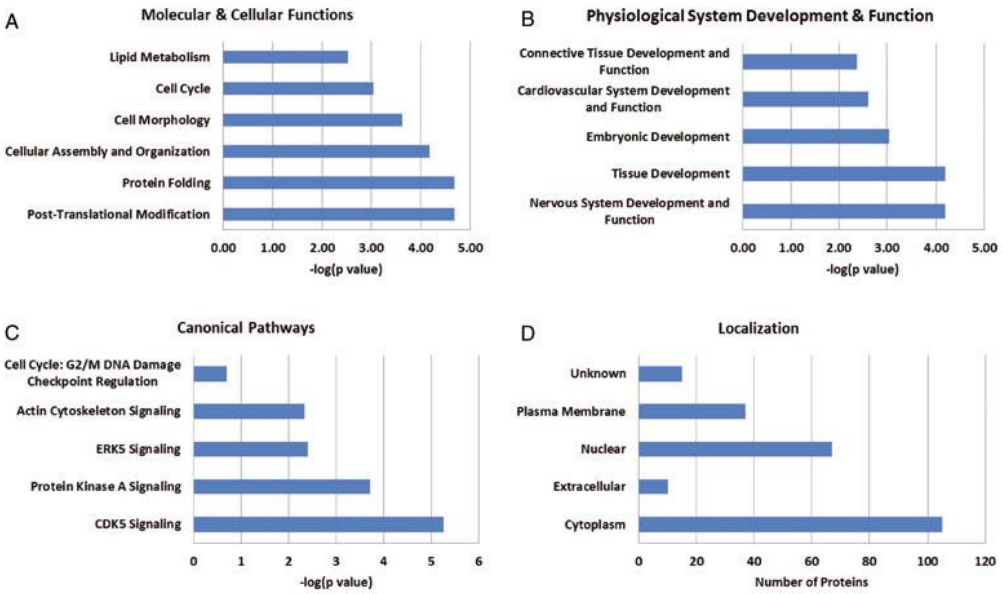

Figure 3. Ingenuity pathway analysis of APP-mediated differential protein expression in B103 cells showing over-represented categories associated with (A) molecular and cellular function, (B) physiological system development and function, (C) canonical pathways, and (D) cell localization.

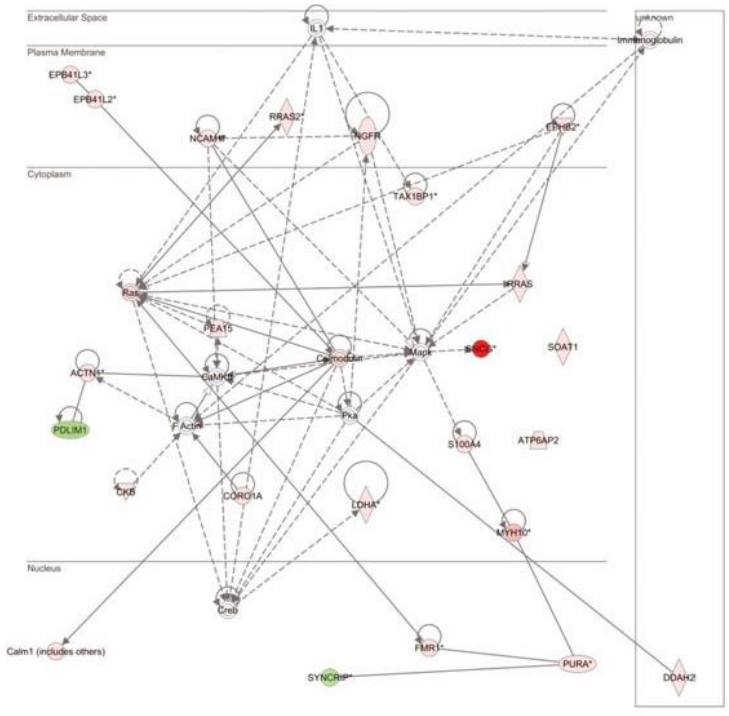

Figure 4. Top-scoring pathway from Ingenuity pathway analysis associated with cellular assembly and organization based on differentially expressed proteins identified from B103 cells expressing APP-695. The network diagram uses different shapes to represent protein functions: enzymes (diamond), kinases (inverted triangle), transporters (trapezoid), and other (circles). Single lines represent protein–protein interactions; solid or dashed lines represent direct or indirect interactions, respectively. Proteins that regulate another protein are indicated by arrows.

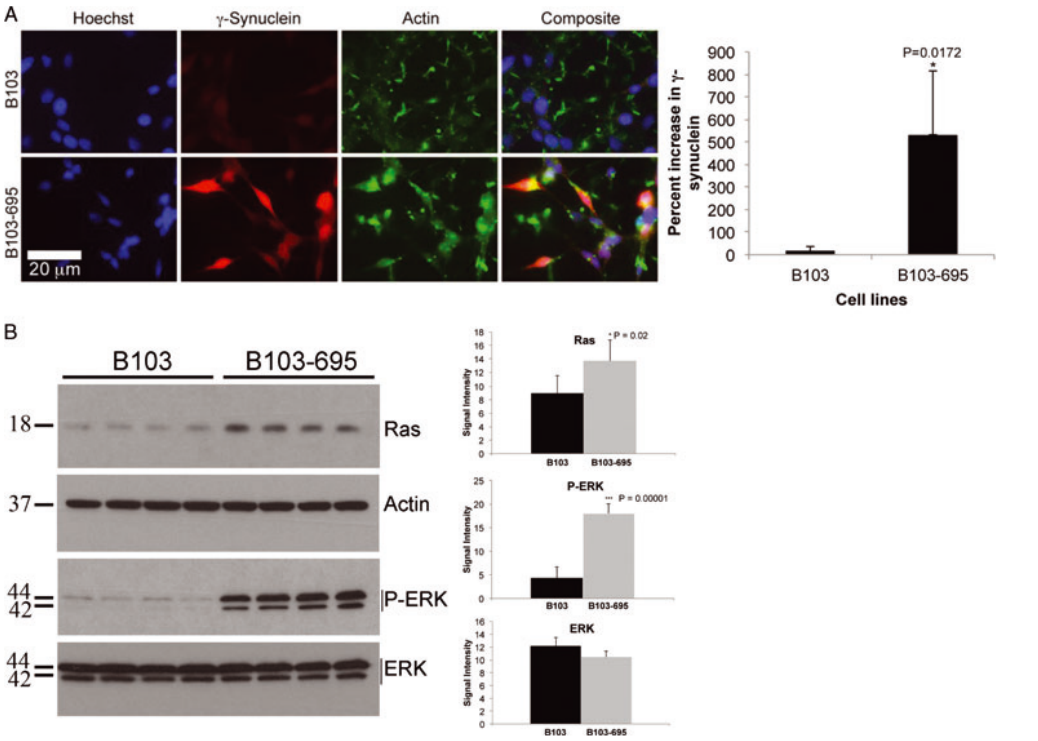

Figure 5. (A) Immunostaining: B103 and B103–695 cells were co-immunostained using γ-synuclein (rabbit polyclonal) and actin (mouse monoclonal) primary antibodies and Alexa Fluor 594 anti-rabbit and Alexa Fluor 488 anti-mouse secondary antibodies. Hoechst was used to visualize the nuclei. The expression of γ-synuclein was significantly higher in B103–695 than that in B103 cells and it seems to localize to the nucleus and cytoplasm. Images were taken on a Zeiss fluorescent microscope fitted with an Axiocam MRm camera and analyzed using AxioVision Rel 4.8 software (magnification: 63×). The bar graph shows the percent increase in γ-synuclein intensity measured using ImageJ, image analysis tool, after converting the images to 8-bit gray. The intensity of γ-synuclein in three independent images taken from B103 and B103–695 cells were normalized to the intensity of Hoechst within the same sample for comparison. (B) Western blot validation: Equal amounts of proteins from B103 and B103–695 cell extracts done in quadruplicate were separated on a 15% Tris-glycine gel and probed with Ras, and P-ERK antibodies. Both Ras and P-ERK were significantly increased in B103–695 cells compared to B103 cells (bar graphs labeled Ras and P-ERK). Re-probe of the Ras blot with actin antibody shows equal amount of proteins on gel and re-probe of P-ERK blot with ERK antibody shows no change in expression of ERK upon expression of APP (bar graph labeled ERK).

due to the limited antibody reactivity on Western blots as immunostaining analysis using the anti-γ-synuclein antibody showed a significant increase in this protein in B103–695 cells compared to B103 (Fig. 5A). Co-staining of the cells with an actin antibody showed altered actin staining in B103–695, providing some additional support to the functional enrichment analysis results in which actin cytoskeleton signaling and subsequent cytoskeletal organization could potentially be altered through APP expression.

Gamma synuclein, a member of the synuclein family, was the most significantly upregulated protein, showing a 59.6-fold increase. It is important to note that even with relatively high variability at the peptide level, low ratio counts and such a significant increase in protein expression for γ-synuclein, we were able to obtain fairly consistent protein ratio values across three biological replicates with the SILAC analysis (17% RSD) and also validate with an alternative protein expression measurement approach. Increased expression of γ-synuclein mRNA has been observed in the brains of AD patients, supporting its potential contribution in AD pathology [31]. γ-synuclein has also been shown to bind microtubule and promote tubulin polymerization and cell adhesion [32]. Studies in cancer cells have shown that it enhances cell migration and protects against mitotic inhibitor-mediated apoptosis. It was initially identified as a breast cancer specific gene and was associated with breast tumor progression [33, 34]. γ–Synuclein has been shown to interact with the checkpoint protein BubR1 to bring about the defects in mitosis [35, 36].

Ras, a small GTPase, is involved in signal transduction regulating cell growth, differentiation, and survival. Increased Ras expression has been implicated in AD brains

but the functional significance of this in AD pathology development is not known [37]. Interestingly, nerve growth factor receptor protein in the plasma membrane, which is upregulated in our dataset as a result of APP expression in B103 cells, has been shown to increase activation of Ras protein(s) in the cytoplasm [38]. Ras activation consequently results in increased MAP-kinase activity. It is possible that a Ras-mediated cell signaling cascade may play a role in the aberrant cell cycle activation and neurodegeneration associated with pathology development in AD.

Mitogen-activated protein kinase (MAPK) functions downstream from Ras in this signal transduction pathway and responds to extracellular signals by inducing different cellular functions such as proliferation, mitosis, differentiation, and apoptosis. Ras activation of the MAPK signaling pathway has been well established. Although the Ras–MAPK signaling pathway has a well-known role in cancer, there is increasing evidence for its involvement in neurodegenerative disease as well [39]. The Ras–MAPK signaling pathway has been found to be induced during very early stages of AD, prior to the formation of plaques and tangles [40, 41]. MAPK is also involved in the regulation of γ-synuclein mRNA expression [42]. Analysis of the active phosphorylated form of mitogen-activated protein kinase P44/42 MAPK (ERK1/2) showed that it is significantly induced in B103–695 cells while the nonphospho ERK levels were unaffected by APP expression (Fig. 5B). Given potential crosstalk between PKA and MAPK signaling, we also investigated the impact of siRNA-mediated knockdown and chemical inhibition of PKA and found no effect on ERK phosphorylation status (data not shown). These findings suggest that APP expression specifically affects activation of ERK and do not have any effect on the expression of the protein.

Downregulated proteins in the pathway shown in Fig. 4 include PD2 and LIM domain 1 (PDLIM1) protein, a transcription regulator that has been shown to be responsive to hypoxia and also oxidative stress [43]. Differential PDLIM1 mRNA expression in human vastus lateralis muscle has been associated with Huntington's disease, making PDLIM1 a potential biomarker [44]. SYNCRIP is a member of the heterogeneous nuclear ribonucleoprotein family, and was recently identified in a microarray study as a gene potentially involved in AD [45]. Our SILAC study provides additional evidence for these potential markers of AD at the protein level.

3.4 Implications in AD

Bioinformatic analysis of the 102 statistically significant proteins identified numerous proteins with roles in a variety of neurological diseases. We have listed differentially expressed proteins from our SILAC analysis that have been implicated in neurodegenerative disease in Table 1 as determined by IPA analysis, reporting only those proteins with ratios having less than 30% RSD values. For example, hypoxanthine phosphoribosyltransferase 1 was increased 10-fold and nerve growth factor receptor was increased 3.5-fold, and both of these proteins have been associated with neurodegeneration [46]. Nerve growth factor receptor as well as γ-synuclein also have emerging roles in AD [47]. There are two different types of nerve growth factor receptors; the low-affinity nerve growth factor receptor, also known as $p75^{NTR}$, which binds all neurotrophins and the Trk family of tyrosine kinase receptors that bind specific neurotrophins. Both of these receptors have been associated with neurodegeneration and are implicated in AD pathology as these receptors bind Aβ, and are upregulated in AD [48, 49].

B103 cells expressing APP showed a decrease in Reticulon 4 (RTN4), an endoplasmic reticulum (ER) associated protein that is involved in neuroendocrine secretion. RTN4 has been shown to inhibit neurite outgrowth, and consequently has also been named neurite outgrowth inhibitor or Nogo. Increased expression of RTN4 has been shown to decrease Aβ peptide production by reducing beta-site APP cleaving enzyme 1 activity [50]. Park et al. found that RTN4 and its receptor RTN4R demonstrate altered subcellular localization in AD. In normal brain, RTN4 shows reduced cellular and enhanced neuropil localization whereas in AD brain, it shows enhanced cellular localization. Similarly, while RTN4R is mainly localized to cell soma in normal brain, it showed reduced cellular localization with more diffuse staining in the neuropil and plaques in AD brain. RTN4R was also found to physically interact with APP and Aβ, limiting Aβ accumulation [51]. Another protein that showed downregulation in the B103–695 cells is the eukaryotic translation initiation factor 4A2 (eIF4A2), which showed a 7.98-fold decrease and is also associated with the ER. A decrease in expression of the proteins associated with ER may indicate that expression of APP leads to an induction of ER stress. ER responds to stress by activating various signaling pathways including the unfolded protein response, which leads to attenuation of protein translation. Studies have shown that APP induces ER stress-mediated apoptosis in cells and further studies are necessary to confirm that APP expression in B103 cells lead to an induction in ER stress-associated signaling pathways [52]. In AD, ER stress has been shown to induce inflammation, which leads to enhanced pathology development in AD. Moreover, eIF4A2 has been suggested as one of the two suitable reference genes for RT-qPCR studies in human AD post-mortem brain samples, as its mRNA is stably expressed [53].

Several studies also indicate a link between APP processing and lipid metabolism (see the reviews [54, 55]). Analysis of cellular distribution of APP, BACE, and γ-secretase have shown that these proteins colocalize in the lipid-rich raft domains leading to enhanced amyloidogenic processing of APP whereas α-secretase-mediated cleavage occurs at membrane domains outside of the lipid rafts [56]. It has also been shown that people with high-cholesterol levels have increased risk of developing AD. Analysis of data from AD patients have shown that people carrying the apolipoproteins E4 allele (ApoE4) are more prone to get the disease than those carrying apolipoprotein E2 or E3 allele [57, 58]. It is hypothesized that ApoE4 is a genetic risk factor for AD however, not all carriers of ApoE4 get the disease.

Table 1. Selected differentially expressed proteins implicated in neurodegenerative disease that were identified in B103–695 cells using SILAC-based quantitative proteomic analysis

Fold change	SD	ID	Symbol	Entrez gene name	Location
59.650	10.17	F1LQ96	SNCG	Synuclein, gamma (breast cancer-specific protein 1)	Cytoplasm
11.433	2.78	Q811A3	PLOD2	Procollagen-lysine, 2-oxoglutarate 5-dioxygenase 2	Cytoplasm
8.363	0.78	F1LSL3	ITPR3	Inositol 1,4,5-trisphosphate receptor, type 3	Cytoplasm
7.953	0.78	B2B9B0	EPHB2	EPH receptor B2	Plasma membrane
4.284	0.65	D3ZZ63	FLNC	Filamin C, gamma	Cytoplasm
3.819	0.41	F1MA96	NCAM1	Neural cell adhesion molecule 1	Plasma membrane
3.770	0.85	P50442	GATM	Glycine amidinotransferase (*L*-arginine:glycine amidinotransferase)	Cytoplasm
3.638	0.52	F1LNX0	DDAH1	Dimethylarginine dimethylaminohydrolase 1	Cytoplasm
3.547	0.21	Q5HZV9	PPP1R7	Protein phosphatase 1, regulatory subunit 7	Nucleus
3.519	0.15	P07174	NGFR	Nerve growth factor receptor	Plasma membrane
2.970	0.59	P70636	LAMA5	Laminin, alpha 5	Extracellular space
2.872	0.27	Q6MG60	DDAH2	Dimethylarginine dimethylaminohydrolase 2	Unknown
2.768	0.17	F1M5W8	AFAP1L2	Actin filament-associated protein 1-like 2	Cytoplasm
2.765	0.08	P05942	S100A4	S100 calcium-binding protein A4	Cytoplasm
2.657	0.43	F1LNU6	FADS2	Fatty acid desaturase 2	Plasma membrane
2.653	0.42	Q80WE1	FMR1	Fragile X mental retardation 1	Nucleus
2.557	0.17	F1LYK7	CFL2	Cofilin 2 (muscle)	Nucleus
2.375	0.40	F1LZM7	HSDL2	Hydroxysteroid dehydrogenase like 2	Cytoplasm
2.317	0.19	D4A4T0	STUB1	STIP1 homology and U-box-containing protein 1, E3 ubiquitin protein ligase	Cytoplasm
2.309	0.10	Q91ZN1	CORO1A	Coronin, actin-binding protein, 1A	Cytoplasm
2.298	0.22	F1LV02	DBI	Diazepam-binding inhibitor (GABA receptor modulator, acyl-CoA-binding protein)	Cytoplasm
2.292	0.18	F1LND7	FDPS	Farnesyl diphosphate synthase	Cytoplasm
2.206	0.17	Q68G41	ECI1	enoyl-CoA delta isomerase 1	Cytoplasm
2.156	0.38	Q4G053	SAMD9L	Sterile alpha motif domain containing 9-like	Unknown
2.144	0.16	P40615	DKC1	Dyskeratosis congenita 1, dyskerin	Nucleus
2.118	0.08	P10868	GAMT	Guanidinoacetate *N*-methyltransferase	Cytoplasm
2.072	0.06	Q63081	PDIA6	Protein disulfide isomerase family A, member 6	Cytoplasm
1.880	0.03	P13233	CNP	2′,3′-cyclic nucleotide 3′ phosphodiesterase	Cytoplasm
1.865	0.03	D4ABV5	Calm1	Calmodulin 1	Nucleus
1.853	0.05	D3ZM53	Ywhaq	Tyrosine 3-monooxygenase/tryptophan 5-monooxygenase activation protein, theta polypeptide	Cytoplasm
1.850	0.21	D4A2V9	GPI	Glucose-6-phosphate isomerase	Extracellular space
1.831	0.28	P16617	PGK1	Phosphoglycerate kinase 1	Cytoplasm
1.819	0.13	P21263	NES	Nestin	Cytoplasm
1.733	0.13	P07335	CKB	Creatine kinase, brain	Cytoplasm
1.714	0.10	O35244	PRDX6	Peroxiredoxin 6	Cytoplasm
−2.015	0.41	Q6URK4	HNRNPA3	Heterogeneous nuclear ribonucleoprotein A3	Nucleus
−2.143	0.05	D4A8D5	FLNB	Filamin B, beta	Cytoplasm
−2.342	0.03	F1M3G6	HSPH1	Heat shock 105kDa/110kDa protein 1	Cytoplasm
−2.941	0.06	Q5U1Z3	RTN4	Reticulon 4	Cytoplasm
−3.017	0.10	Q7TP47	SYNCRIP	Synaptotagmin binding, cytoplasmic RNA-interacting protein	Nucleus
−3.615	0.06	P52944	PDLIM1	PDZ and LIM domain 1	Cytoplasm
−7.977	0.07	F1LP27	EIF4A2	Eukaryotic translation initiation factor 4A2	Cytoplasm

Fold change for expression ratios less than 1 were reported as the negative reciprocal of the expression ratio.

The exact mechanism by which ApoE4 affects pathology development in AD is not clear. It has been shown that ApoE4 promotes the aggregation of Aβ leading to accelerated plaque formation and cognitive deficit [59, 60]. Also, it appears that ApoE4 is less effective in clearing Aβ, thus leading to its accumulation [61]. Studies in mouse models of AD have shown that drugs that lower cholesterol levels can reduce the levels of Aβ and therefore plaque pathology [62]. Our analysis showed a 2–3-fold increase in expression of sterol *O*-acetyl transferase 1 and Acyl CoA: cholesterol acyl transferase 2 in cells expressing APP compared to the parental B103 cells. These enzymes are involved in esterification of cholesterol and play a role in controlling the equilibrium between free and esterified cholesterol.

These enzymes have been shown to have an effect on APP processing; RNAi-mediated inhibition of ACAT1 led to a decrease in processing of APP to generate Aβ indicating that changes in cholesterol esterification can influence pathology development in AD [63]. Studies by others have shown that Acyl CoA: cholesterol acyl transferase 2 can more efficiently esterify cholesterol than ACAT1 [64]. The upregulation of these enzymes in B103–695 cells suggests that APP may affect modification of lipids that in turn affects APP processing. Alterations in cholesterol esterification may influence the membrane lipid composition and therefore APP processing. Altogether these data suggest that APP and lipids may be regulated by a feed-forward mechanism, where the expression and processing of APP affects lipid composition and function that in turn induces further APP processing.

Analyses of AD brains have shown aberrant expression of cell cycle regulatory proteins in neurons. The roles of the cell cycle regulators in neurons as well as the mechanisms that lead to the induced expression of these proteins are not known. It is possible that either APP or a metabolite of APP may enhance expression of proteins such as γ-synuclein and Ras, thus affecting cell proliferation of transformed cells and degeneration of terminally differentiated cells. γ-Synuclein has already been shown to bind and alter microtubule dynamics. Our co-immunostaining analysis with actin and γ-synuclein antibodies show altered localization of actin in the cells expressing APP. This is a significant finding and suggests that APP-mediated induction in γ-synuclein may lead to alterations in cytoskeletal and microtubule-associated proteins, which in turn affects neuronal signaling and synaptic function in AD. Since γ-synuclein affects the mitotic checkpoint, it is possible that the neuronal expression of this protein may not only alter the neuronal cytoskeleton but also affects the differentiation state of neurons. Neurons are terminally differentiated cells and do not have an active cell cycle machinery and therefore may respond to cell cycle activation by undergoing apoptosis instead of transformation. In addition to a role in AD, studies from different groups have shown that cancers of different organs show increased levels of APP or a metabolite of APP. Thus, a careful analysis of APP function may enhance our knowledge on the role of APP in bringing about pathologies associated with not only AD but also cancers of different organs.

4 Concluding remarks

This study represents the first comprehensive proteomic analysis of B103 and B103–695 rat neuronal-like cells, including relative quantitation of protein expression using SILAC-based proteomics. Several proteins were identified as being significantly upregulated or downregulated in B103–695 cells, many with potential implications in AD pathology. The comprehensive dataset provides insight into proteins that may be affected by APP-695 expression and provides a foundation for future mechanistic studies. The proteins identified are associated with a number of diverse processes including cellular assembly and organization, cell cycle, lipid metabolism, protein folding, PTMs, as well as physiological system development and function. These findings suggest that several different processes are influenced by APP expression, which may contribute to synaptic dysfunction, amyloid plaque formation, and AD pathology.

This research was supported by grants from the Alzheimer's association (IIRG-08–90842 to JP), NIH-NIA (1R21AG031429–01A2 to JP), and funds from the USF Health Byrd Alzheimer's Institute, Department of Molecular Medicine, and Department of Cell Biology, Microbiology, and Molecular Biology at USF, Tampa. We thank Dr. Jeremiah Tipton and the Center of Drug Discovery and Innovation Proteomics Facility for use of the Orbitrap XL mass spectrometer. We also thank Dr. Bonnie Goodwin, who received the B103 cells from Dr. Dave Schubert at Salk Institute, for cells used in this study.

The authors have declared no conflict of interest.

5 References

[1] Kosik, K. S., Joachim, C. L., Selkoe, D. J., *Proc. Natl. Acad. Sci. U S A* 1986, *83*, 4044–4048.

[2] Selkoe, D. J., *Neuron* 1991, *6*, 487–498.

[3] Alzheimer, A., Stelzmann, R. A., Schnitzlein, H. N., Murtagh, F. R., *Clin. Anat.* 1995, *8*, 429–431.

[4] Naslund, J., Schierhorn, A., Hellman, U., Lannfelt, L., Roses, A. D., Tjernberg, L. O., Silberring, J., Gandy, S. E., Winblad, B., Greengard, P., Nordstedt, C., Terenius, L., *Proc. Natl. Acad. Sci. U S A* 1994, *91*, 8378–8382.

[5] Iwatsubo, T., Odaka, A., Suzuki, N., Mizusawa, H., Nukina, N., Ihara, Y., *Neuron* 1994, *13*, 45–53.

[6] Mori, H., Takio, K., Ogawara, M., Selkoe, D. J., *J. Biol. Chem.* 1992, *267*, 17082–17086.

[7] Duff, K., Eckman, C., Zehr, C., Yu, X., Prada, C. M., Perez-tur, J., Hutton, M., Buee, L., Harigaya, Y., Yager, D., Morgan, D., Gordon, M. N., Holcomb, L., Refolo, L., Zenk, B., Hardy, J., Younkin, S., *Nature* 1996, *383*, 710–713.

[8] Suzuki, N., Cheung, T. T., Cai, X. D., Odaka, A., Otvos, L., Jr., Eckman, C., Golde, T. E., Younkin, S. G., *Science* 1994, *264*, 1336–1340.

[9] Hernandez-Ortega, K., Ferrera, P., Arias, C., *J. Neurosci. Res.* 2007, *85*, 1744–1751.

[10] Judge, M., Hornbeck, L., Potter, H., Padmanabhan, J., *Mol. Neurodegener.* 2011, *6*, 80–100.

[11] Suzuki, T., Oishi, M., Marshak, D. R., Czernik, A. J., Nairn, A. C., Greengard, P., *Embo J.* 1994, *13*, 1114–1122.

[12] Lee, M. S., Kao, S. C., Lemere, C. A., Xia, W., Tseng, H. C., Zhou, Y., Neve, R., Ahlijanian, M. K., Tsai, L. H., *J. Cell Biol.* 2003, *163*, 83–95.

[13] Shin, R. W., Ogino, K., Shimabuku, A., Taki, T., Nakashima, H., Ishihara, T., Kitamoto, T., *Acta Neuropathol.* 2007, *113*, 627–636.

[14] Ueberham, U., Hilbrich, I., Ueberham, E., Rohn, S., Glockner, P., Dietrich, K., Bruckner, M. K., Arendt, T., *Neurobiol. Aging* 2012, *33*, 2827–2840.

[15] Bowser, R., Smith, M. A., *J. Alzheimers Dis.* 2002, *4*, 249–254.

[16] Busser, J., Geldmacher, D. S., Herrup, K., *J. Neurosci.* 1998, *18*, 2801–2807.

[17] Andorfer, C., Acker, C. M., Kress, Y., Hof, P. R., Duff, K., Davies, P., *J. Neurosci.* 2005, *25*, 5446–5454.

[18] Herrup, K., Arendt, T., *J Alzheimers Dis.* 2002, *4*, 243–247.

[19] Jordan-Sciutto, K., Rhodes, J., Bowser, R., *Mech. Ageing Dev.* 2001, *123*, 11–20.

[20] Malik, B., Currais, A., Andres, A., Towlson, C., Pitsi, D., Nunes, A., Niblock, M., Cooper, J., Hortobagyi, T., Soriano, S., *Cell Cycle* 2008, *7*, 637–646.

[21] McShea, A., Harris, P. L., Webster, K. R., Wahl, A. F., Smith, M. A., *Am. J. Pathol.* 1997, *150*, 1933–1939.

[22] Schubert, D., Behl, C., *Brain Res.* 1993, *629*, 275–282.

[23] Jin, L., Ninomiya, H., Roch, J., Schubert, D., Masliah, E., Otero, D., Saitoh, T., *J. Neurosci.* 1994, *14*, 5461–5470.

[24] Wisniewski, J. R., Zougman, A., Nagaraj, N., Mann, M., *Nat. Methods* 2009, *6*, 359–362.

[25] Cox, J., Mann, M., *Nat. Biotech.* 2008, *26*, 1367–1372.

[26] Benjamini, Y., Hochberg, Y., *J. Roy. Stat. Soc. Ser. B.* 1995, *57*, 289–300.

[27] Nikolic, M., Dudek, H., Kwon, Y. T., Ramos, Y. F., Tsai, L. H., *Genes Dev.* 1996, *10*, 816–825.

[28] Tsai, L. H., Takahashi, T., Caviness, V. S., Jr., Harlow, E., *Development* 1993, *119*, 1029–1040.

[29] Su, S. C., Tsai, L. H., *Annu. Rev. Cell Dev. Biol.* 2011, *27*, 465–491.

[30] Rakic, S., Davis, C., Molnar, Z., Nikolic, M., Parnavelas, J. G., *Cereb. Cortex* 2006, *16 Suppl 1*, i35–i45.

[31] Rockenstein, E., Hansen, L. A., Mallory, M., Trojanowski, J. Q., Galasko, D., Masliah, E., *Brain Res.* 2001, *914*, 48–56.

[32] Zhang, H., Kouadio, A., Cartledge, D., Godwin, A. K., *Exp. Cell Res.* 2011, *317*, 1330–1339.

[33] Ji, H., Liu, Y. E., Jia, T., Wang, M., Liu, J., Xiao, G., Joseph, B. K., Rosen, C., Shi, Y. E., *Cancer Res.* 1997, *57*, 759–764.

[34] Jia, T., Liu, Y. E., Liu, J., Shi, Y. E., *Cancer Res.* 1999, *59*, 742–747.

[35] Inaba, S., Li, C., Shi, Y. E., Song, D. Q., Jiang, J. D., Liu, J., *Breast Cancer Res. Treat.* 2005, *94*, 25–35.

[36] Gupta, A., Inaba, S., Wong, O. K., Fang, G., Liu, J., *Oncogene* 2003, *22*, 7593–7599.

[37] Lüth, H. J., Holzer, M., Gertz, H. J., Arendt, T., *Brain Res.* 2000, *852*, 45–55.

[38] Tinhofer, I., Maly, K., Dietl, P., Hochholdinger, F., Mayr, S., Obermeier, A., Grunicke, H. H., *J. Biol. Chem.* 1996, *271*, 30505–30509.

[39] Ferrer, I., Blanco, R., Carmona, M., Ribera, R., Goutan, E., Puig, B., Rey, M. J., Cardozo, A., Viñals, F., Ribalta, T., *Brain Pathol.* 2001, *11*, 144–158.

[40] Gärtner, U., Holzer, M., Heumann, R., Arendt, T., *Neuro. Report* 1995, *6*, 1441–1444.

[41] Gärtner, U., Holzer, M., Arendt, T., *Neuroscience* 1999, *91*, 1–5.

[42] Li, M., Yin, Y., Hua, H., Sun, X., Luo, T., Wang, J., Jiang, Y., *J. Biol. Chem.* 2010, *285*, 30480–30488.

[43] Basu, A., Drame, A., Muñoz, R., Gijsbers, R., Debyser, Z., De Leon, M., Casiano, C. A., *The Prostate* 2012, *72*, 597–611.

[44] Strand, A. D., Aragaki, A. K., Shaw, D., Bird, T., Holton, J., Turner, C., Tapscott, S. J., Tabrizi, S. J., Schapira, A. H., Kooperberg, C., Olson, J. M., *Human Mol. Genet.* 2005, *14*, 1863–1876.

[45] Guttula SV, A. A., Gumpeny, R. S., *Int. J. Alzheimer's Dis.* 2012, *2012*, 1643–1650.

[46] Terrisse, L., Poirier, J., Bertrand, P., Merched, A., Visvikis, S., Siest, G., Milne, R., Rassart, E., *J. Neurochem.* 1998, *71*, 1643–1650.

[47] Navarro, A., del Valle, E., Astudillo, A., González del Rey, C., Tolivia, J., *Exp. Neurol.* 2003, *184*, 697–704.

[48] Yaar, M., Zhai, S., Fine, R. E., Eisenhauer, P. B., Arble, B. L., Stewart, K. B., Gilchrest, B. A., *J. Biol. Chem.* 2002, *277*, 7720–7725.

[49] Podlesniy, P., Kichev, A., Pedraza, C., Saurat, J., Encinas, M., Perez, B., Ferrer, I., Espinet, C., *Am. J. Pathol.* 2006, *169*, 119–131.

[50] Dasgupta, P., Sun, J., Wang, S., Fusaro, G., Betts, V., Padmanabhan, J., Sebti, S. M., Chellappan, S. P., *Mol. Cell. Biol.* 2004, *24*, 9527–9541.

[51] Park, J. H., Gimbel, D. A., GrandPre, T., Lee, J.-K., Kim, J.-E., Li, W., Lee, D. H. S., Strittmatter, S. M., *J. Neurosci.* 2006, *26*, 1386–1395.

[52] Takahashi, K., Niidome, T., Akaike, A., Kihara, T., Sugimoto, H., *J. Neurochem.* 2009, *109*, 1324–1337.

[53] Penna, I., Vella, S., Gigoni, A., Russo, C., Cancedda, R., Pagano, A., *Int. J. Mol. Sci.* 2011, *12*, 5461–5470.

[54] Di Paolo, G., Kim, T. W., *Nat. Rev. Neurosci.* 2011, *12*, 284–296.

[55] Grimm, M. O., Rothhaar, T. L., Hartmann, T., *Exp. Brain Res.* 2012, *217*, 365–375.

[56] Wahrle, S., Das, P., Nyborg, A. C., McLendon, C., Shoji, M., Kawarabayashi, T., Younkin, L. H., Younkin, S. G., Golde, T. E., *Neurobiol. Dis.* 2002, *9*, 11–23.

[57] Corder, E. H., Saunders, A. M., Strittmatter, W. J., Schmechel, D. E., Gaskell, P. C., Small, G. W., Roses, A. D., Haines, J. L., Pericak-Vance, M. A., *Science* 1993, *261*, 921–923.

[58] Roses, A. D., Saunders, A. M., Alberts, M. A., Strittmatter, W. J., Schmechel, D., Gorder, E., Pericak-Vance, M. A., *Jama* 1995, *273*, 374–376.

[59] Costa, D. A., Nilsson, L. N., Bales, K. R., Paul, S. M., Potter, H., *J. Alzheimers Dis.* 2004, *6*, 509–514.

[60] Ma, J., Yee, A., Brewer, H. B. Jr., Das, S., Potter, H., *Nature* 1994, *372*, 92–94.

[61] Holtzman, D. M., Bales, K. R., Tenkova, T., Fagan, A. M., Parsadanian, M., Sartorius, L. J., Mackey, B., Olney, J., McKeel, D., Wozniak, D., Paul, S. M., *Proc. Natl. Acad. Sci. USA* 2000, *97*, 2892–2897.

[62] Hutter-Paier, B., Huttunen, H. J., Puglielli, L., Eckman, C. B., Kim, D. Y., Hofmeister, A., Moir, R. D., Domnitz, S. B., Frosch, M. P., Windisch, M., Kovacs, D. M., *Neuron* 2004, *44*, 227–238.

[63] Huttunen, H. J., Greco, C., Kovacs, D. M., *FEBS Lett.* 2007, *581*, 1688–1692.

[64] Temel, R. E., Gebre, A. K., Parks, J. S., Rudel, L. L., *J. Biol. Chem.* 2003, *278*, 47594–47601.

Appendix B – Electrophoresis: Neuroproteomics Special Issue, Supporting Information

Supplementary Table 2. Significant hits identified using Perseus. Fold change for expression ratios < 1 were reported as the negative reciprocal of the expression ratio.

Majority Protein Name	Majority Protein ID	Gene	Fold Change
Synuclein, gamma, isoform CRA	D4ACB0	Sncg	59.6
Sodium channel	F1LQQ7	Scn7a	32.2
Taste receptor type 2 member 135	F1LS99	Tas2r135	29.3
Myosin-10	F1LQ02	Myh10	19.7
Uncharacterized protein (Fragment)	F1M6H4		13.2
RCG25923, isoform CRA	D3ZQR7	Plod2	11.4
Hypoxanthine-guanine phosphoribosyltransferase	F1LNY0	Hprt1	10.2
Renin receptor	Q6AXS4	Atp6ap2	8.8
Microtubule-associated protein 1A	D4ACP6	Map1a	8.6
Echinoderm microtubule-associated protein-like 1	Q4V8C3	Eml1	8.5
Inositol 1,4,5-trisphosphate receptor type 3	C7E1V1	Itpr3	8.4
Ephrin receptor	F1MAJ0	Ephb2	8.0
Armc6 protein	B2RYL4	Armc6	7.6
Uncharacterized protein	F1MAA7	Lamc1	7.3
Astrocytic phosphoprotein PEA-15	Q5U318	Pea15	6.4
Prefoldin subunit 2	B0BN18	Pfdn2	5.5
Ras-related protein R-Ras	D3Z8L7	Rras	5.1
Cell adhesion molecule 4	Q1WIM1	Cadm4	5.0
B-cell receptor-associated protein 29	Q5XIU4	Bcap29	4.4
Transcriptional activator protein Pur-alpha (Fragments)	F1LPS8	Pura	4.3
PHD and RING finger domain-containing protein 1	Q63625	Phrf1	4.3
Prefoldin 5 (Predicted), isoform CRA	B5DFN4	Pfdn5	4.3
Uncharacterized protein	D3ZHA0	Flnc	4.3
Uncharacterized protein (Fragment)	F1LUD3	Ahnak2	4.2
Uncharacterized protein	D4A6U8	Tia1	4.1
Uncharacterized protein (Fragment)	F1M692		4.1
Fructose-bisphosphate aldolase C	P09117	Aldoc	4.1
Uncharacterized protein	D4A5F0	Fam114a1	3.9
RCG38845, isoform CRA	F1LZC5	Ndufa13	3.8
Neural cell adhesion molecule 1	F1LUV9	Ncam1	3.8
CD97 molecule	E9PT32	Cd97	3.8
Glycine amidinotransferase, mitochondrial	P50442	Gatm	3.8
N(G),N(G)-dimethylarginine dimethylaminohydrolase 1	O08557	Ddah1	3.6
Apolipoprotein D	P23593	Apod	3.6
Protein phosphatase 1 regulatory subunit 7	Q5HZV9	Ppp1r7	3.5
Tumor necrosis factor receptor superfamily member 16	P07174	Ngfr	3.5
Calcium-regulated heat stable protein 1	Q9WU49	Carhsp1	3.3
Sterol O-acyltransferase 1	O70536	Soat1	3.3
Uncharacterized protein (Fragment)	F1M903	Arhgap23	3.2
DnaJ (Hsp40) homolog, subfamily B, member 4	Q5XIP0	Dnajb4	3.2
Transglutaminase 2, C polypeptide	Q6P6R6	Tgm2	3.2
Erythrocyte protein band 4.1-like 3, isoform CRA	Q9JMB3	Epb4.1l3	3.1
3-hydroxyisobutyrate dehydrogenase, mitochondrial	P29266	Hibadh	3.1
ERO1-like protein alpha	D3ZNL3	Ero1l	3.0
Phosphatidylinositide phosphatase SAC1	F1LYT0	Sacm1l	3.0
Laminin chain (Fragment)	F1MAN8	Lama5	3.0
N(G),N(G)-dimethylarginine dimethylaminohydrolase 2	Q6MG60	Ddah2	2.9
Sperm antigen with calponin homology and coiled-coil domains 1	D3ZSR4	Cytsb	2.8
2-hydroxyacyl-CoA lyase 1	Q8CHM7	Hacl1	2.8

Msh2 protein	B1WBQ7	Msh2	2.8
Uncharacterized protein (Fragment)	F1M5W8	Afap1l2	2.8
Protein S100-A4	P05942	S100a4	2.8
Uncharacterized protein	D3ZC00		2.8
Tax1-binding protein 1 homolog	F1LS64	Tax1bp1	2.7
Fatty acid desaturase 2	Q9Z122	Fads2	2.7
Fragile X mental retardation protein 1 homolog	E9PSS4		2.7
Uncharacterized protein	D4A389		2.6
Uncharacterized protein (Fragment)	F1M2X2		2.6
Uncharacterized protein (Fragment)	F1LYK7	Cfl2	2.6
RCG46052	D3ZKH6	Rabgap1l	2.5
Hydroxysteroid dehydrogenase-like protein 2	Q4V8F9	Hsdl2	2.4
Probable saccharopine dehydrogenase	Q6AY30	Sccpdh	2.3
Uncharacterized protein (Fragment)	F1M8Y4	Depdc6	2.3
STIP1 homology and U-Box containing protein 1, isoform CRA	D4A4T0	Stub1	2.3
L-lactate dehydrogenase	B5DEN4	Ldha	2.3
Coronin-1A	Q91ZN1	Coro1a	2.3
Acyl-CoA-binding protein	P11030	Dbi	2.3
Uncharacterized protein	D3ZFJ2		2.3
Ac2-125	Q7TPK0	Fdps	2.3
Brain-specific alpha actinin 1 isoform	Q6T487	Actn1	2.2
Large neutral amino acids transporter small subunit 1	Q63016	Slc7a5	2.2
Growth arrest-specific protein 7	O55148	Gas7	2.2
Enoyl-CoA delta isomerase 1, mitochondrial	P23965	Eci1	2.2
Uncharacterized protein	D4ACC2	LOC100361376	2.2
Similar to protein 4.1G (Predicted), isoform CRA	D3ZSM1	Epb4.1l2	2.2
Uncharacterized protein	E9PTD6	Samd9l	2.2
H/ACA ribonucleoprotein complex subunit 4	P40615	Dkc1	2.1
Guanidinoacetate N-methyltransferase	D4ADW8	Gamt	2.1
Protein disulfide-isomerase A6	Q63081	Pdia6	2.1
RGD1308350 protein (Fragment)	Q5I0K2	RGD1308350	2.0
Uncharacterized protein	D3ZZ09	Vgll3	2.0
RCG25591, isoform CRA	B2RYD7	RGD1311563	1.9
2,3-cyclic-nucleotide 3-phosphodiesterase	P13233	Cnp	1.9
Calmodulin	D4ADE9	Calm1	1.9
14-3-3 protein theta	P68255	Ywhaq	1.9
Glucose-6-phosphate isomerase	Q6P6V0	Gpi	1.9
Phosphoglycerate kinase 1	P16617	Pgk1	1.8
Nestin	P21263	Nes	1.8
Tubulin polymerization-promoting protein family member 3	Q5PPN5	Tppp3	1.8
Psmg4 protein	B2RZB8	Psmg4	1.8
Creatine kinase B-type	P07335	Ckb	1.7
Peroxiredoxin-6	O35244	Prdx6	1.7
Mannose-P-dolichol utilization defect 1	D3Z865	Mpdu1	1.7
Uncharacterized protein	D3ZVA5	Fbll1	1.3
Membrane-associated DHHC13 zinc finger protein	E9PU37	Zdhhc13	1.2
Heterogeneous nuclear ribonucleoprotein A3	Q6URK4	Hnrnpa3	-2.0
Filamin, beta (Predicted)	D3ZD13	Flnb	-2.1
Heat shock protein 105 kDa	Q66HA8	Hsph1	-2.3
Reticulon-4	F1LQN3	Rtn4	-2.9
Heterogeneous nuclear ribonucleoprotein Q	D3ZME6	Syncrip	-3.0
PDZ and LIM domain protein 1	P52944	Pdlim1	-3.6
Eukaryotic initiation factor 4A-II	Q5RKI1	Eif4a2	-8.0

Appendix C – Electrophoresis: Permissions

JOHN WILEY AND SONS LICENSE
TERMS AND CONDITIONS

This Agreement between Dale Chaput ("You") and John Wiley and Sons ("John Wiley and Sons") consists of your license details and the terms and conditions provided by John Wiley and Sons and Copyright Clearance Center.

License Number	3678290608737
License date	Jul 29, 2015
Licensed Content Publisher	John Wiley and Sons
Licensed Content Publication	Electrophoresis
Licensed Content Title	SILAC-based proteomic analysis to investigate the impact of amyloid precursor protein expression in neuronal-like B103 cells
Licensed Content Author	Dale Chaput,Lisa Hornbeck Kirouac,Harris Bell-Temin,Stanley M. Stevens,Jaya Padmanabhan
Licensed Content Date	Dec 19, 2012
Pages	10
Type of use	Dissertation/Thesis
Requestor type	Author of this Wiley article
Format	Electronic
Portion	Full article
Will you be translating?	No
Title of your thesis / dissertation	Mass Spectrometry based investigation of APP-dependent mechanisms in neurodegeneration
Expected completion date	Nov 2015
Expected size (number of pages)	200
Requestor Location	Dale Chaput 3532 Palm Crossing Dr. Unit 304 TAMPA, FL 33613 United States Attn: Dale Chaput
Billing Type	Invoice
Billing Address	Dale Chaput 3532 Palm Crossing Dr. Unit 304 TAMPA, FL 33613 United States Attn: Dale Chaput
Total	0.00 USD
Terms and Conditions	

TERMS AND CONDITIONS

This copyrighted material is owned by or exclusively licensed to John Wiley & Sons, Inc. or one of its group companies (each a"Wiley Company") or handled on

behalf of a society with which a Wiley Company has exclusive publishing rights in relation to a particular work (collectively "WILEY"). By clicking "accept" in connection with completing this licensing transaction, you agree that the following terms and conditions apply to this transaction (along with the billing and payment terms and conditions established by the Copyright Clearance Center Inc., ("CCC's Billing and Payment terms and conditions"), at the time that you opened your Rightslink account (these are available at any time at http://myaccount.copyright.com).

Terms and Conditions

- The materials you have requested permission to reproduce or reuse (the "Wiley Materials") are protected by copyright.

- You are hereby granted a personal, non-exclusive, non-sub licensable (on a stand-alone basis), non-transferable, worldwide, limited license to reproduce the Wiley Materials for the purpose specified in the licensing process. This license is for a one-time use only and limited to any maximum distribution number specified in the license. The first instance of republication or reuse granted by this licence must be completed within two years of the date of the grant of this licence (although copies prepared before the end date may be distributed thereafter). The Wiley Materials shall not be used in any other manner or for any other purpose, beyond what is granted in the license. Permission is granted subject to an appropriate acknowledgement given to the author, title of the material/book/journal and the publisher. You shall also duplicate the copyright notice that appears in the Wiley publication in your use of the Wiley Material. Permission is also granted on the understanding that nowhere in the text is a previously published source acknowledged for all or part of this Wiley Material. Any third party content is expressly excluded from this permission.

- With respect to the Wiley Materials, all rights are reserved. Except as expressly granted by the terms of the license, no part of the Wiley Materials may be copied, modified, adapted (except for minor reformatting required by the new Publication), translated, reproduced, transferred or distributed, in any form or by any means, and no derivative works may be made based on the Wiley Materials without the prior permission of the respective copyright owner. You may not alter, remove or suppress in any manner any copyright, trademark or other notices displayed by the Wiley Materials. You may not license, rent, sell, loan, lease, pledge, offer as security, transfer or assign the Wiley Materials on a stand-alone basis, or any of the rights granted to you hereunder to any other person.

- The Wiley Materials and all of the intellectual property rights therein shall at all times remain the exclusive property of John Wiley & Sons Inc, the Wiley Companies, or their respective licensors, and your interest therein is only that of having possession of and the right to reproduce the Wiley Materials pursuant to Section 2 herein during the continuance of this Agreement. You agree that you own no right, title or interest in or to the Wiley Materials or any of the intellectual property rights therein. You shall have no rights hereunder other than the license as provided for above in Section 2. No right, license or interest to any trademark, trade name, service mark or other branding ("Marks") of WILEY or its licensors is granted hereunder, and you agree that you shall not assert any such right, license or interest with respect thereto.

- NEITHER WILEY NOR ITS LICENSORS MAKES ANY WARRANTY OR REPRESENTATION OF ANY KIND TO YOU OR ANY THIRD PARTY, EXPRESS, IMPLIED OR STATUTORY, WITH RESPECT TO THE MATERIALS OR THE ACCURACY OF ANY INFORMATION CONTAINED IN THE MATERIALS, INCLUDING, WITHOUT LIMITATION, ANY IMPLIED WARRANTY OF MERCHANTABILITY, ACCURACY, SATISFACTORY QUALITY, FITNESS FOR A PARTICULAR PURPOSE, USABILITY, INTEGRATION OR NON-INFRINGEMENT AND ALL SUCH WARRANTIES ARE HEREBY EXCLUDED BY WILEY AND ITS LICENSORS AND WAIVED BY YOU

- WILEY shall have the right to terminate this Agreement immediately upon breach of this Agreement by you.

- You shall indemnify, defend and hold harmless WILEY, its Licensors and their respective directors, officers, agents and employees, from and against any actual or threatened claims, demands, causes of action or proceedings arising from any breach of this Agreement by you.

- IN NO EVENT SHALL WILEY OR ITS LICENSORS BE LIABLE TO YOU OR ANY OTHER PARTY OR ANY OTHER PERSON OR ENTITY FOR ANY SPECIAL, CONSEQUENTIAL, INCIDENTAL, INDIRECT, EXEMPLARY OR PUNITIVE DAMAGES, HOWEVER CAUSED, ARISING OUT OF OR IN CONNECTION WITH THE DOWNLOADING, PROVISIONING, VIEWING OR USE OF THE MATERIALS REGARDLESS OF THE FORM OF ACTION, WHETHER FOR BREACH OF CONTRACT, BREACH OF WARRANTY, TORT, NEGLIGENCE, INFRINGEMENT OR OTHERWISE (INCLUDING, WITHOUT LIMITATION, DAMAGES BASED ON LOSS OF PROFITS, DATA, FILES, USE, BUSINESS OPPORTUNITY OR CLAIMS OF THIRD PARTIES), AND WHETHER OR NOT THE PARTY HAS BEEN ADVISED OF THE POSSIBILITY OF SUCH DAMAGES. THIS LIMITATION SHALL APPLY NOTWITHSTANDING ANY FAILURE OF ESSENTIAL PURPOSE OF ANY LIMITED REMEDY PROVIDED HEREIN.

- Should any provision of this Agreement be held by a court of competent jurisdiction to be illegal, invalid, or unenforceable, that provision shall be deemed amended to achieve as nearly as possible the same economic effect as the original provision, and the legality, validity and enforceability of the remaining provisions of this Agreement shall not be affected or impaired thereby.

- The failure of either party to enforce any term or condition of this Agreement shall not constitute a waiver of either party's right to enforce each and every term and condition of this Agreement. No breach under this agreement shall be deemed waived or excused by either party unless such waiver or consent is in writing signed by the party granting such waiver or consent. The waiver by or consent of a party to a breach of any provision of this Agreement shall not operate or be construed as a waiver of or consent to any other or subsequent breach by such other party.

- This Agreement may not be assigned (including by operation of law or otherwise) by you without WILEY's prior written consent.

- Any fee required for this permission shall be non-refundable after thirty (30) days from receipt by the CCC.

- These terms and conditions together with CCC&#65533;s Billing and Payment terms and conditions (which are incorporated herein) form the entire agreement between you and WILEY concerning this licensing transaction and (in the

absence of fraud) supersedes all prior agreements and representations of the parties, oral or written. This Agreement may not be amended except in writing signed by both parties. This Agreement shall be binding upon and inure to the benefit of the parties' successors, legal representatives, and authorized assigns.

- In the event of any conflict between your obligations established by these terms and conditions and those established by CCC's Billing and Payment terms and conditions, these terms and conditions shall prevail.
- WILEY expressly reserves all rights not specifically granted in the combination of (i) the license details provided by you and accepted in the course of this licensing transaction, (ii) these terms and conditions and (iii) CCC's Billing and Payment terms and conditions.
- This Agreement will be void if the Type of Use, Format, Circulation, or Requestor Type was misrepresented during the licensing process.
- This Agreement shall be governed by and construed in accordance with the laws of the State of New York, USA, without regards to such state's conflict of law rules. Any legal action, suit or proceeding arising out of or relating to these Terms and Conditions or the breach thereof shall be instituted in a court of competent jurisdiction in New York County in the State of New York in the United States of America and each party hereby consents and submits to the personal jurisdiction of such court, waives any objection to venue in such court and consents to service of process by registered or certified mail, return receipt requested, at the last known address of such party.

WILEY OPEN ACCESS TERMS AND CONDITIONS

Wiley Publishes Open Access Articles in fully Open Access Journals and in Subscription journals offering Online Open. Although most of the fully Open Access journals publish open access articles under the terms of the Creative Commons Attribution (CC BY) License only, the subscription journals and a few of the Open Access Journals offer a choice of Creative Commons Licenses:: Creative Commons Attribution (CC-BY) license Creative Commons Attribution Non-Commercial (CC-BY-NC) license and Creative Commons Attribution Non-Commercial-NoDerivs (CC-BY-NC-ND) License. The license type is clearly identified on the article.

Copyright in any research article in a journal published as Open Access under a Creative Commons License is retained by the author(s). Authors grant Wiley a license to publish the article and identify itself as the original publisher. Authors also grant any third party the right to use the article freely as long as its integrity is maintained and its original authors, citation details and publisher are identified as follows: [Title of Article/Author/Journal Title and Volume/Issue. Copyright (c) [year] [copyright owner as specified in the Journal]. Links to the final article on Wiley's website are encouraged where applicable.

The Creative Commons Attribution License

The Creative Commons Attribution License (CC-BY) allows users to copy, distribute and transmit an article, adapt the article and make commercial use of the article. The CC-BY license permits commercial and non-commercial re-use of an open access article, as long as the author is properly attributed.

The Creative Commons Attribution License does not affect the moral rights of

has not endorsed this translation."

Use by commercial "for-profit" organisations

Use of Wiley Open Access articles for commercial, promotional, or marketing purposes requires further explicit permission from Wiley and will be subject to a fee. Commercial purposes include:

- Copying or downloading of articles, or linking to such articles for further redistribution, sale or licensing;
- Copying, downloading or posting by a site or service that incorporates advertising with such content;
- The inclusion or incorporation of article content in other works or services (other than normal quotations with an appropriate citation) that is then available for sale or licensing, for a fee (for example, a compilation produced for marketing purposes, inclusion in a sales pack)
- Use of article content (other than normal quotations with appropriate citation) by for-profit organisations for promotional purposes
- Linking to article content in e-mails redistributed for promotional, marketing or educational purposes;
- Use for the purposes of monetary reward by means of sale, resale, licence, loan, transfer or other form of commercial exploitation such as marketing products
- Print reprints of Wiley Open Access articles can be purchased from: corporatesales@wiley.com

Further details can be found on Wiley Online Library
http://olabout.wiley.com/WileyCDA/Section/id-410895.html

Other Terms and Conditions:

v1.9

Questions? customercare@copyright.com or +1-855-239-3415 (toll free in the US) or +1-978-646-2777.

Appendix D – Methods in Neuroproteomics

Proteomic analysis of limited protein quantities from human brain tissue using gel-aided sample preparation (GASP)

Dale Chaput, Stanley M. Stevens Jr.

Department of Cell Biology, Microbiology, and Molecular Biology, University of South Florida, Tampa, FL.

Corresponding author: smstevens@usf.edu

Running head: Gel-aided sample preparation (GASP)

Summary

One challenge associated with mass spectrometry-based proteomics is the preparation of samples from small amounts of starting material. Studies using primary cell cultures isolated from various tissues often provided limited numbers of cells (eg. microglia). Additionally, accessibility to human tissue and the quantity of tissue that can be obtained is also often limited. To date, a number or proteomic sample processing methods have been used, some of which show variable results when working with small amounts of protein. We have successfully implemented a gel-aided sample processing (GASP) method for proteomic analysis of cell lysates and human brain tissue samples with as low as 1µg of protein. Based on proteome coverage obtained using high-resolution mass spectrometry, GASP is a reliable and reproducible method for processing samples with limited amounts of protein.

Key Words

Proteomics, gel-aided sample processing, GASP, protein

1. Introduction

A number of sample preparation strategies have been developed for various proteomics applications. In-solution digests are useful when the sample buffer is compatible with digestion and downstream analytical detection, primarily relying on urea for sample lysis and protein solubilization. Additionally, SDS-PAGE and 2-dimensional electrophoresis (2-DE) are commonly used for protein separation/fractionation followed by in-gel digest of proteins [128, 129, 383]. While these techniques are commonly used, lysis buffer compatibility is usually limited to mild reagents when mass spectrometry is the downstream characterization technique. Another point to consider is that solubilization of membrane proteins and other hydrophobic proteins often requires harsher lysis buffers that include detergents, such as sodium dodecyl sulfate (SDS), which increase protein solubilization, and therefore increase proteome coverage [384]. While detergents increase protein solubilization, they are typically incompatible with mass spectrometry as they can suppress analyte ion formation and reduce chromatography performance and, therefore, detergent removal improves protein identification [385, 386]. The Mann lab developed the filter-aided sample preparation (FASP) method for removing ionic detergents, which uses a filter for buffer exchange followed by protein digestion [217]. While FASP is a commonly used and efficient method for proteomic sample processing using SDS, it also has its limitations; for example, it relies on filters that are known to absorb proteins, especially hydrophobic proteins, and these filters occasionally fail to retain protein. These issues can be particularly problematic when working with limited amounts of protein as the majority of it may be retained by the filter or lost entirely.

Recently, a gel-aided sample preparation (GASP) approach was described [387] that demonstrated effective and reproducible protein recovery when working with very small amounts of protein. During GASP, protein samples are combined with acrylamide to generate a solidified piece of gel matrix that encapsulates the protein lysate. The gel is minced to increase buffer access, while

proteins are retained in the gel. After washing the gel pieces, proteins are digested overnight as in a typical in-gel digestion, and peptides can be subsequently extracted. To determine the effectiveness of GASP in the analysis of brain-derived cell and tissue lysate, we report the application of the GASP method for proteomic analysis of limited amounts of protein extracted from human brain tissue.

2. Materials

Solutions should be prepared using HPLC-grade water, or at minimum nanopure water, and analytical grade reagents.

2.1 Lysis buffer composition

1. Lysis buffer composition: 4% SDS, 100mM dithiothreitol (DTT), 100mM Tris pH 7.4, protease and phosphatase inhibitors (optional). A stock of 100mM Tris pH 7.4 can be prepared in advance and stored at room temperature. We prepare 100mM Tris pH 7.4 by solubilizing Tris-base in water and adjusting the pH with HCl. 4% SDS (w/v) and 100mM DTT should be prepared fresh before each use in 100mM Trish pH 7.4.
2. Pierce 660 assay reagent and ionic detergent compatibility reagent (IDCR) (Pierce).

2.2 Acrylamide and polymerization reagents

1. Protogel (40% w/v, 37.5:1, acrylamide/bisacrylamide solution, National Diagnostics).
2. 10% ammonium persulfate (APS) (w/v) should be made fresh before each use. To make 10% APS, add 100mg APS to 850µl water, for a final volume of 1ml. Amounts can be scaled depending on the requirements for the experiment.
3. Tetramethylethylenediamine (TEMED).
4. Spin-X filter inserts (Costar, Corning) are used to mince gel pieces and should be placed in 2ml centrifuge tubes.

2.3 GASP buffers

1. Fixing solution: 50% methanol, 40% acetic acid, 10% water (v/v/v).

2. Wash solution: 6M urea in 100mM Tris pH 8.5. A stock of 100mM Tris pH 8.5 can be prepared in advance and stored at room temperate. 6M urea should be prepared fresh for each experiment.
3. Dehydrating solution: acetonitrile.
4. Rehydrating solution: 50mM ammonium bicarbonate (ABC) in water.
5. Peptide extraction solution: 5% formic acid (v/v) in water.

2.4 Digest solution resuspension and composition.

1. Resuspend 200µg lyophilized Trypsin/Lys-C (Promega) in 20µl resuspension buffer (50mM acetic acid). Dilute to 0.1µg/µl using 25mM ammonium bicarbonate (ABC). Depending on the amount of trypsin required, Trypsin/Lys-C can be further diluted using 25mM ABC.

2.5 LC-MS/MS Peptide Resuspension Buffer

1. 1% acetonitrile, 0.1% formic acid, water.

3. Methods

3.1. Sample Lysis

1. Weight brain tissue samples and calculate required lysis buffer volume based on the addition of 5µl lysis buffer/1mg tissue weight.
2. Add lysis buffer to cell pellet or tissue. Incubate at 95°C for 5 minutes. Centrifuge at 16,000x*g* for 10 minutes to pellet any remaining insoluble material. When working with small cell pellets or pieces of tissue, there should only be a minimal pellet, if any can be seen at all. After the addition of 4% SDS lysis buffer, boiling, and sonication, protein samples should be kept at room temperature when in use to avoid SDS precipitation.
3. Determine protein concentration using the Pierce 660 assay supplemented with ionic detergent compatibility reagent (IDCR) (*see* **Note 1**).

3.2. Gel-Aided Sample Processing (GASP)

All procedures carried out at room temperature unless otherwise specified.

1. Bring desired amount of protein to 50-100µl in 100mM Tris pH 7.4. Add an equal volume of Protogel (40%) to achieve a 20% acryalmide solution (*see* **Note 2**). Gently mix until homogenous and incubate at room temperature for 20 minutes.
2. Add 5µl 10% APS and 5µl TEMED to lysate/acrylamide. Let gel polymerize for 15 minutes, or until solid (*see* **Note 3**).
3. Transfer gel piece to a Spin-X filter insert placed in a 2ml centrifuge tube (*see* **Note 4**). Centrifuge at 16,000x*g* for 5 minutes. If a significant amount of gel has not passed through filter, re-position the gel in the filter and re-centrifuge (*see* **Note 5**).
4. Add 1ml fixing solution to the minced gel pieces. Incubate while vortexing for 10 minutes (*see* **Note 6**). Briefly centrifuge the samples and discard the supernatant (*see* **Note 7**).
5. Wash 1: Add 500µl of 6M urea to gel pieces. Incubate while vortexing for 10 minutes.
6. Dehydrate gel pieces with 1ml of acetonitrile and incubate while vortexing for 10 minutes. The gel pieces will turn white. Briefly centrifuge and discard supernatant.
7. Wash 2: Add 500µl of 50mM ABC to gel pieces. Incubate while vortexing for 10 minutes.
8. Dehydrate gel pieces with 1ml of acetonitrile. Incubate while vortexing, until gel pieces turn white. Briefly centrifuge and discard supernatant.
9. Repeat dehydration with 500µl acetonitrile for 10 minutes while vortexing.
10. Add Trypsin/Lys-C solution to the dry gel pieces (1:50, w/w, enzyme:substrate). Bring the volume of the Trypsin/Lys-C solution to twice the volume of the original gel piece using 25mM ABC (*see* **Note 8**). Incubate at 37°C overnight (~16 hrs).

3.3. Peptide Extraction

1. Add 1 volume (equal to the volume of the overnight digest solution) of acetonitrile (*see* **Note 9**). Incubate while vortexing for 10 minutes.
2. The supernatant contains desired peptides. Briefly centrifuge and transfer the supernatant to a fresh, labelled 1.5ml centrifuge tube.
3. Rehydrate gel pieces with 1 volume of 5% formic acid in water. Incubate while vortexing for 10 minutes.
4. Dehydrate gel pieces with 1 volume of acetonitrile. Incubate while vortexing for 10 minutes.
5. Briefly centrifuge and pool supernatant with previously collected supernatant.
6. Further dehydrate gel pieces with 1 volume of acetonitrile. Incubate while vortexing for 10 minutes.
7. Briefly centrifuge and pool supernatant.
8. Completely dry peptides in a vacuum concentrator (*see* **Note 10**). Resuspend peptides in 0.1% formic acid, 1% acetonitrile. Vortex for 5 minutes. Place in sonicator bath for 10 minutes. Centrifuge at 16,000x*g* for 10 minutes. Transfer to autosampler vial (*see* **Note 11**).

3.4. Database Searching

1. GASP results in the addition of propionamide on N-termini of lysine, cysteine, and histidine residues. Need to consider as variable modification in database searches (*see* **Note 12**).

4. Notes

1. While we use the Pierce 660 assay for determining protein concentration, other protein assays may be compatible with the lysis buffer as well. The use of IDCR with the 660 assay when using the 4% SDS, 100mM DTT lysis buffer is critical in order to obtain fairly accurate measurements of total protein amounts (for downstream mass spectrometry-based quantitation).

2. If sample/lysate volume is 100µl, add 100µl of 40% acrylamide. The desired concentration is 20% acrylamide.
3. If the gel does not harden, more acrylamide and APS can be added.
4. The gel piece should be oriented so that the widest part is against the filter (see Figure 1a). It is important to use 2ml centrifuge tubes as volumes of 1.5ml are used during some steps.
5. Not all gel pieces will pass through the Spin-X filter. Any gel pieces that do not pass through and remain in the filter should be added to the minced gel pieces in the centrifuge tube.
6. All steps involving incubation while vortexing were performed using a Fisher Scientific vortex mixer at setting 1 (lowest setting, approximately 300rpm).
7. All supernatant removal and discard steps should be performed using gel loading tips. A gel loading tip can be attached to a 1ml pipette tip to more conveniently remove large supernatant volumes (see Figure 1b).
8. If the total volume of the lysate and acrylamide was 100µl (ex. 50µl lysate and 50µl acrylamide), dilute Trypsin/Lys-C to 200µl for overnight incubation.
9. A 'volume' should be equal to the volume used above (in **Note 8**). For example, if Trypsin/Lys-C was diluted to a final volume of 200µl, a 'volume' is 200µl.
10. Additional desalting steps are not necessary but could be incorporated into the protocol.
11. Resuspend dried peptides in ~0.5-1µl more than intended to transfer to autosampler vial whenever possible. Use a gel loading tip to transfer sample to the autosampler vial being careful to avoid any pelleted insoluble material or gel pieces.
12. Monomeric acrylamide reacts with nucleophilic amino acids and can result in the addition of propionamide to the N-termini of cysteine, histidine, and lysine residues. This needs to

be considered as a variable modification when searching raw data files. In our experience, based on the total number of propionaminde modifications, lysine undergoes this modification the most, followed by histidine and then cysteine.

Table 1. Number of proteins identified from human tissue after GASP. GASP was used to process 0.5µg, 5µg, 10µg, 25µg, and 50µg of protein from 2 biological replicates (Rep 1 and Rep 2) of human brain tissue. Peptides were separated on an EasyNano-LC with a 50cm C18 reverse-phase (RP)-UPLC column and analyzed on a Q-Exactive Plus with a 1 hour gradient. The number of proteins identified with a reported intensity value increases as the amount of protein increases. Additionally, the number of proteins identified with a minimum of 2 peptides is reported.

	Number of Quantified Proteins		*Number of Proteins Identified with Minimum 2 peptides*	
GASP Amount (µg)	**Rep 1**	**Rep 2**	**Rep 1**	**Rep 2**
0	1023	832	700	507
5	1960	1882	1555	1447
10	2076	2148	1642	1667
25	2210	2012	1744	1589
50	2163	2252	1683	986

Table 2. Protein quantitation accuracy following GASP of human tissue. Generating a ratio of intensity values comparing 0.5µg and 5µg digests, we would expect a 25-fold increase in intensity from the 5µg digest. The average median ratio of 5µg/0.5µg protein intensities was 28.51, slightly above the expected increase. We speculate, based on the peptide digest amount resuspended and analysed by LC-MS/MS, that with the 50µg GASP we are surpassing the column loading capacity of the analytical column which is affecting protein quantitation .

Ratio	**Median Ratio**	**Avg. Median**	**St. Dev.**
5/0.5 – 1	26.497	28.51	2.85
5/0.5 – 2	30.53		
10/5 - 1	2.168	1.92	0.35
10/5 - 2	1.677		
25/10 - 1	2.305	2.29	0.02
25/10 - 2	2.277		
50/25 - 1	1.377	0.99	0.54
50/25 - 2	0.618		

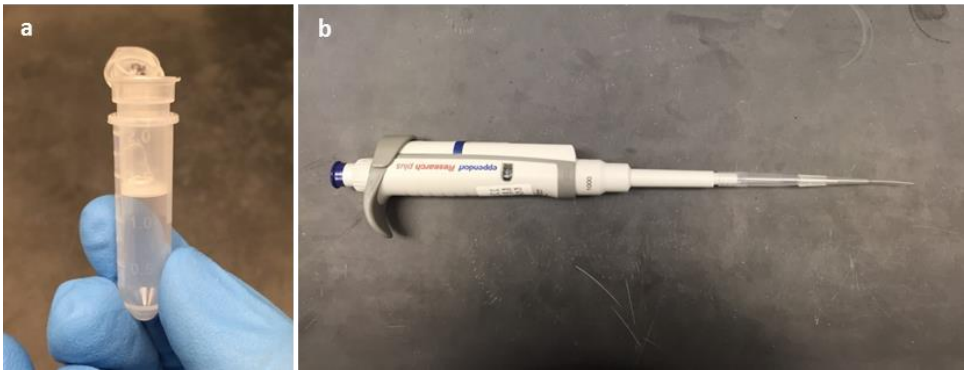

Figure 1. Orientation of gel in Spin-X filter insert and attachment of gel loading tip for GASP. (a) Orientation of gel piece in Spin-X filter before centrifugation**. b)** Gel-loading pipet tip stacked on 1ml pipet tip.